**University of Dundee**

**DOCTOR OF PHILOSOPHY**

**Developing nomograms and predictive models based on Multiparametric MRI characterised localised prostate cancer**

Alqahtani, Saeed

*Award date:*
2022

*Licence:*
Copyright of the Author. All Rights Reserved
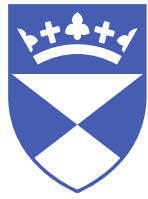
[Link to publication](#)

# Developing nomograms and predictive models based on Multiparametric MRI characterised localised prostate cancer.

by

Saeed Alqahtani

A Thesis Submitted in Fulfilment of the Requirements of the University of Dundee
for the Degree of Doctor of Philosophy (Ph.D.)

**May 2022**

## **Acknowledgements**

First, I would like to express my sincere gratitude to my supervisors Prof Zhihong Huang and Prof Ghulam Nabi for their great support and advice in conducting this study and in helping me to complete my thesis. Beside my supervisors, I would like to thank my Thesis Monitoring Committee, Dr Nikola Krstajic and Dr Svetlana Zolotovskaya, for their insightful comments and suggestions.

My sincere thanks to Dr Magdalena Szewczyk-Bieda and Dr Cheng Wei for their close technical support in MRI analyses. Special thanks also to Dr Jennifer Wilson who played a vital role in reporting the histopathology.

My appreciation also goes out to my colleagues and friends who motivated and advised me during my PhD project. Finally, I would like to thank my wife and my family: my parents, my brothers and my sisters, for their tremendous understanding and encouragement over the past few years.

## <u>Declarations:</u>

I, Saeed Alqahtani, hereby certify that this thesis is written by me, is my own work and has not been submitted in any other degree qualification except as specified.

Signature of candidate

I confirm that Saeed Alqahtani has completed the minimum duration period of registration of full-time study at the University of Dundee and has fulfilled the conditions of the University of Dundee, thereby qualifying him to submit this thesis in application for the degree of Doctor of Philosophy.

Prof. Zhihong Huang

Prof. Ghulam Nabi

# Contents:

## List of Figures:

**List of Tables:**

## <u>Abbreviations</u>

**AS**          Active surveillance

**ADC**        Apparent diffusion coefficient

**AUC**        Area under the curve

**BIRADS**   Breast imaging reporting and data system

**BPH**        Benign prostate hypertrophy

**c-statistic**  Concordance statistic

**csPCa**     Clinically significant cancer

**cT**          Clinical tumour stage

**CZ**          Central zone

**DCE**        Dynamic contrast enhanced

**DRE**        Digital rectal examination

**DWI**        Diffusion-weighted imaging

**ECE**        Extra capsular extension

**EPE**        Extra prostatic tumour extension

**ERC**        Endo-rectal coil

**ESUR**      European Society of Urogenital Radiology

**GS**          Gleason score

**AJCC**      American Joint Committee on Cancer

**UICC**      International Union Against Cancer

**HIFU**      High-intensity focused ultrasound

**IQR**        Interquartile range

**ISUP**      International Society of Urological Pathology

**$K_{ep}$**        Reverse reflux rate constant

**$K_{trans}$**     Transfer constant

**m**           Mean

**M**           Median

**MP-MRI**   Multiparametric MRI

**MRI**        Magnetic resonance imaging

**MRSI**      Magnetic resonance spectroscopic imaging

**NVB**        Neurovascular bundle

**OR**          Odds ratio

**PIRADS**    Prostate imaging reporting and data system

**PCa**    Prostate cancer

**PPA-coil**    Pelvic-phased-array coil

**PSA**    Prostate specific antigen

**PSAD**    Prostatic specific antigen density

**PZ**    Peripheral zone

**RP**    Radical prostatectomy

**SB**    Systematic random biopsy

**SD**    Standard deviation

**SVI**    Seminal vesicle invasion

**T1W**    T1-weighted

**T2W**    T2-weighted

**TB**    MR/US fusion targeted biopsy

**TRUS**    Transrectal ultrasound

**TZ**    Transitional zone

**US**    Ultrasound

**TR**    Transrectal

**TP**    Transperineal

## Abstract

Multiparametric magnetic resonance imaging (MP-MRI) and MRI targeted biopsies (TB) are a new standard in prostate cancer (PCa) screening and diagnosis. Guidelines already include this approach for patients at risk. First, this thesis aimed to assess whether pre-biopsy MRI can narrow the discrepancy of histopathological grades between biopsy and radical prostatectomy (RP) using the Prostate Imaging Reporting and Data System (PIRADS). Second, this thesis aimed to develop a prediction model to identify patients who will benefit from performing systematic random biopsy (SB) at the time of TB.

330 men treated consecutively by RP with localised PCa were included in this study. The MRI and histopathology of the biopsies and RP specimens were assessed respectively. A multivariate model was constructed using logistic regression analysis to assess the ability of MRI to predict upgrading in biopsy Gleason score (GS) in a nomogram. A decision-analysis curve was constructed assessing the impact of the nomogram using different thresholds for probabilities of upgrading. In the SB and TB study, 198 patients with positive MRI findings who underwent both TB and SB were prospectively recruited in this study. The first outcome was to compare the detection rate of clinically significant prostate cancer (csPCa) in SB and TB. For the second outcome, a multivariate analysis using a logistic regression model and nomogram construction were used to identify patients who will benefit from SB in addition to TB. A decision-analysis curve was constructed assessing the impact of the nomogram using different thresholds for probabilities of our model. Statistical analyses were performed using IBM SPSS (version 23.0) and RStudio (version 4.0.3)

Using multivariate analysis, the PIRADS v2.0 score significantly improved the predictive ability of MRI scans for upgrading of biopsy GS (p=0.001, 95% CI [0.06-

0.034]), which improved the C-index of predictive nomogram significantly (0.90 vs. 0.64, p<0.05). Moreover, the detection rate of csPCa using SB and TB was 51.0% (101/198) and 56.1% (111/198), respectively, adopting a patients-based biopsy approach. The detection rate of csPCa was higher using a combined biopsy (64.6%; 128/198) compared to a TB (56.1%; 111/198) alone. This was statistically significant ($\chi2$=15.06, df (degree of freedom) = 1, P<0.001). In the multivariate analysis, age, prostate-specific antigen density (PSAD) and PIRADS score were found to predict the detection of significant PCa by SB in addition to TB. A nomogram based on the model showed good discriminative ability (C-index; 78%).

In conclusion, MP-MRI using PIRADS score was shown to be an independent predictor of postoperative GS upgrading, and that this should be taken into consideration while offering treatment options to men with localised PCa. There was a significant difference in the detection of csPCa using a combined biopsy approach. The developed nomogram could help identify those patients at risk of having PCa who will benefit from adding SB biopsy in addition to TB.

# Chapter 1 Introduction

## 1.1 Motivations and research objectives

Histology from biopsies categorised into GS is the only confirmatory test for cancer diagnosis and is most commonly used for risk stratification of men with a recent diagnosis of PCa. Based on the above, men are counselled for various treatment options. With increasing therapeutic options available to men with a diagnosis of PCa, scrutiny of information from biopsy grade becomes increasingly important. There is around 35.5% (range: 14–51%) upgrading of biopsy GS on LRP (1). Many factors contribute to the discrepancy between needle biopsy and corresponding radical surgery GS. Under calling of Gleason cribriform Gleason pattern 4 as pattern 3 or the presence of borderline grades due to barely appreciable glandular differentiation under microscope and lack of sampling of tertiary grade disease on biopsies are known contributors. Factors such as age, size of prostate, extent of cancer on biopsy needle and number of biopsy samples (extended/ or mapping) are also known to impact on the incidence of upgrading (2).

In light of a number of studies reporting upgrading or undergrading of PCa on needle biopsies, there is the potential for under treatment or overtreatment (i.e. radiotherapy and hormone duration). Several publications (3,4) and consensus updates on the Gleason grading system have partially addressed this issue including recommending deriving GS by adding the most common and highest Gleason pattern on the biopsy rather than original method of adding the primary and second most common patterns (5). Moreover, upgrading, if suspected, has long-term outcome implications. Corcoran et al (6) showed that even after adjusting for known preoperative variables (including clinical stage, PSA, number of positive cores, and percentage of positive cores) upgrade to a higher GS remained a strong and

independent predictor of biochemical recurrence after attempted local curative therapy, this underscores the importance of gaining more information to predict upgrading of biopsy GS in men diagnosed with PCa as this may serve as a marker of biologically aggressive disease.

Pre-biopsy MRI has recently been shown to hold great promise in the detection and characterisation of PCa (7). A negative scan (no lesion seen on the MRI scan) showed a high negative predictive value for the presence of significant PCa (8). Song et al (9) reported a high predictive value of PIRADS v2 in predicting upgrading of GS from biopsy, however this study was retrospective and MRI was obtained at least 3 weeks following biopsies, an approach known to impact the interpretation of images. Post-biopsy haemorrhage is the most common false-positive finding for PCa (10). In this study, there was no attempt to align histopathological sectioning to MRI using recently reported 3D-mould technology. Therefore, the objective of the first part of the thesis was:

1. To evaluate whether pre-biopsy MRI had the potential to narrow the discrepancy of histopathological grades between transrectal ultrasound (TRUS) biopsy and radical prostatectomy (RP) using PIRADS v2.0

Recent trends and evidence support pre-biopsy MRI with selective targeting of suspected malignant lesions using MRI/ultrasound (US) and TB methods (11) . The burgeoning interest in fusion imaging has arisen to address the main limitations of SB: over detection of clinically insignificant cancers and possibly under detection of csPCa. A number of recent reports support the utility of pre-biopsy multi-parametric magnetic resonance imaging (mpMRI) to address the limitations of SB, and the advantage of increased csPCa detection (12–14). Pre-biopsy MRI in MRI directed pathways have been reported to detect a higher number of csPCa. However,

benefits of image-guided targeting performed in combination with systematic sampling or alone remains poorly defined. Drost et al. in a recent systematic review, used a mixed population (with or without image fusion targeting of suspicious areas) to answer this question, however image fusion methods were not used in all the cases of included studies and hence the benefits of targeting suspicious areas with the image fusion approach, with or without addition of systematic biopsy sampling, remains unclear (15) .

Image fusion approach makes use of information from MRI to direct biopsy needles under real-time US guidance (12,16,17) . Studies have shown that mpMRI combined with TB technology is a promising tool in the diagnosis of PCa (12,18,19) . In light of a number of previous trials showing the significant benefits of image TB, research is now focused on whether random biopsies are required at all in the detection of prostate cancer (20–22) . This question is pertinent to settle an ongoing debate as studies have also highlighted that TB with the addition of systematic random biopsy is superior to systematic random biopsy alone either in terms of capturing csPCa or even in terms of post-procedural morbidity (11) . In a large retrospective study, from centres in Europe and the USA, Dell'Oglio et al. aimed at findings a group of men where systematic biopsies could be avoided all together in men with MRI-facilitated targeted biopsy approach. The authors failed to achieve their objectives and concluded that systematic sampling should be combined with the image guided fusion biopsies (23) . In a large multicentre prospective study, researchers concluded a higher detection rate for clinically significant prostate cancer for a combined approach (TB and SB) biopsy method, however  different image fusion systems including cognitive guidance were used in targeted biopsy approach (21). Furthermore, the study did not use PIRADS v2 categorisation and no standardised

protocol was used for MRI imaging. This allowed biases and heterogeneity into the reported data. Our study is a protocol-driven prospective investigation with standardised US/MRI fusion protocol. We assessed clinical variables that could help in identifying patients who may benefit from systematic random biopsies in addition to fusion targeted approach. The comprehensive analysis and outcomes using methodology of this study has not been reported in the literature (24,25), in particularly net clinical benefit of the approach.

The aim of the second part of the thesis was to:

1. compare the diagnostic accuracy of MRI/US fusion targeted biopsies, systematic biopsies and combined approaches in the detection of csPCa and define predictive factors where a combined approach could be used.

2. Quantify additional benefits of adding systematic biopsies to the targeted biopsies approach by constructing a nomogram and assessing its net-clinical benefits.

## 1.2 Content of the thesis

This thesis includes five chapters. Chapter I introduction: the purpose and background of this project.

Chapter II reviews the literature and summarises the knowledge related to my project, including prostate anatomy, diagnosis and treatment of prostate cancer, the principles and applications of MP-MRI are revealed. Finally, how to construct a nomogram and decision curve analysis.

Chapter III (Prediction of prostate cancer Gleason score upgrading): contains methods and materials of the first study, analysis, results and discussion. (First paper)

Chapter IV (Predicting the performance of concurrent SB during TB sampling of MP-MRI) contains methods and materials of the second study, analysis, results and discussion. (Second paper)

Chapter V Conclusion and future work: Pre-biopsy MRI and PIRADS score significantly and independently predict GS upgrading, a nomogram using clinical variables can assist decision-making during the counselling of patients to have systematic sampling of the prostate in addition to an image fusion biopsy approach. The further work also is mentioned in this chapter.

## 1.3 Publication from the thesis

1/ **Alqahtani S**, Wei C, Zhang Y, Szewczyk-Bieda M, Wilson J, Huang Z, Nabi G. Prediction of prostate cancer Gleason score upgrading from biopsy to radical prostatectomy using pre-biopsy multiparametric MRI PIRADS scoring system. Scientific reports. 2020 May 7;10(1):1-9.
**(Chapter 3)**

2/ **Alqahtani, S**.; Zhang, X.; Wei, C.; Zhang, Y.; Szewczyk-Bieda, M.; Wilson, J.; Huang, Z.; Nabi, G. Predicting the Performance of Concurrent Systematic Random Biopsies during Image Fusion Targeted Sampling of MultiParametric MRI Detected Prostate Cancer. A Prospective Study (PRESET Study). Cancers 2022, 14, 1
**(Chapter 4)**

## 1.4 Publication related to the thesis

1/Wei C, Zhang Y, Malik H, Zhang X, **Alqahtani S**, Upreti D, Szewczyk-Bieda M, Lang S, Nabi G. Prediction of postprostatectomy biochemical recurrence using quantitative ultrasound Shear wave elastography imaging. Frontiers in oncology. 2019 Jul 9; 9:572.

# Chapter 2 Literature review

## 2.1 Anatomy and histology of the prostate gland

The prostate is a male organ surrounding the urethra, lying between the urinary bladder superiorly and the urogenital diaphragm inferiorly. It is a fibro-muscular glandular structure measuring approximately 3 cm in length.

The prostate is conical in shape and has a base superiorly against the bladder neck, and an apex lies on the superior surface of the urogenital diaphragm (Figure 2-1). The mid-prostate locates between the base superiorly and the apex inferiorly (26).
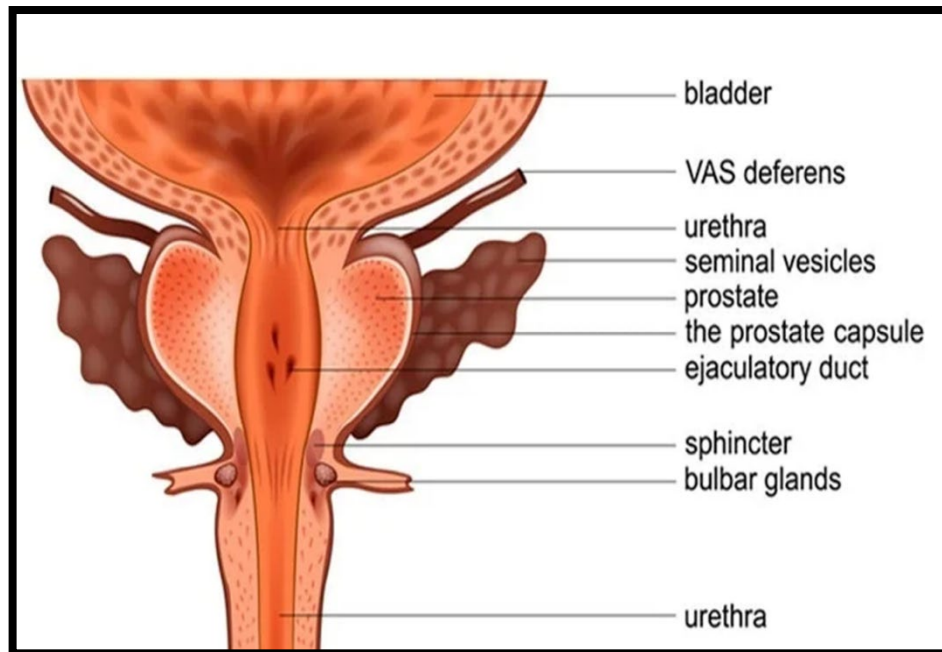


Figure 2-1 The anatomical features of the prostate gland with other surrounding pelvic structures (27).

McNeal (28) defined three separate zones of the prostate: the central zone (CZ); the peripheral zone (PZ); and the transition zone. All differed histologically and biologically. The CZ is located posterosuperiorly to the transitional zone (TZ), which is located centrally and surrounds the proximal part of the urethra. The PZ makes up the main body of the gland (approximately 65%) and is located in the posterior and

inferior parts of the prostate; 75% of malignancy is found in this zone (28) (Figure 2-2).
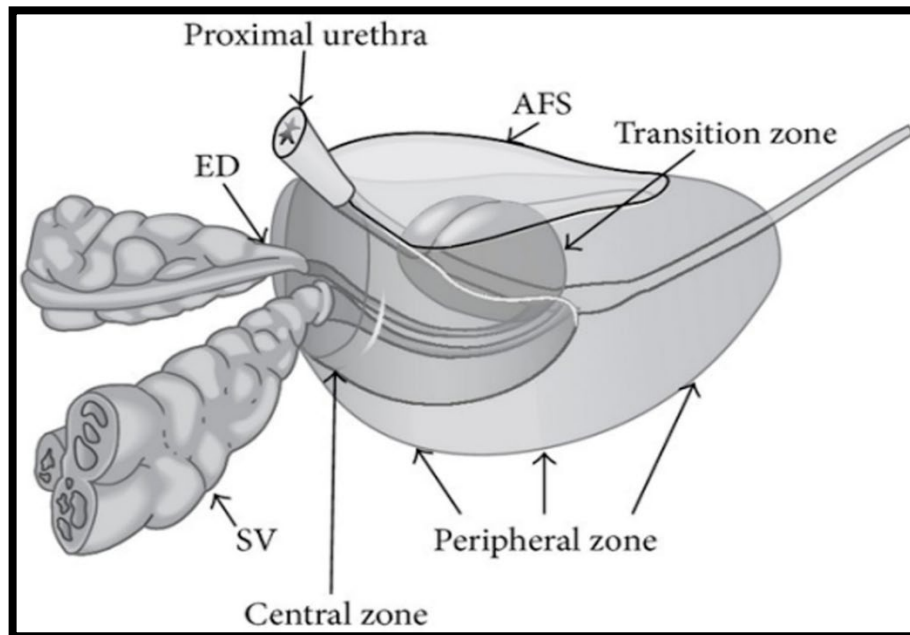


Figure 2-2 Zonal anatomy of the prostate and their relation to each other (29).

Histologically, the prostate gland is made up of epithelial and stromal components. The epithelial part is at most represented by the acinar glands that are lined with secretory stratified columnar epithelia cells. These glands are separated by the connective tissue stroma which consists of fibroblast, nerves, smooth muscle fibres, and rarely, adipocytes (30).

The function of the prostate gland is to produce a fluid that, together with sperm cells from the testicles and fluids from other glands, makes up semen. The muscles of the prostate also ensure that the seminal fluid is pressed into the urethra and then expelled outwards during ejaculation (28).

## 2.2 Prostate cancer (PCa)

The second most frequently diagnosed cancer in males worldwide, PCa continues to be a major health issue (31). Approximately 1.11 million men are diagnosed with PCa and 307,000 deaths by PCa occur per year (32). Higher than 95% of PCa are referred to as acinar or conventional types (30).

According to studies, the incidence of PCa relates to increases in age (33,34). From the results shown, almost 37% of PCa tumours were seen in males under the age of 65. Patients aged 65 to 74 years old with PCa were the largest group, accounting for 36% all cases. 27% of PCa was detected in males 75 years of age and older. Therefore, patients over the age of 65 accounted for 63% of all PCa.

GS is thought to be the gold standard for PCa aggressiveness and determination. It is based on the observation of acini under the microscope by a pathologist. Cancer epithelial cells have larger nuclei and more prominent nucleoli than normal epithelial cells, and there are no basal cells (35).

### 2.2.1 Diagnosis

High levels of PSA and an irregular digital rectal exam (DRE) are indicators of high PCa risk. A biopsy can be used to confirm a diagnosis of PCa. Low-grade indolent PCa may not progress to a clinically significant tumour. High-grade PCa can be aggressive, easily spread, and result in death. However, PSA detection, biopsies, and DRE have limited sensitivity and accuracy. This is because 70-80% of cases with high PSA have benign prostatic hyperplasia (BPH) or prostatitis, so the specificity of PSA to PCa is low. DRE can only be used to assess tumours from the posterior of the prostate. Moreover, it cannot detect the number of lesions, as tumour cells may be mixed with normal prostate tissue. A biopsy taken from a multifocal

PCa lesion can show Gleason underscoring (36). In addition, patients with low-grade PCa identified by biopsies may have aggressive lesions outside of the biopsied region, especially in bigger prostate. This might result in Gleason underscoring. Adding pre-biopsy MRI in the diagnosis and characterisation of PCa has recently been shown to be very promising (7).

A number of recent reports have supported the use of pre-biopsy MRI to address many of the limitations of SB, with the prominent advantage being the increased detection of csPCa (7,37–39).

## 2.2.2 Grading and staging

Used to grade PCa (40), the GS system was named after Gleason, a pathologist, who defined five degrees of increasing aggressiveness (grading) based on the extent to which tumour cells are structured into identifiably glandular structures (glandular differentiation) at low magnification:

**Grade 1** – Small uniform glands with minimal nuclear changes.

**Grade 2** – Medium sized acini still separated by stromal tissue but more closely arranged.

**Grade 3** – These tumours have marked variation of glandular size and organization, as well as stromal tissue infiltration.

**Grade 4** – Marked cytological atypia with extensive infiltration.

**Grade 5** – Sheets of undifferentiated cancer cells.

Since PCa has more than two grades in heterogeneity, the GS system combines a primary score, which is the most prevalent, with a secondary grade, which is the second most prevalent, to assess PCa. GS is obtained by combining the primary and secondary grades. Consequently, the GS ranges from 2 (1+1) to 10 (5+5) (41).

The TNM classification, developed and maintained by the American Joint Committee on Cancer (AJCC) and the International Union Against Cancer (UICC) for the 7th edition in 2010 (42), is used to stage PCa.

**Primary tumour assessment (T):**

**T1** - Clinically inapparent tumour neither palpable nor visible by imaging.

**T1c** - Tumour identified by needle biopsy (for example, because of elevated PSA).

**T2** - Tumour confined within the prostate.

**T3** - Tumour extends through the prostate capsule.

**T3a** - Extracapsular extension **T3b** =Tumour invades seminal vesicles

**T4** - Tumour is fixed or invades adjacent structures other than seminal vesicles, such as external sphincter, rectum, bladder, levator muscles and/or pelvic wall.

**Regional lymph node involvement (N):**

**NX** - Regional lymph nodes were not assessed.

**N0** - No regional lymph node metastasis.

**N1** - Metastasis in regional.

**Distant Metastasis (M):**

**M1** - Distant metastasis**.**

**M1a** - Non-regional lymph node(s).

**M1b** - Bone(s).

**M1c** - Other sites.

### 2.2.3 Treatment

PCa treatment requires the collaboration of a multidisciplinary team including urologists, histopathologists, radiologists, and radiation oncologists.

Age, original PSA, clinical staging (TNM), GS, urinary function, and comorbidities all play a role in treatment planning (43). A patient's life expectancy and the disease's biological characteristics, as well as the disease's predicted aggressiveness, are important factors to consider before starting any PCa treatment plan. A patient's preferences for various treatment choices should also be taken into account, by considering treatment risks before taking any decision.

Clinically localised PCa is defined by a tumour confined to the prostate gland or a Clinical stage of T2 or less (44). It is widely treated with the following:

1- Active surveillance (AS)

- Regularly monitoring of the disease is usually preferred for those with very-low-risk and low-risk PCa.

2. Radical prostatectomy (RP)

- Removing the whole prostate gland. Seminal vesicles and certain nearby lymph nodes may be removed based on tumour staging (44).

3. Radiotherapy

- Radiotherapy aims to destroy PCa cells without causing too much damage to healthy cells. External radiotherapy uses high-energy X-ray beams targeted at the prostate from outside the body. Brachytherapy is another type of radiotherapy where tiny radioactive seeds are internally put into the prostate.

4. Hormonal therapy

- Androgen suppression treatment is another name for hormone therapy. The goal is to lower or avoid male hormones, known as androgens, from fuelling PCa cells in the body. Hormonal therapy may also be used in conjunction with other treatments, such as radiotherapy, to improve the efficacy of the treatment (45).

5. Focal therapy

- High-intensity focused ultrasound (HIFU) uses high-frequency ultrasound energy to heat and destroy cancer cells in the prostate. Recently, patients with clinically significant nonmetastatic PCa can be given focal treatment using HIFU since it is effective in the medium term and has a low-risk of urinary and rectal side effects (46).

## 2.3 Multiparametric MRI of the prostate gland

MRI of the prostate is performed using a 1.5 or 3 Tesla MRI scanner and a pelvicphased-array coil (PPA-coil) placed over the pelvis, with or without an endorectal coil (ERC) depending on the clinical condition. The use of an ERC can increase image quality, as it is located in the rectum just posterior to the prostate gland as well as to fixate the prostate during the scan, potentially reducing motion artefacts. However, the ERC has some drawbacks, including longer scanning times, increased costs and lower patient compliance due to the coil's placement in the rectum. The additional image resolution of the ERC is valuable on 1.5 T MRI, whereas it is more questionable on 3 T. Most prostatic MRI examinations can be conducted with acceptable image quality without an ERC due to increased spatial resolution (the ability to distinguish two dense structures from each other) and increased signal-to-noise ratio on 3 T MRI (47). However, a recent study found that 3 T MRI with and without an ERC evidenced similar diagnosis of overall and index PCa (48). According to the European Society of Urogenital Radiology's (ESUR) MR prostate guidelines, the use of an ERC is optional for detection and preferable for staging at 3 T MRI (49).

The quality of an MRI image is also influenced by the patient's preparation. The administration of an oedema prior to the examination and injection of an antispasmodic agents may diminish rectal peristaltic motion and reduce intra-luminal air which can cause MRI artefacts (50).

The development of MP-MRI provides new possibilities in the detection, lesion characterisation and staging of PCa due to its high quality and soft-tissue contrast. Several published data (12,51–53) have illustrated the rapidly growing use of MP-MRI as the most sensitive and specific diagnostic imaging modality for PCa

management. MP-MRI can reveal details about morphological, metabolic and cellular changes in the prostate as well as to characterise tissue vascularity (54,55). The use of MP-MRI criteria to follow up malignancy recurrence and treatment decisions may decrease the population needing TRUS biopsies by allowing these biopsies to be targeted to high-risk groups. Pre-biopsy MP-MRI, used as a triage, could improve the detection of clinically significant cancer (12).

MP-MRI contains different MRI sequences: anatomical imaging; diffusion weighted imaging (DWI); dynamic contrast enhanced imaging (DCE); and spectroscopic imaging (MRSI). The information from these techniques can be combined to provide more accurate results.

## 2.3.1 Anatomical MR imaging for prostate gland

Anatomical MRIs include T2-weighted (T2W) and T1-weighted (T1W) images. These display the anatomy of the prostate and its adjacent structure with high resolution. As part of MP-MRI, anatomical MRIs are useful when combined with other functional MRI techniques such as DWI and DCE imaging to obtain the optimal accuracy of the result (49).

## 2.3.1.1 T1-weighted MRI

T1W imaging is used in conjunction with T2W imaging to detect post-biopsy haemorrhage and assess the prostate's contour and neurovascular bundles (NVB). Because of its low spatial resolution, T1W imaging cannot be used to assess intra-prostatic zonal anatomy (56). On T2W imaging, post-biopsy haemorrhage can mimic PCa because both cancerous lesions and haemorrhage can appear as dark (hypo-intense) areas. It has been reported that it affects between 28 and 95% of patients (10,57,58). However, only haemorrhage on T1W imaging will appear as a high signal

intensity area, which can be used to rule out false-positive findings on T2W imaging (10) (Figure 2-3).
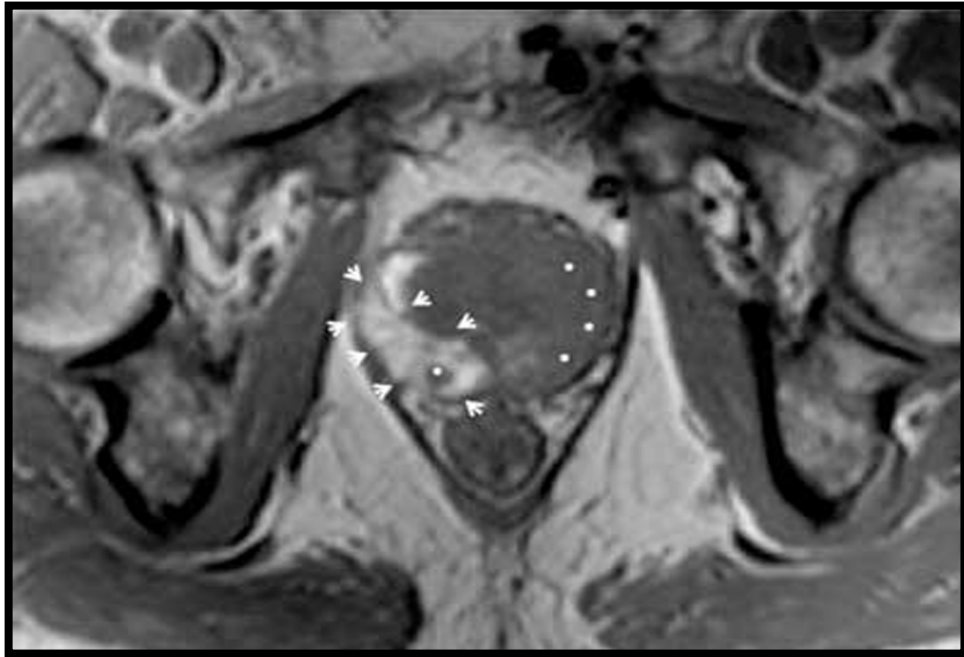


Figure 2-3 Axial T1 showing diffuse hyperintense signal in the right PZ (arrowheads) due to post-biopsy haemorrhage with area free of T1 hyperintense blood (asterisks) matched the PCa lesions (T1 haemorrhage exclusion sign).

The extent of haemorrhage in a PCa lesion is smaller than in adjacent benign tissue, and the presence of the excluded haemorrhage sign on T1W imaging combined with a homogeneous low signal intensity area on T2W imaging is highly accurate for PCa detection (58).

### 2.3.2.2 T2-weighted MRI

By providing a good picture of the prostatic zonal anatomy, T2W imaging with high spatial resolution can be used to detect, localise, and stage PCa (51). Often, the PZ has a higher signal intensity due to the high content of water in the glandular tissue as opposed to the transitional and CZ which often have a lower signal intensity (Figure 2.4A). The transitional and CZ is often referred in combination as the central

gland, as the two zones can be difficult to differentiate on MRI. However, awareness about the location and features of the CZ is important because its manifestation may mimic PCa, resulting in a false positive reading on MRI (Figure 2.4B). However, PCa in the CZ is uncommon, but when it is located there it is usually more aggressive (59).
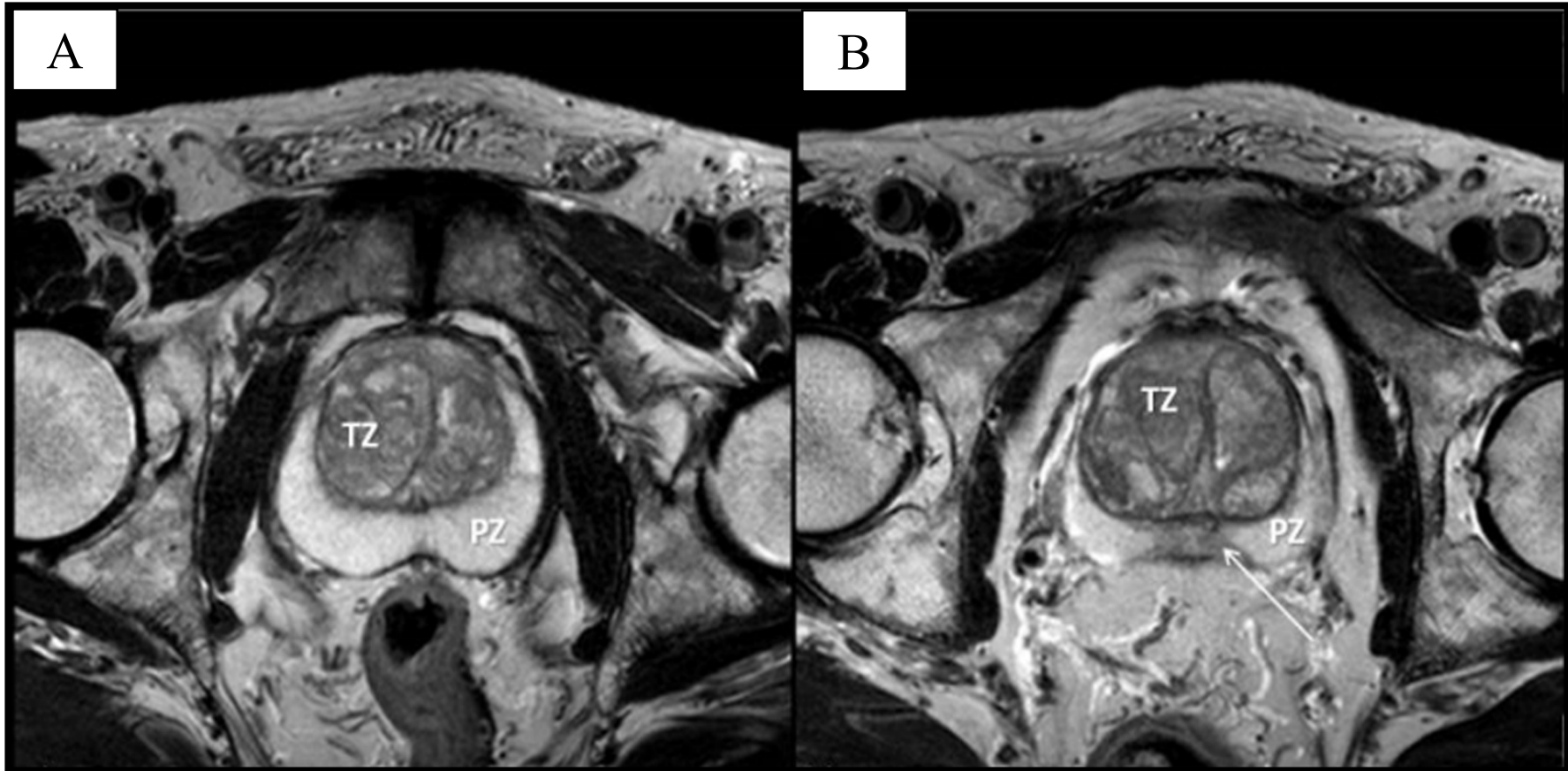
Figure 2-4 Normal prostate anatomy. (A) T2W images show the PZ and TZ in the axial plane. (B) Axial T2W image at the prostatic base shows the CZ (white arrow) as a hypointense area surrounding the ejaculatory ducts (60).

The prostatic capsule appears as a thin fibro-muscular fringe with lower signal intensity surrounding the prostate. In contrast to the higher signal intensity from the homogeneous benign PZ, PCa in the PZ typically appears as a round or oval area of low signal intensity (61,62) (Figure 2-5). On T2W imaging, however, some PCa lesions are iso-intense and cannot be seen. The use of T2W imaging alone therefore has limitations.
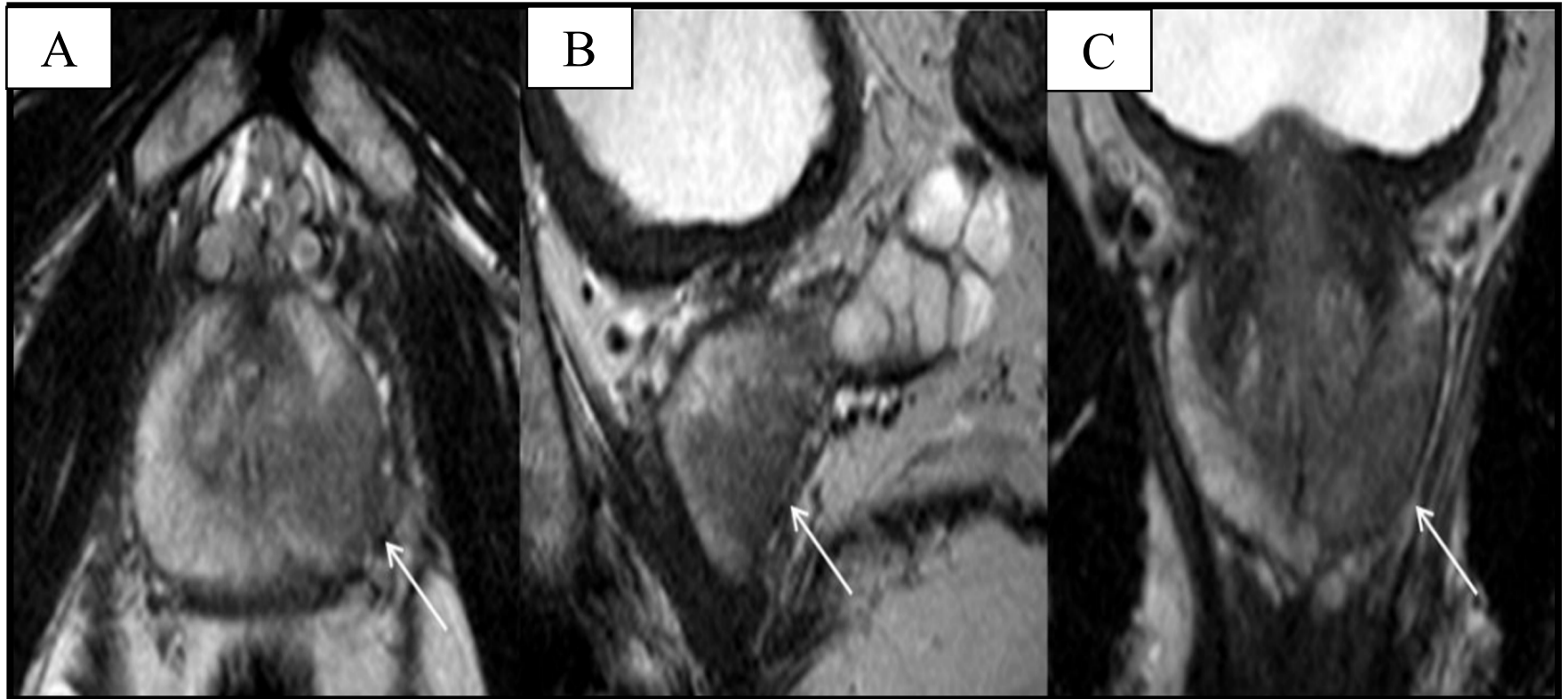
Figure 2-5 On (A) axial, (B) sagittal, and (C) coronal views, T2W imaging of a PCa lesion in the left PZ (white arrow) (60).

PCa occurring in the TZ is not as clearly defined because it often has lower and mixed signal intensities due to benign prostatic hyperplasia nodules that may interfere with diagnosis and mimic PCa. PCa in the TZ is characterised by a homogeneous low signal intensity area usually anteriorly located and has a lenticular shape (Figure 2-6) (63).
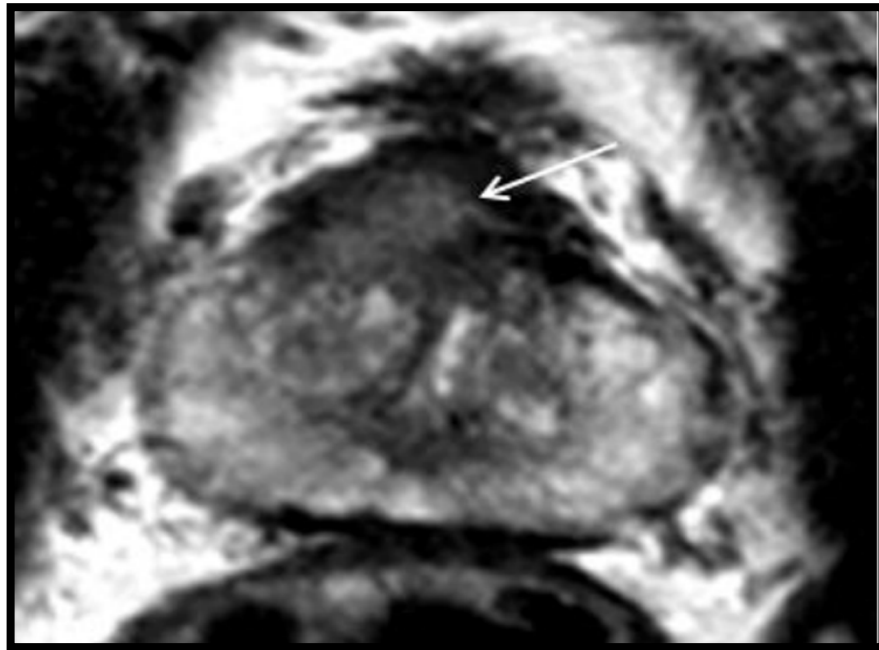


Figure 2-6 Axial T2W image of a PCa lesion in the prostate's right anterior part (white arrow) (60).

The degree of signal intensity on T2W imaging has been related to the GS as cancers with a Gleason grade 4 or 5 become more hypointense than cancers with a Gleason grade 3 (64). Further, the cancer's growth pattern may affect the appearance where sparse tumours with increased intermixed benign prostatic tissue appear more like normal PZ than more dense tumours (65). Moreover, several benign lesions in the prostate such as haemorrhage, atrophy, BPH, calcifications, and prostatitis may present as a low signal intensity region on T2W imaging, resulting in false-positive readings. According to a meta-analysis, T2W imaging alone had a sensitivity and specificity of 0.57-0.62 and 0.74-0.78, respectively (66). Due to this moderate sensitivity and specificity, T2W imaging can be used in

conjunction with other functional MRI techniques such as DWI and DCE imaging to improve diagnostic performance (67).

## 2.3.2 Functional MR imaging for prostate gland

### 2.3.2.1 Diffusion weighted imaging (DWI)

DWI is a non-invasive functional MRI technique that measures changes in water molecule diffusion as a result of microscopic structural changes. DWI generates different signal intensities that quantify the movement of free water molecules by applying different gradients (b-values) to the water protons in the tissue (68). The glandular structures in normal prostatic tissue, particularly in the PZ, allow water molecules to move freely without restriction. PCa often depletes glandular structures and causes restricted diffusion by containing more densely packed cells. Diffusion changes result in changes in the signal intensity on DWI: regions with restricted diffusion appear bright on DWI. DWI is usually performed with different b-values where low b-values (0-100) indicate a signal decay caused by perfusion in the tissue, whereas higher b-values represent water movement in the extracellular and intracellular compartment (69). DWI can be used to detect and characterise lesions by providing both qualitative and quantitative information about tissue cellularity and structure Therefore, a qualitative assessment of a region with high signal intensity on high b-value DWI often represents a region with restricted diffusion caused by tightly packed cells.

The apparent diffusion coefficient (ADC) is calculated using the signal intensity changes of at least two b-values to quantitatively assess the degree of diffusion restriction. ADC is calculated using built-in software in the MRI scanner or workstation. An $ADC_{map}$ is created based on the ADC value in each voxel of the

prostate. Restricted diffusion causes a reduction in the ADC value and appears dark on the ADC$_{map}$ (69,70).

Compared to surrounding normal tissue, PCa has higher cellular density and restricted diffusion. As a result, PCa lesions appear bright on DWI with high b-values but dark on the ADC$_{map}$ with lower ADC tumour values (70–72). As a result, DWI can help distinguish between malignant and benign tumours, and the use of DWI in the diagnosis of PCa has been shown to add sensitivity and especially specificity to T2W imaging carried out on its own (Figure 2-7) (73).
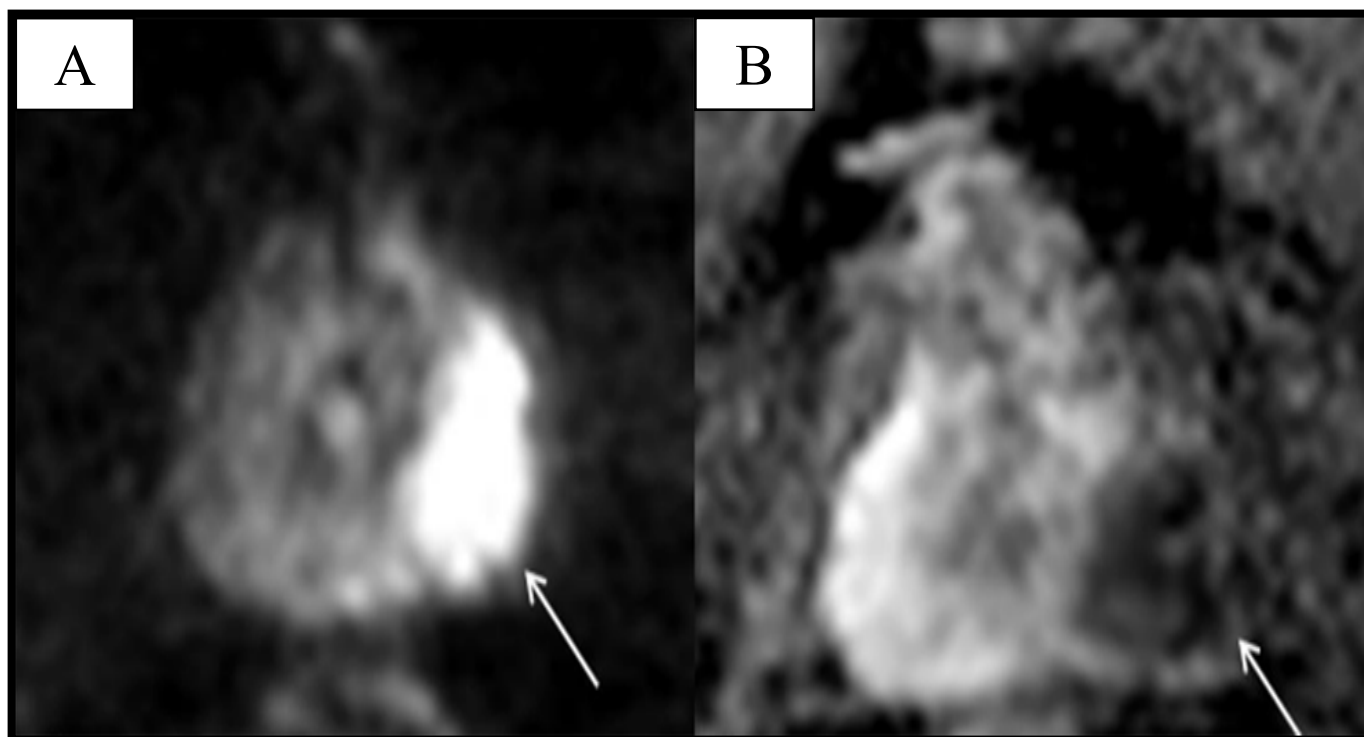
Figure 2-7 (A) DWI of PCa in the left PZ (white arrow) b1400 (B) ADC$_{map}$ (60).

According to studies, the mean ADC tumour value measured from the cancerous lesion on the ADCmap and the GS have an inverse relationship (74–77), implying that ADC tumour values can be used as a non-invasive marker of tumour aggression. Attempts have been made to define precise cut-off values to distinguish malignant from healthy tissue and to further differentiate between GS groups. However, a wide range and inconsistency in mean ADC tumour values have been reported due to different study methodologies with different b-values, different MRI scan and field strengths, as well as patient variability between studies (74,76,78). Furthermore, remarkable overlap exists between ADC values from malignant and benign prostatic tissue, along with wide variability depending on the zonal origin. As a result, no agreement has been reached on absolute ADC tumour cut-off values for different GS (79–81).

### 2.3.2.2 Dynamic contrast-enhanced MRI

DCE-MRI exploits the fact that malignant and benign prostatic tissues frequently have distinct contrast enhancement profiles. The DCE-MRI method is based on changes in the pharmacokinetic features of the tissue mainly due to angiogenesis. DCE-MRI includes a series of fast high-temporal (the ability to make fast and accurate images in rapid succession) T1W images before, during and after a quick intravenous injection of a gadolinium-based contrast agent. Since prostatic tissue is usually heavily vascularised, a simple examination of pre- and post-contrast images is insufficient for PCa characterisation (82). Compared to normal prostatic tissue, PCa often causes angiogenesis and increased vascular permeability, resulting in a high and early contrast enhancement peak (increased enhancement) accompanied by fast washout of the contrast (Figure 2-8) (83,84).
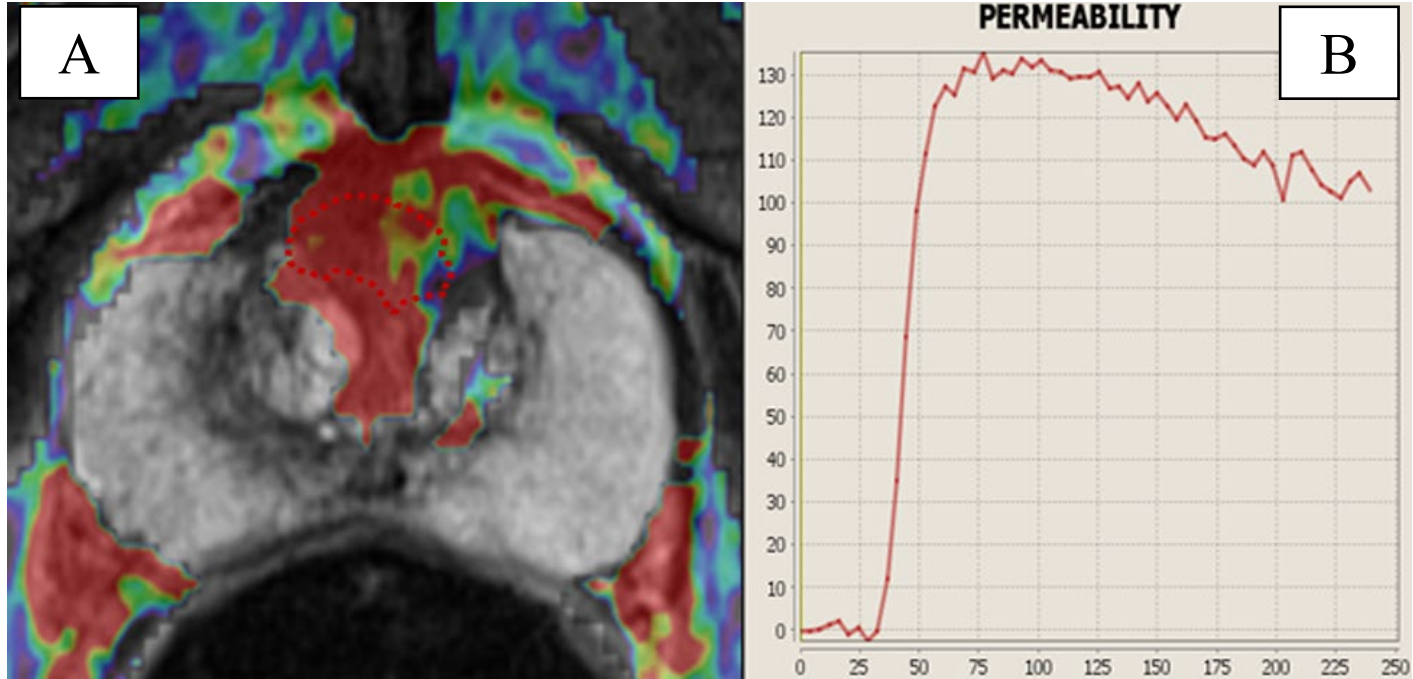
Figure 2-8 (A) DCE-MRI colour map shows early focal contrast enhancement in the TZ tumour (Red dotted circle). (B) DCE-curve which is a typical malignant curve with a high peak, rapid early enhancement (high wash-in rate) and early wash-out.

The pharmacokinetic features of the tissue can be defined using a number of methods. Qualitatively by visualising enhancement curves, and quantitatively by using detailed pharmacokinetic models to calculate the contrast exchange rate between different cellular compartments, or semi-quantitatively, by measuring various enhancement curve kinetic parameters such as wash-in/wash-out rate, time to peak. In addition, various post-processing software tools are used to analyse and describe the DCE-MRI, including overlaid colourised enhancement maps used to detect pathological changes and PCa. Previous research has shown that using DCE-MRI in combination with other MRI modalities can enhance PCa detection diagnostic accuracy (85,86) and improve extra capsular extension (ECE) detection (87). The utility of DCE-MRI primarily adds sensitivity to the MP-MRI performance and is essential for the detection of local recurrence. However, Baur et al (88) have stated that DCE-MRI did not add significant value to the detection of PCa. DCE-MRI has a low specificity as benign conditions such as hyper-vascularised BPH nodules and prostatitis can mimic pathological enhancement patterns. To reach the optimum sensitivity and accuracy for PCa evaluation, DCE-MRI should be used in combination with other MRI modalities such as T2W imaging and DWI (85,89).

### 2.3.2.3 Magnetic resonance spectroscopic imaging

MRSI displays the relative concentrations of chemicals within small volumes of interest, providing metabolic information about prostate tissue (voxels). Citrate is abundant in normal prostate tissue (higher in the PZ compared with the central or transition zone levels). Because the cells in PCa switch from a citrate producing to a citrate oxidising metabolism, citrate levels in PCa cells are decreased or undetectable. Choline levels are also elevated in proliferating malignant tissue due

to a high phospholipid cell membrane turnover (Figure 2-9). As a result, MRSI detects tumours based on an increased choline to citrate ratio (90).

However, because MRSI is technically challenging and requires a high level of expertise as well as a longer scan time, which is frequently combined with the use of an ERC, many centres do not include it in their standard protocol. MRSI is not required for prostate examination according to the ESUR MR prostate guidelines (91).
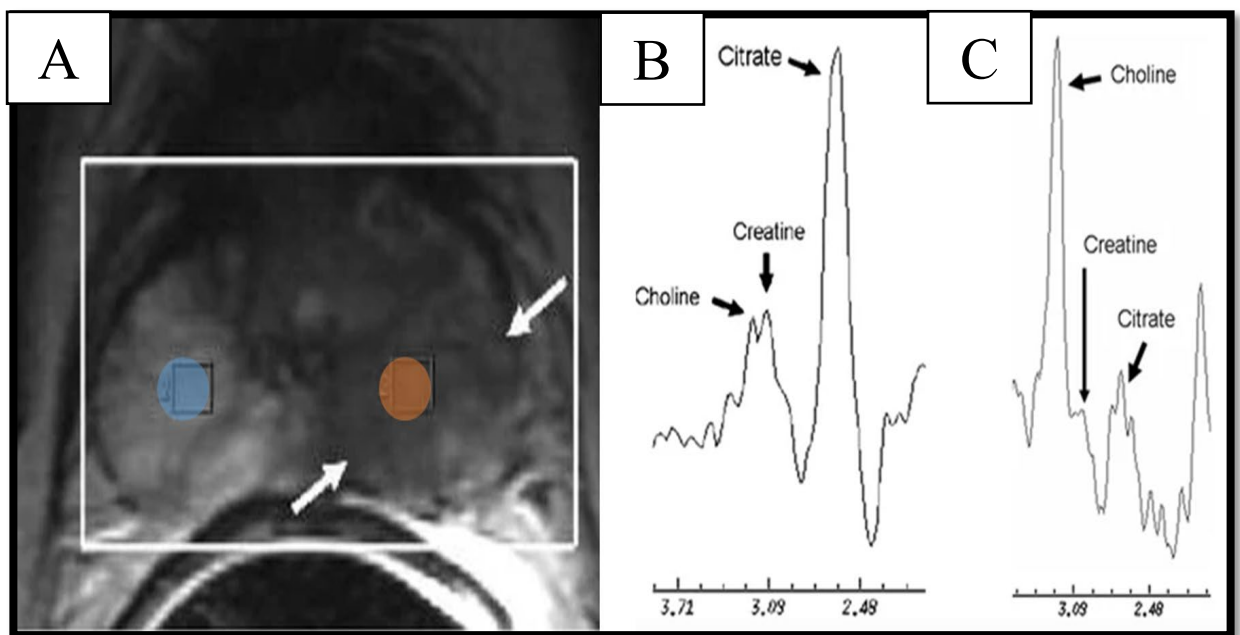


Figure 2-9 (A) The MRSI was acquired from the whole prostate showing a large low signal intensity lesion (arrows) in the left PZ. (B) The right voxel from the PZ (blue circle) shows the high signal intensity with the normal metabolic profile of the prostatic gland, high level of citrate and lower level of choline. (C) The corresponding spectrum from the left voxel shows increased choline and reduced citrate, indicative for a metabolic profile of prostatic cancer (orange circle) combined with the low signal intensity on MRI (92).

## 2.4 Prostate Imaging-Reporting and Data system (PIRADS)

The basic principle of a scoring system for MP-MRI readings is to detect abnormal regions and grade each region based on the appearance on the MP-MRI according to the degree of suspicion of PCa. However, interpreting prostate MP-MRI is difficult, requiring a steep learning curve; experienced readers are significantly more accurate than inexperienced readers (93,94). MP-MRI diagnostic accuracy varies between studies (95,96), owing to differences in study protocols' diagnostic criteria, MRI machines and expertise, which has sparked a debate about MP-MRI's readiness for routine use (97). Lack of standardisation and a consistent scoring system has been a source of debate for MP-MRI. As a result, clinical guidelines were recently published in order to promote high-quality MP-MRI acquisition and evaluation. The guidelines, including clinical indications for MP-MRI and a structured uniform PIRADS to standardise prostatic MP-MRI readings, are based on evidence from the literature and consensus from ESUR prostate MRI experts (49,98).

The PIRADS classification system, like the Breast imaging reporting and data system (BIRADS) for breast imaging, is a scoring system for prostate MP-MRI. It should include: 1) a graphic prostate scheme with 16-27 regions based on a five-point Likert scale; 2) a PIRADS score for each individual lesion; and 3) the largest lesion's maximum diameter. For each suspicious lesion within the prostate, all MRI modalities – such as T2W, DWI, and DCE imaging – are scored independently (1-5) on a five-point scale, and the sum of all individual scores (ranging from 3-15 for three modalities) constitutes the PIRADS summation score. Further, each lesion is assigned a final overall score (ranging from 1 to 5) based on the likelihood of clinically significant PCa being present (98) (Table 2-1).

| Score | Criteria |
|---|---|
| | **T2WI imaging for PZ** |
| 1 | Signal intensity is uniformly hyperintense (normal). |
| 2 | Either Linear or wedge-shaped hypointensity or diffuse mild hypointensity with an indistinct margin. |
| 3 | Non-circumscribed, rounded, moderate hypointensity or heterogeneous signal intensity. Others that don't fit into the categories of 2, 4, or 5. |
| 4 | The focus/mass is circumscribed, homogenous, moderately hypointense, and confined to the prostate, with <1.5 cm in greatest dimension. |
| 5 | Identical to 4, but with ≥1.5cm in greatest dimension or definite extraprostatic extension/invasive behaviour. |
| | **T2WI imaging for TZ** |
| 1 | A round, fully encapsulated nodule or a normal-appearing TZ (rare) (An example of a typical nodule). |
| 2 | A mostly encapsulated nodule or a circumscribed nodule that is homogeneous but not encapsulated. ("atypical nodule") or a homogeneous mildly hypointense area between nodules. |
| 3 | Non-circumscribed, rounded, moderate hypointensity or heterogeneous signal intensity. Others that don't fit into the categories of 2, 4, or 5. |
| 4 | Lenticular or non-circumscribed, homogeneous, moderately hypointense, and with <1.5 cm in greatest dimension |
| 5 | Identical to 4, but with ≥1.5cm in greatest dimension or definite extraprostatic extension/invasive behaviour. |
| | **Diffusion weighted imaging** |
| 1 | No abnormality on ADC and high b-value DWI. |
| 2 | Hypointense linear/wedge shaped on ADC and/or hyperintense linear/wedge shaped on high b-value DWI. |
| 3 | On ADC, focal hypointense (distinct from background) and/or focal hyperintense on high b-value DWI; may be markedly hypointense on ADC or markedly hyperintense on high b-value DWI, but not both. |
| 4 | On ADC, the focal region is markedly hypointense, and on high b-value DWI, it is markedly hyperintense; <1.5cm in greatest dimension. |
| 5 | Identical to 4, but with ≥1.5cm in greatest dimension or definite extraprostatic extension/invasive behaviour. |
| | **Dynamic contrast enhanced imaging** |
| - | No early or concurrent enhancement; or diffuse multifocal enhancement NOT corresponding to a focal finding on T2W and/or DWI; or focal enhancement corresponding to a lesion showing BPH characteristics on T2WI (including features of extruded BPH in the PZ). |
| + | Focal, it occurs before or at the same time as enhancement of adjacent normal prostatic tissues and it corresponds to a suspicious T2W and/or DWI finding. |
| | **Overall final score** |
| 1 | Clinically significant tumour is highly unlikely to be present. |
| 2 | Clinically significant tumour is unlikely to be present. |
| 3 | Clinically significant tumour is equivocal. |
| 4 | Clinically significant tumour is likely to be present. |
| 5 | Clinically significant tumour is highly likely to be present. |

Table 2.1 T2W, DWI, and DCE imaging are classified using the PIRADS system. On T2W imaging, the PZ and TZ have significantly different anatomical appearances, so different PIRADS criteria are used for the two zones (49,98).

Each lesion should be evaluated for possible extra prostatic tumour extension (EPE) in addition to the PIRADS classification. The ESUR MR prostate guidelines include a table of MP-MRI findings along with a risk score stratified into different EPE criteria with concomitant tumour characteristics/findings (Table 2-2).

| Criteria | Findings | Score |
|---|---|---|
| Extracapsular extension | Abutment | 1 |
| | Irregularity | 3 |
| | Thickening of the neurovascular bundle | 4 |
| | Bulge, capsule loss | 4 |
| | Extracapsular disease that can be measured | 5 |
| Seminal vesicles Expansion | Expansion of the seminal vesicles | 1 |
| | Low T2 signal | 2 |
| | Filling in of angle | 3 |
| | Enhancement and impeded diffusion | 4 |
| Distal sphincter | Adjacent tumour | 3 |
| | Effacement of the sphincter muscle with a low signal | 3 |
| | Sphincter enhancement that is abnormal | 4 |
| Neck of the bladder | Adjacent tumour | 2 |
| | Low T2 signal in bladder muscle | 3 |
| | Enhancement that extends into the bladder neck is abnormal | 4 |

Table 2.2 EPE risk scoring of extra prostatic extension (49).

T4-disease includes invasion into the bladder neck, external distal sphincter, rectum, and/or side of the pelvic wall, although only the first two T4-findings are included in the ESUR EPE risk scoring. The most commonly used MRI modality for EPE assessment is anatomical T2W imaging. However, some of the categories (for

example, Seminal vesicle invasion (SVI)) also include functional imaging findings (enhancement and impeded diffusion risk score 4). Suspicion of EPE should be given an overall score ranging from 1 to 5 based on the likelihood of EPE being present. Therefore, the five-point scale is considered a continuum of risk with higher scores indicating a higher risk of EPE. However, not all categories include the total score range of 1-5, and functional imaging results, for example, are excluded from ECE evaluation. Functional imaging has been shown in previous studies to aid in the detection of ECE (99,100), particularly in less experienced readers. As a result, when applying functional imaging findings, personal opinion may influence the interpretation and overall impression of possible ECE.

## 2.5 Histological grades between biopsy and radical prostatectomy

Several studies have examined the relationship between the GS at needle biopsy and the RP (101). Following the consensus conferences of the International Society of Urological Pathology (ISUP), the Gleason grading system was updated in 2005 and again in 2014 (4,102). The ISUP recently endorsed the use of a validated Grade Group stratification system ranging from 1 (GS 6) to 5 (GS 9 or 10) in conjunction with the overall Gleason system to reduce the number of grading categories and facilitate more accurate disease stratification (102).

With an increase in men undergoing treatment other than RP, such as radiation therapy or AS, where the only tissue sampled is on the needle biopsy, biopsy grade has become more important in recent years. Not only is there a risk of undertreatment due to needle biopsy undergrading, but overtreatment (i.e. additional radiotherapy) is also a concern for men whose biopsies are overgraded. The issue of accounting for tertiary grade patterns is significant as they can be seen in nearly 20% of RP specimens (103). Despite recent advances, traditional diagnostic pathways still rely on TRUS guided prostate biopsy to obtain systematic needle biopsies of the prostate, which has recently been shown to have a sensitivity of only 48% for the diagnosis of 'clinically significant' cancer, defined as a GS of at least 4 + 3 or a maximum core length of at least 6 mm (7).

Epstein et al (2) found that the rate of upgrading from GS 6 on biopsy to GS 7 on RP was 36.3%. The incidence of upgrading can be influenced by several quantifiable factors including serum PSA levels, pathology weight, age, the extent of cancer on biopsy, and needle biopsy sampling. The difference in experience and skill in grading among pathologists is a more difficult variable to quantify, although it has been

shown that needle biopsy and RP GS are more closely matched when graded by urologic pathologists rather than general pathologists (101,104).

The incidence of downgrading was also reported by Epstein JI et al (2), who found that 12% of cases with a biopsy diagnosis of 3 + 4 = 7 had GS 5–6 at RP. One explanation for these cases is that Gleason pattern 4 was overgraded due to tangentially sectioned small glands of pattern 3 on biopsy. Alternatively, the assigned biopsy GS may have been accurate in some cases, with such small foci of Gleason pattern 4 in the RP that it was either not recorded or unsampled deeper within the paraffin block. In cases where the GS 5–6 versus GS 3 + 4 = 7 on biopsy is borderline, it is probably better to diagnose the case as GS 6 because undergrading due to sampling error is acceptable compared to overgrading due to grading error.

Audenet et al (105) proposed a nomogram to predict the likelihood of upgrading patients on biopsy. This nomogram included several clinical variables such as age, PSA density, percentage of positive cores, and DRE in a first cohort of 896 patients. The accuracy of this model suggests that clinical factors are insufficient for assessing the disease's risk prior to treatment.

However, several studies have found that MP-MRI correlates with pathologic grade at surgery and can accurately distinguish between patients with low- and high-risk PCa (106,107). Ongoing efforts are being made to combine both imaging and conventional clinical variables in order to narrow the discrepancy between the GS of biopsy and RP Specimens and to improve the accuracy of predicting the upgrading.

## 2.6 MRI-targeted biopsy

In order to perform targeted prostate biopsy, three methods of MRI guidance are available: (1) cognitive fusion, in which the US operator simply points the biopsy needle at the prostate region reviewed prior to MRI that revealed a lesion; (2) direct MRI-guided biopsy, performed inside an MRI tube; and (3) software coregistration of stored MRI with real-time US, performed with a fusion unit. Each approach has its own set of benefits and drawbacks (108).

Cognitive fusion is simple, fast and requires no additional tools beyond the MRI and a conventional TRUS facility. The US operator does not need any additional training beyond that needed for traditional TRUS biopsy. In the comprehensive review of Moore et al (109), cognitive fusion was used in some 22 different studies. Although the evidence was minimal, cognitive fusion appears to be more accurate than conventional SB. The potential for human error in interpreting from MRI to TRUS without an actual overlay is a disadvantage of cognitive fusion.

Direct MRI-guided biopsy is conducted in-bore, that is within the MRI tube, by a radiologist who fuses a prior MRI demonstrating a lesion with a contemporaneous MRI to confirm the location of the biopsy needle. The patient is rescanned after each biopsy sample to confirm localisation. Only a few targeted cores are typically taken; systematic sampling is not done. The Barentsz group at Radboud University in Nijmegen, the Netherlands, published a major experience with in-bore biopsy (110). The small number of cores taken, the precise localisation of the biopsy, and the reduced detection of insignificant tumours are all advantages of this procedure. The drawbacks of this method include the time and expense required, along with the in-bore time and the two MRI sessions necessary to obtain the biopsy specimens. Furthermore, since only suspicious lesions are sampled, tissues with a 'normal' MRI

appearance are missed, which is problematic because any false-negative aspects of prostate MRI are unknown. The third approach for MRI guidance of prostate biopsy is MRI–TRUS fusion. In this method, the operator images the prostate using US, as performed for the past several decades. When viewing the prostate, the MRI of that prostate, which is performed beforehand and stored in the device, is fused with real-time ultrasound using a digital overlay, allowing the target(s) previously delineated by a radiologist to be brought into the aiming mechanism of the US. The fusion produces a three-dimensional reconstruction of the prostate, and the aiming and monitoring of biopsy sites takes place on the reconstructed model. This approach has the drawbacks of being indirect, requiring the use of an additional device, and requiring advanced operator training. The benefit is that it can be conducted within minutes in an outpatient clinic setting under local anaesthesia (108). The best MRI-TB method remains a matter of debate in the literature. However, several studies have concluded that MRI–TRUS fusion-guided biopsy is significantly more reliable and cost-effective than visual registration and in-bore biopsy (111,112).

MRI targeted fusion biopsy has been shown to outperform SB in the diagnosis of clinically significant cancer in many previous studies (12,17,113). Despite the improved detection of clinically significant cancers with MRI-targeted biopsies, debate still remains whether MRI-TB can be used instead of or in addition to SB. Ahdoot et al (20) found that combined biopsy improved the detection of all PCa in patients with MRI-visible lesions. However, MRI-TB alone underestimated the tumour's histologic grade. Following RP, upgrades to grade group 3 or higher on histopathological analysis were significantly lower after combined biopsy.

## 2.7 Nomogram construction

Iasonos et al (114) published the following steps (Table 2-3). The first step in developing a nomogram is to clearly define the population to which it will be applied in clinical practice. The population should be defined with detailed inclusion and exclusion criteria. When creating nomograms, it is preferable to use population-level data because it allows the model to be more generalisable. Clinicians' abilities to correctly apply a nomogram's predicted probabilities is entirely dependent on their understanding of the population on which the nomogram was based.

| Initial steps in constructing nomogram |
| --- |
| Define the patient population: Data source in Single institution, Multicentre |
| Identify the outcome of interest: What dose does the nomogram predict? |
| Make a list of all the predictors that you are considering. |
| Construct the nomogram: Model selection, Select variables |
| Validation: Data source (Internal data, External data) |

Table 2.3 Important Steps in constructing a Nomogram.

The operational definition of the outcome of interest is the second step in creating a nomogram. When creating nomograms, it is crucial to precisely and accurately describe the outcome. The entire point of a nomogram is to be able to predict the probability of an outcome occurring. As a result, the result must be as precise and accurate as possible, as well as simple to understand for both clinicians and patients. The third step is to select several covariates (variables) with a pathophysiological link to the desired outcome. All potential variables associated with an outcome should be included in the model when creating a nomogram, as long as they fit into

39

the pathophysiology of developing the outcome. The covariates should be chosen in advance and based on clinical evidence rather than statistical significance.

The fourth step in creating a nomogram is to choose a prediction model, enter the covariates into the model, and make sure that the prediction model's statistical assumptions (regression) are met. The type of regression to use for a nomogram is determined by the outcome's scale of measurement. Logistic regression, multinomial logistic regression, and proportional odds regression are used to construct nomograms for categorical and ordinal outcomes. If the 'time-to-event' for developing an outcome is the basis for constructing a nomogram, then Cox regression analysis can be used. Multiple regression may be used to build nomograms for continuous outcomes. Poisson regression or negative binomial regression can be used to construct nomograms for count outcomes (naturally skewed distributions).

The prediction model is finalised using validation, discrimination, and calibration methods in the fifth step. Cross-validation (split-group validation and bootstrap validation) and external validation are two methods of validation (to see if the model holds up with a new population or dataset). The predictive accuracy of discrimination refers to how well a model distinguishes between patients who have and do not have the desired outcome. Discrimination is evaluated by the concordance index (or C-index) obtained from ROC analyses (c-statistics or area under the curve (AUC)). The calibration of regression models is calculated by plotting the predicted probabilities of the model against the actual probabilities.

The final step is to interpret the validated nomogram and evaluate it for concordance and model fit. Each covariate's relative effects are converted to a point scale ranging from 0 to 100. These 'scores' for each covariate are added together and correspond

to the regression model's predicted probability of a patient having the outcome of interest (Figure 2-10).
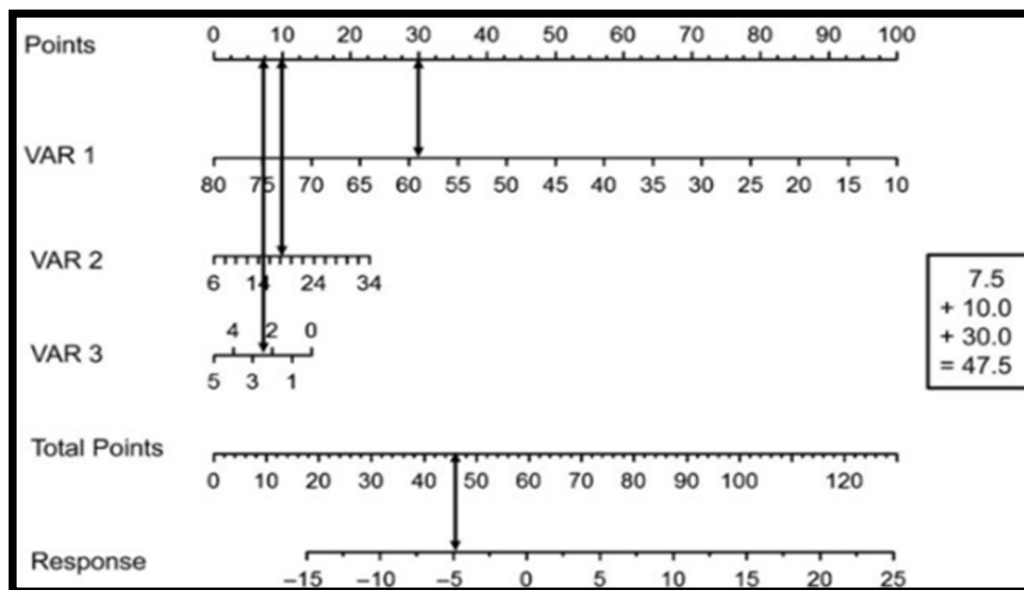


Figure 2-10 The nomogram depicts the impact of various predictive variables on various horizontal lines. The lengths of the different lines vary depending on the influence of each predictor. The greater the influence of a horizontal line, the longer it is. A number of points on the respective horizontal line represent the influence of each predictor. The anticipated magnitude of response can be read on the response horizontal line at the bottom of the nomogram by adding the points associated with each predictor (115).

The clinical utility of nomograms has been a source of debate. Increases in predictive accuracy related to the use of nomograms cannot only be statistically significant but also clinically meaningful. For example, preoperative nomograms estimating the risk of positive surgical margins, and lymph node metastases, may help clinicians in identifying patients who would derive greater benefit from more extensive surgery. Patients and physicians may benefit from postoperative nomograms that estimate recurrence, cancer specific survival, overall survival, the benefit of adjuvant therapies, and the impact of treatment on quality of life. However, their proper clinical application requires a thorough understanding of the nomogram-specific question,

study population, method of construction, and outcome, in order to accurately determine its applicability to a specific patient's clinical condition. Furthermore, the ability to analyse nomogram performance and assess limitations is needed in order to properly advise patients on the context, precision, and assumptions underlying nomogram risk estimations (116–118).

## 2.8 Decision-analysis curve

The definitive answer to determine if nomogram assisted decisions improve patient outcomes lies in prospective evaluation and randomising patients to nomogram or non-nomogram-based decisions and comparing the outcomes. However prospective validation of every nomogram prior to use is time consuming and impractical. Other method exists to evaluate the effects of prediction models on clinical decisions (118). Vickers and Elkin suggested decision analysis curves to estimate the clinical utility of prediction models using the threshold probability (probability that triggers a medical intervention by a physician or patient, equating to the probability at which the harm of a false-positive intervention exceeds the harm of a false-negative non-intervention) (119). The net benefit (defined as the fraction of true-positives subtracted by the fraction of false-positives weighted by the relative harm of a false-positive and false-negative result) is calculated using the threshold probability. A decision analysis curve is generated by plotting the net benefit against the threshold probability, which can then be used to assess the net benefit of nomogram at various threshold probabilities, compared to the net benefit of decisions made under the assumption that either all or none of the patients have the outcome of interest. For example, if a physician's threshold probability of dissecting the seminal vesicle during a RP is either < 5% or >50% risk of SVI, decisions curve analysis at these threshold probabilities are irrelevant because the net benefit is the same if all or none of the patients have SVI (Figure 2-11).
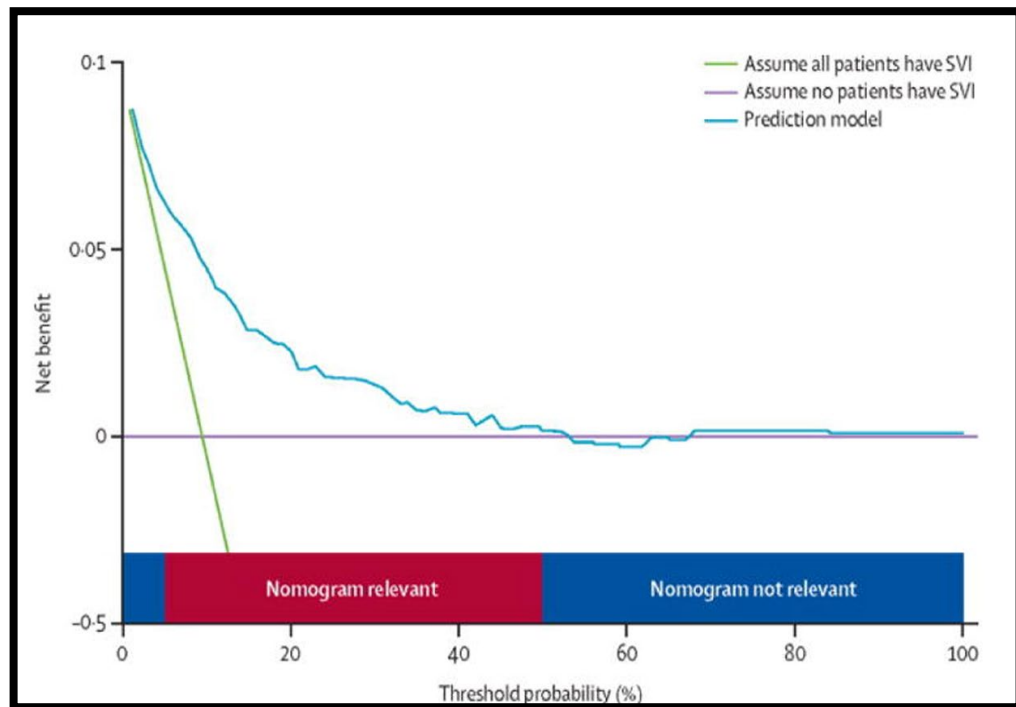
Figure 2-11 At a threshold probability of < 5%, > 50%, the nomogram is irrelevant (118).

## 2.9 Summary

The prostate gland is a conical fibromuscular pelvic organ containing three zones surrounded by extraperitoneal fat. PCa is an androgen-dependent malignancy which is the most common cancer in male patients and the second most common cause of cancer-related deaths. GS is believed to be the reference standard for PCa determination and aggressiveness. Several recent reports support the utility of pre-biopsy MP-MRI and image fusion of MRI with real-time US to address many of the limitations.

Firstly, an increase or 'upgrade' in GS in prostate cancer following biopsies remains a significant challenge to overcome. The second limitation addressed in this thesis was the development of a prediction model to identify patients who may benefit from performing SB at the time of TB in men suspected of having prostate cancer.

In the following chapters, the first part was aimed to evaluate whether pre-biopsy MRI has the potential to narrow the discrepancy of histopathological grades between biopsy and radical prostatectomy using PIRADS v2.0. Moreover, the second part was aimed to compare the diagnostic accuracy of TB, SB and combined approaches in the detection of csPCa and define predictive factors where combined approach could be used, and to quantify additional benefits of adding SB to TB methods by constructing a nomogram and assessing its net-clinical benefits.

# Chapter 3 Prediction of prostate cancer Gleason score upgrading

## 3.1 Materials and methods

### 3.1.1 Study population

This is a study with prior Caldicott institutional approval (Caldicott/IGTCAL5626). All experiments including the study protocol followed approved institutional guidelines. The study had ethical approval (14/ES/1070) with each participant providing informed consent to the use of their imaging data. Between July 2014 and January 2019, 330 men treated by LRP who were diagnosed with localised PCa with raised PSA or/and abnormal DRE were retrospectively included in this study. They were offered MP-MRI and those with positive MRI results (PIRADS score 3 and above) subsequently had a TRUS-guided prostate biopsy (12 cores). Of these patients, eight were excluded because of contraindication to MRI such as a heart pacemaker and metallic foreign body including three claustrophobic patients. Further analysis occurred with the remaining 322 patients (Figure 3-1).
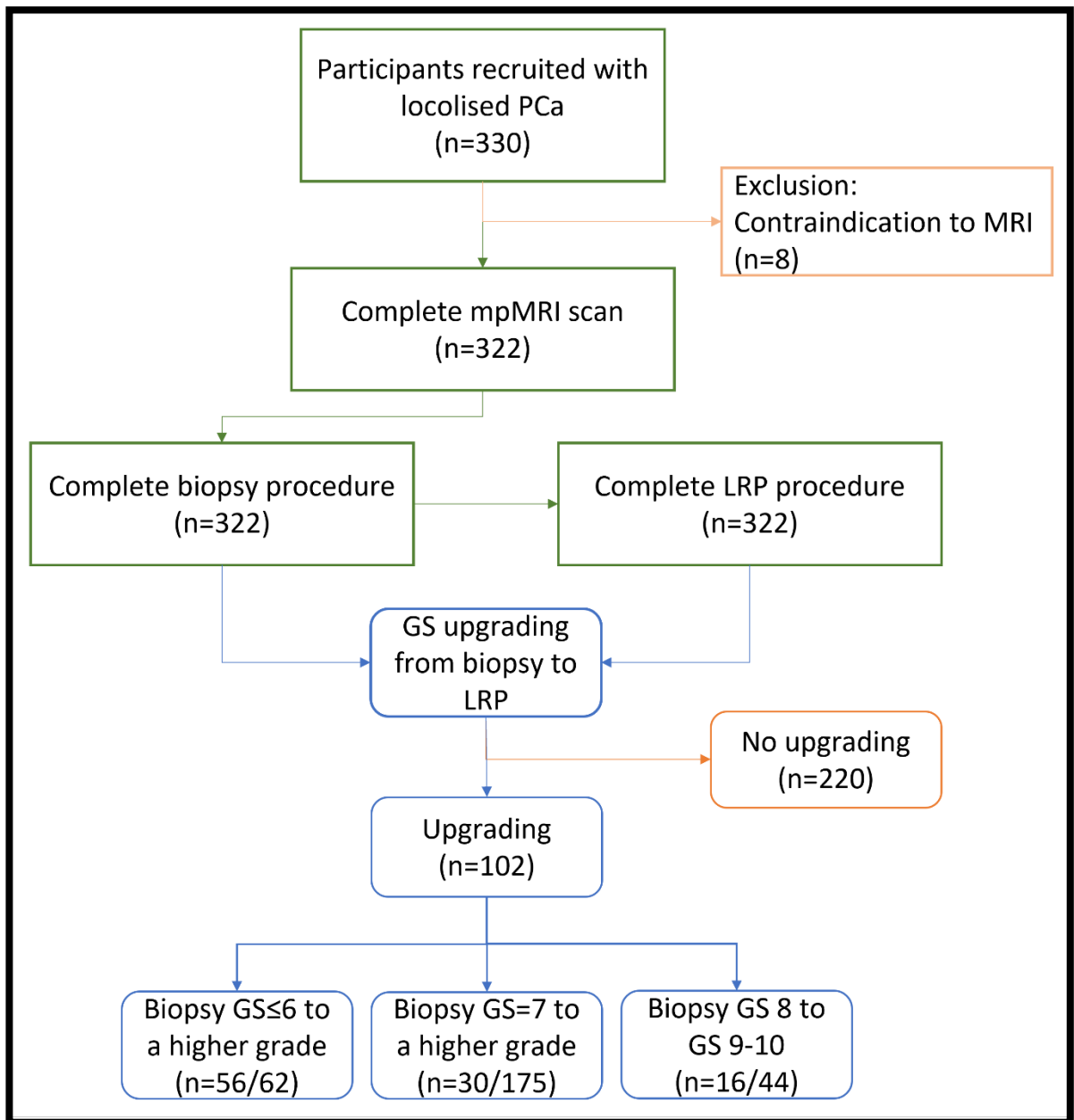
Figure 3-1 Flowchart of the study.

The clinical, pathological and imaging factors information of the patients, including age, weight, preoperative PSA, PSAD, number of positive cores, maximum percentage of cancer per core and PIRADS v2.0 score on MP-MRI were recorded. GS upgrading defined as a biopsy GS increasing from lower to higher grade on reported before (2).Table 3-1 summarises the baseline characteristics between upgraded and non-upgraded groups of the cohort.

We hypothesised that pre-biopsy MRI with PIRADS classification of a suspicious area in prostatic cancer would improve predictions of GS upgrading from biopsy to RP. Upgrading of GS on histology was defined as change of GS from lower to higher grade between biopsy and histology from RP.

|  | Total | Upgrading | No upgrading |
|---|---|---|---|
| **Number of patients** | 322 | 102 | 220 |
| **Age (y), mean ± SD (range)** | 66.83±5.9(44-77) | 66.82±6.12(49-77) | 66.85±5.9(44-77) |
| **Prostate Weight mean ± SD (range)** | 63.7±30.13(12-207) | 65.3±26.2(20-155) | 63.1±31.78(12-207) |
| **PSA level (ng/ml), mean ± SD (range)** | 11.1±7.39(0.1-47.7) | 12.6±9.98 (2-47.7) | 10.39±5.7(0.1-41) |
| **PSA Density (ng/ml$^2$), mean ± SD (range)** | 0.261±0.234 (0.001-3.48) | 0.212±0.183(0.035-1.11) | 0.203±0.254(0.00198-3.48) |
| **Number of positive cores** | 4.8±3.4(1-12) | 4.1±3.07(1-12) | 5.08±3.42(1-12) |
| **Maximum percentage of cancer per core** | 50.2±30.4(5-100) | 42.5±30.6(5-100) | 53.3±29.52(5-100) |
| **PIRADS from MP-MRI Benign (1,2)** | 17 (5%) | 4 (4%) | 13 (6%) |
| **PIRADS 3** | 21 (7%) | 6 (6%) | 15(7%) |
| **PIRADS 4** | 78 (24%) | 26 (26%) | 52 (23%) |
| **PIRADS 5** | 206 (64%) | 66 (65%) | 140 (64%) |

Table 3.1 Patient characteristics.

### 3.1.2 MRI protocol and PIRADS score

All patients' MP-MRI scans were performed on 3T scanner (TIM Trio, Siemens, Erlangen, Germany) 2 weeks before TRUS-guided biopsies. The MP-MRI protocol was derived from the European Society of Uro-radiology Guidelines 2012 for the detection of PCa and the subsequent publication of version 2 (120). Table 3-2 briefly summarises the MRI acquisition parameters. Localiser images were acquired in all three imaging planes, whereby the plane of the prostate was defined in relation to the rectal wall.

| | T1WI | High resolution T2WI | | | | DWI | | | DCE |
|---|---|---|---|---|---|---|---|---|---|
| | Axial | Sagittal | Axial | Coronal | | DWI | DWI high b-value | | Dyn Gd-MRI |
| Sequence | 2DTSE | 2DTSE | 2DTSE | 2DTSE | | 2DEPI | 2DEPI | | 3D VIBE |
| TR (ms) | 650 | 6000 | 4000 | 5000 | | 3300 | 3300 | | 4.76 |
| TE (ms) | 11 | 102 | 100 | 100 | | 95 | 95 | | 2.45 |
| Flip angle (°) | 150 | 140 | 150 | 150 | | – | – | | 10 |
| Slice thickness (mm) | 3 | 3 | 3 | 3 | | 3 | 3 | | 3 |
| Slice gap (mm) | 0.6 | 0.6 | 0.6 | 0.6 | | 0 | 0 | | 0.6 |
| Resolution (pixels) | 320 | 320 | 320 | 320 | | 192 | 192 | | 192 |
| FOV (mm) | 200 | 200 | 200 | 200 | | 280 | 280 | | 280 |
| b-values (s/mm$^2$) | – | – | – | – | | 50,100,500, 1000 | 2000 | | – |
| Temporal resolution (s) | – | – | – | – | | – | – | | 4 |

Table 3.2 MRI acquisition parameters.

The MP-MRI images were analysed and scored by experienced uro-radiologists using PIRADS v2.0; and the radiologists were blinded to all patients' pathology results (Figure 3-2).
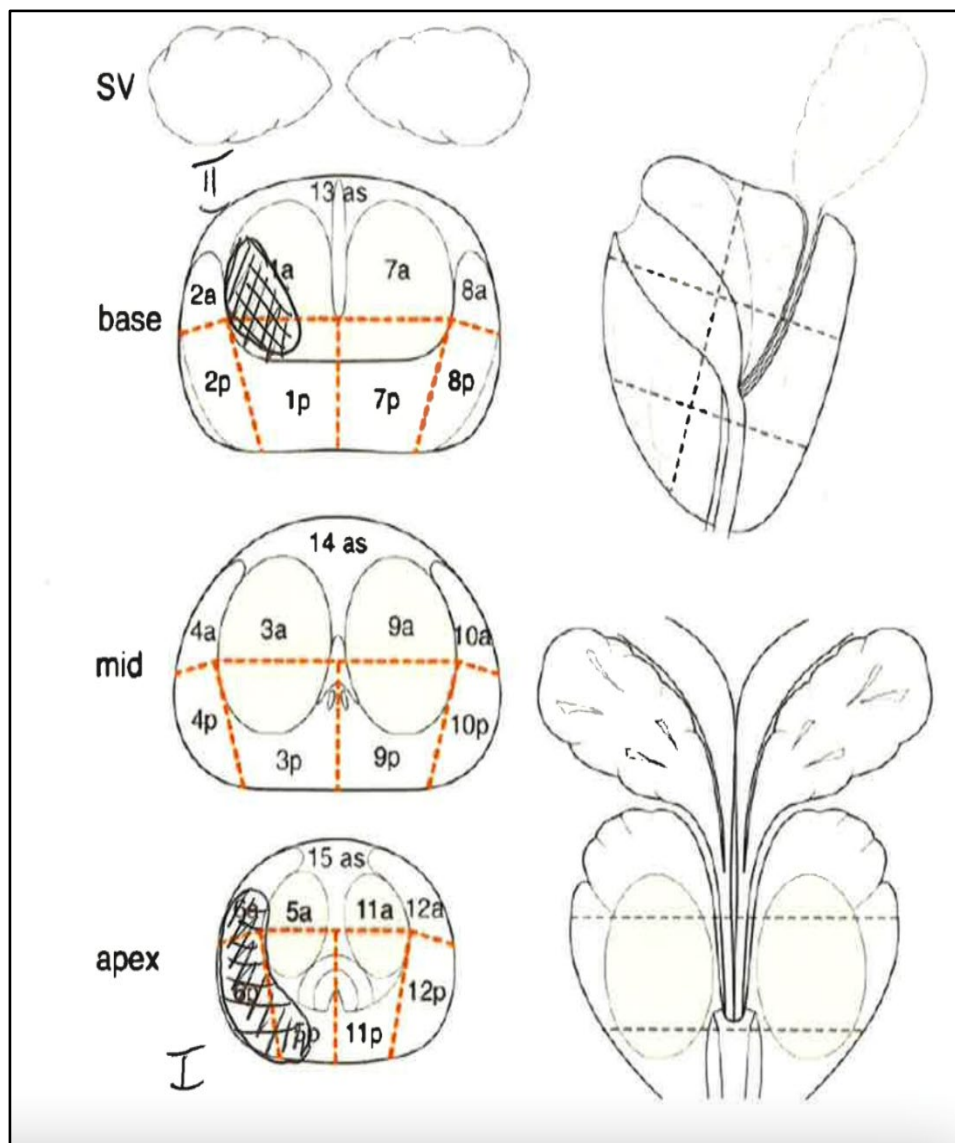


*Figure 3-2 lesions localised and graded in MRI*

PIRADS v2.0 assessment categories were described as follows: score 1, clinically significant cancer is highly unlikely to be present; score 2, clinically significant cancer is unlikely to be present; score 3, the presence of clinically significant cancer is

equivocal; score 4, clinically significant cancer is likely to be present; and score 5,

clinically significant cancer is highly likely to be present (Figure 3-3).
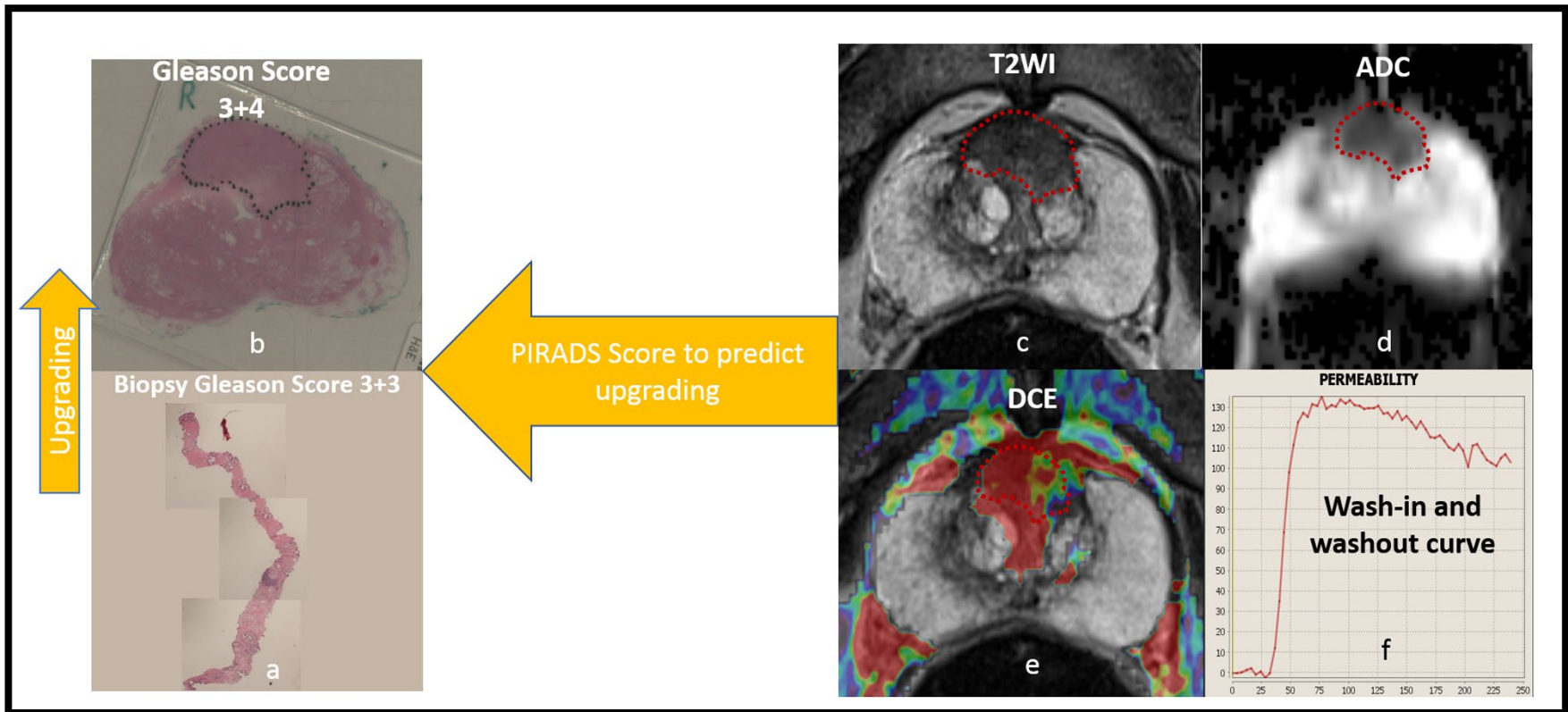
Figure 3-3 a: A 73-year-old man with GS 6 disease on prostate cancer on TRUS-Guided biopsies. b: The grade was upgrading to GS 7 on whole mount RP specimen c: Axial T2-weighted image shows ill-defined homogeneous low-signal-intensity on the CZ (d), ADC shows restricted diffusion in low-signal mass, and (e) DCE shows fast and strong enhancement and early contrast agent washout (type 3 curve) (e,f). The lesion was scored as PIRADS v2.0 5 (>1.5cm) and based on the parameters described here.

### 3.1.3 Histopathology data and analysis

The biopsy results were analysed by experienced pathologists, who were blinded to MRI findings. The GS for each patient was obtained. The radical prostate specimens for histology were sliced in patient-specific moulds to aid orientations between imaging and histology, which were fabricated using a 3D printer as described by our group and others previously (121,122). Specifically, patient specific 3D printed moulds were made prior to surgery based on the T2-weighted MRI prostate capsule the moulds were customised for each patient using MIMICS and Solidworks.

### 3.1.4  Mould design: a better standard reference

Figure 3-4 depicted the method for creating patient-specific moulds based on MR imaging and prostate sectioning during histopathology processing, but there is still a thorough discussion below.
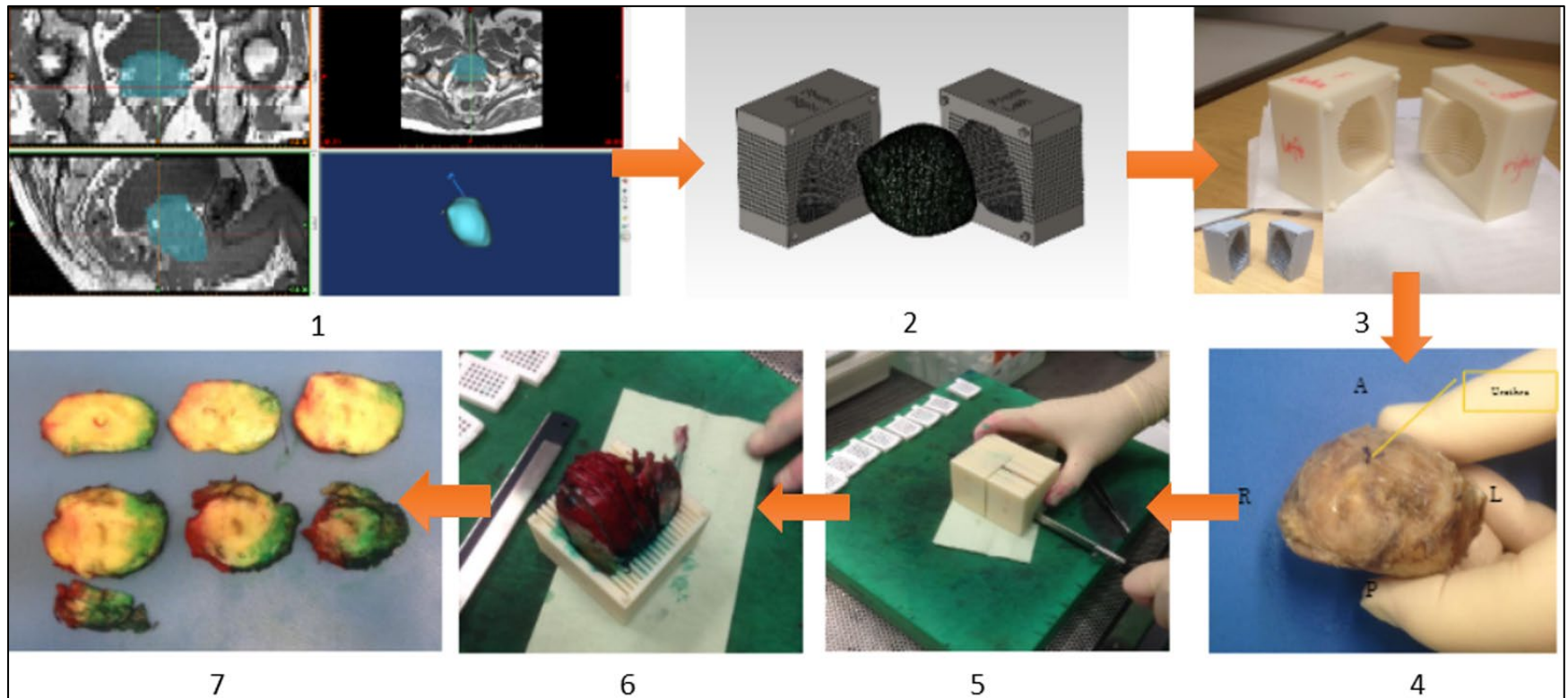
Figure 3-4 Steps of Method: (1) segmentation of MRI data in biomedical software MIMICS, (2) mould making in CAD software SolidWorks, (3) 3D printout from rapid prototyping machine Uprint, (4) post-radical prostatectomy specimen before dyeing and mould placement, (5) slicing of the prostate specimen with a single-blade, (6) final slices shown in the mould, and (7) the tissue slices are arranged from the apex to the base (123).

There are three factors to consider while creating such a mould and guaranteeing a higher pathological standard reference for prostate specimens:

1. Prostate gland segmentation in MR images: a critical step in customising each patient's prostate. The outer dimensions of the mould block had to be modified because the size of the gland differed across patients.

2. Measuring the real size of each prostate: following surgery, prostate specimens were somewhat altered, and the size measurement allowed the final design of the mould to be adjusted to match the prostate.

3. Aligning Cutting Slots: For each patient, the number of slots needs to be changed.

Participants received MRI scan. T2WI was used to produce three planar images of the prostate (axial, coronal, and sagittal). The scan resolution for the axial image was 0.63 x 0.63 mm2, and each slice was 3mm thick with a 0.6mm gap. After a thorough examination of these 2D pelvic pictures, skilled radiologists used the programme MIMICS (Medical Image Segmentation for Engineering on Anatomy) to determine the prostate capsule's borders in one direction, the prostate was segmented. There were 7-12 2D pictures in the axial direction (Figure 3-5 and Figure 3-6) that could be fused and verified to create a 3D model, saved as stereolithographic (STL) file.
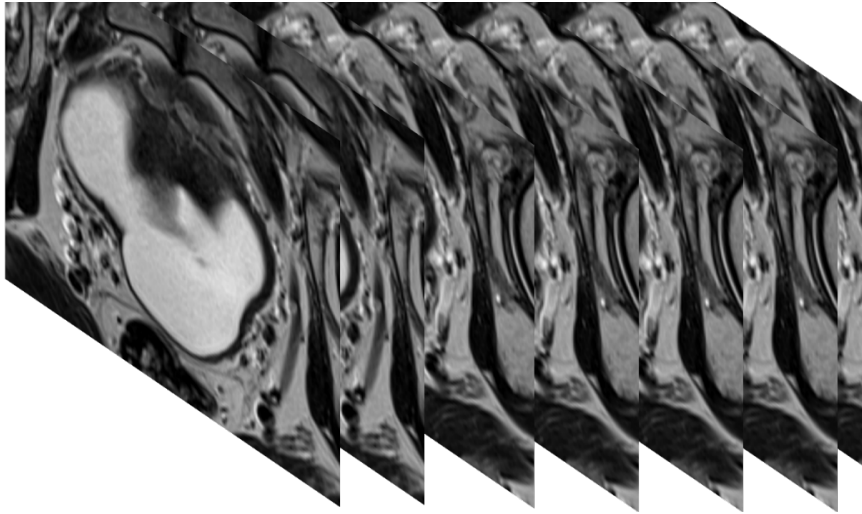
*Figure 3-5 MRI's slices for a specific patient*
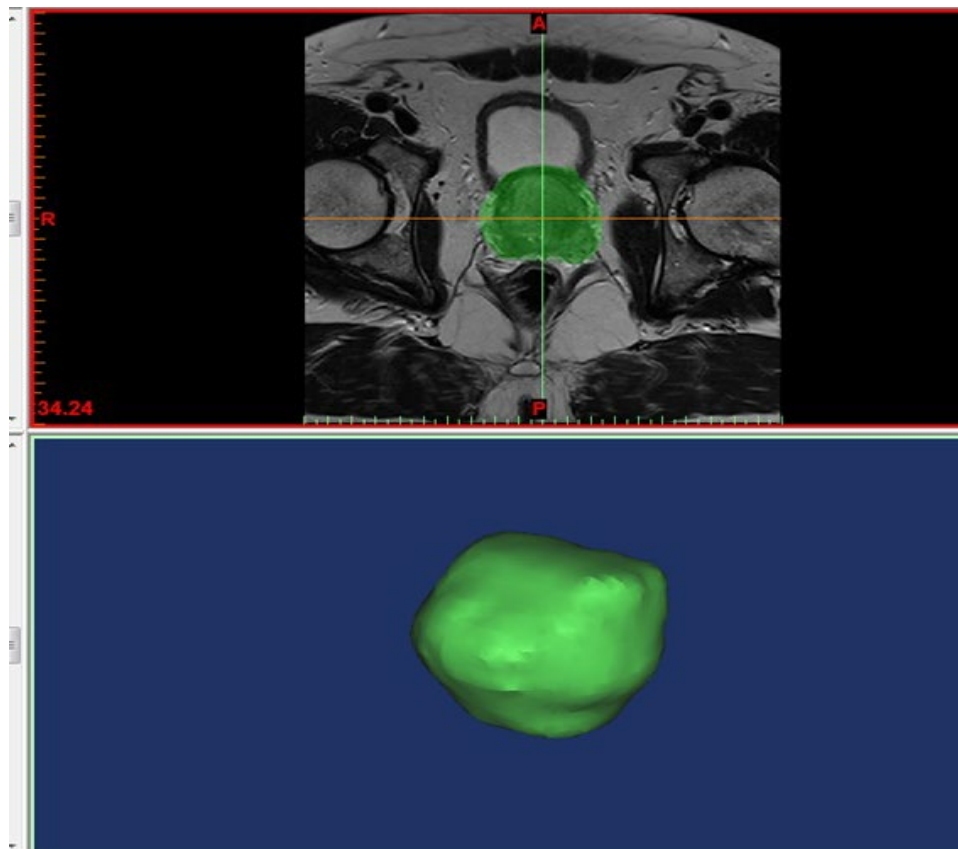


*Figure 3-6 Segmentation of the prostate (green area) of MR imaging*

One 3D model was merged and transformed into an object simulated in MIMICS software depicting the patient's prostate topography in the axial direction of segmentation and validation with the other two directions. To avoid any minor errors, the 3D prostate model was checked and then compared to the prior prostate measurement before any modifications were made. When the fused 3D model's capsule was verified, it was rough, thus smoothing was performed to the capsule's surface. The coarse model was loaded into the software of the CAD Meshmixer (2011 Autodesk, Inc.) to make the mould creation process easier by smoothing it out. To reduce file size, the smoothed model was also saved as a mesh model in STL format, which was then imported back into MIMICS for triangle reduction.

SolidWorks (3D CAD analysis software, design software, Dassault Systèmes SolidWorks Corp. USA) was used to import the triangle-reduced mesh model as a SolidWorks Part (SLDPRT) model. The mesh or the triangular surfaces of the SLDPRT model had to be regulated under a particular range for a successful conversion; otherwise, the importing process would be impacted and even collapse. After wrapping the solid simulated prostate model in a cubic or rectangular shaped block for the model and performing a "subtraction" (combine in feature) on the two models, the interior cavity that exactly housed the patient's prostate was generated in the newest model. Because patients' prostates had diverse forms and sizes, the outer dimensions of the moulds varied. After determining the prostrates positioning in the mould, slots for specimens sectioning were put in the mould in an axial direction based on 2D images from axial MR imaging. The size is 1.2 mm thick of each slot, easy to cut off with a 0.245mm thick single trimming blade (Feather Safety Razor Co., LTD. Medical Division) with a 3-6 mm spacing that reflected the thickness of each axial imaging slice. The slots can either be sagittal or coronal in orientation,

depending on the patients' prostate models fusing direction. The mould was then split into two parts (left and right) utilising feature split for prostate specimen embedding. The two distinct sections that had been modified as SLDPRT files were re-saved as STL files.

Around 200 moulds were created with the assistance of the two 3D printers over the next three years, and Figure 3-7 shows some of the 3D printed models.
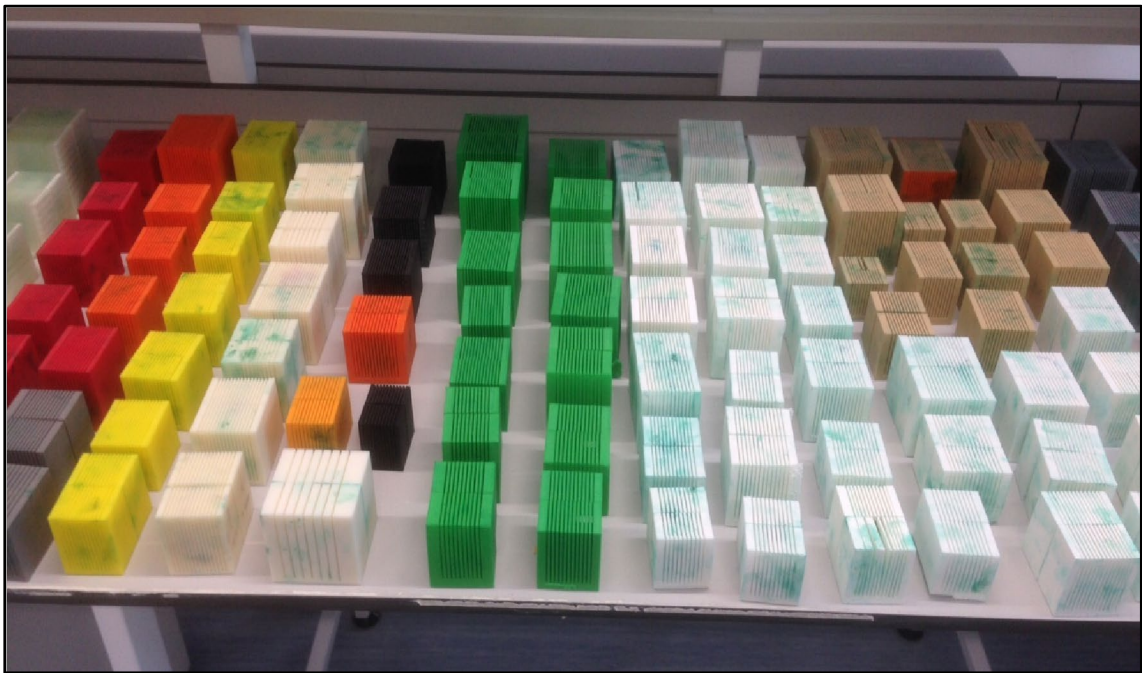


*Figure 3-7 a view of all printed moulds*

The average mould required 120 minutes to design, 4 to 7 hours to print and an expense for materials of less than $7 (121).

The collection of the prostate specimen was made from patients in the operating room and sent to the pathology lab, where it was formalin fixed at room temperature for about 48-72 hours. The specimen was painted green on the left side and red on the right side before being cut in the mould, and the seminal vesicles were removed according to the mould from the apex to the prostate base. The proper orientation had to be confirmed while inserting the prostate specimen into the mould hence the

sliced histopathological specimens that would be showing their corresponding MRI scanning slices. Prostate is cut by using a single blade during sectioning, and by applying it gently and very slowly to prevent any specimen friction or movement (Figure 3-8). All histopathological sections were taken after slicing and kept separately in tissue blocks for future analysis.
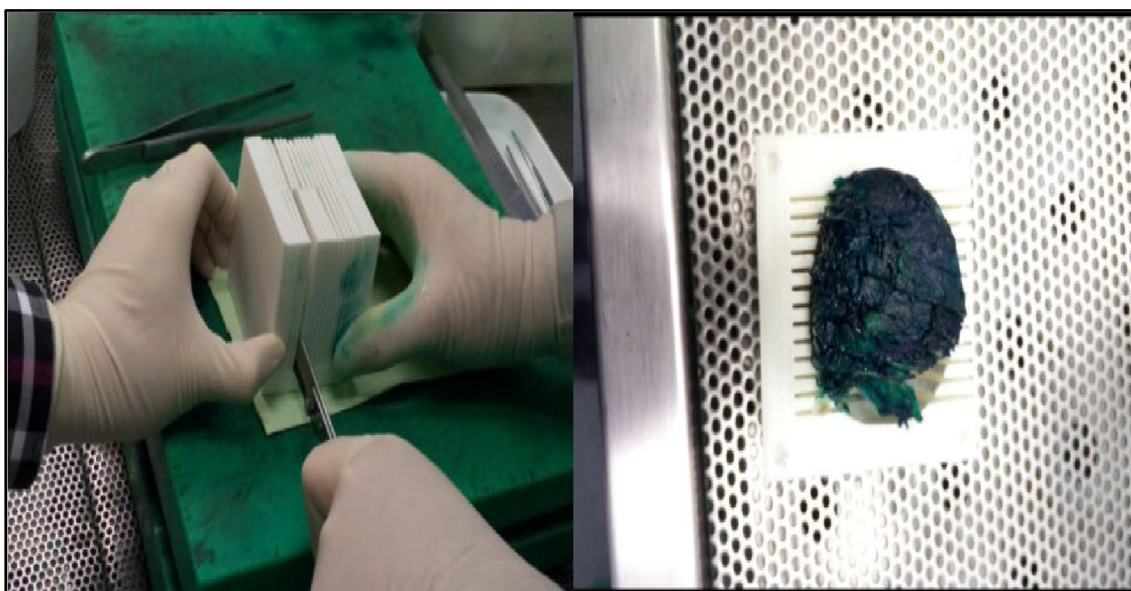


*Figure 3-8 Cutting procedures and specimens after cutting*

### 3.1.5 Statistical analysis

Baseline characteristics of patients and pathological outcomes were compared using a chi-square test for categorical data (PIRADS score) and a Student t-test or ANOVA for continuous data (age, weight, PSA level, PSAD, number of positive cores and maximum percentage of cancer per core).

Univariate logistic regression was applied to investigate the association of clinical variables with the upgrading of biopsy GS. Variables with P<0.05 in the univariate analysis were further assessed using a multivariate logistic regression analysis to identify factors predictive of GS upgrading.

The parameter in the logistic regression model is measured. Specifically, In a logistic regression model, the probability of a binary response in an event is measured using a linear combination of independent variables. The dependent variable's binary value (0 and 1) represents two outcomes, such as death/survival, pass/fail, ill/healthy.

In order to estimate the area under the curve (AUC) for predicting GS upgrading to determine the diagnostic performance of clinical variables with or without PIRADS score, a receiver operating characteristic (ROC) curve analysis was conducted.

AUC reflects the discriminable ability between negative and positive probabilities based on independent variables. The accuracy of diagnosis could be improved by selecting single or combinable variables with optimal AUC as a test of diagnostic performance.

In addition, logistic regression model coefficients were used to perform a nomogram predicating the probability of GS upgrading. Non-informative or non-significant variables in univariate logistic regression for GS upgrading were removed.

The value of concordance indexes (c-index) were calculated and compared. The c-index should be between 0.5 and 1, with 0.5 indicating that the model is unable to predict the event. In contrast, when the C index is equal to 1, predicted results are completely consistent with actual results. Normally, a C index of 0.70 to 0.90 is considered to be of high accuracy. The bias-corrected calibrated values were generated from internal validation based on 200 bootstrap resamples, which ensures the excellent performance of a nomogram while it has been used in a new cohort.

A decision-analysis curve was constructed assessing impact of nomogram using different thresholds probabilities of upgrading (none of the GS upgrade to all GS upgrade).

Analyses were performed using SPSS 22 (IBM Corporation, New York, US) and R software. The alpha level was set at 0.05 to determine two-tailed significance.

## 3.2 Result

### 3.2.1 Upgrading cohort characteristics

In total, 322 men were included in our study. Table 3-3 shows the concordance between the biopsy and prostatectomy GS sums. Of these, (102/322; 31.6%) had GS upgrading from biopsy to LRP.

Almost half of this upgrading was from biopsy GS ≤6 disease (56/102; 55%). Majority of the low-risk patients GS≤6 on biopsy were upgraded (56/62; 90%). More than half of whole cohort (175/322; 54%) had a GS 7 on prostate biopsy and (30/175; 17%) men had GS upgrading.

Finally, eighty-five of the cohort (85/322; 26%) had a GS≥8 on prostate biopsy and (16/85; 18.8%) men had GS upgrading from GS 8 on prostate biopsy to GS >8 at LRP.

| Biopsy Gleason sum | Radical prostatectomy Gleason sum | | | | |
|:---:|:---:|:---:|:---:|:---:|:---:|
| | 6 | 7 | 8 | 9-10 | Total |
| **1-5** | 0 | 3 | 0 | 1 | 4 |
| **6** | 6 | 46 | 2 | 4 | 58 |
| **7** | 0 | 145 | 14 | 16 | 175 |
| **8** | 0 | 19 | 9 | 16 | 44 |
| **9-10** | 0 | 2 | 3 | 36 | 41 |
| **Total** | 6 | 215 | 28 | 73 | 322 |

Table 3.3 Comparison between biopsy and RP GS sum.

The correlation between PIRADS score and pathologic GS at LRP is demonstrated in Figure 3-9. Of the 322 patients, the distribution of PIRADS score was as follows: score 1 and 2 in 17 (17/322; 5%) patients, score 3 in 21 (21/322; 7%) patients, score 4 in 78 (78/322; 24%) patients, and score 5 in 206 (206/322; 64%) patients.



| | Radical prostatctomy GS 6 | Radical prostatctomy GS 7 | Radical prostatctomy GS 8-10 | Totall |
|---|---|---|---|---|
| ■ PIRADS (5) | 28 | 103 | 75 | 206 |
| ■ PIRADS (4) | 21 | 43 | 14 | 78 |
| ■ PIRADS (3) | 5 | 15 | 1 | 21 |
| ■ PIRADS (1,2) | 7 | 10 | 0 | 17 |

■ PIRADS (1,2)　■ PIRADS (3)　■ PIRADS (4)　■ PIRADS (5)
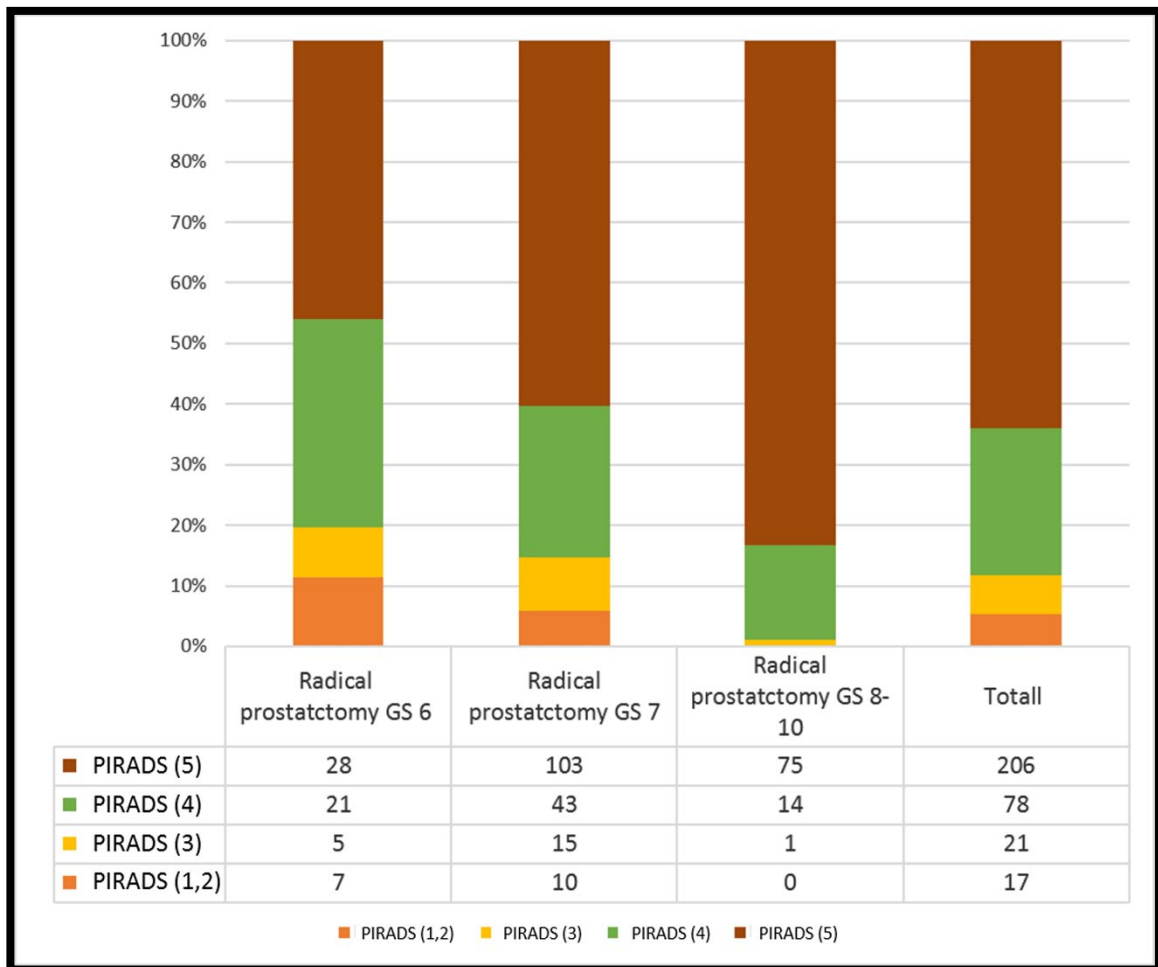
Figure 3-9 RP GS stratified according to PIRADS score.

## 3.2.2 Predicting of GS upgrading

Table 3-4 shows the outcomes of the logistic regression analysis and predictive variables of GS upgrading. On univariate analyses, increased preoperative prostate specific antigen levels, number of positive cores, maximum percentage of cancer per core and PIRADS ≥ 4 were all significantly associated with GS upgrading (p<0.05). Age, weight of prostate and PSA density did not show any significance (p>0.05) which were excluded from further analyses. In the multivariate analyses, PIRADS ≥ 4 and higher PSA level were both statistically significant and independently predictive of GS upgrading (p=0.001 and 0.003, respectively). In Figure 3-10, PIRADS v2.0 score with PSA value show a higher accuracy than PSA alone for predicting GS upgrading (AUC=0.90 and 0.64, respectively, p<0.001).

| | Univariate | | | Multivariate | |
|---|---|---|---|---|---|
| | OR (95% CI) | *P*-value | | OR (95% CI) | *P*-value |
| **Age** | 1.005 (0.962-1.041) | 0.799 | | | |
| **Pathology weight** | 1.002(0.931-1.009) | 0.540 | | | |
| **Number of positive cores** | 0.86(0.87-0.96) | 0.005 | | 0.970(0.98-1.01) | **0.69** |
| **PSA level (ng/ml)** | 1.040 (1.009-1.073) | 0.001 | | 1.09(1.030-1.160) | **0.003** |
| **PSA Density (ng/ml$^2$)** | 1.15 (0.44-3.04) | 0.76 | | | |
| **Maximum percentage of cancer per core** | 0.988 (0.980-0.96) | 0.002 | | 0.970 (0.84-1.12) | **0.62** |
| **PIRADS** **≤3** **>3** | **1 (reference)** **0.017(0.08-0.04)** | **-** **0.001** | | **1 (reference)** **0.014 (0.06-0.034)** | **-** **0.001** |

Table 3.4 Univariate and multivariate logistic regression analysis.
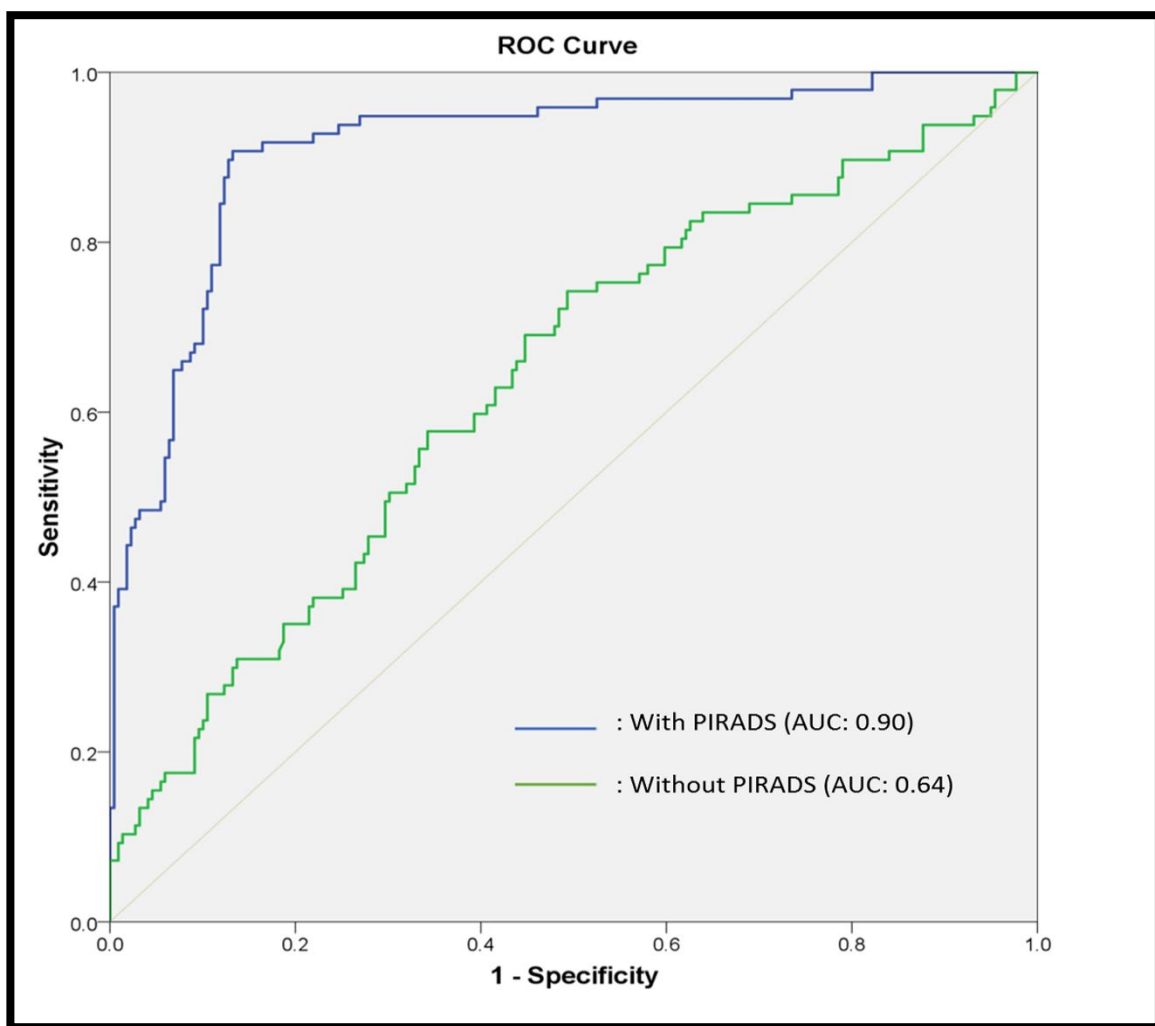
Figure 3-10 ROC curve of the clinical variables with and without PIRADS score.

### 3.2.3 Impact of PIRADS score on prediction of GS upgrading in relation to other factors

Figures 3-11 **a1** and **a2** show the nomograms constructed for upgradation of biopsy GS with and without PIRADS v2.0 score data. In the nomograms, a longer scale indicated higher percentage of impact and larger points were suggesting probability of upgrading. PIRADS score had the greatest impact followed by PSA level. The maximal point of each parameter was set at 10. The summation of the points of individual parameter could be found in the total points, and then the corresponding probability of GS upgrading was obtained. In the model including the PIRADS, the PIRADS occupied the longest bar in the nomogram, indicating PIRADS score had the greatest impact on the probability of GS upgrading, followed by PSA level, number of positive cores, maximum percentage of cancer per core. By contrast, the model without the PIRADS, PSA took up the largest points for the probability of GS upgrading. The second significant parameter was number of positive cores, with increase by about 3.5 point compared with the model including PIRADS.

C-index of the established nomogram which had PIRADS v2.0 score variable to predict the GS upgrading in the cohort was significantly higher than that of the nomogram without PIRADS score (0.90 [95% CI 0.87-0.89] vs. 0.64 [95% CI, 0.57-0.70], p=0.001). This result demonstrated that the model with PIRADS score had better performance to evaluate the predictive ability of GS upgrading.

The nomograms were then validated using 200 bootstrap samples, internal calibration curves are shown in Figures 3-11 **b1** and **b2**. The calibration plot for internal validation more intuitively reflected the predictive ability of two models. The internal calibration plot (b1) showed excellent agreement between the predictive

probabilities and actual probabilities. Compared with the model without PIRADS score (b2), left model covered additional fitting probability ranges involving below 20% and higher than 80%.
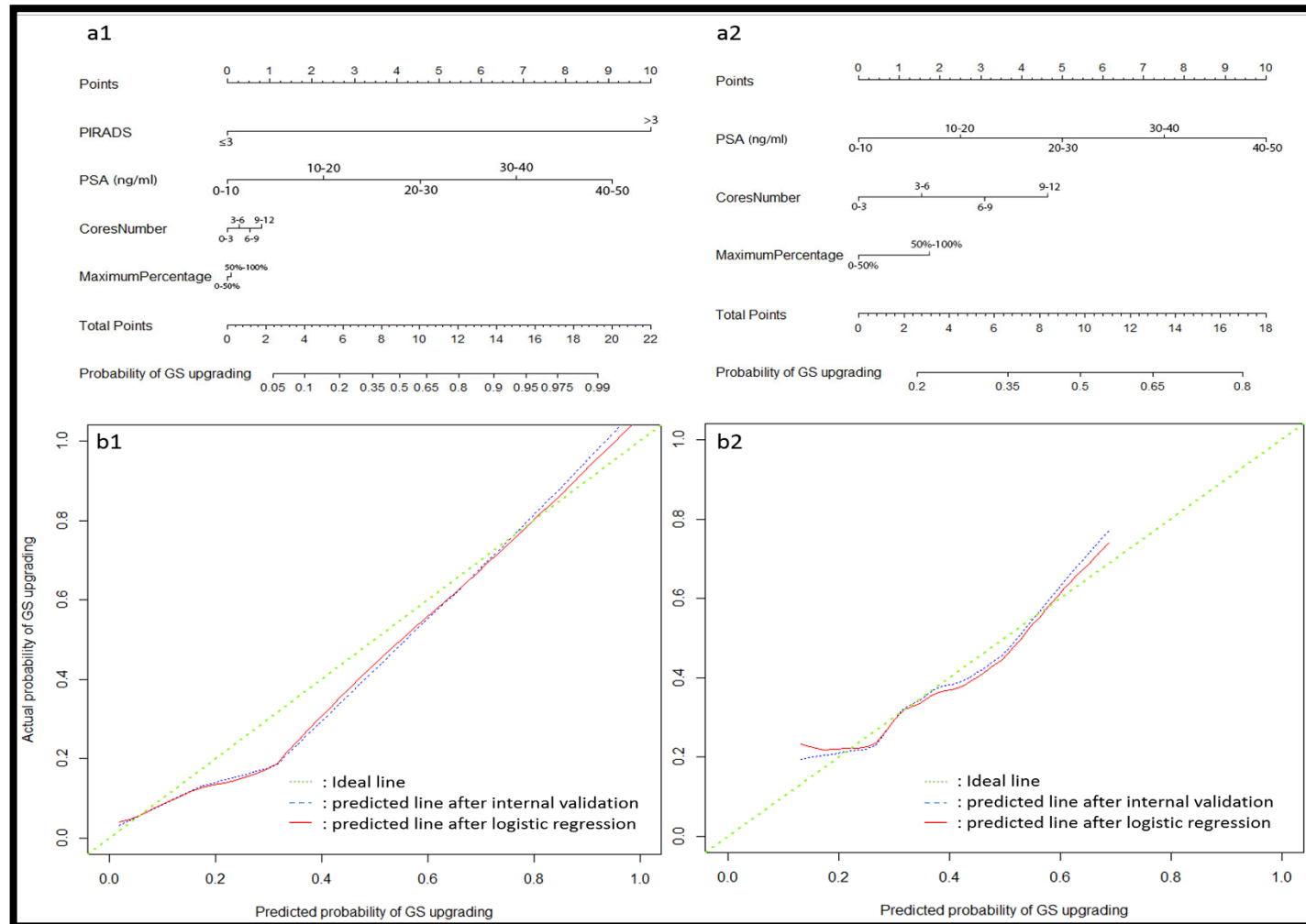
Figure 3-11 The nomograms of GS upgrading prediction with (a1) and without PIRADS score (a2). Calibration plots of observed and predicted probability of GS upgrading with (b1) and without PIRADS score (b2).

### 3.2.4 Decision curve analysis

The decision analysis curve is shown in Figure 3-12. The net benefit for the model using PIRADS score was significantly higher at all thresholds compared with the model without PIRADS score. As seen in Figure 3-12, the decision curve line (depicted by a red line) of the model without the PIRADS scores remained close to the line with threshold probabilities ranging from 0 to 0.25. In contrast, a higher positive net benefit was obtained in the range of threshold probabilities ranging from 0.05 to 1.0 in the model with PIRADS scores.

In the DCA curve, the line of the model without PIRADS score showed almost the same benefit to the line of 'intervention for all patient' from probability between 0%-20%, then dropped to about a low net benefit of around 0.01 at 40% probability of GS upgrading. However, the net benefit for the model with PIRADS was higher than 0.2 at 40% probability of GS upgrading. Even through at a high probability of > 80%, it still had net benefit.
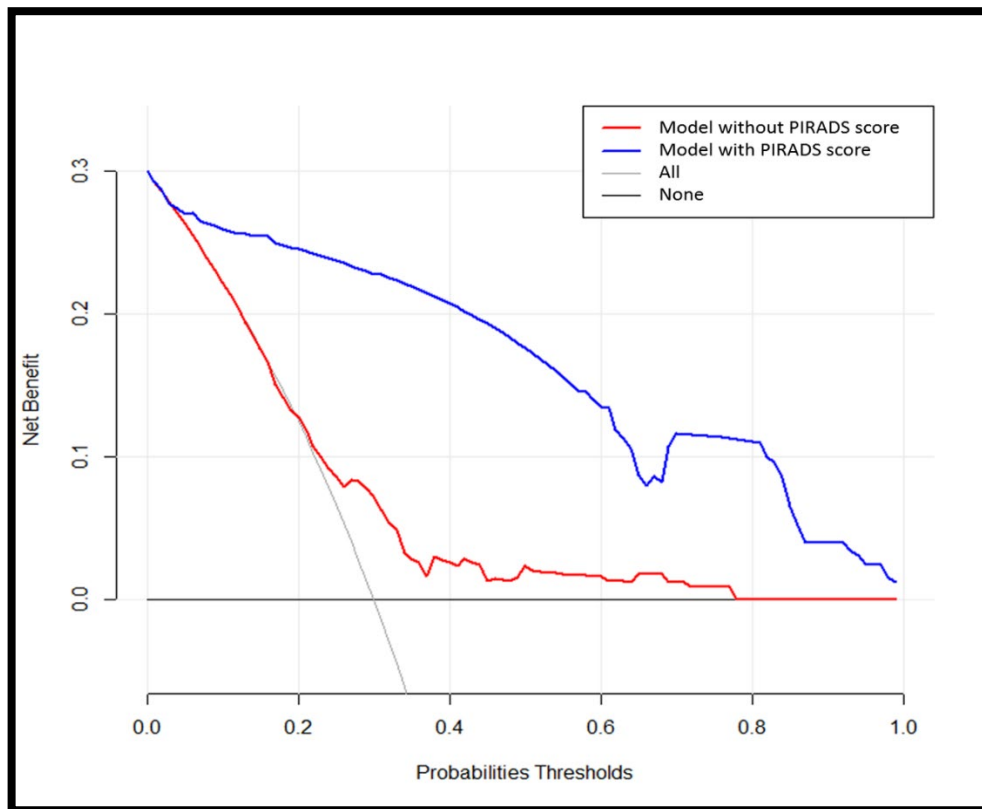
Figure 3-12 Decision analysis demonstrated a high net benefit of PIRADS score model across a wide range of threshold probabilities. Prediction model without PIRADS score (red line); prediction model with PIRADS score (blue line).

## 3.3 Discussion

This is the first study to bring together information of PIRADS scores in pre-biopsy MRI and an improved image oriented histopathological grossing of RP specimen by making the use of the mould, bridging the gap in the existing literature. As the T2 image is the best sequence for the anatomic information on MRI (123) we demonstrated that the mould can be used to accurately register histopathologic and MRI findings. Anatomical registration of preoperative MRI and prostate whole-mount obtained with 3D-printed, patient-specific, MRI-derived moulds versus conventional whole-mount sectioning was compared by Daniel et al (124). He concluded that anatomical registration of MRI and ex vivo prostate whole-mounts using MRI-derived moulds is significantly better than the conventional method (0.95/0.85 respectively) (P < 0.0001). Our results indicate a significant advantage (C-index 0.90 vs 0.64) of using the prediction model including PIRADS scores added to conventional clinic-pathological characteristics (PSA level, percentage of cancer on core-biopsies, gland size etc.) of men with PCa confirmed by systematic transrectal random biopsies relative to a model without PIRADS scores. Age has been considered an important predictor of GS upgrading in a previous study (125). However, in our study age was not associated with the upgrading of GS due to the limited sample size similar to the findings of song (9). Prostate biopsy GS upgrading remains a challenge for physicians managing localised PCa, as better knowledge of contributing factors and how to narrow the gap is lacking (2). To inform any consensus, we need an improved understanding of the role imaging can play, in particular pre-biopsy MRI, in predicting GS change and adverse downstream oncological outcomes. Although, recent improvements have been made in refining biopsy strategies and in reducing

sampling errors, a significant and continued effort is still needed to identify men at risk of GS upgrading.

Wang et al (126) reported a nomogram with C-index of 0.795 using preoperative factors without imaging data in a non-screened population from China. This is similar to our study as the healthcare system for the cohort reported here did not have men screened for PCa. Table 3-5 shows the predictive ability of various reported nomograms in upgrading of biopsy GS of PCa in screened populations (1,126–129). The upgrading rate of biopsy GS seen in our cohort is similar to a larger cohort of 2982 patients reported previously (127). A higher percentage of men with a GS of 6 were upgraded in the present study. It is interesting that despite the higher number of cores obtained in the present study (12 in number) in comparison with 6-10 biopsy cores obtained in study by Chun FK et al (127); upgrading rates remain comparable.

A number of previous studies have carried out multivariate analyses of factors responsible for upgrading of biopsy GS including construction of nomograms (Table 3-5).

| Author | year | Number of patients | Performance (C-index) | Significant parameters on multivariate analysis |
|---|---|---|---|---|
| Chun, FK | 2006 | 2982 | 0.804 | PSA level, clinical stage and primary and secondary GS |
| Kulkarni, GS | 2007 | 175 | 0.71 | PSA level and the level of pathologist expertise |
| Budäus, L | 2010 | 414 | 0.708 | PSA level, clinical stage, prostate volume and percent of positive cores |
| Wang, JY | 2014 | 220 | 0.789 | PSA level, clinical stage, and primary and secondary GS |
| Biming, He | 2016 | 411 | 0.753 | Primary and secondary GS and obesity |
| This study | 2019 | 322 | 0.90 | PSA level and PIRADS score on MP-MRI |

Table 3.5 Comparison between previous and current studies.

In predictive oncology, nomograms have huge potential to help clinicians determine the risk of disease progression and identify those who would experience a greater benefit from multimodality therapy. This approach may result in avoiding unnecessary treatment and improve quality of life by reducing side effects of therapy through better and more precise approach. However, a careful approach is needed to construct nomogram based on specific question, the study population, the method of construction, and its ability to apply to a particular clinical situation. We have followed guidelines described in previous publications (118,130,131) in constructing nomogram in this study including selection of variables and statistical methods. The nomogram in the present study has been internally validated (Cross-validation and bootstrapping).

External validation of nomogram was not carried out in the present study as this would require further prospective multi-centre recruitment of a cohort. Since D'Amico pioneered this approach (132), none of the reported predictive nomograms have included imaging features of the disease. Furthermore, the advantage of our nomogram is a higher overall accuracy (discriminant properties) and closer agreement between predicted and observed values (superior calibration). Estimating clinical utility of nomograms in prognosticating an outcome of intervention remains core value of translational research in precision medicine. Vickers and Elkin (119) have introduced decision analysis curves estimating probabilities of benefits and harms that a diagnostic test or intervention can trigger at various thresholds. Addition of PIRADS score to nomogram achieved a higher net benefit of decisions making in comparison to leaving out PIRADS score as shown in the decision analysis curve constructed in the present study. The thresholds ranged from no upgrading of disease to all men having upgrading of disease following LRP.

Predicting final histopathological GS of PCa remains a highly desirable information for physicians counselling men with localised PCa for various modalities of treatment and long-term disease recurrence. At present, various nomograms are used mainly taking into consideration clinical factors such as age, pre-operative PSA level and number of biopsy cores involved with the cancer. Notwithstanding this, there is still a large histopathological discrepancy between biopsy and final RP GS. The present study reports a nomogram based on pre-biopsy MP-MRI grade (PIRADS score) of cancer along with other known clinical parameters. The nomogram clearly showed an improved prediction of final GS and the findings have a large implication for clinicians and researchers in this area. The majority of low-risk patients were upgraded to a higher risk in this study. Low-risk patients with an elevated PSA or those for whom expert pathological review is not possible may benefit from a repeat biopsy, as evidence suggests that additional biopsy cores improve GS accuracy for patients opting for AS (128). We envisage that this and further research should take us close to precise prediction of final GS of histopathology in PCa and thereby an improved and informed decision making by stakeholders including patients in the management of localised PCa.  This will have huge benefits for improved GS prediction for men opting for AS and focal therapy besides those opting for radical prostatectomy.

There are limitations to this study. The study was conducted retrospectively at a single centre with dedicated uro-radiologist and pathologist, and the rate of upgrading may be different in small centres. Moreover, overall accuracy of our model, although higher than previous was not perfect (90%). Additionally, performance of our model needs further validation in an external data set. PIRADS v2.0 is a step forward in simplifying the initial standardisation efforts made in PIRADS

v1, but it will undoubtedly require more changes as research progresses, experience grows, technology advances and this may impact the external validation of the present nomogram. Although, there may be inter-reader variability between the readers of MRI however, Greer et al (133) in a multi-reader study (showed high sensitivity and agreement (>90%) between prostate specialists for PIRADS v2.0. Finally, the accuracy of our model could still be improved by integrating additional predictor variables, such as the novel genomic and other biomarkers (134,135). The growing field of artificial intelligence and machine learning using radiomics approach may improve our ability to define tumour characteristics and classification. This undoubtedly may impact results of the study in the future. Finally, with emerging evidence supporting MRI facilitated biopsy targeting of suspicious areas using ultrasound, the rate of upgrading and the future implications for the practice may change (136). There is an emerging evidence that TB may improve our ability to narrow the upgrading gap between the biopsies and RP histology(137,138); however no predictive nomogram information was available from both the studies. Our ongoing work through randomised intervention in MR/US fusion should be able to provide more information (139)

# Chapter 4 Predicting the performance of concurrent SB during TB sampling of MP-MRI

## 4.1 Materials and methods

### 4.1.1 Study population and power calculation

The study had ethical approval (14/ES/1070) and all participants provided informed consent for their imaging data to be used. The study also had Caldicott institutional approval (Caldicott/IGTCAL6358) to link data with electronic systems wherever needed for follow-up outcomes. The study period was between April 2015 and March 2020.

The inclusion criteria were age between 40 to 76; abnormal DRE; PSA≤ 20 ng/ml; and MRI <T3 disease. Exclusion criteria were repeat biopsies; prior radiotherapy to prostate; and diagnosis of acute prostatitis with 12 months or history of PCa. All participants had pre-biopsy MP-MRI and only MRI positive (PIRADS≥3) were recruited into the study (n=198). Of these patients, 78/198 (39%) underwent radical prostatectomy. Patients then underwent prostate biopsy by MR/US fusion technique (Hitachi HI-RVS; Europe Holding, Steinhausen, Switzerland) by operator 1. This was followed by a standard 12-core TRUS biopsy by a second operator (blinded to the MRI results).

In considering performing a McNemar matched test, a minimum sample size of 110 men undergoing both SB and TB prostate biopsy methods would be required to yield 90% power with a significance level of 0.05 (α = .05) which would also allow 20% of dropout rate. csPCa detection rate via Sb and TB were found in previous study (140). Therefore, we recruited more patients than the minimum required number from the sample estimation to ensure achievement of study power and significance level.

## 4.1.2 MRI techniques

Two weeks before TRUS-guided biopsies, all patients had MP-MRI scans on a 3T scanner (TIM Trio, Siemens, Erlangen, Germany). The MP-MRI procedure was adapted from version 2 of the European Society of Uro-radiology Guidelines for the detection of prostate cancer, which were published in 2012. Phased-array coil was placed around the pelvis's patient while was lying on his back. A gadolinium contrast agent (Dotarem, Guerbet, France) was inserted to acquire DCE sequence with dose equal to 2 mlkg-1 of Dotarem. The scan took approximately an hour to include the following anatomical and functional sequences:

- High-resolution T2 spin echo (SE) pulse sequence, acquired in the sagittal, axial and coronal oblique planes.

- T1 SE pulse sequence of the pelvis acquired in the axial oblique plane.

- T1 SE axial sequence of abdomen and pelvis.

- T2 3D SPACE sequence for fusion biopsy planning.

- T2W fast spin echo sequence of abdomen and pelvis in coronal plane.

- DWI.

- DCE.

The MP-MRI images were analysed and scored by experienced uro-radiologists using PIRADS v2.0; and the radiologists were blinded to all patients' pathology results.

## 4.1.3 Biopsy procedures and histopathological analysis

Data from an MRI scan was obtained two weeks prior to the biopsy. MRI images were loaded into the HI-RVS software (Hitachi-Real-time Virtual Sonography) via a USB device. Prior to the MRI/US fusion biopsy, the prostate MRI was used as a map to target prostate lesions, register three points (the apex, base, and posterior of the prostate) and create a 3D-reconstruction of the prostate (Figure 4-1).
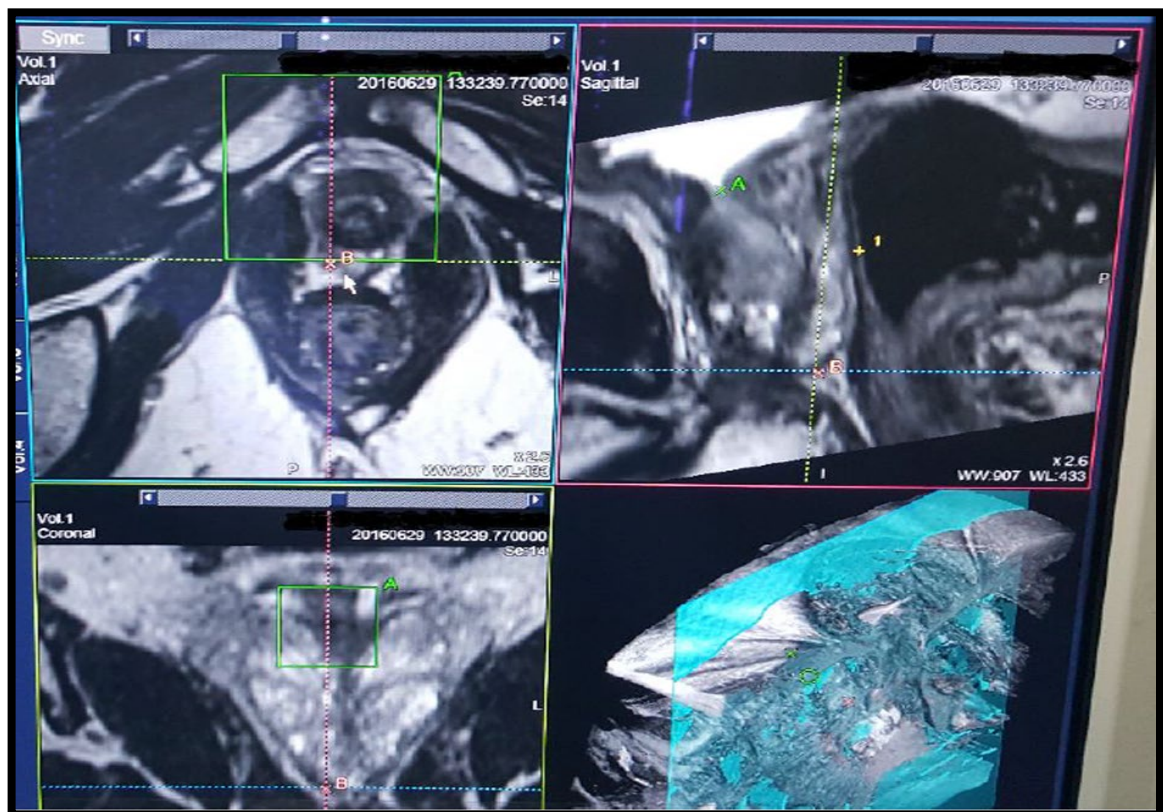


Figure 4-1 An MRI of the prostate taken before the biopsy is used as a map.

The patient was then placed on the table in left lateral decubitus so that an NHS-accredited, well-trained radiologist and/or urologist could perform an MRI/US fusion biopsy. While under local anaesthetic (Lidocaine, Hydrochloride injection 1%) diluted with normal saline, the operator inserted the endo-cavity (trans-rectal) biplane transducers (EUP-CC531) with a frequency between (8.0-4.0) MHz to perform the biopsy. The transducer was joined to a biopsy gun (BARD, 22mm penetration length,

18 gauge) to obtain the biopsy cores, and Electro-Magnetic (EM) sensors (EZU-RV2S) **(**Figure 4-2**)** were affixed to EM field generator stand. These were put close to the patient to transmit the signal to the sensor, allowing for more precise target location.



*Figure 4-2 EMS with a trans-rectal ultrasound transducer*

The fusion device's screen was divided into two screens: the left screen with a pre-biopsy MR image; and the right screen with real-time ultrasound to fuse and align the targeted lesion on the MRI. These would be aligned and fused with the US which would be used to guide the biopsy needle to the region of interest (ROI) in the MRI where the targeted lesion was located (Figure 4-3).
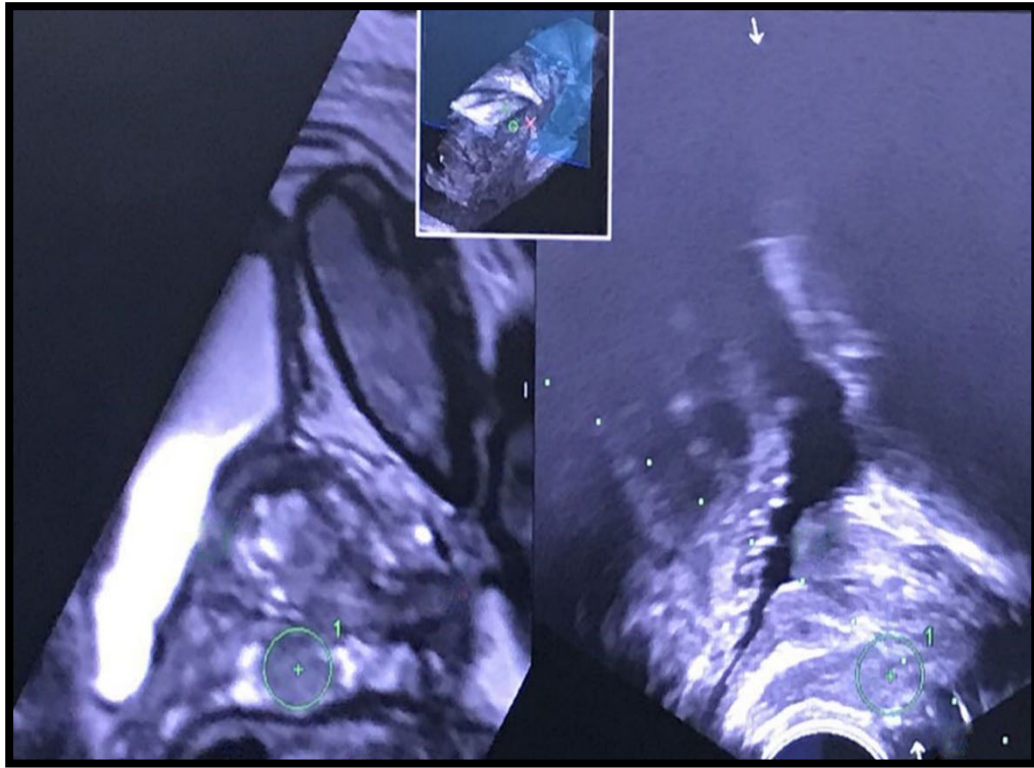
Figure 4-3 (A) The left window displays an MRI of the prostate, and (B) the right side window (US window) and the green circled region shows the index lesion where the biopsy can be taken from.

Three cores of tissue were obtained in the fusion TB approach from previously identified MP-MRI lesions using superimposed T2-weighted sequence on the real-time TRUS image.

On the exact same day as the MRI/US fusion biopsy, the systematic random 12-core biopsies (Figure 4-4) were performed by an experienced urologist or specialist nurse following targeting.
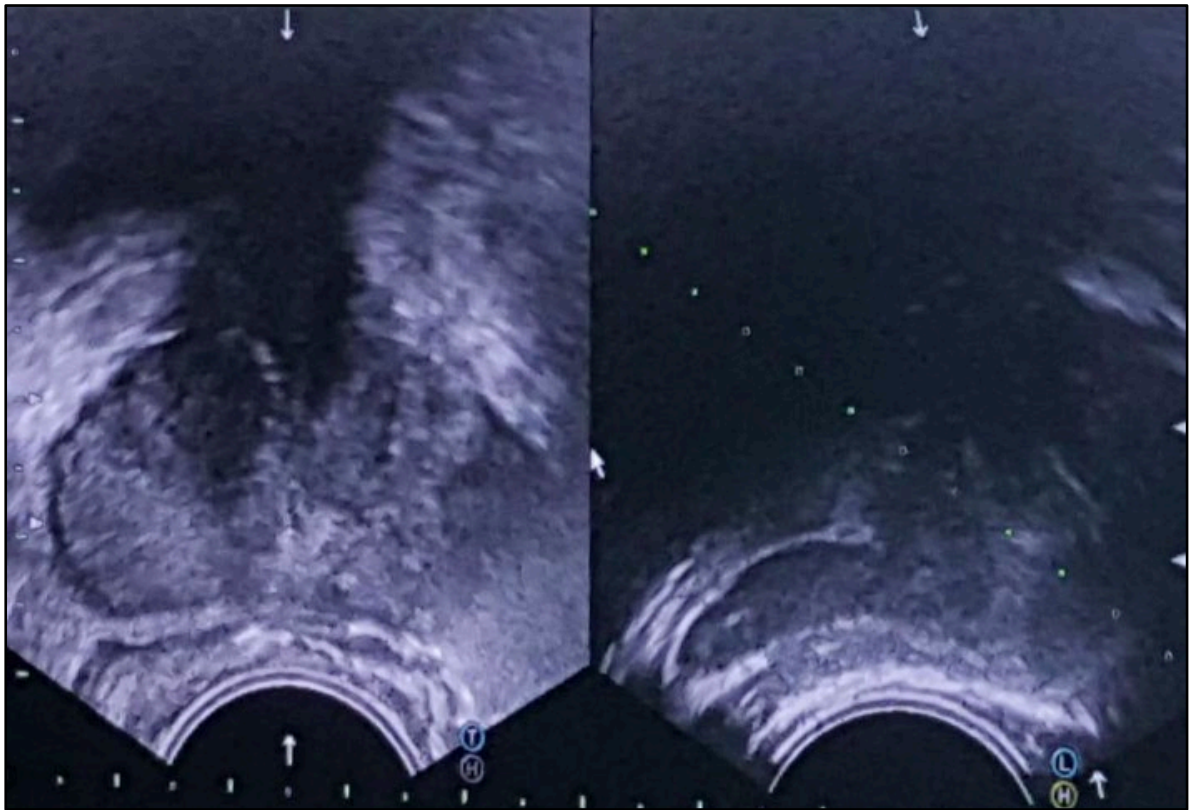
*Figure 4-4 TRUS guided prostate biopsy*

The SB was typically the 12 cores approach, collected in an extended sextant template of biopsies from the lateral and medial aspects of the base, mid, and apical prostate on the left and right sides

The twelve core locations are:

1. Right upper lateral

2. Right base

3. Right mid lateral

4. Right para-midline

5. Right lower lateral

6. Right apex

7. Left upper lateral

8. Left base

9. Left mid lateral

10. Left para-midline

11. Left lower lateral

12. Left apex

The pathologist identified all the cores and recorded their Gleason score (Table 4-1).

| | Core Location | Score | % Involved |
|---|---|---|---|
| 1 | Right upper lateral | 4+4 | 40 |
| 2 | Right base | 5+4 | 100 |
| 3 | Right mid lateral | 4+5 | 100 |
| 4 | Right Para midline | 4+5 | 100 |
| 5 | Right lower lateral | 4+5 | 100 |
| 6 | Right apex | 4+5 | 100 |
| 7 | Left base | 4+3 | 20 |
| 8 | Left upper lateral | 4+3 | 80 |
| 9 | Left para midline | 4+3 | 100 |
| 10 | Left para midline | 4+3 | 100 |
| 11 | Left lower lateral | 4+3 | 100 |
| 12 | Left apex | 4+3 | 50 |

Table 4.1 SB report for all the 12 cores

The biopsy results were analysed by experienced uro-pathologists (blinded to the MRI findings). The GS for each patient was obtained.

A subset of cohort (n=78) underwent RP and prostate glands were assessed by mould-based histopathological orientation as described in our previous study (121,122). A genitourinary pathologist with 10 years of experience independently reviewed step-section histologic slides of the prostatectomy specimen for each case. This pathologist was unaware of the MRI and biopsy findings. The pathologist identified all the lesions for each case and recorded their Gleason score (Figure 4-

5) summarises the study protocol in brief. This was used as a reference standard to assess the diagnostic accuracy of both SB and TB in detecting csPCa.
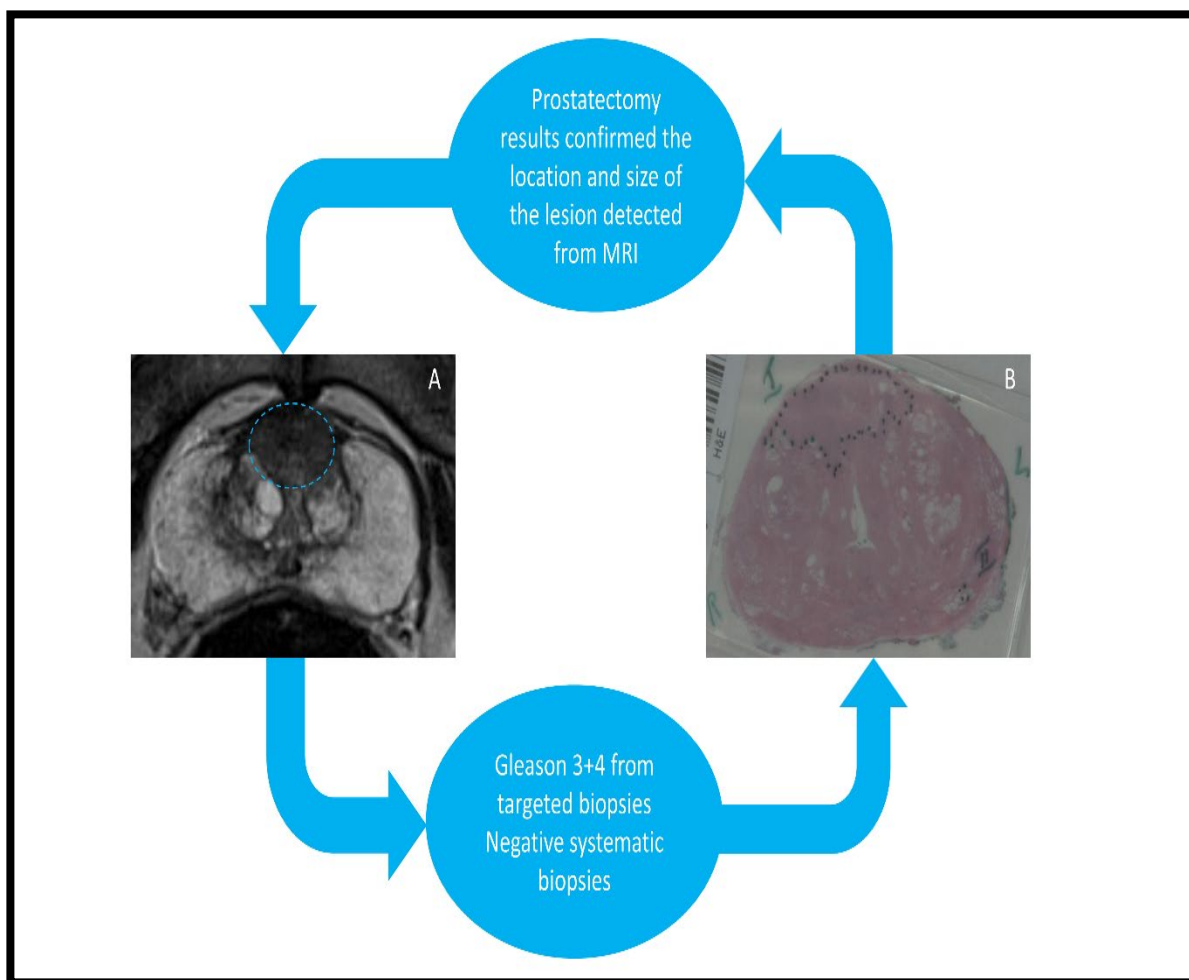


*Figure 4-5 A: A 76 years old patient with a PIRADS 5 lesion detected from 3T MRI in anterior zone with a high PSA and abnormal DRE. B: Patient-specific 3D Mould based grossing of radical prostatectomy slice shows a 3+4 GS cancer located in the anterior zone*

## 4.1.4 Outcomes

Primary outcome of the study was to compare the detection rate of clinically significant PCa using both SB and TB approaches alone and in combination. This was assessed both at biopsy and RP stages. Significant PCa was defined as the presence of PCa with GS ≥3+4 (International Society for Urological Pathology [ISUP]

grade 2 or more). The secondary outcome was to asses net clinical benefit of the approaches using nomogram and decision-analysis methods.

## 4.1.5 Statistical analysis

Patient's age (in years), PSA, prostate volume (ml), and PSAD were collected. PSAD was calculated using PSA divided by the MRI-derived prostate volume (ellipsoid method). Number of lesions, index lesion size (mm), PIRADS category, and lesion location were measured by MP-MRI. Each lesion was counted only once. Index lesion size was the size of lesion with the highest PIRADS score. Continuous data were first tested to see if they were normally distributed by the Kolmogorov-Smirnov Test of Normality. The mean (m) and standard deviation (SD) were described if the variable followed a normal distribution. The median (M) and interquartile range (IQR) were presented if the variable was not normally distributed. Categorical variables were reported as frequencies and proportions. Cross tabulation was carried out in order to compare the proportions of significant PCa patients by SB, TB, and combined SB+TB.

The McNemar chi-square test was conducted in patients who were given both diagnostic tests. McNemar chi-square, degree of freedom (df) and P-value were calculated and presented. A two-step Logistic regression was performed to identify explanatory variables of significant PCa. First, the patient's age, PSAD, lesion size, PIRADS and number of lesions were individually put into a univariate logistic regression model where the outcome was defined as having significant PCa or not. Statistically significant variables were then put into the multivariate logistic regression model. Odds ratio (OR), 95% confidence interval (95% CI) of OR, and P values were recorded.

A nomogram was created based on the statistically significant variables in the final model. The discriminative ability of the predictive model was tested by ROC curve and the concordance statistic (c-statistic) was presented. The predicted probabilities of significant PCa were plotted against observed probabilities to test the calibration of the model. Decision curve analysis was applied to determine the benefit of the nomogram.

In the subgroup analysis, prostatectomy was performed in a group of 78 patients (112 lesions). The detection rate of true significant PCa lesions via SB, TB and combined SB+TB was compared using the McNemar chi-square test. Statistical analyses were conducted by SPSS V23.0 and R V4.0.3. The Bonferroni adjustment, which adjusted P value by times of tests, was used accounting for multiple testing. The alpha level (adjusted P- value) was set at 0.05/times of tests to determine two-tailed significance for the McNemar chi-square test.

## 4.2 Result

### 4.2.1 Patient's characteristics

The participating patients' demographic data are shown in Table 4-2. A total of 198 patients who underwent both SB and fusion TB in the same setting were recruited into the study.

Several clinical variables included baseline information (age, PSA level (ng/ml), PSAD (ng/ml2), and prostate volume (ml)) and MP-MRI features (number of lesions seen on MRI, index lesion size (mm), PIRADS score 3,4,5 and lesion location transition zone (TZ), PZ, and both zones (TZ+PZ).

| | Variables | Overall (n=198) |
|---|---|---|
| **Basic information** | Age, median (IQR), in years | 67 (71-61) |
| | Prostate specific antigen (PSA), median (IQR), ng/ml | 8.2 (10.6-6.4) |
| | Prostate volume, median (IQR), ml | 47 (63-33) |
| | PSA Density, median (IQR), ng/ml$^2$ | 0.18(0.27-0.11) |
| **MP-MRI** | Number of lesions, n (%) | |
| | 1 | 102 (51.5%) |
| | 2 | 75 (38%) |
| | 3 | 14 (7%) |
| | 4 | 6 (3%) |
| | 5 | 1 (0.5%) |
| | Index lesion size, median (IQR), mm | 16 (25-13) |
| | Prostate Imaging Reporting and Data System (PIRADS score), n (%) | |
| | PIRADS 3 | 22 (11%) |
| | PIRADS 4 | 55 (28%) |
| | PIRADS 5 | 121(61%) |
| | Lesion location, n (%) | |
| | Peripheral zone (PZ) | 79 (40%) |
| | Transition zone (TZ) | 44 (22%) |
| | Both zones (TZ-PZ) | 75 (38%) |
| **Targeted (TB)/Systematic random (SB) biopsy** | Detection of prostate cancer (PCa) in TB, n (%) | 129 (65%) |
| | Detection of prostate cancer (PCa) in SB, n (%) | 127 (64%) |

Table 4.2 Descriptive characteristics of 198 patients who underwent MP-MRI of the prostate and subsequent systematic random and TB at our centre.

## 4.2.2 Comparison of the detection rate of significant prostate cancer between SB, TB and combined approaches

The detection rate of csPCa using random biopsy was 51.0% (101/198) and using TB was 56.1% (111/198). This was not statistically significant (the McNemar chi-square test was $\chi^2=2.273$, df= 1, P=0.132, OR=0.63 (95% CI, 0.34 to 1.16). There were 17 patients (17/198; 8.5%) where the TB approach alone missed clinically significant cancers (8 from the same site and 9 from normal looking prostate on MRI (Figure 4-6).
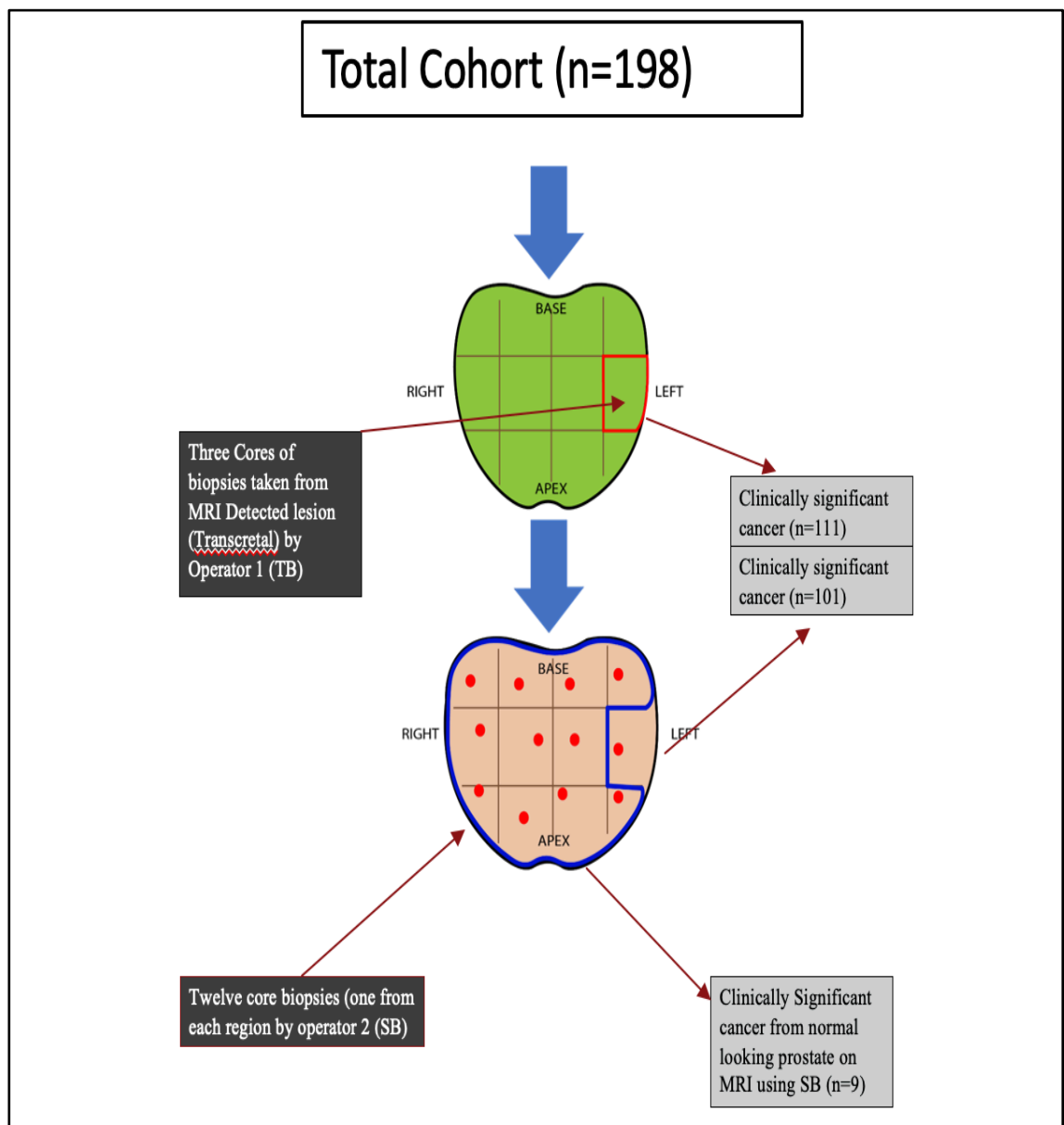


Figure 4-6 The detection rate of significant prostate cancer between SB, TB based on patients' level.

There were 84 patients (84/198;42.4%) where the positive cores on systematic sampling and TB detected csPCa (72 from the same sector of index lesion and 12 from different sectors away from index lesion). When the TB is negative (69/198; 34.8%), the SB detected clinically insignificant cancer in 12 patients (12/69; 17.3%) and detected csPCa in 8 patients (8/69;11.6%). Twenty-seven (27/198; 13.6%) men were upgraded to csPCa based on TB while 17 patients (17/198; 8.5%) were upgraded based on SB ($\chi2$=2.27, P=0.13).

The detection rate of significant PCa was higher using combined biopsy (64.6%; 128/198) in comparison to TB (56.1%; 111/198). The McNemar chi-square test result with Yates correction was statistically significant ($\chi2$=15.06, df= 1, P<0.001). There was an 8.5% increase in significant PCa detection rate at the patient level using combined biopsy methods compared to using TB alone. The results are shown in Table 4-3.

| Systematic random Biopsy (SB) | | Fusion Targeted biopsy (TB) | | | | |
|---|---|---|---|---|---|---|
| | | No Cancer | Low-Risk Cancer | Intermediate-Risk Cancer | High-Risk Cancer | Total |
| | | | Gleason 3+3 | Gleason 3+4 | Gleason > 3+4 | |
| No Cancer | | 49 | 3 | 9 | 10 | 71 |
| Low-Risk Cancer | Gleason 3+3 | 12 | 6 | 6 | 2 | 26 |
| Intermediate-Risk Cancer | Gleason 3+4 | 4 | 8 | 15 | 6 | 33 |
| High-Risk Cancer | Gleason > 3+4 | 4 | 1 | 18 | 45 | 68 |
| Total | | 69 | 18 | 48 | 63 | 198 |

Table 4.3 Biopsy findings per patient of SB compared with TB for the total cohort of 198 men. Orange shading indicates men in whom SB upgraded the prostate cancer risk category in relation to TB. Blue shading indicates men in whom TB upgraded prostate cancer risk.

We further validated the findings using a subset of cohort where the histopathology of RP was used as a reference standard. There were 170 clinically significant cancers (170/190; 89.4%) seen on RP histopathology using mould-based approach and counting each focus of cancer. 112 were targeted using the MRI/US image fusion method. The TB approach detected 70 of these (70/112; 62.5%), whereas the SB approach detected 54 (54/112; 48.2%). The difference was statistically significant (the McNemar chi-square test result was $\chi2=6.618$, df= 1, P=0.010, OR=0.36 (95% CI, 0.17 to 0.77). The combined approach to 112 lesions detected more cancers than SB or TB alone (79/112; 70.5%). Compared to SB, the combined approach detected 22.3% more cancers (70.5% vs 48.2%). The McNemar chi-square test result with Yates correction was statistically significant ($\chi2=23.04$, df= 1, P<0.001). Similarly, the combined approach detected 8% more cancers in comparison to TB (70.5% vs. 62.5%). The McNemar chi-square test result with Yates correction was statistically significant ( $\chi2=7.111$, df= 1, P=0.008.).

Interestingly, there were 11 cancers (11/190; 5.8 %) which were labelled as clinically insignificant and all were upgraded to clinically significant using the TB approach. In comparison, there were 24 (24/190; 12.6%) cancers labelled as clinically insignificant and 20 (20/190; 10.5%) were upgraded using the SB approach. The McNemar chi-square test result with Yates correction was $\chi2=0.450$, df= 1, P=0.502, OR=1.50 (95% CI, 0.61 to 3.67. This was not statistically significant (Figure 4-7).

## Radical prostatectomy cohort (n=78)

TB

SB

Clinically significant prostate lesions (n= 170/190 )

| Radical Prostatectomy (RP) | | | |
|---|---|---|---|
| | Low-Risk Cancer | Intermediate-Risk Cancer | High-Risk Cancer |
| Fusion Targeted Biopsy (TB) | Gleason 3+3 | Gleason 3+4 | Gleason > 3+4 | Total |
| No Cancer | 18 | 68 | 21 | 107 |
| Low-Risk Cancer Gleason 3+3 | 0 | 8 | 3 | 11 |
| Intermediate-Risk Cancer Gleason 3+4 | 1 | 29 | 10 | 40 |
| High-Risk Cancer Gleason > 3+4 | 1 | 10 | 21 | 32 |
| Total | 20 | 115 | 55 | 190 |

| Radical Prostatectomy (RP) | | | |
|---|---|---|---|
| | Low-Risk Cancer | Intermediate-Risk Cancer | High-Risk Cancer |
| Systematic Random Biopsy (SB) | Gleason 3+3 | Gleason 3+4 | Gleason > 3+4 | Total |
| No Cancer | 11 | 54 | 21 | 86 |
| Low-Risk Cancer Gleason 3+3 | 4 | 16 | 4 | 24 |
| Intermediate-Risk Cancer Gleason 3+4 | 3 | 26 | 5 | 34 |
| High-Risk Cancer Gleason > 3+4 | 2 | 19 | 25 | 46 |
| Total | 20 | 115 | 55 | 190 |

| Radical Prostatectomy (RP) | | | |
|---|---|---|---|
| | Low-Risk Cancer | Intermediate-Risk Cancer | High-Risk Cancer |
| Combined Biopsy (SB+TB) | Gleason 3+3 | Gleason 3+4 | Gleason > 3+4 | Total |
| No Cancer | 11 | 37 | 13 | 61 |
| Low-Risk Cancer Gleason 3+3 | 4 | 19 | 1 | 24 |
| Intermediate-Risk Cancer Gleason 3+4 | 3 | 35 | 8 | 46 |
| High-Risk Cancer Gleason > 3+4 | 2 | 24 | 33 | 59 |
| Total | 20 | 115 | 55 | 190 |

Upgraded Lesions    Downgraded Lesions

Figure 4-7 The detection rate of significant PCa via SB, TB and combined SB+TB on RP lesions.

Table 4-4 shows the difference in prostate cancer lesion upgrading between SB and TB (112)

| SB | TB | | Total lesions |
|---|---|---|---|
| | Upgrading | Not upgrading | |
| **Upgrading** | 3 | 12 | 15 |
| **No upgrading** | 8 | 89 | 97 |
| **Total lesions** | 11 | 101 | 112 |

Table 4.4 Upgrading lesions between SB and TB (112)

The proportion of lesion upgrading between SB and TB are 9.8% (11/112) and 13.4% (15/112), respectively. This was not statistically significant (the McNemar chi-square test result with Yates correction is $\chi^2$=0.450, df= 1, P=0.502, Odds ratio OR=1.50 (95% CI, 0.61 to 3.67). Table 4-5 shows the difference in prostate cancer lesion upgrading between combined biopsies and TB

| SB+TB | TB | | Total lesions |
|---|---|---|---|
| | Upgrading | Not upgrading | |
| **Upgrading** | 8 | 7 | 15 |
| **Not upgrading** | 3 | 94 | 97 |
| **Total lesions** | 11 | 101 | 112 |

Table 4.5 Upgrading lesions between combined biopsy (SB+TB) and TB (112)

The proportion of lesion upgrade between combined biopsy and TB are 13.4% (15/112) and 9.8% (11/112), respectively. This was not statistically significant (the McNemar chi-square test result with Yates correction is $\chi^2$=0.900, df= 1, P=0.343, Odds ratio OR=2.33 (95% CI, 0.60 to 9.02. Table 4-6 shows the

difference in prostate cancer lesion upgrading between combined biopsies and SB

| SB+TB | SB | | Total lesions |
|---|---|---|---|
| | Upgrade | Not upgrade | |
| **Upgrading** | 10 | 5 | 15 |
| **No upgrading** | 5 | 92 | 97 |
| **Total lesions** | 15 | 97 | 112 |

Table 4.6 Upgrading lesions between combined biopsy (SB+TB) and SB (112)

The proportion of lesion upgrading between combined biopsy and SB are both 13.4% (15/112). The result was not statistically significant (the McNemar chi-square test result with Yates correction is $\chi^2$=0.100, df= 1, P=0.752, Odds ratio OR=1.00 (95% CI, 0.29 to 3.45).

## 4.2.3 Univariate and multivariate logistic regression analysis and developed nomogram

In univariate logistic regression, patient's age, PSAD, lesion size and PIRADS were all significant predictors of significant PCa detected by random biopsy (Table 4-7) and therefore were put into multivariate analysis. A 6% increase in odds of significant PCa by random biopsy was associated with each one-year increase in age (OR= 1.06, 95%CI 1.01-1.12). Per 1ng/ml2 increase of PSAD was associated with an almost 26-fold increase in odds of significant PCa (OR= 25.63, 95%CI 1.93-341.27). Having PIRADS-5 was another significant predictor of significant PCa using random biopsy which was associated with a 6-fold increase in odds compared to those with PIRADS-3 (OR=5.94, 95%CI 1.77-19.93).

| Covariate | N | Univariate Logistic Regression | | | | Multivariate Logistic Regression | | | |
|---|---|---|---|---|---|---|---|---|---|
| | | OR | 95%CI | | P value | OR | 95%CI | | P value |
| | | | Lower | Upper | | | Lower | Upper | |
| **Age (year)** | 198 | 1.07 | 1.02 | 1.12 | 0.009 | 1.06 | 1.01 | 1.12 | 0.036 |
| **PSAD** | 198 | 92.79 | 7.61 | 1130.69 | <0.001 | 25.63 | 1.93 | 341.27 | 0.014 |
| **Lesion size** | 198 | 1.06 | 1.03 | 1.10 | <0.001 | 1.02 | 0.98 | 1.06 | 0.399 |
| **PIRADS** | 198 | | | | <0.001 | | | | 0.001 |
| **3** | 22 | Ref | - | | - | Ref | - | | - |
| **4** | 55 | 1.69 | 0.49 | 5.80 | 0.406 | 1.51 | 0.42 | 5.43 | 0.525 |
| **5** | 121 | 9.46 | 3.00 | 29.84 | <0.001 | 5.94 | 1.77 | 19.93 | 0.004 |
| **Number of Lesions** | | | | | 0.309 | | | | |
| **1** | 102 | Ref | - | | - | | | | |
| **2** | 75 | 1.11 | 0.61 | 2.02 | 0.730 | | | | |
| **3 and above** | 21 | 2.16 | 0.81 | 5.80 | 0.125 | | | | |

Table 4.7 Univariate and multivariate logistic regression analysis.

The statistically significant independent variables from the multivariate logistic regression model (age, PSAD and PIRADS) were used to develop a nomogram to predict the probability of significant PCa using SB (Figure 4-8).

The model demonstrated good discriminative ability (C-statistic= 0.779, 95%CI 0.714-0.843) (Figure 4-9).

The calibration plot demonstrated good agreement between the model predictions and actual observations for detecting csPCa via SB (Figure 4-10).
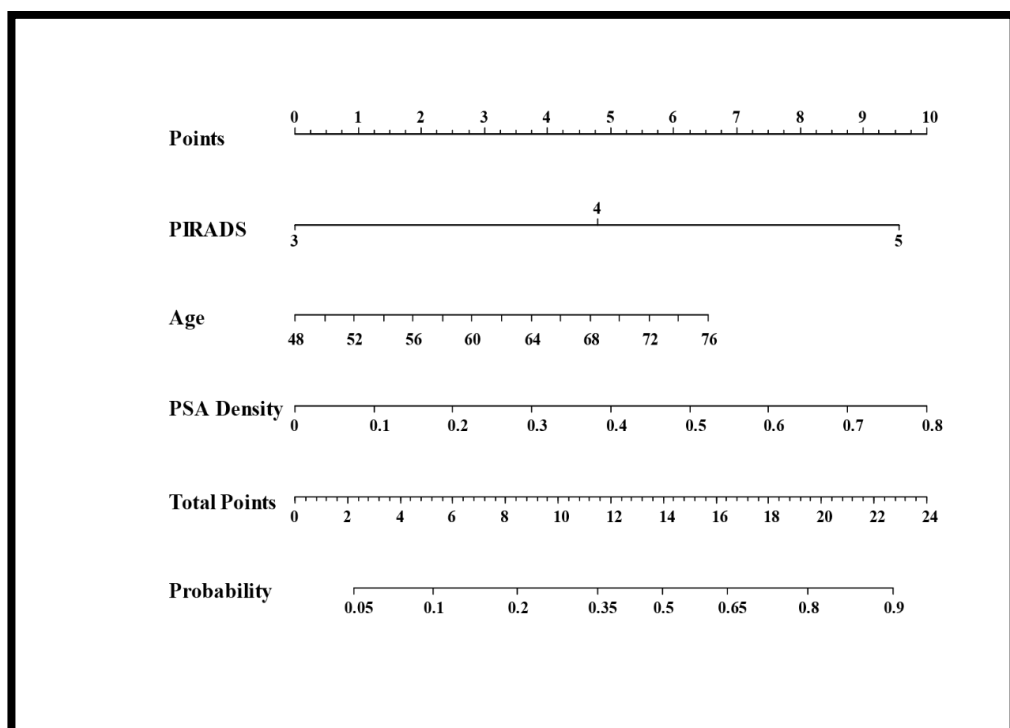


Figure 4-8 Nomogram with significant clinical variables to predict patients who will benefit from performing SB in addition to fusion TB.
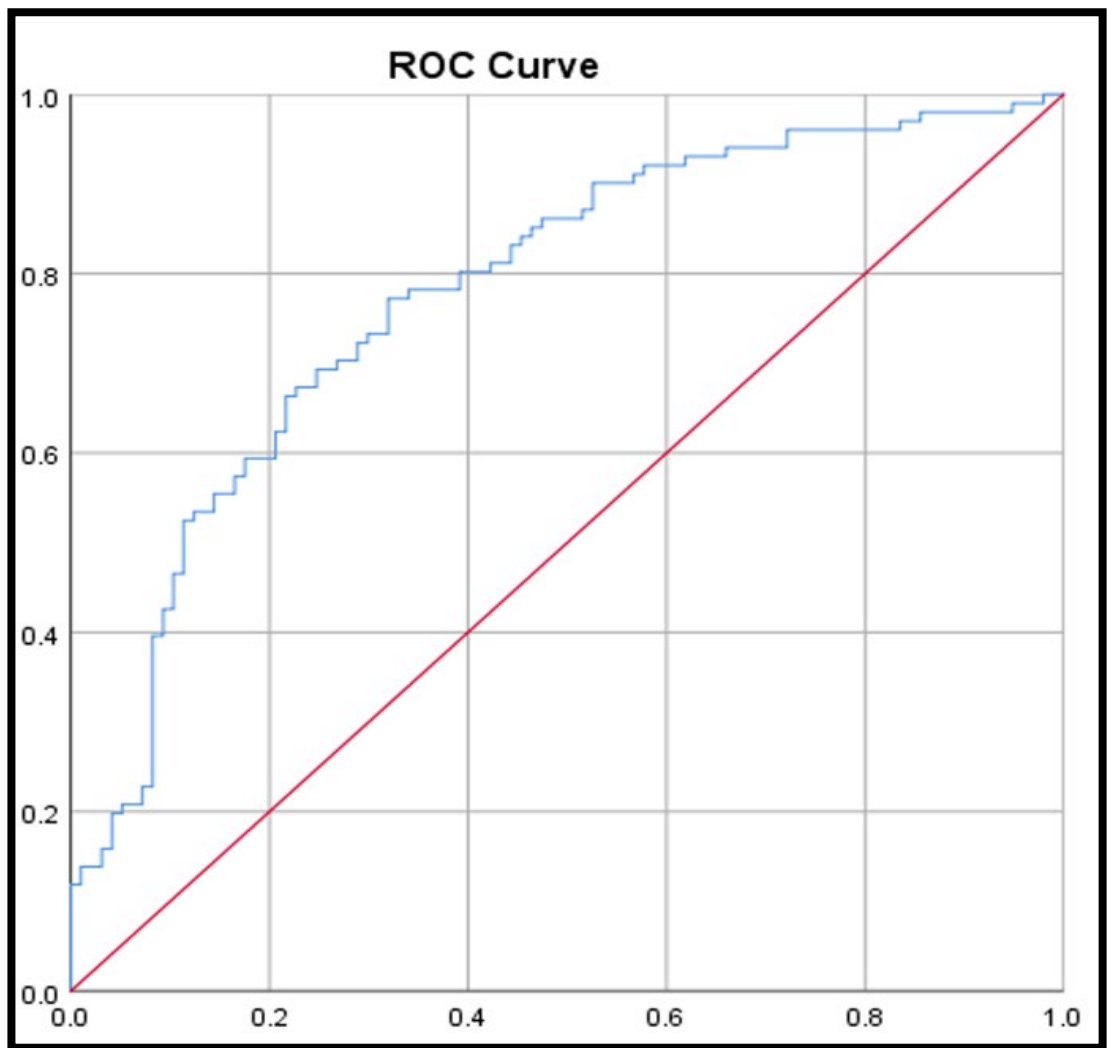
Figure 4-9 ROC curve and AUC for model discriminative ability.
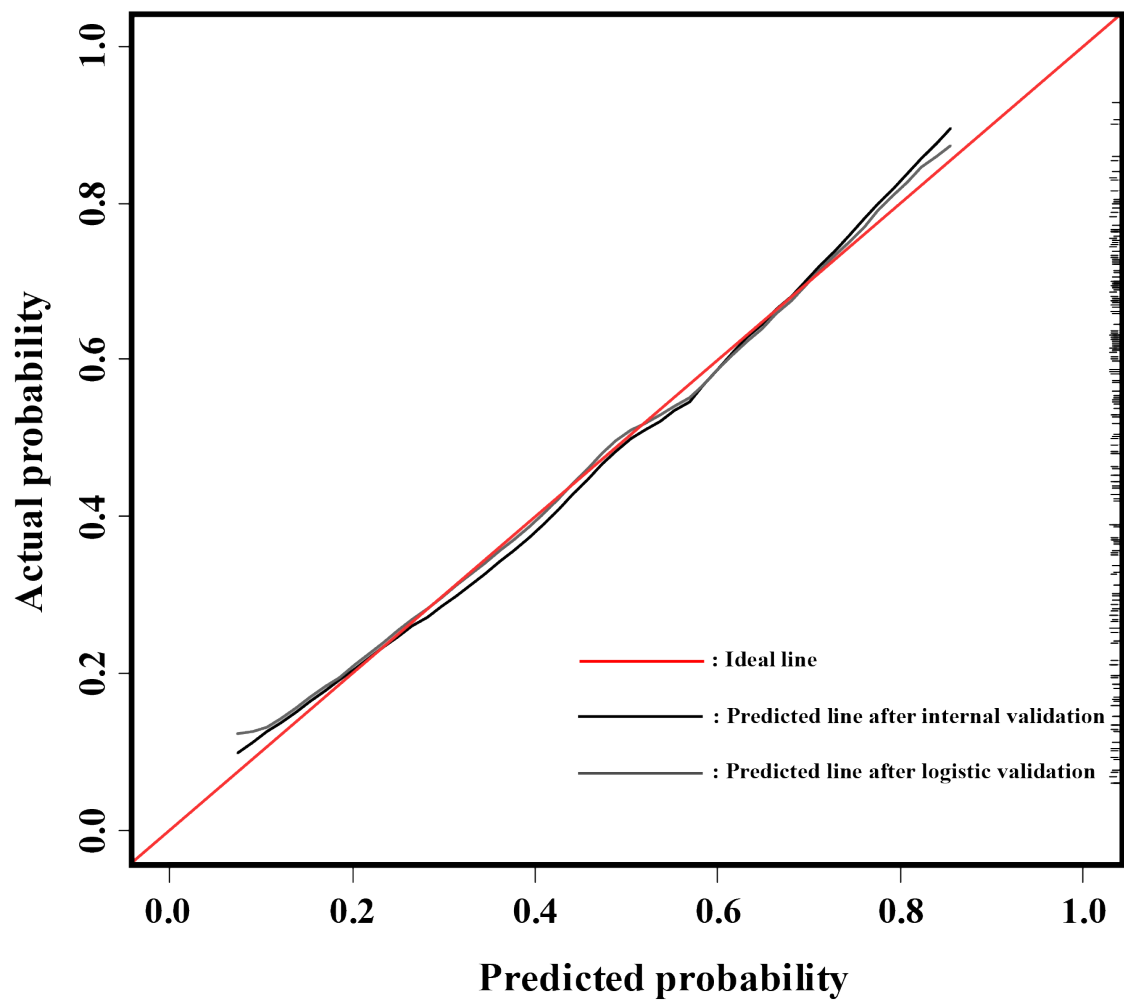
Figure 4-10 Model calibration plot for observed and predicted probability.

## 4.2.4 Decision curve analysis

The outcomes of the decision analysis curve are shown in Figure 4-11. The net benefit of performing SB in addition to TB on all cases is depicted by the grey line, whereas the black line represents the net benefit of not doing SB (only TB performed). The net benefit of using our prediction model was to identify patients who will benefit from SB in addition to TB at risk of having csPCa. Our nomogram increased the overall net clinical benefit when the threshold probability was <60% and improved the diagnosis of significant cancer compared to avoiding SB biopsy in all.
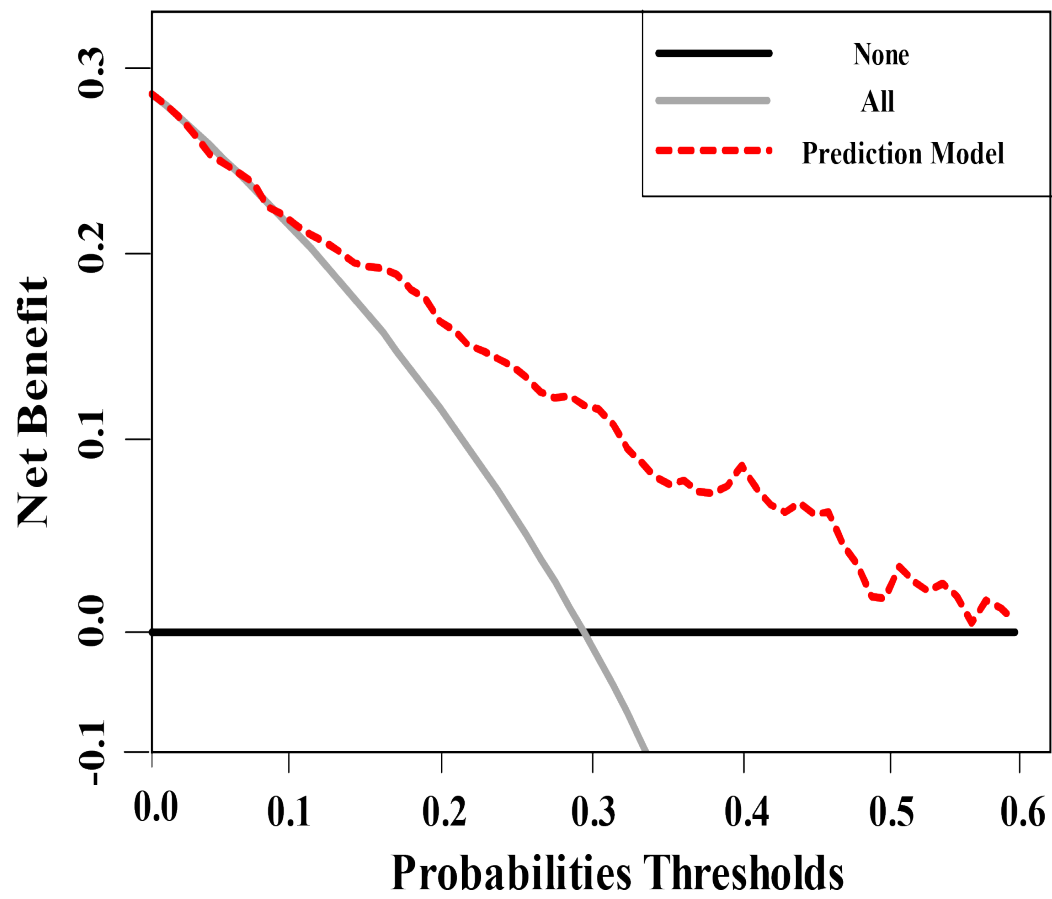
Figure 4-11 Decision analysis demonstrated a high net benefit of the model across a wide range of threshold probabilities.

## 4.3 Discussion

This study assessed the detection rate of clinically significant cancers using image fusion targeting, random systematic sampling and combination approaches. Patients-based analyses were further validated using lesion-based data from RP histology. There were statistically significant higher detection rates for the combined biopsy approach compared to SB or TB alone. The image-fusion TB approach alone would have missed 17 clinically significant PCa. Therefore, the combined approach detected more clinically significant cancers than either SB or TB alone. These results are similar to those reported by Filson et al (141) but differ to that reported in the PRECISION trial (11). Therefore, in our observations, omitting concurrent SB during image-fusion may run the risk of missing csPCa in around 8.5% of patients. Similar to Cash et al (142), we observed TB missing a small number clinically significant cancers in targeted areas. It is essential that we balance the advantages of concurrent sampling of prostate during targeting against the risks of side effects and increased detection of clinically insignificant cancer. Avoiding or adding SB at the time of fusion TB remains a challenge for physicians, as knowledge and evidence of decision-making contributing factors still remains unknown (143).

Our outcomes from the nomogram indicated the excellent advantage (C-index 78% vs. 70%) of using a multivariable prediction model adjusting for clinical and radiological features (age, PSAD and PIRADS). The nomogram could be used to assist in selecting a group of men where a combined biopsy approach would be more useful.

We also observed no significant advantage of improved characterisation of clinically significant PCa using the TB approach as all cancers labelled as clinically insignificant were upgraded on final histopathology of RP. The challenge of

upgrading or undergrading would continue with both biopsy approaches as seen in our previous study (144). There could be various reasons for this, including inadequate sampling due to cancer heterogeneity, poor visibility of cribriform architecture on MRI and in biopsies (2).

Several retrospective studies have assessed the outcomes of SB in addition to TB for the detection of clinically significant cancers. Sathianathen (145) et al reported a nomogram with C-index=70%. The nomogram was based on clinical variables (biopsy naivety, previous biopsy and AS patients), and imaging variables (number of MRI lesions and PIRADS score). The model provided a higher net clinical benefit at a threshold probability of <30%. The model was meant to predicts csPCa in systematic random cores only (when TB was negative). However, our finding focused on predicting those patients who will benefit from performing SB in addition to fusion TB (irrespective of the target biopsy being positive or negative). Also, unlike their study, our nomogram along with age, PSAD and PIRADS, found that adding these clinical variables to a model yielded a higher C-index (78% vs 70%). In contrast to the present study, Sathianathen et al (145) did not report on a validation cohort using RP as a reference standard. Further, and similar to our study, others have reported the possibility of missing significant cancers if the image fusion targeted approach was offered alone (38,146–148). Dell'Oglio et al (23) failed to identify patients who might benefit from fusion TB alone, therefore, they supported a combination of TB and SB as the preferred approach. In their study, there was no attempt to predict and assess the clinical variables that could help in identifying patients who will have a greater benefit from SB. Lastly, Falagario et al (149) highlighted that smaller lesions in a big prostate were more likely to be missed in TB biopsy, therefore, they developed a nomogram based on MRI volumetric parameters

and clinical information for deciding when SB should be performed in addition to TB. In their study, all patients underwent biparamtric MRI; however, in our analysis we followed the standard method for prostate imaging (MP-MRI) using PIRADS (91). Moreover, the study was a multi-institutional retrospective analysis of the data from two previously published prospective trials with predominant fusion biopsies being cognitive rather than image-fusion using software. All men in the MULTI-IMPROD study (150,151) had transrectal systematic biopsies and these trials were not powered to answer the research question of the present study. In contrast to the present study, Falagario et al (149) provided a range of probabilities of missing clinically significant cancers in men if SB was to be avoided altogether. We reported a set of measurable imaging criteria which can predict the likely benefit of adding SB to TB.

To our knowledge, the present study is the first where lesion-based analyses were carried out using a mould-based approach for a comprehensive pathological analysis. This confirmed that most clinically significant cancers were detected using a combined biopsy approach. Clinically significant PCa were still missed by the biopsies and this may be due to smaller lesions or a cribriform pattern seen on histopathology (152).

Decision-making using critical analysis especially in situations of uncertainty, cost pressures and likely patient morbidity, is inevitably based on evidence or sets of observations. In this study, we have presented a decision-curve analysis estimating the net clinical benefits of offering a diagnostic test (combined approach to biopsy) in comparison to TB or SB approaches alone. The clinical and radiological observations have been used to construct a nomogram which provides the basis of the decision-making curve. The curve includes intervention for all and intervention

for none and provides background to facilitate discussions with patients. A balance has to be achieved between maximising the detection of clinically significant cancers and avoiding the detection of clinically insignificant cancers.

At present, various nomograms are used mainly for taking into consideration clinical factors such as age, pre-operative PSA level and PIRADS score of the suspicious cancers. The present study reports a nomogram based on clinical parameters (age, PSAD and PIRADS). The nomogram clearly showed an improved prediction which can be used to perform additional biopsy and the findings have substantial implications for clinicians and researchers in this area. We envisage that this and further research should take us close to precise decision-making. There will remain a group of men where a SB approach would bring value in addition to a fusion TB approach, and thereby improve informed decision making in the management of men suspected of PCa.

Even though many studies point to the accuracy of MRI/TRUS targeted biopsy in cancer diagnosis, there are few data about the standardisation of the procedure regarding the best approach (transrectal vs. transperineal). Recently there is a study investigating the detection rate of csPCa of TR versus TP targeted biopsy and found that the detection rate for csPCa was lower when the TR (66.7% of the cases) versus the TP (93.3% of the cases) approach was used. Moreover, the TP-targeted biopsies diagnosed more PCa (93.7%) located in the anterior zone of the prostate compared to the TR approach (25%) (153).

Our study had some limitations. This is a single centre study with dedicated uro-radiologists and pathologists. We wanted to explore the association between lesion location and csPCa via SB but due to low numbers of lesions in the TZ, this was not possible. It was not possible to use PIRADS v2.1 , since the enrollment to study

started before its publication, and this is a similar challenge to any other study published recently on this topic (21). We used fusion biopsy via transrectal approach however recent trends suggest that transperineal targeted biopsy could lead to detecting more clinically significant prostate cancer. The nomogram in the present study has been internally validated (Cross-validation and bootstrapping). External validation of the nomogram was not carried out in the present study as this would require further prospective multi-centre recruitment of a cohort.

# Chapter 5 Conclusion and future work

In this thesis, the performance of pre-biopsy MRI for prostate cancer upgrading from biopsy to radical prostatectomy was tested. The results conclude that, a PIRADS score of 4 or 5 are associated with an increased risk of biopsy GS upgrading. In a multivariate analysis, the PIRADS score significantly improved prediction ability of pre-biopsy MRI scans for upgrading of Gleason Score (p=0.001, 95% CI [0.06-0.034]), which improved the C-index of predictive nomogram significantly (0.90 vs. 0.64, p<0.05). Currently, a variety of nomograms are used, with clinical parameters such as age, pre-operative PSA level and the number of biopsy cores involved in the cancer being taken into account. Despite this, there is still a significant histopathological difference between the biopsy and the final RP GS. This study presents a nomogram based on pre-biopsy MP-MRI grade (PIRADS score) and other known clinical parameters. We believe that this will bring us closer to a precise prediction of final GS of histopathology in prostate cancer, allowing stakeholders, including patients, to make better and more informed decisions in the treatment of localised prostate cancer.

In addition to prediction of upgrading GS, further findings also assessed the detection rate of csPCa using SB, TB and combined approaches. The image-fusion TB method would have missed 17 clinically significant PCa if it had been used alone. As a result, the combined approach detected more clinically significant cancers (64.6 %128/198) than either SB or TB alone. The results of the nomogram showed that using a multivariable prediction model that adjusts for clinical and radiological features (age, PSAD and PIRADS) has a significant benefit (C-index 78%). The nomogram might be used to help identify a group of men who would benefit from a

combined biopsy approach. The decision analysis curve confirmed a higher net clinical benefits of a combined approach (TB and SB) at an acceptable threshold. Future research should concentrate on incorporating additional predictor variables, such as novel genomic and other biomarkers to improve the accuracy of the model. The use of radiomics in conjunction with artificial intelligence and machine learning can improve our ability to identify tumour characteristics and classification. This would certainly have an effect on the study's findings in the future. Moreover, the nomogram in the study has been internally validated (Cross-validation and bootstrapping). External validation in a multi-institutional cohort is needed to predict the added values of SB to TB, which may help urologists avoid unnecessary biopsy sampling and reduce the detection of insignificant PCa while maintaining detection of clinically significant cancer.

In addition, understanding the limits of MP-MRI sensitivity for detecting tumours with Gleason pattern 4 is essential. MP-MRI is rapidly being adopted for PCa detection and surveillance, as well as a guide for focal therapy. GS pattern 4 is a heterogenous group that can be further classified into architectural patterns such as poorly formed, cribriform, and fused glands. Improving risk assessment in this group is very crucial, as GS 7 prostate cancer on biopsy is an important clinical threshold for active treatment. Future study is warranted to evaluate the impact of Gleason pattern 4 architectural pattern (cribriform) on the sensitivity of MP-MRI for PCa detection and to compare the results with lesion-based data from RP histology.

# References

1. Budäus L, Graefen M, Salomon G, Isbarn H, Lughezzani G, Sun M, et al. The novel nomogram of Gleason sum upgrade: Possible application for the eligible criteria of low dose rate brachytherapy. Int J Urol. 2010;17(10):862–8.

2. Epstein JI, Feng Z, Trock BJ, Pierorazio PM. Upgrading and Downgrading of Prostate Cancer from Biopsy to Radical Prostatectomy: Incidence and Predictive Factors Using the Modified Gleason Grading System and Factoring in Tertiary Grades. Eur Urol. 2012 May 1;61(5):1019–24.

3. Amin M, Boccon-Gibod L, Egevad L, Epstein JI, Humphrey PA, Mikuz G, et al. Prognostic and predictive factors and reporting of prostate carcinoma in prostate needle biopsy specimens. Scand J Urol Nephrol Suppl. 2005;39(216):20–33.

4. Epstein JI, Allsbrook WC, Amin MB, Egevad LL, Bastacky S, López Beltrán A, et al. The 2005 International Society of Urological Pathology (ISUP) consensus conference on Gleason grading of prostatic carcinoma. Am J Surg Pathol. 2005;29(9):1228–42.

5. Garnett JE, Oyasu R, Grayhack JT. The accuracy of diagnostic biopsy specimens in predicting tumor grades by Gleason's classification of radical prostatectomy specimens. J Urol. 1984;131(4):690–3.

6. Corcoran NM, Hong MKH, Casey RG, Hurtado-Coll A, Peters J, Harewood L, et al. Upgrade in Gleason score between prostate biopsies and pathology following radical prostatectomy significantly impacts upon the risk of biochemical recurrence. BJU Int. 2011;108(8 B):202–10.

7. Ahmed HU, El-Shater Bosaily A, Brown LC, Gabe R, Kaplan R, Parmar MK, et al.

Diagnostic accuracy of multi-parametric MRI and TRUS biopsy in prostate cancer
(PROMIS): a paired validating confirmatory study. Lancet (London, England). 2017
Feb 25;389(10071):815–22.

8.    Itatani R, Namimoto T, Atsuji S, Katahira K, Morishita S, Kitani K, et al. Negative
predictive value of multiparametric MRI for prostate cancer detection: Outcome of
5-year follow-up in men with negative findings on initial MRI studies. Eur J Radiol.
2014 Oct 1;83(10):1740–5.

9.    Song W, Bang SH, Jeon HG, Jeong BC, Seo S Il, Jeon SS, et al. Role of PI-RADS Version
2 for Prediction of Upgrading in Biopsy-Proven Prostate Cancer With Gleason Score
6. Clin Genitourin Cancer. 2018;16(4):281–7.

10.   White S, Hricak H, Forstner R, Kurhanewicz J, Vigneron DB, Zaloudek CJ, et al.
Prostate Cancer: Effect of Postbiopsy Hemorrhage on Interpretation ofMR Images'
From the Departments of Radiology. Radiology. 1995;195:385–90.

11.   Kasivisvanathan V, Rannikko AS, Borghi M, Panebianco V, Mynderse LA, Vaarala
MH, et al. MRI-Targeted or Standard Biopsy for Prostate-Cancer Diagnosis. N Engl J
Med. 2018;1767–77.

12.   Ahmed HU, El-Shater Bosaily A, Brown LC, Gabe R, Kaplan R, Parmar MK, et al.
Diagnostic accuracy of multi-parametric MRI and TRUS biopsy in prostate cancer
(PROMIS): a paired validating confirmatory study. Lancet. 2017;389(10071):815–22.

13.   Pokorny MR, De Rooij M, Duncan E, Schröder FH, Parkinson R, Barentsz JO, et al.
Prospective study of diagnostic accuracy comparing prostate cancer detection by
transrectal ultrasound-guided biopsy versus magnetic resonance (MR) imaging with
subsequent mr-guided biopsy in men without previous prostate biopsies. Eur Urol.

2014;66(1):22–9.

14.    Mottet N, van den Bergh RCN, Briers E, Van den Broeck T, Cumberbatch MG, De

Santis M, et al. EAU-EANM-ESTRO-ESUR-SIOG Guidelines on Prostate Cancer—2020

Update. Part 1: Screening, Diagnosis, and Local Treatment with Curative Intent. Eur

Urol. 2021;79(2):243–62.

15.    Drost FJH, Osses D, Nieboer D, Bangma CH, Steyerberg EW, Roobol MJ, et al.

Prostate Magnetic Resonance Imaging, with or Without Magnetic Resonance

Imaging-targeted Biopsy, and Systematic Biopsy for Detecting Prostate Cancer: A

Cochrane Systematic Review and Meta-analysis. Eur Urol [Internet]. 2020;77(1):78–

94. Available from: https://doi.org/10.1016/j.eururo.2019.06.023

16.    Padhani AR, Weinreb J, Rosenkrantz AB, Villeirs G, Turkbey B, Barentsz J. Prostate

Imaging-Reporting and Data System Steering Committee: PI-RADS v2 Status Update

and Future Directions. Eur Urol. 2019;75(3):385–96.

17.    Kasivisvanathan V, Stabile A, Neves JB, Giganti F, Valerio M, Shanmugabavan Y, et

al. Magnetic Resonance Imaging-targeted Biopsy Versus Systematic Biopsy in the

Detection of Prostate Cancer: A Systematic Review and Meta-analysis(Figure

presented.). Eur Urol. 2019;76(3):284–303.

18.    Sonn GA, Natarajan S, Margolis DJA, MacAiran M, Lieu P, Huang J, et al. Targeted

biopsy in the detection of prostate cancer using an office based magnetic

resonance ultrasound fusion device. J Urol. 2013;189(1):86–92.

19.    Wysock JS, Rosenkrantz AB, Huang WC, Stifelman MD, Lepor H, Deng F-M, et al. A

Prospective, Blinded Comparison of Magnetic Resonance (MR) Imaging–Ultrasound

Fusion and Visual Estimation in the Performance of MR-targeted Prostate Biopsy:

The PROFUS Trial. Eur Urol. 2014 Aug 1;66(2):343–51.

20. Ahdoot M, Wilbur AR, Reese SE, Lebastchi AH, Mehralivand S, Gomella PT, et al. MRI-Targeted, Systematic, and Combined Biopsy for Prostate Cancer Diagnosis. N Engl J Med. 2020;382(10):917–28.

21. Rouvière O, Puech P, Renard-Penna R, Claudon M, Roy C, Mège-Lechevallier F, et al. Use of prostate systematic and targeted biopsy on the basis of multiparametric MRI in biopsy-naive patients (MRI-FIRST): a prospective, multicentre, paired diagnostic study. Lancet Oncol. 2019;20(1):100–9.

22. Elkhoury FF, Felker ER, Kwan L, Sisk AE, Delfin M, Natarajan S, et al. Comparison of Targeted vs Systematic Prostate Biopsy in Men Who Are Biopsy Naive: The Prospective Assessment of Image Registration in the Diagnosis of Prostate Cancer (PAIREDCAP) Study. JAMA Surg. 2019;154(9):811–8.

23. Dell'Oglio P, Stabile A, Soligo M, Brembilla G, Esposito A, Gandaglia G, et al. There Is No Way to Avoid Systematic Prostate Biopsies in Addition to Multiparametric Magnetic Resonance Imaging Targeted Biopsies. Eur Urol Oncol. 2020 Feb 1;3(1):112–8.

24. Siddiqui MM, Rais-Bahrami S, Turkbey B, George AK, Rothwax J, Shakir N, et al. Comparison of MR/ultrasound fusion-guided biopsy with ultrasound-guided biopsy for the diagnosis of prostate cancer. JAMA - J Am Med Assoc. 2015 Jan 27;313(4):390–7.

25. Sonn GA, Chang E, Natarajan S, Margolis DJ, MacAiran M, Lieu P, et al. Value of targeted prostate biopsy using magnetic resonance-ultrasound fusion in men with prior negative biopsy and elevated prostate-specific antigen. Eur Urol. 2014

Apr;65(4):809–15.

26.    Snell RS. Snell's Clinical Anatomy by Regions. 2004.

27.    Liji T. Prostate Gland Anatomy. News-Medical [Internet]. 2019; Available from:

https://www.news-medical.net/health/Prostate-Gland-Anatomy.aspx

28.    McNeal JE. Normal histology of the prostate. Am J Surg Pathol. 1988;

29.    Aaron LT, Franco OE, Hayward SW. Review of Prostate Anatomy and Embryology

and the Etiology of Benign Prostatic Hyperplasia. Vol. 43, Urologic Clinics of North

America. W.B. Saunders; 2016. p. 279–88.

30.    Lopez-Beltran A, Menendez CL, Montironi R, Cheng L. Rare Tumors and Tumor-like

Conditions in Urological Pathology.

31.    Torre LA, Bray F, Siegel RL, Ferlay J, Lortet-Tieulent J, Jemal A. Global cancer

statistics, 2012. CA Cancer J Clin. 2015;65(2):87–108.

32.    IARC. Cancer Fact Sheets:Prostate Cancer. Int Agency Res Cancer [Internet]. 2012;

Available from: http://gco.iarc.fr/today%0Ahttps://gco.iarc.fr/today/data/pdf/fact-

sheets/cancers/cancer-fact-sheets-19.pdf

33.    Bashir MN. MINI-REVIEW Epidemiology of Prostate Cancer. 2015;16(2012):5137–

41.

34.    Yin M, Bastacky S, Chandran U, Becich MJ, Dhir R. Prevalence of Incidental Prostate

Cancer in the General Population: A Study of Healthy Organ Donors. J Urol.

2008;179(3):892–5.

35.    Gleason DF, Mellinger GT, Arduino LJ, Bailar JC, Becker LE, Berman HI, et al.

Prediction of Prognosis for Prostatic Adenocarcinoma by Combined Histological

Grading and Clinical Staging. J Urol. 2017;197(2):S134–9.

36. Bretlau T. Grainger & Allison's Diagnostic Radiology , 6th edition . Acta radiol. 2015;56(12):NP53–NP53.

37. Salami SS, Ben-Levi E, Yaskiv O, Ryniker L, Turkbey B, Kavoussi LR, et al. In patients with a previous negative prostate biopsy and a suspicious lesion on magnetic resonance imaging, is a 12-core biopsy still necessary in addition to a targeted biopsy? BJU Int. 2015;115(4):562–70.

38. Pokorny MR, De Rooij M, Duncan E, Schröder FH, Parkinson R, Barentsz JO, et al. Prospective study of diagnostic accuracy comparing prostate cancer detection by transrectal ultrasound-guided biopsy versus magnetic resonance (MR) imaging with subsequent mr-guided biopsy in men without previous prostate biopsies. Eur Urol. 2014;66(1):22–9.

39. Arumainayagam N, Ahmed HU, Moore CM, Freeman A, Allen C, Sohaib SA, et al. Multiparametric MR imaging for detection of clinically significant prostate cancer: A validation cohort study with transperineal template prostate mapping as the reference standard. Radiology. 2013;268(3):761–9.

40. Gleason DF. Histologic grading of prostate cancer: A perspective. Hum Pathol. 1992;23(3):273–9.

41. Hammerich KH, Ayala GE, Wheeler TM. Anatomy of the prostate gland and surgical pathology of prostate cancer. Prostate Cancer. 2008;(January):1–14.

42. Edge SB, Compton CC. The american joint committee on cancer: The 7th edition of the AJCC cancer staging manual and the future of TNM. Ann Surg Oncol. 2010;17(6):1471–4.

43. Knipper S, Graefen M. Treatment options for localized prostate cancer. Onkologe.

2019;25(3):279–88.

44.    Bott SRJ, Birtle AJ, Taylor CJ, Kirby RS. Prostate cancer management: (2) An update on locally advanced and metastatic disease. Postgrad Med J. 2003;79(937):643–5.

45.    Liede A, Hallett DC, Hope K, Graham A, Arellano J, Shahinian VB. International survey of androgen deprivation therapy (ADT) for non-metastatic prostate cancer in 19 countries. ESMO Open. 2016;1(2):1–9.

46.    Ahmed HU, Zacharakis E, Dudderidge T, Armitage JN, Scott R, Calleary J, et al. High-intensity-focused ultrasound in the treatment of primary prostate cancer: the first UK series. Br J Cancer [Internet]. 2009;101(1):19–26. Available from: http://dx.doi.org/10.1038/sj.bjc.6605116

47.    Bloch BN, Rofsky NM, Baroni RH, Marquis RP, Pedrosa I, Lenkinski RE. 3 Tesla magnetic resonance imaging of the prostate with combined pelvic phased-array and endorectal coils: Initial experience. Acad Radiol. 2004;11(8):863–7.

48.    Mirak SA, Shakeri S, Bajgiran AM, Felker ER, Sung KH, Asvadi NH, et al. Three Tesla Multiparametric Magnetic Resonance Imaging: Comparison of Performance with and without Endorectal Coil for Prostate Cancer Detection, PI-RADS[TM] version 2 Category and Staging with Whole Mount Histopathology Correlation. J Urol. 2019;201(3):496–502.

49.    Barentsz JO, Richenberg J, Clements R, Choyke P, Verma S, Villeirs G, et al. ESUR prostate MR guidelines 2012. Eur Radiol. 2012;22(4):746–57.

50.    Coskun M, Mehralivand S, Shih JH, Merino MJ, Wood BJ, Pinto PA, et al. Impact of bowel preparation with Fleet's[TM] enema on prostate MRI quality. Abdom Radiol. 2020;45(12):4252–9.

51.     Lee DJ, Ahmed HU, Moore CM, Emberton M, Ehdaie B. Multiparametric magnetic resonance imaging in the management and diagnosis of prostate cancer: Current applications and strategies. Curr Urol Rep. 2014;15(3):1–10.

52.     Sciarra A, Barentsz J, Bjartell A, Eastham J, Hricak H, Panebianco V, et al. Advances in magnetic resonance imaging: How they are changing the management of prostate cancer. Eur Urol [Internet]. 2011;59(6):962–77. Available from: http://dx.doi.org/10.1016/j.eururo.2011.02.034

53.     Heijmink SWTPJ, Fütterer JJ, Strum SS, Oyen WJG, Frauscher F, Witjes JA, et al. State-of-the-art uroradiologic imaging in the diagnosis of prostate cancer. Acta Oncol (Madr). 2011;50(SUPPL. 1):25–38.

54.     Turkbey B, Shah VP, Pang Y, Bernardo M, Xu S, Kruecker J, et al. Is apparent diffusion coefficient associated with clinical risk scores for prostate cancers that are visible on 3-T MR images? Int Braz J Urol. 2011;37(2):275–6.

55.     Hambrock T, Hoeks C, Hulsbergen-Van De Kaa C, Scheenen T, Fütterer J, Bouwense S, et al. Prospective assessment of prostate cancer aggressiveness using 3-T diffusion-weighted magnetic resonance imaging-guided biopsies versus a systematic 10-core transrectal ultrasound prostate biopsy cohort. Eur Urol. 2012;61(1):177–84.

56.     Verma S, Rajesh A. A clinically relevant approach to imaging prostate cancer: Self-assessment module. Am J Roentgenol. 2011;196(3 SUPPL.):11–4.

57.     Tamada T, Sone T, Jo Y, Yamamoto A, Yamashita T, Egashira N, et al. Prostate cancer: Relationships between postbiopsy hemorrhage and tumor detectability at MR diagnosis. Radiology. 2008;248(2):531–9.

58. Barrett T, Vargas HA, Akin O, Goldman DA, Hricak H. Value of the hemorrhage exclusion sign on T1-weighted prostate MR images for the detection of prostate cancer. Radiology. 2012;263(3):751–7.

59. Vargas HA, Akin O, Franiel T, Goldman DA, Udo K, Touijer KA, et al. Normal central zone of the prostate and central zone involvement by prostate cancer: Clinical and mr imaging implications. Radiology. 2012;262(3):894–902.

60. Boesen L. Multiparametric MRI in detection and staging of prostate cancer. Dan Med J. 2017;64(2).

61. Cruz M, Tsuda K, Narumi Y, Kuroiwa Y, Nose T, Kojima Y, et al. Characterization of low-intensity lesions in the peripheral zone of prostate on pre-biopsy endorectal coil MR imaging. Eur Radiol. 2002;12(2):357–65.

62. Turkbey B, Albert PS, Kurdziel K, Choyke PL. Imaging localized prostate cancer: Current approaches and new developments. Am J Roentgenol. 2009;192(6):1471–80.

63. Kayhan A. Multi-parametric MR imaging of transition zone prostate cancer: Imaging features, detection and staging. World J Radiol. 2010;2(5):180.

64. Wang L, Mazaheri Y, Zhang J, Ishill NM, Kuroiwa K, Hricak H. Assessment of biologic aggressiveness of prostate cancer: Correlation of MR signal intensity with gleason grade after radical prostatectomy. Radiology. 2008;246(1):168–76.

65. Coefficient D, Sparse T, Langer DL, Trachtenberg J. Intermixed Normal Tissue within Prostate Cancer : Effect on MR Imaging Measurements of Apparent Purpose : Methods : Results : Conclusion : 2008;249(3).

66. Tan CH, Wei W, Johnson V, Kundra V. Diffusion-weighted MRI in the detection of

prostate cancer: Meta-analysis. Am J Roentgenol. 2012;199(4):822–9.

67. Roethke MC, Lichy MP, Jurgschat L, Hennenlotter J, Vogel U, Schilling D, et al. Tumorsize dependent detection rate of endorectal MRI of prostate cancer - A histopathologic correlation with whole-mount sections in 70 patients with prostate cancer. Eur J Radiol. 2011;79(2):189–95.

68. Kingsley PB, Monahan WG. Selection of the Optimum b Factor for Diffusion-Weighted Magnetic Resonance Imaging Assessment of Ischemic Stroke. Magn Reson Med. 2004;51(5):996–1001.

69. Qayyum A. Diffusion-weighted imaging in the abdomen and pelvis: Concepts and applications. Radiographics. 2009;29(6):1797–810.

70. Kim CK, Park BK, Kim B. Diffusion-weighted MRI at 3 T for the evaluation of prostate cancer. Am J Roentgenol. 2010;194(6):1461–9.

71. Somford DM, Fütterer JJ, Hambrock T, Barentsz JO. Diffusion and Perfusion MR Imaging of the Prostate. Magn Reson Imaging Clin N Am. 2008;16(4):685–95.

72. Zelhof B, Pickles M, Liney G, Gibbs P, Rodrigues G, Kraus S, et al. Correlation of diffusion-weighted magnetic resonance data with cellularity in prostate cancer. BJU Int. 2009;103(7):883–8.

73. Wu LM, Xu JR, Ye YQ, Lu Q, Hu JN. The clinical value of diffusion-weighted imaging in combination with T2-weighted imaging in diagnosing prostate carcinoma: A systematic review and meta-analysis. Am J Roentgenol. 2012;199(1):103–10.

74. Verma S, Rajesh A, Morales H, Lemen L, Bills G, Delworth M, et al. Assessment of aggressiveness of prostate cancer: Correlation of apparent diffusion coefficient with histologic grade after radical prostatectomy. Am J Roentgenol. 2011;196(2):374–81.

75.    Hambrock T, Somford DM. Relationship between Apparent Diffusion Coeffi cients at

       3 . 0-T MR Imaging and Gleason Grade in Peripheral Zone Prostate Cancer 1

       Purpose : Methods : Results : Imaging. 2013;259(2):453–61.

76.    Vargas HA, Akin O, Franiel T, Mazaheri Y, Zheng J, Moskowitz C, et al. Diffusion-

       weighted endorectal MR imaging at 3 T for prostate cancer: Tumor detection and

       assessment of aggressiveness. Radiology. 2011;259(3):775–84.

77.    Jung S, Donati OF, Vargas HA, Goldman D, Hricak H, Akin O. Transition zone

       prostate cancer: Incremental value of diffusion-weighted endorectal MR imaging in

       tumor detection and assessment of aggressiveness. Radiology. 2013;269(2):493–

       503.

78.    Thörmer G, Otto J, Reiss-Zimmermann M, Seiwerts M, Moche M, Garnov N, et al.

       Diagnostic value of ADC in patients with prostate cancer: Influence of the choice of

       b values. Eur Radiol. 2012;22(8):1820–8.

79.    Litjens GJS, Hambrock T, Hulsbergen-van De Kaa C, Barentsz JO, Huisman HJ.

       Interpatient variation in normal peripheral zone apparent diffusion coefficient:

       Effect on the prediction of prostate cancer aggressiveness. Radiology.

       2012;265(1):260–6.

80.    Jeoung HK, Jeong KK, Park BW, Kim N, Cho KS. Apparent diffusion coefficient:

       Prostate cancer versus noncancerous tissue according to anatomical region. J Magn

       Reson Imaging. 2008;28(5):1173–9.

81.    Tamada T, Sone T, Jo Y, Toshimitsu S, Yamashita T, Yamamoto A, et al. Apparent

       diffusion coefficient values in peripheral and transition zones of the prostate:

       Comparison between normal and malignant prostatic tissues and correlation with

histologic grade. J Magn Reson Imaging. 2008;28(3):720–6.

82.    Alonzi R, Padhani AR, Allen C. Dynamic contrast enhanced MRI in prostate cancer. Eur J Radiol. 2007;63(3):335–50.

83.    Brawer MK, Deering RE, Brown M, Preston SD, Bigler SA. Predictors of pathologic stage in prostatic carcinoma. The role of neovascularity. Cancer. 1994;73(3):678–87.

84.    Bigler SA, Deering RE, Brawer MK. Comparison of microscopic vascularity in benign and malignant prostate tissue. Hum Pathol. 1993;24(2):220–6.

85.    Verma S, Turkbey B, Muradyan N, Rajesh A, Cornud F, Haider MA, et al. Overview of dynamic contrast-enhanced MRI in prostate cancer diagnosis and management. Am J Roentgenol. 2012;198(6):1277–88.

86.    Hara N, Okuizumi M, Koike H, Kawaguchi M, Bilim V. Dynamic contrast-enhanced magnetic resonance imaging (DCE-MRI) is a useful modality for the precise detection and staging of early prostate cancer. Prostate. 2005;62(2):140–7.

87.    Bloch BN, Furman-Haran E, Helbich TH, Lenkinski RE, Degani H, Kratzik C, et al. Prostate cancer: Accurate determination of extracapsular extension with high-spatial-resolution dynamic contrast-enhanced and T2-weighted MR imaging - Initial results. Radiology. 2007;245(1):176–85.

88.    Wang X, Wang JY, Li CM, Zhang YQ, Wang JL, Wan B, et al. Evaluation of the prostate imaging reporting and data system for magnetic resonance imaging diagnosis of prostate cancer in patients with prostate-specific antigen <20 ng/ml. Chin Med J (Engl). 2016;129(12):1432–8.

89.    Engelbrecht MR, Huisman HJ, Laheij RJF, Jager GJ, Van Leenders GJLH, Hulsbergen-

Van De Kaa CA, et al. Discrimination of prostate cancer from normal peripheral zone and central gland tissue by using dynamic contrast-enhanced MR imaging. Radiology. 2003;229(1):248–54.

90.     Johnson LM, Turkbey B, Figg WD, Choyke PL. Multiparametric MRI in prostate cancer management. Nat Rev Clin Oncol [Internet]. 2014;11(6):346–53. Available from: http://dx.doi.org/10.1038/nrclinonc.2014.69

91.     Schieda N, Quon JS, Lim C, El-Khodary M, Shabana W, Singh V, et al. Evaluation of the European Society of Urogenital Radiology (ESUR) PI-RADS scoring system for assessment of extra-prostatic extension in prostatic carcinoma. Eur J Radiol. 2015 Oct 1;84(10):1843–8.

92.     Vilanova JC, Barceló J. Prostate cancer detection: Magnetic resonance (MR) spectroscopic imaging. Abdom Imaging. 2007;32(2):253–61.

93.     Mullerad M, Hricak H, Wang L, Chen HN, Kattan MW, Scardino PT. Prostate cancer: Detection of extracapsular extension by genitourinary and general body radiologists at MR imaging. Radiology. 2004;232(1):140–6.

94.     Wassberg C, Akin O, Vargas HA, Shukla-Dave A, Zhang J, Hricak H. The incremental value of contrast-enhanced MRI in the detection of biopsy-proven local recurrence of prostate cancer after radical prostatectomy: Effect of reader experience. Am J Roentgenol. 2012;199(2):360–6.

95.     Engelbrecht MR, Jager GJ, Laheij RJ, Verbeek ALM, van Lier HJ, Barentsz JO. Local staging of prostate cancer using magnetic resonance imaging: A meta-analysis. Eur Radiol. 2002;12(9):2294–302.

96.     Pinto F, Totaro A, Palermo G, Calarco A, Sacco E, D'Addessi A, et al. Imaging in

prostate cancer staging: Present role and future perspectives. Urol Int. 2012;88(2):125–36.

97.     Barentsz J, Dickinson L, Sciarra A. Axel Heidenreich. Consensus criteria for the use of magnetic resonance imaging in the diagnosis and staging of prostate cancer: Not ready for routine use. Eur Urol 2011;59:495-7. Eur Urol. 2011;60(1):e5.

98.     Chatfield M. Pi-Rads Prostate Imaging - Reporting and DAta System. Am Coll Radiol [Internet]. 2015; Available from: http://www.acr.org/~/media/ACR/Documents/PDF/QualitySafety/Resources/PIRADS/PIRADS V2.pdf

99.     Rosenkrantz AB, Chandarana H, Gilet A, Deng FM, Babb JS, Melamed J, et al. Prostate cancer: Utility of diffusion-weighted imaging as a marker of side-specific risk of extracapsular extension. J Magn Reson Imaging. 2013;38(2):312–9.

100.    Chong Y, Kim CK, Park SY, Park BK, Kwon GY, Park JJ. Value of diffusion-weighted imaging at 3 T for prediction of extracapsular extension in patients with prostate cancer: A preliminary study. Am J Roentgenol. 2014;202(4):772–7.

101.    Fine SW, Epstein JI. A Contemporary Study Correlating Prostate Needle Biopsy and Radical Prostatectomy Gleason Score. J Urol. 2008;179(4):1335–9.

102.    Epstein JI, Egevad L, Amin MB, Delahunt B, Srigley JR, Humphrey PA. The 2014 international society of urological pathology (ISUP) consensus conference on gleason grading of prostatic carcinoma definition of grading patterns and proposal for a new grading system. Am J Surg Pathol. 2016;40(2):244–52.

103.    Trock BJ, Guo CC, Gonzalgo ML, Magheli A, Loeb S, Epstein JI. Tertiary Gleason Patterns and Biochemical Recurrence After Prostatectomy: Proposal for a Modified

Gleason Scoring System. J Urol [Internet]. 2009;182(4 SUPPL.):1364–70. Available

from: http://dx.doi.org/10.1016/j.juro.2009.06.048

104.    Kuroiwa K, Shiraishi T, Naito S. Gleason score correlation between biopsy and

prostatectomy specimens and prediction of high-grade Gleason patterns:

Significance of central pathologic review. Urology [Internet]. 2011;77(2):407–11.

Available from: http://dx.doi.org/10.1016/j.urology.2010.05.030

105.    Audenet F, Rozet F, Resche-Rigon M, Bernard R, Ingels A, Prapotnich D, et al. Grade

Group Underestimation in Prostate Biopsy: Predictive Factors and Outcomes in

Candidates for Active Surveillance. Clin Genitourin Cancer [Internet].

2017;15(6):e907–13. Available from: https://doi.org/10.1016/j.clgc.2017.04.024

106.    Radtke JP, Schwab C, Wolf MB, Freitag MT, Alt CD, Kesch C, et al. Multiparametric

Magnetic Resonance Imaging (MRI) and MRI–Transrectal Ultrasound Fusion Biopsy

for Index Tumor Detection: Correlation with Radical Prostatectomy Specimen. Eur

Urol [Internet]. 2016;70(5):846–53. Available from:

http://dx.doi.org/10.1016/j.eururo.2015.12.052

107.    Le JD, Tan N, Shkolyar E, Lu DY, Kwan L, Marks LS, et al. Multifocality and prostate

cancer detection by multiparametric magnetic resonance imaging: Correlation with

whole-mount histopathology. Eur Urol [Internet]. 2015;67(3):569–76. Available

from: http://dx.doi.org/10.1016/j.eururo.2014.08.079

108.    Tang et al. 2005. MRI–ultrasound fusion for guidance of targeted prostate biopsy.

Bone. 2008;23(1):1–7.

109.    Moore CM, Robertson NL, Arsanious N, Middleton T, Villers A, Klotz L, et al. Image-

guided prostate biopsy using magnetic resonance imaging-derived targets: A

systematic review. Eur Urol. 2013;63(1):125–40.

110. Hoeks CMA, Schouten MG, Bomers JGR, Hoogendoorn SP, Hulsbergen-Van De Kaa CA, Hambrock T, et al. Three-tesla magnetic resonance-guided prostate biopsy in men with increased prostate-specific antigen and repeated, negative, random, systematic, transrectal ultrasound biopsies: Detection of clinically significant prostate cancers. Eur Urol. 2012;62(5):902–9.

111. Giganti F, Moore CM. A critical comparison of techniques for MRI-targeted biopsy of the prostate. Transl Androl Urol. 2017;6(3):432–43.

112. Tewes S, Hueper K, Hartung D, Imkamp F, Herrmann TRW, Weidemann J, et al. Targeted MRI/TRUS fusion-guided biopsy in men with previous prostate biopsies using a novel registration software and multiparametric MRI PI-RADS scores: first results. World J Urol [Internet]. 2015;33(11):1707–14. Available from: http://dx.doi.org/10.1007/s00345-015-1525-4

113. M. Christopher AMLS. Prostate cancer detection with MR-ultrasound fusion biopsy: the role of systematic and targeted biopsies. Physiol Behav. 2016;176(1):100–106.

114. Iasonos A, Schrag D, Raj G V., Panageas KS. How to build and interpret a nomogram for cancer prognosis. J Clin Oncol. 2008;26(8):1364–70.

115. Reimer M, Hüllemann P, Hukauf M, Keller T, Binder A, Gierthmühlen J, et al. Prediction of response to tapentadol in chronic low back pain. Eur J Pain (United Kingdom). 2017;21(2):322–33.

116. Chun FKH, Karakiewicz PI, Briganti A, Gallina A, Kattan MW, Montorsi F, et al. Prostate Cancer Nomograms: An Update. Eur Urol. 2006;50(5):914–26.

117. Chun FKH, Karakiewicz PI, Huland H, Graefen M. Role of nomograms for prostate

cancer in 2007. World J Urol. 2007;25(2):131–42.

118. Balachandran VP, Gonen M, Smith JJ, DeMatteo RP. Nomograms in oncology: More than meets the eye. Lancet Oncol. 2015;16(4):e173–80.

119. Vickers AJ, Elkin EB. Decision curve analysis: A novel method for evaluating prediction models. Med Decis Mak. 2006;26(6):565–74.

120. Padhani AR, Weinreb J, Rosenkrantz AB, Villeirs G, Turkbey B, Barentsz J. Prostate Imaging-Reporting and Data System Steering Committee: PI-RADS v2 Status Update and Future Directions. Eur Urol. 2018 Jun 13;

121. Sheikh N, Wei C, Szewczyk-Bieda M, Campbell A, Memon S, Lang S, et al. Combined T2 and diffusion-weighted MR imaging with template prostate biopsies in men suspected with prostate cancer but negative transrectal ultrasound-guided biopsies. World J Urol. 2017;35(2):213–20.

122. Wei C, Jin B, Szewczyk-Bieda M, Gandy S, Lang S, Zhang Y, et al. Quantitative parameters in dynamic contrast-enhanced magnetic resonance imaging for the detection and characterisation of prostate cancer. Oncotarget. 2018;9(22):15997–6007.

123. Wei C, Lang S, Bidaut L, Doull RI, Huang Z, Nabi G. Computer Aided Image Analysis and Rapid Prototyping Molds Using Patient-Specific MRI Data For Reliable Comparison Between Imaging and Histopathology of Radical Prostatectomy Specimens. 2014;(January).

124. Costa DN, Chatzinoff Y, Passoni NM, Kapur P, Roehrborn CG, Xi Y, et al. Improved Magnetic Resonance Imaging-Pathology Correlation with Imaging-Derived, 3D-Printed, Patient-Specific Whole-Mount Molds of the Prostate. Invest Radiol.

2017;52(9):507–13.

125.    Jalloh M, Myers F, Cowan JE, Carroll PR, Cooperberg MR. Racial variation in prostate

cancer upgrading and upstaging among men with low-risk clinical characteristics.

Eur Urol [Internet]. 2015;67(3):451–7. Available from:

http://dx.doi.org/10.1016/j.eururo.2014.03.026

126.    Wang JY, Zhu Y, Wang CF, Zhang SL, Dai B, Ye DW. A nomogram to predict gleason

sum upgrading of clinically diagnosed localized prostate cancer among Chinese

patients. Chin J Cancer. 2014;33(5):241–8.

127.    Chun FK-H, Steuber T, Erbersdobler A, Currlin E, Walz J, Schlomm T, et al.

Development and Internal Validation of a Nomogram Predicting the Probability of

Prostate Cancer Gleason Sum Upgrading Between Biopsy and Radical

Prostatectomy Pathology. Eur Urol. 2006 May 1;49(5):820–6.

128.    Kulkarni GS, Lockwood G, Evans A, Toi A, Trachtenberg J, Jewett MAS, et al. Clinical

predictors of gleason score upgrading. Cancer. 2007;109(12):2432–8.

129.    He B, Chen R, Gao X, Ren S, Yang B, Hou J, et al. Nomograms for predicting Gleason

upgrading in a contemporary Chinese cohort receiving radical prostatectomy after

extended prostate biopsy: development and internal validation. Oncotarget.

2016;7(13).

130.    Iasonos A, Schrag D, Raj G V., Panageas KS. How to build and interpret a nomogram

for cancer prognosis. J Clin Oncol. 2008;26(8):1364–70.

131.    Harrell FE. Regression Modeling Strategies [electronic resource] : With Applications

to Linear Models, Logistic and Ordinal Regression, and Survival Analysis in Springer

Series in Statistics. Springer. 2015. 63–102 p.

132. D'AMICO A V., WHITTINGTON R, MALKOWICZ SB, FONDURULIA J, CHEN M-H, TOMASZEWSKI JE, et al. THE COMBINATION OF PREOPERATIVE PROSTATE SPECIFIC ANTIGEN AND POSTOPERATIVE PATHOLOGICAL FINDINGS TO PREDICT PROSTATE SPECIFIC ANTIGEN OUTCOME IN CLINICALLY LOCALIZED PROSTATE CANCER. J Urol. 1998 Dec 1;160(6):2096–101.

133. Greer MD, Shih JH, Lay N, Barrett T, Bittencourt L, Borofsky S, et al. Interreader Variability of Prostate. 2019;(June):1197–205.

134. Kornberg Z, Cooperberg MR, Spratt DE, Feng FY. Genomic biomarkers in prostate cancer. Transl Androl Urol. 2018;7(3):459–71.

135. Sanhueza C, Kohli M. Clinical and Novel Biomarkers in the Management of Prostate Cancer. Curr Treat Options Oncol. 2018;19(2).

136. Kasivisvanathan V, Rannikko AS, Borghi M, Panebianco V, Mynderse LA, Vaarala MH, et al. MRI-targeted or standard biopsy for prostate-cancer diagnosis. N Engl J Med. 2018;378(19):1767–77.

137. Nassiri N, Margolis DJ, Natarajan S, Sharma DS, Huang J, Dorey FJ, et al. Targeted Biopsy to Detect Gleason Score Upgrading during Active Surveillance for Men with Low versus Intermediate Risk Prostate Cancer. J Urol. 2017;197(3):632–9.

138. Le JD, Stephenson S, Brugger M, Lu DY, Lieu P, Sonn GA, et al. Magnetic resonance imaging-ultrasound fusion biopsy for prediction of final prostate pathology. J Urol. 2014;192(5):1367–73.

139. Szewczyk-Bieda M, Wei C, Coll K, Gandy S, Donnan P, Arcot Ragupathy SK, et al. A multicentre parallel-group randomised trial assessing multiparametric MRI characterisation and image-guided biopsy of prostate in men suspected of having

prostate cancer: MULTIPROS study protocol. Trials. 2019;20:638.

140. Philippe Puech MP, Olivier Rouvière MP, Arnauld Villers, Patrick Devos M, Marc
Colombel MP, Marc-Olivier Bitker MP, et al. Prostate cancer Diagnosis:
Multiparametric MR-targeted Biopsy with Cognitive and Transrectal US-MR Fusion
Guidance versus Systematic Biopsy-Prospective Multicenter Study 1. Radiology.
2013;268(2).

141. Filson CP, Natarajan S, Margolis DJA, Huang J, Lieu P, Dorey FJ, et al. Prostate cancer
detection with magnetic resonance-ultrasound fusion biopsy: The role of systematic
and targeted biopsies. Cancer. 2016;122(6):884–92.

142. Cash H, Günzel K, Maxeiner A, Stephan C, Fischer T, Durmus T, et al. Prostate cancer
detection on transrectal ultrasonography-guided random biopsy despite negative
real-time magnetic resonance imaging/ultrasonography fusion-guided targeted
biopsy: reasons for targeted biopsy failure. BJU Int. 2016;118(1):35–43.

143. Connor MJ, Miah S, Jayadevan R, Khoo CC, Eldred-Evans D, Shah T, et al. Value of
systematic sampling in an mp-MRI targeted prostate biopsy strategy. Vol. 9,
Translational Andrology and Urology. 2020. p. 1501–9.

144. Alqahtani S, Wei C, Zhang Y, Szewczyk-Bieda M, Wilson J, Huang Z, et al. Prediction
of prostate cancer Gleason score upgrading from biopsy to radical prostatectomy
using pre-biopsy multiparametric MRI PIRADS scoring system. Sci Rep.
2020;10(1):1–9.

145. Sathianathen NJ, Warlick CA, Weight CJ, Ordonez MA, Spilseth B, Metzger GJ, et al.
A clinical prediction tool to determine the need for concurrent systematic sampling
at the time of magnetic resonance imaging-guided biopsy. BJU Int. 2019 Apr

1;123(4):612–7.

146.    Sathianathen NJ, Butaney M, Bongiorno C, Konety BR, Bolton DM, Lawrentschuk N.
        Accuracy of the magnetic resonance imaging pathway in the detection of prostate
        cancer: a systematic review and meta-analysis. Prostate Cancer Prostatic Dis.
        2019;22(1):39–48.

147.    Muthigi A, George AK, Sidana A, Kongnyuy M, Simon R, Moreno V, et al. Missing the
        Mark: Prostate Cancer Upgrading by Systematic Biopsy over Magnetic Resonance
        Imaging/Transrectal Ultrasound Fusion Biopsy. J Urol. 2017;197(2):327–34.

148.    Siddiqui MM, Rais-Bahrami S, Truong H, Stamatakis L, Vourganti S, Nix J, et al.
        Magnetic Resonance Imaging/Ultrasound–Fusion Biopsy Significantly Upgrades
        Prostate Cancer Versus Systematic 12-core Transrectal Ultrasound Biopsy. Eur Urol.
        2013 Nov 1;64(5):713–9.

149.    Falagario U, Jambor I, Taimen P, Syvänen KT, Kähkönen E, Merisaari H, et al. Added
        value of systematic biopsy in men with a clinical suspicion of prostate cancer
        undergoing biparametric MRI-targeted biopsy: multi-institutional external
        validation study. World J Urol. 2020;

150.    Perez IM, Jambor I, Kauko T, Verho J, Ettala O, Falagario U, et al. Qualitative and
        Quantitative Reporting of a Unique Biparametric MRI: Towards Biparametric MRI-
        Based Nomograms for Prediction of Prostate Biopsy Outcome in Men With a Clinical
        Suspicion of Prostate Cancer (IMPROD and MULTI-IMPROD Trials). J Magn Reson
        Imaging. 2020 May 1;51(5):1556–67.

151.    Jambor I, Boström PJ, Taimen P, Syvänen K, Kähkönen E, Kallajoki M, et al. Novel
        biparametric MRI and targeted biopsy improves risk stratification in men with a

clinical suspicion of prostate cancer (IMPROD Trial). J Magn Reson Imaging. 2017

Oct 1;46(4):1089–95.

152.	Truong M, Hollenberg G, Weinberg E, Messing EM, Miyamoto H, Frye TP. Impact of

Gleason Subtype on Prostate Cancer Detection Using Multiparametric Magnetic

Resonance Imaging: Correlation with Final Histopathology. J Urol. 2017 Aug

1;198(2):316–21.

153.	Pepe P, Garufi A, Priolo G, Pennisi M. Transperineal Versus Transrectal MRI/TRUS

Fusion Targeted Biopsy: Detection Rate of Clinically Significant Prostate Cancer. Clin

Genitourin Cancer. 2017;15(1):e33–6.

## Appendix

Programming for nomogram, calibration and decision curve analysis using RStudio

```
library(foreign)
bc <- read.spss("E:/patients data.sav", use.value.labels=F, to.data.frame=T)
library(rms)
dd <- datadist(bc)
options(datadist="dd")
```

**(First study)**

1/With PI-RADS

```
f1 <- lrm(STATUS ~ PIRADS + PSA + CoresNumber + MaximumPercentage, data
= bc)
lrm(formula = STATUS ~ PIRADS + PSA + CoresNumber + MaximumPercentage,
data = bc)
nom <- nomogram(f1, fun= function(x)1/(1+exp(-x)), # or fun=plogis
lp=F, funlabel="Probability of GS upgrading",maxscale=10, fun.at=c(0.99, 0.975,
0.95, 0.9, 0.8, 0.65, 0.5, 0.35, 0.2, 0.1, 0.05))
plot(nom)
f2 <- lrm(STATUS ~ PIRADS + PSA + CoresNumber + MaximumPercentage,
x=T,y=T,data = bc)
cal2 <- calibrate(f2, cmethod="KM", method="boot", m=110, B=1000)
plot(cal2)
plot(cal2,xlab="Predicted probability of GS upgrading",ylab="Actual probability of
GS upgrading")
```

2/without PI-RADS

```
f3 <- lrm(STATUS ~ PSA + CoresNumber + MaximumPercentage, data = bc)
lrm(formula = STATUS ~ PSA + CoresNumber + MaximumPercentage, data = bc)
nom <- nomogram(f3, fun= function(x)1/(1+exp(-x)), # or fun=plogis
lp=F, funlabel="Probability of GS upgrading",maxscale=10, fun.at=c(0.99, 0.975,
0.95, 0.9, 0.8, 0.65, 0.5, 0.35, 0.2, 0.1, 0.05))
plot(nom)
f4 <- lrm(STATUS ~ PSA + CoresNumber + MaximumPercentage, x=T,y=T,data =
bc)
```

```
cal4 <- calibrate(f4, cmethod="KM", method="boot", m=110, B=1000)
plot(cal4)
plot(cal4,xlab="Predicted probability of GS upgrading",ylab="Actual probability of
GS upgrading")
```

**(Second study)**

Nomogram:

```
bc <- read.spss("E:/filename.sav",
use.value.labels = F,
to.data.frame = T)
dd <- datadist(bc)
options(datadist = "dd")
f1 <-
lrm(Outcome ~ PIRADS + Age + PSAdensity, data = bc)
lrm(formula = Outcome ~ PIRADS + Age + PSAdensity,
data = bc)
# rt2$gender <- factor(rt2$gender,labels=c("F", "M"))
# rt2$stage <- factor(rt2$stage,labels=c("Stage1", "Stage2", "Stage3", "Stage4"))
# rt2$T <- factor(rt2$T,labels=c("T1", "T2", "T3", "T4"))4 rt2$M <-
factor(rt2$M,labels=c("M0", "M1"))
# rt2$N <- factor(rt2$N,labels=c("N0", "N1", "N2", "N3"))6 rt2$risk <-
factor(rt2$risk,labels=c("low", "high"))
nom <- nomogram(
f1,
fun = function(x)
1 / (1 + exp(-x)),
# or fun=plogis+lp = F,
lp=F,
funlabel = "Probability",
maxscale = 10,
fun.at = c(0.99, 0.975, 0.95, 0.9, 0.8, 0.65, 0.5, 0.35, 0.2, 0.1, 0.05))
plot(nom)
```

calibration plot:

```
f2 <- lrm(Outcome ~ PIRADS + Age + PSAdensity, x=T,y=T,data = bc)
```

```r
cal2 <- calibrate(f2, cmethod="KM", method="boot", m=39, B=200)
p <- cal2[,"predy"]
p.app <- cal2[,"calibrated.orig"]
p.cal <- cal2[,"calibrated.corrected"]
xlim <- c(0, 1)
ylim <- c(0, 1)
at <- attributes(cal2)
predicted <- at$predicted
s <- !is.na(p + p.cal)
err <- predicted - approx(p[s], p.cal[s], xout=predicted, ties=mean)$y
cat('\nn=',n <- length(err),  '  Mean absolute error=',
round(mae <- mean(abs(err), na.rm=TRUE),3),'  Mean squared error=',
round(mean(err^2, na.rm=TRUE),5),
'\n0.9 Quantile of absolute error=',
round(quantile(abs(err), .9, na.rm=TRUE),3),     '\n\n', sep='')
plot(p, p.app, xlim=xlim, ylim=ylim,
xlab="Predicted probability",
ylab="Actual probability",
type="n")
lines(p, p.app, lty=1, col='blue') ## change color of apparent
lines(p, p.cal, lty=1, col='red') ## change color of bias-corrected
abline(0,
1,
lty = 1,
lwd = 2,
col = c(rgb(150, 250, 50, max = 255)))
do.call('scat1d', c(list(x=predicted), 'scat1d.opts'))
legend <- list(x=xlim[1] + .55*diff(xlim),
y=ylim[1] + .32*diff(ylim))
legend(legend, c("Apparent", "Bias-corrected", "Ideal"),
lty=c(3,1,2), bty="n")
title(sub=paste("B=", at$B, "repetitions,", at$method),
cex.sub=0.75, adj=0)
```

135

```r
title(sub=paste('Mean absolute error=', round(mae,3),

' n=', n, sep="),

cex.sub=0.75, adj=1)
```

DCA analysis:

```r
library(devtools)

Data <- read.spss("filename.sav",

use.value.labels = F,

to.data.frame = T)

simple <-

decision_curve(

Outcome ~ PIRADS + Age + PSAdensity,

data = Data,

family = binomial(link = 'logit'),

thresholds = seq(0, 0.6, by = 0.01),

confidence.intervals = 0.95,

study.design = 'case-control',

population.prevalence = 0.3)

List <- list(simple)

plot_decision_curve(

List,

curve.names = c('model'),

cost.benefit.axis = FALSE,

col = c('red'),

confidence.intervals = FALSE,

standardize = FALSE,

xlab="Probabilities Thresholds")

table=summary(simple,measure= 'NB')
```

# Raw data 1

| | LRP | NO. | CHI | age | sitename | MRI | PIRAD | PSA | core | percenta | stage | TRUS | Pathology | Weigh | PSAD |
|---|---|---|---|---|---|---|---|---|---|---|---|---|---|---|---|
| 2 | 16/07/2013 | 1 | 1309600031 | 53 | CRC | 3T | 4 | 5.9 | 2 | 20 | T0 | 3+3 | 3+4 | 34.5 | 0.17101 |
| 3 | 09/07/2013 | 2 | 2610500017 | 63 | CRC | 3T | 4 | 8.5 | 3 | 10 | T0 | 3+3 | 3+4 | 29 | 0.2931 |
| 4 | 15/08/2013 | 3 | 2107440077 | 69 | CRC | 3T* | 4 | 11 | 3 | 20 | T2b | 3+4 | 4+5 | 58.5 | 0.18803 |
| 5 | 08/10/2013 | 4 | 1901410099 | 72 | STRACATHRO | 1.5T | 5 | 11.1 | 7 | 50 | T2 | 4+3 | 3+4 | 66 | 0.16818 |
| 6 | 08/10/2013 | 5 | 1604445254 | 69 | STRACATHRO | 1.5T | 4 | 17 | 6 | 70 | T2 | 4+4 | 4+3 | 40 | 0.425 |
| 7 | 12/11/2013 | 6 | 0311450059 | 68 | NINEWELLS | 1.5T | 5 | 9 | 3 | 20 | T0 | 3+3 | 3+4 | 58.5 | 0.15385 |
| 8 | 12/11/2013 | 7 | 0811430375 | 70 | CRC | 3T | 4 | 6.6 | 4 | 20 | T2 | 3+4 | 4+5 | 85 | 0.07765 |
| 9 | 19/11/2013 | 8 | 1708540253 | 59 | STRACATHRO | 1.5T | 4 | 5.5 | 3 | 50 | T2 | 3+4 | 3+4 | 26.5 | 0.20755 |
| 10 | 19/11/2013 | 9 | 0105480738 | 65 | STRACATHRO | 1.5T | 5 | 4.9 | 10 | 50 | T0 | 3+4 | 3+4 | 76.5 | 0.06405 |
| 11 | 10/12/2013 | 10 | 2602490652 | 64 | NINEWELLS | 1.5T | 5 | 23 | 6 | 70 | T2 | 4+4 | 3+4 | 42 | 0.54762 |
| 12 | 16/12/2013 | 11 | 1505470951 | 66 | STRACATHRO | 1.5T | 5 | 22.9 | 6 | 90 | T2 | 4+5 | 4+5 | 48.5 | 0.47216 |
| 13 | 31/12/2013 | 12 | 0711430233 | 70 | CRC | 3T | 5 | 6.5 | 3 | 20 | T1c | 3+4 | 3+4 | 39 | 0.16667 |
| 14 | 27/12/2013 | 13 | 2401430512 | 70 | NINEWELLS | 1.5T | 5 | 11 | 10 | 90 | T2 | 4+3 | 3+4 | 60.5 | 0.18182 |
| 15 | 25/02/2014 | 14 | 0205530052 | 61 | NINEWELLS | 1.5T | 5 | 44 | 11 | 90 | T2 | 4+4 | 4+5 | 61 | 0.72131 |
| 16 | 04/03/2014 | 15 | 2401570012 | 57 | CRC | 3T | 3 | 7.8 | 2 | 100 | T2 | 3+4 | 3+4 | 26 | 0.3 |
| 17 | 18/03/2014 | 16 | 2608495079 | 65 | NINEWELLS | 1.5T | 4 | 21.6 | 1 | 10 | T2 | 3+3 | 4+5 | 73 | 0.29589 |
| 18 | 18/03/2014 | 17 | 0810500574 | 64 | NINEWELLS | 1.5T | 4 | 9 | 4 | 25 | T0 | 3+3 | 3+3 | 114.5 | 0.0786 |
| 19 | 25/03/2014 | 18 | 0106410059 | 73 | CRC | 3T | 5 | 7.4 | 4 | 10 | T2 | 3+4 | 4+5 | 58 | 0.12759 |
| 20 | 15/04/2014 | 19 | 0903560038 | 58 | CRC | 3T | 5 | 8.1 | 1 | 80 | T2 | 4+5 | 4+5 | 53 | 0.15283 |
| 21 | 15/04/2014 | 20 | 2311540653 | 60 | CRC | 3T | 5 | 34 | 7 | 90 | T2 | 4+5 | 4+5 | 39.5 | 0.86076 |
| 22 | 29/04/2014 | 21 | 3006480171 | 66 | NINEWELLS | 1.5T | 5 | 13.6 | 7 | 70 | T1c | 4+3 | 4+5 | 53 | 0.2566 |
| 23 | 29/04/2014 | 22 | 1505470293 | 67 | NINEWELLS | 1.5T | 5 | 10.2 | 5 | 40 | T1c | 3+4 | 4+3 | 49.5 | 0.20606 |
| 24 | 07/05/2014 | 23 | 0407430318 | 71 | STRACATHRO | 1.5T | 5 | 10 | 6 | 60 | T2 | 3+4 | 3+4 | 37.5 | 0.26667 |
| 25 | 06/05/2014 | 24 | 1106410173 | 73 | STRACATHRO | 1.5T | 5 | 10.6 | 10 | 100 | T2b | 4+5 | 4+5 | 94.5 | 0.11217 |
| 26 | 20/04/2014 | 25 | 2710450011 | 69 | STRACATHRO | 1.5T | 5 | 33.2 | 1 | 70 | T3 | 4+3 | 4+5 | 51.5 | 0.64466 |
| 27 | 27/05/2014 | 26 | 1511430079 | 71 | CRC | 3T | 5 | 11.4 | 4 | 80 | T2 | 4+4 | 4+5 | 61 | 0.18689 |
| 28 | 26/05/2014 | 27 | 1608509796 | 64 | Queens Margaret | 1.5T | 5 | 6.9 | 5 | 90 | T3c | 4+4 | 4+5 | 52.5 | 0.13143 |
| 29 | 03/06/2014 | 28 | 0607536179 | 61 | CRC | 3T | 5 | 18.4 | 8 | 80 | T2B | 3+5 | 3+5 | 72.5 | 0.25379 |
| 30 | 13/06/2014 | 29 | 2305460074 | 68 | STRACATHRO | 1.5T | 5 | 6.5 | 7 | 100 | T2 | 4+4 | 3+4 | 48.5 | 0.13402 |
| 31 | 18/06/2014 | 30 | 1508500312 | 64 | CRC | 3T | 5 | 8 | 5 | 80 | T2 | 4+3 | 4+3 | 52 | 0.15385 |
| 32 | 18/06/2014 | 31 | 2802550152 | 59 | CRC | 3T* | N | 6.1 | 2 | 10 | T1c | 3+3 | 3+3 | 49.5 | 0.12323 |
| 33 | 01/07/2014 | 32 | 2704473595 | 67 | CRC | 3T | 5 | 8.1 | 2 | 30 | T1c | 5+4 | 3+5 | 50.5 | 0.1604 |
| 34 | 08/07/2014 | 33 | 1604470275 | 67 | STRACATHRO | 1.5T | N | 8 | 3 | 20 | T1c | 3+4 | 3+4 | 58 | 0.13793 |
| 35 | 09/07/2014 | 34 | 2605470113 | 67 | CRC | 3T* | 3 | 16 | 2 | 20 | T1c | 3+4 | 3+4 | 160 | 0.1 |
| 36 | 29/07/2014 | 35 | 2705480390 | 66 | CRC | 3T | 5 | 20.1 | 5 | 15 | T1c | 3+5 | 3+4 | 77.5 | 0.25935 |
| 37 | 29/07/2014 | 36 | 0712500154 | 64 | STRACATHRO | 1.5T | 4 | 10 | 6 | 80 | T2c | 4+3 | 3+4 | 49.5 | 0.20202 |
| 38 | 12/08/2014 | 37 | 0106420313 | 72 | NINEWELLS | 1.5T | 5 | 19.6 | 5 | 90 | T2 | 3+3 | 3+4 | 52 | 0.37692 |
| 39 | 25/08/2014 | 38 | 0906472490 | 67 | STRACATHRO | 1.5T | 5 | 23 | 9 | 70 | T1c | 3+4 | 3+4 | 118 | 0.19492 |
| 40 | 02/09/2014 | 39 | 0808500074 | 64 | CRC | 3T* | 5 | 10.5 | 2 | 25 | T1c | 3+3 | 3+4 | 43 | 0.24419 |
| 41 | 02/09/2014 | 40 | 3008531350 | 61 | STRACATHRO | 1.5T | 3 | 20.5 | 2 | 5 | T1c | 3+3 | 3+4 | 155 | 0.13226 |
| 42 | 09/09/2014 | 41 | 0909420211 | 72 | STRACATHRO | 1.5T | N | 5.7 | 1 | 10 | T1c | 3+4 | 3+4 | 125.5 | 0.04542 |
| 43 | 15/09/2014 | 42 | 1902530330 | 61 | STRACATHRO | 1.5T | 5 | 9.4 | 12 | 100 | T1c | 5+4 | 4+5 | 52.5 | 0.17905 |
| 44 | 23/09/2014 | 43 | 0603470017 | 67 | CRC | 3T | 5 | 10.2 | 4 | 20 | T1c | 3+4 | 3+4 | 46 | 0.22174 |
| 45 | 23/09/2014 | 44 | 1804490350 | 65 | VICTORIA HOS | 1.5T | N | 4.6 | 3 | 30 | T1c | 3+3 | 3+4 | 62.5 | 0.0736 |
| 46 | 30/09/2014 | 45 | 1408420058 | 72 | STRACATHRO | 1.5T | 3 | 12.5 | 3 | 5 | T1c | 3+3 | 3+4 | 137 | 0.09124 |
| 47 | 30/09/2014 | 46 | 0604440197 | 70 | Queens Margaret | 1.5T | 4 | 10 | 8 | 90 | T2 | 4+4 | 4+3 | 48 | 0.20833 |

| | | | | | | | | | | | | | | | |
|---|---|---|---|---|---|---|---|---|---|---|---|---|---|---|---|
| 48 | 21/10/2014 | 47 | 2911430115 | 71 | CRC | 3T | 5 | 42 | 3 | 50 | T2 | 3+4 | 4+5 | 45.5 | 0.92308 |
| 49 | 21/10/2014 | 48 | 0509410472 | 73 | CRC | 3T* | 5 | 25 | 7 | 100 | T2 | 3+4 | 4+5 | 105.5 | 0.23697 |
| 50 | 14/10/2014 | 49 | 1205500235 | 64 | CRC | 3T | 4 | 11 | 1 | 10 | T1c | 3+3 | 3+4 | 50.5 | 0.21782 |
| 51 | 03/11/2014 | 50 | 1811380077 | 76 | STRACATHRO | 1.5T | 5 | 8.9 | 5 | 60 | T1c | 4+5 | 4+5 | 50.5 | 0.17624 |
| 52 | 01/11/2014 | 51 | 1802530355 | 61 | CRC | 3T | 5 | 37 | 2 | 20 | T2 | 3+3 | 3+4 | 63 | 0.5873 |
| 53 | 01/11/2014 | 52 | 1308530315 | 61 | NINEWELLS | 1.5T | 5 | 26.5 | 11 | 100 | T2 | 3+4 | 3+4 | 51.5 | 0.51456 |
| 54 | 28/11/2014 | 53 | 2903420130 | 72 | NINEWELLS | 1.5T | 4 | 11.1 | 4 | 20 | T2 | 5+3 | 3+5 | 48 | 0.23125 |
| 55 | 16/12/2014 | 54 | 0510490433 | 65 | CRC | 3T | 3 | 8.5 | 1 | 20 | T1c | 4+3 | 4+3 | 127.5 | 0.06667 |
| 56 | 05/01/2015 | 55 | 1102530115 | 62 | STRACATHRO | 1.5T | 5 | 6.9 | 2 | 20 | T1c | 3+4 | 3+4 | 34 | 0.20294 |
| 57 | 05/01/2015 | 56 | 1704493412 | 66 | CRC | 3T | 4 | 9.8 | 2 | 20 | T1c | 4+4 | 4+3 | 67.5 | 0.14519 |
| 58 | 13/01/2015 | 57 | 0402475372 | 68 | CRC | 3T* | 3 | 8.6 | 5 | 70 | T1c | 3+4 | 3+4 | 121 | 0.07107 |
| 59 | 13/01/2015 | 58 | 0512400059 | 75 | CRC | 3T* | 5 | 8 | 4 | 70 | T2 | 4+3 | 3+4 | 38 | 0.21053 |
| 60 | 09/01/2015 | 59 | 1503560074 | 59 | CRC | 3T* | N | 6.8 | 1 | 10 | T1c | 3+3 | 3+3 | 74 | 0.09189 |
| 61 | 27/01/2015 | 60 | 1803410256 | 74 | CRC | 3T | 3 | 11 | 12 | 90 | T1c | 3+3 | 3+4 | 34 | 0.32353 |
| 62 | 03/02/2015 | 61 | 2603425218 | 73 | CRC | 3T* | 4 | 12.1 | 5 | 30 | T0 | 4+4 | 4+3 | 53 | 0.2283 |
| 63 | 03/02/2015 | 62 | 1806485575 | 67 | NINEWELLS | 1.5T | 5 | 15.2 | 4 | 30 | T2 | 3+4 | 3+4 | 70 | 0.21714 |
| 64 | 17/02/2015 | 63 | 1011440091 | 71 | NINEWELLS | 1.5T | 5 | 7.1 | 2 | 20 | T2 | 3+3 | 3+4 | 59.5 | 0.11933 |
| 65 | 20/02/2015 | 64 | 0311461131 | 69 | NINEWELLS | 1.5T | 5 | 47 | 3 | 40 | T2 | 4+3 | 3+5 | 55 | 0.85455 |
| 66 | 24/02/2015 | 65 | 1305500474 | 65 | CRC | 3T* | 5 | 28 | 12 | 80 | T1c | 3+5 | 3+5 | 54.5 | 0.51376 |
| 67 | 10/03/2015 | 66 | 2806490251 | 66 | CRC | 3T* | 5 | 10 | 1 | 5 | T1c | 3+3 | 3+3 | 72 | 0.13889 |
| 68 | 17/03/2015 | 67 | 0803460198 | 69 | CRC | 3T* | 4 | 0.9 | 3 | 60 | T1c | 4+4 | 4+4 | 36.5 | 0.02466 |
| 69 | 31/03/2015 | 68 | 1803535474 | 62 | NINEWELLS | 3T* | 5 | 9 | 8 | 80 | T1c | 4+5 | 3+5 | 69 | 0.13043 |
| 70 | 31/03/2015 | 69 | 1211460193 | 69 | STRACATHRO | 1.5T | 5 | 10 | 10 | 50 | T2 | 4+5 | 4+5 | 44 | 0.22727 |
| 71 | 21/04/2015 | 70 | 0506530175 | 62 | STRACATHRO | 1.5T | 5 | 15.5 | 8 | 80 | T2 | 4+4 | 4+5 | 68 | 0.22794 |
| 72 | 28/04/2015 | 71 | 1809575451 | 58 | NINEWELLS | 1.5T | 5 | 12.2 | 12 | 90 | T1c | 4+5 | 4+5 | 52 | 0.23462 |
| 73 | 28/04/2015 | 72 | 0302455310 | 70 | NINEWELLS | 1.5T | 5 | 10 | 3 | 20 | T2 | 4+4 | 4+4 | 55 | 0.18182 |
| 74 | 12/05/2015 | 73 | 0212412213 | 74 | NINEWELLS | 1.5T | 5 | 19.4 | 3 | 70 | T2 | 4+4 | 4+3 | 65 | 0.29846 |
| 75 | 19/05/2015 | 74 | 0110430018 | 72 | CRC | 3T | 5 | 6.7 | 5 | 70 | T2 | 4+3 | 4+3 | 70.5 | 0.09504 |
| 76 | 02/06/2015 | 75 | 1907530258 | 62 | NINEWELLS | 1.5T | 4 | 9.4 | 9 | 50 | T2 | 3+4 | 3+4 | 47 | 0.2 |
| 77 | 02/06/2015 | 76 | 0705410072 | 74 | STRACATHRO | 1.5T | 5 | 7.5 | 6 | 50 | T2 | 4+3 | 3+4 | 101 | 0.07426 |
| 78 | 09/06/2015 | 77 | 1110510012 | 64 | STRACATHRO | 1.5T | 5 | 7.9 | 5 | 80 | T0 | 4+5 | 4+5 | 59 | 0.1339 |
| 79 | 23/06/2015 | 78 | 2212430132 | 72 | STRACATHRO | 1.5T | 5 | 13.3 | 2 | 10 | T1c | 4+3 | 3+5 | 108 | 0.12315 |
| 80 | 30/06/2015 | 79 | 2706440538 | 71 | NINEWELLS | 1.5T | 4 | 4.5 | 2 | 30 | T2 | 4+3 | 4+3 | 62 | 0.07258 |
| 81 | 14/07/2015 | 80 | 2512510514 | 64 | CRC | 3T | N | 10 | 3 | 20 | T1c | 4+3 | 4+3 | 86 | 0.11628 |
| 82 | 21/07/2015 | 81 | 1211550095 | 60 | CRC | 3T | 5 | 8.1 | 10 | 90 | T2 | 3+4 | 3+4 | 68.5 | 0.11825 |
| 83 | 04/08/2015 | 82 | 2511520311 | 63 | CRC | 3T | 3 | 4.2 | 3 | 20 | T2 | 4+5 | 4+3 | 35.5 | 0.11831 |
| 84 | 11/08/2015 | 83 | 2111530131 | 62 | CRC | 3T | 5 | 8.8 | 1 | 30 | T1c | 3+4 | 3+4 | 73.7 | 0.1194 |
| 85 | 11/08/2015 | 84 | 3001500131 | 65 | NINEWELLS | 1.5T | 4 | 6.8 | 4 | 30 | T1c | 3+4 | 3+4 | 72.3 | 0.09405 |
| 86 | 01/09/2015 | 85 | 2405490072 | 66 | STRACATHRO | 1.5T | 5 | 3.1 | 6 | 40 | T0 | 4+4 | 4+3 | 57 | 0.05439 |
| 87 | 01/09/2015 | 86 | 1010410016 | 74 | NINEWELLS | 1.5T | 4 | 7.6 | 1 | 20 | T1c | 3+4 | 3+4 | 120 | 0.06333 |
| 88 | 22/09/2015 | 87 | 1212420276 | 73 | NINEWELLS | 1.5T | 5 | 2 | 6 | 90 | T2 | 4+4 | 4+5 | 42 | 0.04762 |
| 89 | 07/10/2015 | 88 | 2711462196 | 69 | STRACATHRO | 1.5T | 5 | 10.3 | 9 | 90 | T1c | 4+5 | 4+5 | 128.3 | 0.08028 |
| 90 | 05/10/2015 | 89 | 2312510138 | 64 | NINEWELLS | 1.5T | 5 | 11.3 | 3 | 75 | T2 | N | 4+5 | 71.5 | 0.15804 |
| 91 | 05/10/2015 | 90 | 2308450010 | 70 | CRC | 3T | 5 | 11.7 | 1 | 30 | T1c | 3+4 | 4+3 | 45.6 | 0.25658 |
| 92 | 09/10/2015 | 91 | 1501560115 | 59 | NINEWELLS | 1.5T | 4 | 2.1 | 6 | 75 | T2 | 3+4 | 3+4 | 31.2 | 0.06731 |
| 93 | 09/10/2015 | 92 | 0807460079 | 69 | STRACATHRO | 1.5T | 5 | 10.7 | 6 | 20 | T1c | 3+4 | 3+4 | 118 | 0.09068 |

| | Date | | ID | Age | Centre | Field | | | | | T | G1 | G2 | | |
|---|---|---|---|---|---|---|---|---|---|---|---|---|---|---|---|
| 94 | 09/10/2015 | 93 | 0605440034 | 71 | CRC | 3T | 5 | 8.5 | 2 | 70 | T1c | 3+4 | 3+4 | 69.5 | 0.1223 |
| 95 | 26/10/2015 | 94 | 2003440275 | 71 | NINEWELLS | 1.5T | 5 | 10.1 | 1 | 50 | T1c | 3+4 | 3+4 | 161.4 | 0.06258 |
| 96 | 26/10/2015 | 95 | 2709510677 | 64 | CRC | 3T | 5 | 10.8 | 10 | 90 | T2 | 4+3 | 4+3 | 51.5 | 0.20971 |
| 97 | 03/11/2015 | 96 | 2203460555 | 69 | CRC | 3T | 5 | 10.9 | 11 | 90 | T1c | 4+3 | 3+4 | 40.5 | 0.26914 |
| 98 | 28/10/2015 | 97 | 1604560037 | 59 | CRC | 3T | 5 | 9.3 | 11 | 100 | T2 | 4+3 | 4+5 | 59.5 | 0.1563 |
| 99 | 17/11/2015 | 98 | 1309490171 | 66 | CRC | 3T | 5 | 8.1 | 6 | 80 | T2 | 5+4 | 4+3 | 43.2 | 0.1875 |
| 100 | 17/11/2015 | 99 | 0712480277 | 67 | STRACATHRO | 1.5T | 5 | 9.2 | 2 | 30 | T2 | 4+3 | 3+4 | 72.5 | 0.1269 |
| 101 | 24/11/2015 | 100 | 1012420094 | 67 | STRACATHRO | 1.5T | 5 | 11.4 | 3 | 10 | T2 | 3+3 | 3+4 | 60.5 | 0.18843 |
| 102 | 08/12/2015 | 101 | 1207450235 | 70 | STRACATHRO | 1.5T | 5 | 9 | 1 | 30 | T2 | 3+3 | 3+5 | 69.7 | 0.12912 |
| 103 | 08/12/2015 | 102 | 0903395193 | 76 | STRACATHRO | 1.5T | 5 | 22 | 1 | 10 | T2 | 4+4 | 4+3 | 83 | 0.26506 |
| 104 | 15/12/2015 | 103 | 1906570078 | 58 | CRC | 3T | 3 | 0.9 | 1 | 60 | T2 | 3+4 | 3+4 | 47 | 0.01915 |
| 105 | 05/01/2016 | 104 | 2405530236 | 62 | STRACATHRO | 1.5T | 5 | 3.8 | 6 | 90 | T2 | 4+4 | 4+3 | 32.8 | 0.11585 |
| 106 | 29/12/2015 | 105 | 0103420193 | 73 | CRC | 3T | 4 | 5 | 2 | 80 | T2 | 3+4 | 3+4 | 36 | 0.13889 |
| 107 | 29/12/2015 | 106 | 2011440157 | 71 | NINEWELLS | 1.5T | N | 7.6 | 1 | 5 | T2 | 3+3 | 3+4 | 99.25 | 0.07657 |
| 108 | 19/01/2016 | 107 | 2406530159 | 62 | STRACATHRO | 1.5T | 4 | 6 | 1 | 20 | T1c | 3+4 | 3+4 | 75.9 | 0.07905 |
| 109 | 19/01/2016 | 108 | 2303530059 | 62 | STRACATHRO | 1.5T | 4 | 11 | 2 | 10 | T1c | 3+3 | 3+3 | 115.4 | 0.09532 |
| 110 | 25/01/2016 | 109 | 2904450238 | 71 | CRC | 3T | 5 | 11.2 | 14 | 90 | T2 | 4+4 | 3+5 | 65 | 0.17231 |
| 111 | 25/01/2016 | 110 | 1605575577 | 59 | STRACATHRO | 1.5T | 5 | 22 | 3 | 80 | T3b | 4+5 | 4+5 | 89 | 0.24719 |
| 112 | 26/01/2016 | 111 | 0402460111 | 70 | not suit for MRI | | no mri | 7.1 | 7 | 70 | T1c | N | 3+4 | 71.8 | 0.09889 |
| 113 | 26/01/2016 | 112 | 2608540031 | 62 | NINEWELLS | 1.5T | 5 | 9 | 1 | 30 | T1c | 3+4 | 3+4 | 39.8 | 0.22613 |
| 114 | 09/02/2016 | 113 | 2706490055 | 67 | STRACATHRO | 1.5T | 4 | 8.7 | 1 | 5 | T1c | 4+3 | 4+3 | 58.5 | 0.14872 |
| 115 | 09/02/2016 | 114 | 1704510295 | 65 | CRC | 3T | 3 | 9.7 | 6 | 80 | T2 | 3+4 | 3+4 | 128 | 0.07578 |
| 116 | 16/02/2016 | 115 | 0906490170 | 67 | CRC | 3T* | 5 | 8.3 | 2 | 25 | T2b | 3+4 | 3+4 | 62.5 | 0.1328 |
| 117 | 16/02/2016 | 116 | 1312430117 | 73 | STRACATHRO | 1.5T | 5 | 9.4 | 8 | 80 | T1c | 3+4 | 3+4 | 58 | 0.16207 |
| 118 | 01/03/2016 | 117 | 1601390491 | 77 | STRACATHRO | 1.5T | 5 | 47.7 | 1 | 10 | T2 | 3+4 | 3+5 | 43 | 1.1093 |
| 119 | 01/03/2016 | 118 | 2507460156 | 70 | STRACATHRO | 1.5T | 5 | 16 | 5 | 70 | T3a | 3+3 | 3+4 | 73.5 | 0.21769 |
| 120 | 08/03/2016 | 119 | 0212460013 | 70 | CRC | 3T* | 5 | 4.6 | 1 | 50 | T2c | 3+4 | 3+4 | 76 | 0.06053 |
| 121 | 08/03/2016 | 120 | 1611520096 | 64 | NINEWELLS | 1.5T | 5 | 15.8 | 10 | 60 | T2 | 3+4 | 3+5 | 90 | 0.17556 |
| 122 | 22/03/2016 | 121 | 3103450036 | 71 | CRC | 3T | 3 | 12.6 | 1 | 10 | T2 | 3+3 | 3+4 | 90.8 | 0.13877 |
| 123 | 22/03/2016 | 122 | 1502450054 | 71 | CRC | 3T | 4 | 11.2 | 12 | 80 | T2 | 3+4 | 3+4 | 76 | 0.14737 |
| 124 | 29/03/2016 | 123 | 2702433359 | 73 | CRC | 3T | 5 | 9.8 | 1 | 50 | T3a | 3+4 | 3+4 | 44.5 | 0.22022 |
| 125 | 29/03/2016 | 124 | 0309440017 | 72 | NINEWELLS | 1.5T | 5 | 12 | 3 | 10 | T2c | 3+4 | 3+5 | 39 | 0.30769 |
| 126 | 12/04/2016 | 125 | 1205490213 | 67 | Claustrophobic | | cl | 2.9 | 3 | 40 | T2 | 4+3 | 3+5 | 81 | 0.0358 |
| 127 | 15/04/2016 | 126 | 1911520199 | 64 | CRC | 3T | 5 | 9 | 2 | 70 | T1c | 3+4 | 3+4 | 54.5 | 0.16514 |
| 128 | 03/05/2016 | 127 | 2802445456 | 72 | NINEWELLS | 1.5T | 5 | 17.4 | 5 | 100 | T2c | 3+4 | 4+3 | 89 | 0.19551 |
| 129 | 03/05/2016 | 128 | 1508400032 | 76 | CRC | 3T | 5 | 19.1 | 7 | 60 | T1c | 4+3 | 4+3 | 41.5 | 0.46024 |
| 130 | 10/05/2016 | 129 | 1509440011 | 72 | CRC | 3T* | 4 | 5.7 | 2 | 40 | T2 | 3+4 | 4+4 | 77 | 0.07403 |
| 131 | 10/05/2016 | 130 | 0605460590 | 70 | CRC | 3T* | 5 | 7.9 | 1 | 60 | T2b | 4+4 | 4+3 | 110 | 0.07182 |
| 132 | 19/05/2016 | 131 | 2801420077 | 74 | NINEWELLS | 1.5T | 5 | 15.8 | 12 | 95 | T3a | 4+5 | 4+5 | 61.5 | 0.25691 |
| 133 | 31/05/2016 | 132 | 2905500115 | 66 | NINEWELLS | 1.5T | 5 | 2.9 | 1 | 50 | T1c | 4+3 | 4+3 | 64 | 0.04531 |
| 134 | 31/05/2016 | 133 | 1003420257 | 74 | NINEWELLS | 1.5T | 5 | 9 | 8 | 30 | T1c | 3+3 | 3+4 | 93.5 | 0.09626 |
| 135 | 14/06/2016 | 134 | 1304410196 | 75 | CRC | 3T | 5 | 5.4 | 9 | 80 | T0 | 3+3 | 4+3 | 31 | 0.17419 |
| 136 | 14/06/2016 | 135 | 1608390373 | 77 | Claustrophobic | | cl | 5.6 | 10 | 70 | T2b | 4+5 | 4+5 | 20 | 0.28 |
| 137 | 21/06/2016 | 136 | 2309395277 | 77 | PERTH | 1.5T | 5 | 7 | 4 | 80 | T2c | 4+3 | 3+4 | 61.5 | 0.11382 |
| 138 | 21/06/2016 | 137 | 1107390516 | 77 | PERTH | 1.5T | 4 | 5.1 | 1 | 10 | T3a | 3+3 | 3+4 | 106.5 | 0.04789 |
| 139 | 05/07/2016 | 138 | 1508410097 | 75 | NINEWELLS | 1.5T | 4 | 8 | 1 | 50 | T2c | 3+4 | 3+4 | 170 | 0.04706 |
| 140 | 05/07/2016 | 139 | 0911460136 | 70 | STRACATHRO | 1.5T | N | 15 | 2 | 10 | T2 | 3+3 | 4+5 | 66.5 | 0.22556 |
| 141 | 12/07/2016 | 140 | 1010535552 | 63 | STRACATHRO | 1.5T | 4 | 4.6 | 6 | 30 | T2 | 4+5 | 4+5 | 39 | 0.11795 |
| 142 | 12/07/2016 | 141 | 2008490793 | 67 | PERTH | 1.5T | 5 | 19 | 6 | 60 | T1c | 4+4 | 4+5 | 103 | 0.18447 |
| 143 | 27/07/2016 | 142 | 1705500056 | 66 | CRC | 3T | 4 | 6.5 | 6 | 40 | T2c | 4+3 | 4+3 | 38.9 | 0.1671 |
| 144 | 27/07/2016 | 143 | 2111510033 | 65 | STRACATHRO | 1.5T | 5 | 14.4 | 7 | 80 | T2c | 4+3 | 4+3 | 60 | 0.24 |
| 145 | 16/08/2016 | 144 | 2906532096 | 63 | STRACATHRO | 1.5T | 5 | 10.8 | 3 | 10 | T2 | 3+4 | 3+4 | 46.4 | 0.23276 |
| 146 | 16/08/2016 | 145 | 2110410094 | 75 | CRC | 3T | 5 | 11.3 | 2 | 40 | T2c | 3+5 | 3+5 | 61.5 | 0.18374 |
| 147 | 19/08/2016 | 146 | 0406530831 | 63 | STRACATHRO | 1.5T | 4 | 4 | 1 | 30 | T1c | 3+4 | 3+4 | 36 | 0.11111 |
| 148 | 23/08/2016 | 147 | 0710475594 | 69 | CRC | 3T | 5 | 12 | 1 | 15 | T1c | 3+4 | 3+4 | 85.5 | 0.14035 |
| 149 | 23/08/2016 | 148 | 0311450113 | 71 | CRC | 1.5T | 5 | 7.1 | 1 | 50 | T2c | 3+4 | 3+5 | 86 | 0.08256 |
| 150 | 06/09/2016 | 149 | 1103440055 | 72 | NINEWELLS | 1.5T | 5 | 14.4 | 8 | 70 | T1c | 4+3 | 4+3 | 42 | 0.34286 |
| 151 | 13/09/2016 | 150 | 2209500079 | 66 | CRC | 3T | 4 | 4.8 | 7 | 20 | T1 | 3+3 | 3+4 | 35.5 | 0.13521 |
| 152 | 13/09/2016 | 151 | 1103430394 | 73 | PERTH | 1.5T | 4 | 9 | 7 | 60 | T1c | 3+4 | 3+4 | 45.1 | 0.19956 |
| 153 | 27/09/2016 | 152 | 1709450339 | 71 | NINEWELLS | 1.5T | 5 | 16 | 4 | 30 | T1 | 4+4 | 4+5 | 54.2 | 0.2952 |
| 154 | 30/09/2016 | 153 | 0906580536 | 58 | CRC | 3T | 5 | 7 | 8 | 40 | T1c | 4+3 | 3+4 | 54.3 | 0.12891 |
| 155 | 04/10/2016 | 154 | 0706510054 | 65 | CRC | 3T | 5 | 14 | 3 | 60 | T2c | 3+4 | 4+5 | 87 | 0.16092 |

139

| | | | | | | | | | | | | | | |
|---|---|---|---|---|---|---|---|---|---|---|---|---|---|---|
| 155 | 04/10/2016 | 154 | 0706510054 | 65 | CRC | 3T | 5 | 14 | 3 | 60 | T2c | 3+4 | 4+5 | 87 | 0.16092 |
| 156 | 04/10/2016 | 155 | 2705430059 | 73 | CRC | 3T | 5 | 13.9 | 1 | 30 | T2c | 3+4 | 3+4 | 207 | 0.06715 |
| 157 | 11/10/2016 | 156 | 0608555339 | 61 | STRACATHRO | 1.5T | 5 | 9.3 | 5 | 40 | T1c | 3+4 | 3+4 | 68 | 0.13676 |
| 158 | 18/10/2016 | 157 | 0211442216 | 72 | CRC | 3T | 3 | 30 | 1 | 10 | T1c | 4+3 | 4+5 | 100 | 0.3 |
| 159 | 18/10/2016 | 158 | 1609590058 | 57 | CRC | 3T | 4 | 8.5 | 4 | 10 | T2a | 3+3 | 3+4 | 60 | 0.14167 |
| 160 | 25/10/2016 | 159 | 1712400398 | 76 | CRC | 3T | 4 | 7.5 | 3 | 10 | T2a | 3+3 | 3+4 | 71.5 | 0.1049 |
| 161 | 25/10/2016 | 160 | 1704400236 | 76 | STRACATHRO | 1.5T | 5 | 6 | 1 | 50 | T2 | 4+4 | 4+5 | 118 | 0.05085 |
| 162 | 08/11/2016 | 161 | 2707500011 | 66 | CRC | 3T | 5 | 3.8 | 2 | 5 | T2c | 3+3 | 3+4 | 46.3 | 0.08207 |
| 163 | 08/11/2016 | 162 | 2303420415 | 74 | CRC | 3T | 5 | 9 | 10 | 80 | T2c | 4+4 | 4+5 | 88.5 | 0.10169 |
| 164 | 15/11/2016 | 163 | 2901470297 | 69 | NINEWELLS | 1.5T | 4 | 7.1 | 8 | 40 | T1c | 3+4 | 3+4 | 61.5 | 0.11545 |
| 165 | 15/11/2016 | 164 | 1712509799 | 66 | CRC | 3T | 3 | 8 | 2 | 20 | T1c | 3+4 | 3+4 | 78.8 | 0.10152 |
| 166 | 11/11/2016 | 165 | 3110560011 | 60 | CRC | 3T | 5 | 11.8 | 12 | 80 | T3b | 4+4 | 4+5 | 36 | 0.32778 |
| 167 | 06/12/2016 | 166 | 0810640392 | 52 | CRC | 3T | 3 | 8 | 6 | 50 | T0 | 4+3 | 3+4 | 34.5 | 0.23188 |
| 168 | 06/12/2016 | 167 | 1908420030 | 74 | CRC | 3T | 5 | 8 | 2 | 5 | T2a | 3+3 | 3+4 | 63 | 0.12698 |
| 169 | 29/11/2016 | 168 | 1903560934 | 60 | CRC | 3T | 5 | 6.4 | 10 | 100 | T2c | 3+5 | 3+4 | 57 | 0.11228 |
| 170 | 20/12/2016 | 169 | 1207430153 | 73 | CRC | 3T | 4 | 8 | 3 | 10 | T2c | 3+4 | 3+4 | 47.8 | 0.16736 |
| 171 | 23/12/2016 | 170 | 0104610158 | 55 | CRC | 3T | 5 | 7.6 | 5 | 80 | T2c | 4+3 | 3+5 | 36.7 | 0.20708 |
| 172 | 10/01/2017 | 171 | 1104440016 | 72 | STRACATHRO | 1.5T | 5 | 11.1 | 2 | 20 | T2c | 3+3 | 4+3 | 62 | 0.17903 |
| 173 | 10/01/2017 | 172 | 1507430019 | 73 | STRACATHRO | 1.5T | 5 | 15 | 7 | 40 | T2c | 4+4 | 4+5 | 57.2 | 0.26224 |
| 174 | 23/01/2017 | 173 | 0903565412 | 61 | CRC | 3T | 4 | 7 | 5 | 40 | T2 | 3+3 | 3+4 | 120 | 0.05833 |
| 175 | 31/01/2017 | 174 | 3101500117 | 67 | CRC | 3T | 5 | 8 | 2 | 30 | T2c | 4+4 | 3+4 | 47.5 | 0.16842 |
| 176 | 31/01/2017 | 175 | 1805532391 | 64 | CRC | 3T | 5 | 10.6 | 2 | 80 | T2c | 4+3 | 4+3 | 66.5 | 0.1594 |
| 177 | 03/02/2017 | 176 | 1806461293 | 71 | PERTH | 1.5T | 4 | 9.6 | 2 | 60 | T3 | 3+4 | 3+4 | 52.7 | 0.18216 |
| 178 | 07/02/2017 | 177 | 1308551231 | 62 | CRC | 3T | 5 | 14.5 | 10 | 90 | T2c | 4+3 | 4+3 | 51 | 0.28431 |
| 179 | 13/02/2017 | 178 | 0201420716 | 75 | CRC | 3T | 4 | 14.2 | 6 | 90 | T2c | 4+3 | 3+4 | 82.8 | 0.1715 |
| 180 | 22/02/2017 | 179 | 0704430118 | 74 | NINEWELLS | 1.5T | 5 | 10.1 | 4 | 20 | T2 | 3+4 | 3+4 | 107 | 0.09439 |
| 181 | 22/02/2017 | 180 | 1204520011 | 65 | NINEWELLS | 1.5T | 5 | 5.6 | 3 | 20 | T3a | 3+3 | 3+4 | 68.5 | 0.08175 |
| 182 | 28/02/2017 | 181 | 1901490394 | 68 | PERTH | 1.5T | 5 | 11.2 | 10 | 60 | T3a | 4+3 | 4+3 | 92 | 0.12174 |
| 183 | 02/03/2017 | 182 | 1503470296 | 70 | NINEWELLS | 1.5T | 5 | 0.1 | 6 | 40 | T2 | 3+4 | 3+4 | 52.3 | 0.00191 |
| 184 | 06/03/2017 | 183 | 2909440036 | 73 | STRACATHRO | 1.5T | 5 | 6.5 | 1 | 10 | T3a | 3+3 | 4+5 | 54 | 0.12037 |
| 185 | 14/03/2017 | 184 | 0202450090 | 72 | STRACATHRO | 1.5T | 5 | 17.7 | 12 | 95 | T2c | 3+4 | 4+3 | 46.5 | 0.38065 |
| 186 | 17/03/2017 | 185 | 1611540070 | 63 | NINEWELLS | 1.5T | 5 | 19.2 | 1 | 40 | T3a | 3+3 | 3+4 | 90.5 | 0.21215 |
| 187 | 27/03/2017 | 186 | 0210410116 | 76 | NINEWELLS | 1.5T | 5 | 8.2 | 9 | 90 | T3a | 4+3 | 3+4 | 33.7 | 0.24332 |
| 188 | 28/03/2017 | 187 | 2504420196 | 75 | NINEWELLS | 1.5T | 5 | 25 | 6 | 80 | T2c | 4+3 | 4+3 | 56.3 | 0.44405 |
| 189 | 04/04/2017 | 188 | 0405550154 | 62 | NINEWELLS | 1.5T | 5 | 6.5 | 8 | 50 | T3a | 4+4 | 4+5 | 45.5 | 0.14286 |
| 190 | 11/04/2017 | 189 | 0605523215 | 65 | CRC | 3T | 5 | 10.8 | 3 | 40 | T2c | 4+3 | 4+5 | 75.5 | 0.14305 |
| 191 | 11/04/2017 | 190 | 1709470178 | 70 | CRC | 3T | 5 | 9.3 | 4 | 30 | T2b | 3+4 | 3+4 | 50.5 | 0.18416 |
| 192 | 11/04/2017 | 191 | 1302560212 | 61 | NINEWELLS | 1.5T | 4 | 3.5 | 7 | 90 | T2 | 4+4 | 4+5 | 34.5 | 0.10145 |
| 193 | 25/04/2017 | 192 | 0501431152 | 74 | NINEWELLS | 1.5T | 5 | 10.6 | 6 | 80 | T3a | 4+5 | 4+5 | 58 | 0.18276 |
| 194 | 28/04/2017 | 193 | 2205500295 | 67 | CRC | 3T | 3 | 6.9 | 2 | 60 | T2c | 3+4 | 3+4 | 79.5 | 0.08679 |
| 195 | 02/05/2017 | 194 | 0704550636 | 62 | CRC | 3T | 5 | 6.9 | 3 | 25 | T1c | 3+3 | 3+4 | 59 | 0.11695 |
| 196 | 02/05/2017 | 195 | 1610412133 | 77 | STRACATHRO | 1.5T | 5 | 11.9 | 2 | 50 | T2b | 3+3 | 3+4 | 44 | 0.27045 |
| 197 | 16/05/2017 | 196 | 0404490190 | 68 | CRC | 3T | 5 | 9.2 | 3 | 40 | T2c | 3+3 | 3+4 | 71 | 0.12958 |
| 198 | 16/05/2017 | 197 | 0910450293 | 72 | STRACATHRO | 1.5T | 4 | 23 | 3 | 10 | T2c | 3+4 | 3+4 | 82.5 | 0.27879 |
| 199 | 17/05/2017 | 198 | 2703640617 | 53 | CRC | 3T | 5 | 22 | 12 | 70 | T3b | 3+4 | 4+5 | 58.3 | 0.37736 |
| 200 | 23/05/2017 | 199 | 309510058 | 66 | STRACATHRO | 1.5T | 3 | 10 | 3 | 40 | T2a | 3+4 | 3+4 | 147 | 0.06803 |
| 201 | 30/05/2017 | 200 | 2809610134 | 56 | NINEWELLS | 1.5T | 5 | 13 | 3 | 75 | T2c | 3+4 | 3+5 | 71 | 0.1831 |
| 202 | 31/05/2017 | 201 | 1201640016 | 53 | STRACATHRO | 1.5T | 5 | 7.3 | 11 | 90 | T3a | 4+4 | 3+5 | 45 | 0.16222 |
| 203 | 06/06/2017 | 202 | 1402470339 | 70 | CRC | 3T | 5 | 11.7 | 9 | 70 | T2c | 4+5 | 3+5 | 68.9 | 0.16981 |
| 204 | 09/06/2017 | 203 | 0107730057 | 44 | | | 4 | 3.2 | 2 | 20 | T2 | 4+3 | 3+4 | 28.8 | 0.11111 |
| 205 | 12/06/2017 | 204 | 1910550272 | 62 | | | N | 8.3 | 7 | 40 | T2c | 3+4 | 3+4 | 51.5 | 0.16117 |
| 206 | 13/06/2017 | 205 | 0705550354 | 62 | CRC | 3T | 4 | 15 | 6 | 85 | T2c | 3+4 | 4+5 | 76 | 0.19737 |
| 207 | 13/06/2017 | 206 | 1103430297 | 74 | | | 4 | 11.3 | 1 | 20 | T2a | 3+3 | 4+3 | 56.5 | 0.2 |
| 208 | 21/06/2017 | 207 | 1607520397 | 65 | CRC | 3T | 4 | 7.2 | 6 | 75 | T3a | 4+3 | 4+5 | 91 | 0.07912 |
| 209 | 27/06/2017 | 208 | 0302480439 | 69 | | | 5 | 6.2 | 5 | 30 | T2c | 3+4 | 3+4 | 52 | 0.11923 |
| 210 | 30/06/2017 | 209 | 3007580390 | 59 | CRC | 3T | 5 | 15.9 | 12 | 90 | T3a | 4+5 | 4+5 | 94 | 0.16915 |
| 211 | 04/07/2017 | 210 | 1802420592 | 75 | CRC | 3T | 5 | 9.7 | 3 | 100 | T2c | 3+4 | 3+4 | | #DIV/0! |
| 212 | 25/07/2017 | 211 | 2404470132 | 70 | CRC | 3T | 4 | 5.9 | 1 | 80 | T2a | 3+4 | 4+3 | | #DIV/0! |
| 213 | 25/07/2017 | 212 | 0108530493 | 64 | CRC | 3T | 5 | 16.4 | 7 | 90 | T2b | 4+4 | 4+5 | | #DIV/0! |
| 214 | 08/08/2017 | | 1604490071 | 68 | | | 5 | 23.5 | 10 | 90 | T2C | 3+4 | 3+4 | 55.5 | 0.42342 |
| 215 | 15/08/2017 | | 911580573 | 58 | | | 5 | 11.5 | 10 | 60 | T2c | 4+4 | 4+3 | 50.5 | 0.22772 |
| 216 | 15/08/2017 | | 2405430290 | 76 | | | 5 | 8.5 | | | T2c | 3+4 | 4+3 | 32.5 | 0.26154 |

| # | Date | ID | Age | | | | | | | T | | | | |
|---|---|---|---|---|---|---|---|---|---|---|---|---|---|---|
| 217 | 22/08/2017 | 1511610433 | 55 | | | N | 7.5 | 1 | 20 | T2c | 3+3 | 3+3 | 68 | 0.11029 |
| 218 | 22/08/2017 | 108470032 | 70 | | | 5 | 24.4 | 12 | 100 | T3b | 4+3 | 3+5 | 47.9 | 0.50939 |
| 219 | 29/09/2017 | 1608530310 | 64 | | | 5 | 9.8 | 10 | 80 | T2C | 3+4 | 3+4 | 29.2 | 0.33562 |
| 220 | 18/09/2017 | 2310500070 | 66 | | | 5 | 15.5 | 1 | 5 | | 4+4 | 4+5 | 42 | 0.36905 |
| 221 | 25/09/2017 | 711540659 | 62 | | | 5 | 6.2 | | | | 3+4 | 4+5 | | |
| 222 | 03/10/2017 | 1602590095 | 58 | | | 5 | 6.4 | 5 | 30 | T2C | 3+4 | 3+4 | 57.8 | 0.11073 |
| 223 | 29/09/2017 | 2803490315 | 68 | | | N | 5.1 | 6 | 20 | T2c | 3+4 | 3+4 | 125.2 | 0.04073 |
| 224 | 10/10/2017 | 402470834 | 70 | | | 5 | 10 | 1 | 10 | T2c | 3+4 | 3+4 | 55 | 0.18182 |
| 225 | 06/10/2017 | 3112430158 | 73 | | | 5 | 9.2 | 4 | 20 | T3b | 4+4 | 4+5 | 54.2 | 0.16974 |
| 226 | 07/11/2017 | 1708550097 | 62 | | | 4 | 6.1 | 3 | 20 | T2c | 3+3 | 3+4 | 66.9 | 0.09118 |
| 227 | 04/11/2017 | 3006420217 | 75 | | | 4 | 12.7 | 2 | 10 | T2c | 3+4 | 3+4 | 182.5 | 0.06959 |
| 228 | 04/11/2017 | 2805490177 | 68 | | | 5 | 19.4 | 9 | 70 | T2c | 4+3 | 4+3 | 43.5 | 0.44598 |
| 229 | 22/11/2017 | 403540011 | 63 | | | 4 | 6.4 | 1 | 25 | T2c | n | 3+4 | 69.8 | 0.09169 |
| 230 | 14/10/2017 | 1809440297 | 73 | | | 5 | 34.9 | 3 | 40 | T3a | 4+4 | 4+5 | 70.2 | 0.49715 |
| 231 | 13/10/2017 | 509490611 | 68 | | | 4 | 8 | 5 | 80 | T3a | 3+4 | 3+4 | 54 | 0.14815 |
| 232 | 21/12/2017 | 2012500595 | 66 | | | 3 | 5.6 | 5 | 15 | T2c | 3+4 | 3+4 | 165.5 | 0.03384 |
| 233 | 21/12/2017 | 605520097 | 65 | | | 5 | 5.9 | 10 | 90 | T3a | 3+3 | 3+4 | 110.5 | 0.05339 |
| 234 | 19/12/2017 | 2104521270 | 65 | | | 5 | 6.2 | 5 | 40 | T2c | 4+3 | 4+3 | 52 | 0.11923 |
| 235 | 01/11/2017 | 1111410119 | 76 | | | 5 | 6.6 | 5 | 40 | T3a | 4+4 | 4+3 | 40.4 | 0.16337 |
| 236 | 24/01/2018 | 910630011 | 63 | | | 4 | 0.1 | 4 | 30 | T2c | 3+4 | 3+4 | 65 | 0.00154 |
| 237 | 18/01/2018 | 1402500416 | 68 | | | 4 | 7.5 | 3 | 30 | T2c | 4+3 | 4+3 | 83 | 0.09036 |
| 238 | 23/01/2018 | 911420096 | 76 | | | 4 | 10.6 | 6 | 40 | T2c | 3+4 | 3+4 | 112 | 0.09464 |
| 239 | 24/01/2018 | 2904450351 | 73 | | | 5 | 13 | 6 | 80 | T3a | 4+5 | 4+5 | 123 | 0.10569 |
| 240 | 26/01/2018 | 1710460210 | 72 | | | 4 | 6.8 | 4 | 40 | T2c | 4+5 | 4+5 | 36.9 | 0.18428 |
| 241 | 09/01/2018 | 1807510395 | 67 | | | 5 | 5.9 | 8 | 40 | T2c | 3+4 | 3+4 | 80.5 | 0.07329 |
| 242 | 11/01/2018 | 602450438 | 73 | | | 5 | 23.4 | 5 | 40 | T2c | 5+4 | 4+5 | 109 | 0.21468 |
| 243 | 16/01/2018 | 611500299 | 68 | | | 5 | 8.7 | 1 | 10 | T3a | 4+3 | 4+3 | 41 | 0.2122 |
| 244 | 22/01/2018 | 1209530112 | 65 | | | 5 | 12.7 | 12 | 90 | T3a | 4+5 | 4+5 | 50.5 | 0.25149 |
| 245 | 03/01/2018 | 907610293 | 57 | | | 5 | 7 | 3 | 10 | T2c | 3+3 | 3+4 | 28 | 0.25 |
| 246 | 06/02/2018 | 503530077 | 65 | | | n | 7.9 | 1 | 20 | T2c | 4+3 | 4+3 | 37.8 | 0.20899 |
| 247 | 15/02/2018 | 1706470630 | 70 | | | 5 | 8.5 | 1 | 5 | T2c | 4+4 | 4+3 | 82.4 | 0.10316 |
| 248 | 20/02/2018 | 212510037 | 67 | | | 4 | 9.6 | 2 | 10 | T2c | 3+3 | 3+4 | 76 | 0.12632 |
| 249 | 26/02/2018 | 803520018 | 66 | | | 5 | 8 | 7 | 80 | T2c | 3+4 | 3+4 | 36.2 | 0.22099 |
| 250 | 27/02/2018 | 1508560196 | 62 | | | 5 | 5.6 | 4 | 80 | T2c | 3+3 | 3+4 | 60 | 0.09333 |
| 251 | 06/03/2018 | 1001440153 | 74 | | | 4 | 6.6 | 3 | 60 | T2c | 4+4 | 4+3 | 48.2 | 0.13693 |
| 252 | 14/03/2018 | 1512500070 | 68 | | | n | 7.1 | 5 | 40 | T2c | 4+3 | 3+4 | 16 | 0.44375 |
| 253 | 15/03/2018 | 1305540239 | 64 | | | 4 | 11.1 | 3 | 40 | T2c | 4+3 | 4+5 | 41.7 | 0.26619 |
| 254 | 20/03/2018 | 1410530272 | 65 | | | 4 | 4.5 | 2 | 10 | T2a | 3+3 | 3+4 | 19.7 | 0.22843 |
| 255 | 26/03/2018 | 208520139 | 66 | | | 5 | 8.5 | | | T2c | | 3+4 | 40.2 | 0.21144 |
| 256 | 27/03/2018 | 1401510434 | 67 | | | n | 8.4 | 3 | 10 | T2c | 4+3 | 3+4 | 142 | 0.05915 |
| 257 | 08/04/2018 | 1505690153 | 49 | | | n | 6.1 | 5 | 50 | T2c | 3+3 | 3+4 | 20 | 0.305 |
| 258 | 15/04/2018 | 810420015 | 76 | | | n | 7.1 | 6 | 30 | T2c | 4+3 | 4+3 | 35 | 0.20286 |
| 259 | 16/04/2018 | 1911506250 | 68 | | | 5 | 5.2 | 2 | 50 | T2c | 3+3 | 3+4 | 52 | 0.1 |
| 260 | 17/04/2018 | 3004560453 | 62 | | | 5 | 44 | 1 | 5 | T2c | 3+3 | 3+4 | 138.5 | 0.31769 |
| 261 | 24/04/2018 | 806505435 | 68 | | | 5 | 16.9 | 1 | 30 | T2c | 4+3 | 4+3 | 67.2 | 0.25149 |
| 262 | 10/05/2018 | 202590038 | 59 | | | 4 | 2.4 | 3 | 20 | T2C | 4+3 | 4+3 | 55 | 0.04364 |
| 263 | 25/05/2018 | 1001625277 | 56 | | | 4 | 15.2 | 5 | 60 | T2C | 3+4 | 3+4 | 48 | 0.31667 |
| 264 | 15/05/2018 | 503460079 | 72 | | | 5 | 6.9 | 4 | 30 | T2C | 3+4 | 3+4 | 38.5 | 0.17922 |
| 265 | 29/05/2018 | 1611600073 | 58 | | | 3 | 6 | 11 | 40 | T3b | 4+3 | 4+3 | 26.9 | 0.22305 |
| 266 | 30/05/2018 | 2202620230 | 56 | | | 4 | 11.2 | 10 | 90 | T2c | 3+3 | 3+4 | 80.5 | 0.13913 |
| 267 | 05/06/2018 | 1105615499 | 57 | | | 5 | 5.9 | 9 | 80 | T2c | 3+4 | 3+4 | 51 | 0.11569 |
| 268 | 21/06/2018 | 2512560015 | 62 | | | 5 | 18 | 7 | 90 | T3a | 4+5 | 4+5 | 65.6 | 0.27439 |
| 269 | 22/06/2018 | 708480314 | 70 | | | 5 | 6.7 | 9 | 80 | T3a | 4+5 | 4+5 | 49 | 0.13673 |
| 270 | 18/06/2018 | 1302480111 | 70 | | | 3 | 8.6 | 6 | 5 | T2C | 4+3 | 3+4 | 52.25 | 0.16459 |
| 271 | 19/06/2018 | 2007430096 | 75 | | | 5 | 14.6 | 5 | 40 | T3a | 4+5 | 4+5 | 43 | 0.33953 |
| 272 | 21/06/2018 | 2512560015 | 62 | | | 5 | 18 | 7 | 90 | T3a | 4+5 | 4+5 | 65.6 | 0.27439 |
| 273 | 22/06/2018 | 708480314 | 70 | | | 4 | 6.4 | 9 | 80 | T3a | 4+5 | 4+5 | 49 | 0.13061 |
| 274 | 02/07/2018 | 2805430573 | 75 | | | 5 | 9.4 | 2 | 20 | T2c | 3+4 | 3+4 | 44.5 | 0.21124 |
| 275 | 10/07/2018 | 1201550033 | 63 | | | 5 | 6.9 | 5 | 70 | T2c | 3+4 | 3+4 | 36.3 | 0.19008 |
| 276 | 12/07/2018 | 1601580118 | 60 | | | 5 | 6.9 | 6 | 90 | T2c | 3+4 | 3+4 | 44 | 0.15682 |
| 277 | 30/07/2018 | 209570172 | 61 | | | 5 | 18.7 | 11 | 80 | T3b | 4+5 | 4+5 | 45 | 0.41556 |

| | Date | ID | Age | | | | | | | T | Gleason | Gleason | | |
|---|---|---|---|---|---|---|---|---|---|---|---|---|---|---|
| 278 | 17/07/2018 | 2612450211 | 73 | | | 5 | 6.9 | 2 | 50 | T2c | 3+4 | 3+4 | 62.5 | 0.1104 |
| 279 | 20/07/2018 | 206580339 | 60 | | | 5 | 6.6 | 12 | 80 | T3b | 4+5 | 4+5 | 41 | 0.16098 |
| 280 | 14/08/2018 | 1012460533 | 72 | | | 5 | 10.7 | 8 | 90 | T3b | 5+5 | 5+4 | 66 | 0.16212 |
| 281 | 21/08/2018 | 2503430090 | 75 | | | 4 | 3.5 | 4 | 60 | T2c | 4+4 | 3+4 | 47 | 0.07447 |
| 282 | 22/08/2018 | 403500052 | 68 | | | 5 | 7 | 4 | 70 | T2c | 4+4 | 3+4 | 31 | 0.22581 |
| 283 | 30/08/2018 | 203420098 | 76 | | | 4 | 4.9 | 10 | 80 | T3a | 4+3 | 3+4 | 29 | 0.16897 |
| 284 | 11/09/2018 | 209460016 | 72 | | | 5 | 8.2 | 3 | 50 | T2c | 4+3 | 4+3 | 76 | 0.10789 |
| 285 | 10/09/2018 | 1109460198 | 72 | | | 4 | 8.5 | 3 | 15 | T2c | 3+3 | 4+3 | 43 | 0.19767 |
| 286 | 13/09/2018 | 1806450518 | 73 | | | 5 | 8.6 | 4 | 80 | T2c | 3+5 | 3+5 | 82 | 0.10488 |
| 287 | 18/10/2018 | 1201450195 | 70 | | | 4 | 13 | | | T3a | 3+3 | 4+5 | 39 | 0.33333 |
| 288 | 18/09/2018 | 704572273 | 61 | | | 5 | 41.7 | 5 | 100 | T3b | 4+5 | 4+5 | 12 | 3.475 |
| 289 | 20/09/2018 | 1611590019 | 59 | | | no mri | 16.4 | 10 | 90 | T2c | 3+4 | | | |
| 290 | 19/09/2018 | 1810440211 | 74 | | | 5 | 9.5 | | | T3b | 3+4 | 4+4 | 73 | 0.13014 |
| 291 | 02/10/2018 | 3010450079 | 75 | | | 5 | 27 | 6 | 15 | T3a | 4+4 | 4+4 | 85 | 0.31765 |
| 292 | 05/10/218 | 2009440358 | 74 | | | 4 | 24.7 | 1 | 10 | T2c | 3+4 | 3+4 | 55.9 | 0.44186 |
| 293 | 19/10/2018 | 607590076 | 59 | | | 5 | 5.4 | 4 | 30 | T3a | 4+3 | 4+4 | 48 | 0.1125 |
| 294 | 23/10/2018 | 2002590958 | 59 | | | 5 | 5.4 | 3 | 20 | T2a | 4+5 | 4+5 | 35 | 0.15429 |
| 295 | 30/10/2018 | 1710490098 | 69 | | | 4 | 5.2 | 3 | 30 | T3a | 3+4 | 3+4 | 49 | 0.10612 |
| 296 | 01/11/2018 | 108420337 | 76 | | | 4 | 17.1 | 1 | 10 | T2a | 3+4 | 3+4 | 39 | 0.43846 |
| 297 | 06/11/2018 | 112645658 | 54 | | | 5 | 12 | 4 | 50 | T3b | 4+5 | 5+4 | 34 | 0.35294 |
| 298 | 13/11/2018 | 3003450433 | 73 | | | 5 | 8.8 | 2 | 60 | T3a | 4+3 | 4+4 | 68 | 0.12941 |
| 299 | 14/11/2018 | 2109420316 | 75 | | | no mri | 7.2 | 1 | 25 | T3a | 4+4 | 4+4 | | |
| 300 | 19/11/2018 | 606550135 | 63 | | | 5 | 16 | 11 | 80 | T3a | 4+5 | 4+5 | 73 | 0.21918 |
| 301 | 20/11/2018 | 1012565556 | 62 | | | 4 | 5.9 | 3 | 10 | T2c | 3+3 | 3+4 | 30 | 0.19667 |
| 302 | 07/11/2018 | 2808605714 | 58 | | | 5 | 6 | 8 | 90 | T2c | 4+4 | 4+4 | 60 | 0.1 |
| 303 | 31/10/2018 | 604630492 | 55 | | | n | 7.1 | 1 | 10 | T2a | 3+4 | 3+4 | | |
| 304 | 27/11/2018 | 2312550733 | 63 | | | clu | 6.7 | 5 | 90 | T3a | 4+3 | 4+3 | | |
| 305 | 03/12/2018 | 2903570310 | 61 | | | 4 | 8.7 | 4 | 10 | T2c | 4+4 | 3+4 | 51 | 0.17059 |
| 306 | 04/12/2018 | 1609570014 | 61 | | | 4 | 5.4 | 6 | 100 | T2c | 3+4 | 3+4 | 25 | 0.216 |
| 307 | 05/12/2018 | 3103552335 | 63 | | | 5 | 8.2 | 2 | 20 | T3a | 4+3 | 4+3 | 53 | 0.15472 |
| 308 | 06/12/2018 | 1203515251 | 67 | | | 4 | 10 | 3 | 80 | T3b | 3+4 | 3+4 | 124 | 0.08065 |
| 309 | 11/12/2018 | 1507580118 | 60 | | | 5 | 18.5 | 10 | 90 | T2c | 3+4 | 3+4 | 31 | 0.59677 |
| 310 | 12/12/2018 | 806560630 | 62 | | | 5 | 11.2 | 3 | 10 | T2c | 4+3 | 3+4 | 57 | 0.19649 |
| 311 | 13/12/2018 | 1111490031 | 69 | | | 4 | 6.3 | 7 | 70 | T2a | 3+4 | 3+4 | 45 | 0.14 |
| 312 | 17/12/2018 | 805620435 | 56 | | | 3 | 6 | 0 | 0 | T2c | n | 3+4 | 31 | 0.19355 |
| 313 | 18/12/2018 | 2202540512 | 64 | | | 4 | 19.4 | 10 | 80 | T2c | 3+4 | 3+4 | 30 | 0.64667 |
| 314 | 19/12/2019 | 2106530137 | 65 | | | 5 | 9.6 | 4 | 20 | T2c | 4+4 | 4+3 | 35 | 0.27429 |
| 315 | 28/12/2018 | 708450016 | 73 | | | 5 | 8.2 | 7 | 70 | T2c | 3+3 | 4+3 | 34 | 0.24118 |
| 316 | 04/01/2019 | 2701456053 | 73 | | | no mri | 11 | 6 | 20 | T3a | 4+4 | 4+4 | | |
| 317 | 08/01/2019 | 1812420412 | 76 | | | 5 | 13 | 4 | 90 | T2c | 4+3 | 3+4 | 49 | 0.26531 |
| 318 | 09/01/2019 | 2105512097 | 67 | | | 5 | 7.7 | 12 | 90 | T3b | 4+5 | 4+5 | 41 | 0.1878 |
| 319 | 14/01/2019 | 1106500016 | 68 | | | 4 | 18 | 12 | 90 | T3b | 4+5 | 4+5 | 29 | 0.62069 |
| 320 | 15/01/2019 | 803590032 | 59 | | | 5 | 19 | 12 | 90 | T3a | 4+5 | 4+5 | 31 | 0.6129 |
| 321 | 17/01/2019 | 2506630139 | 55 | | | 5 | 9.4 | 12 | 90 | T3a | 4+3 | 4+3 | 48 | 0.19583 |
| 322 | 24/01/2019 | 1402560117 | 62 | | | 5 | 9.4 | 10 | 70 | T2c | 4+3 | 3+4 | 70 | 0.13429 |
| 323 | 22/01/2019 | 1506470416 | 71 | | | no mri | 7.2 | 1 | 5 | T2c | 4+3 | 4+3 | | |
| 324 | 21/01/2019 | 806559179 | 63 | | | 4 | 10.5 | 1 | 10 | T2a | 3+4 | 3+4 | 117 | 0.08974 |
| 325 | 29/01/2019 | 307440095 | 74 | | | 5 | 6.3 | 1 | 25 | T2c | 3+4 | 3+4 | 80 | 0.07875 |
| 326 | 05/02/2019 | 2904470158 | 71 | | | 5 | 5.4 | 6 | 60 | T2c | 3+4 | 4+3 | 38 | 0.14211 |
| 327 | 12/02/2019 | 206560095 | 62 | | | 5 | 8.3 | 12 | 100 | T3b | 4+3 | 4+3 | 36 | 0.23056 |
| 328 | 19/02/2019 | 406460094 | 72 | | | 5 | 7.9 | 12 | 100 | T3a | 4+5 | 5+4 | 45 | 0.17556 |
| 329 | 25/02/2019 | 412560038 | 62 | | | 5 | 7.4 | 5 | 50 | T2c | 3+4 | 3+4 | 37 | 0.2 |
| 330 | 06/03/2019 | 3107570370 | 61 | | | 5 | 8.1 | 1 | 60 | T2c | 4+5 | 4+5 | 64 | 0.12656 |
| 331 | 07/03/2019 | 1702620654 | 56 | | | 3 | 8.2 | 3 | 20 | T2c | 3+4 | 3+4 | 88 | 0.09318 |

| No. | Study ID | age* | Date of MRI Scan | PSA (ng/ml) | MRI Result | lesion focus | Highest PIRADS | location | target lesion size (mm) | Biopsy Type | biopsy result | Highest G Grade | Location | Fusion | Highest G Grade |
|---|---|---|---|---|---|---|---|---|---|---|---|---|---|---|---|
| 1 | T0001IC | 64 | 17/02/2015 | 7.9 | P | 1 | 5 | 9p, 10p | 14 | F | P | 3+4 | 1, 2, 4, 6, 9, 11 | P | 3+3 |
| | | | | | | 2 | 3 | 1a | 10 | | | | | | 3+3 |
| | | | | | | 3 | 3 | 9a | 13 | | | | | | |
| | | | | | | 4 | 3 | 3a | 20 | | | | | | |
| 4 | T0004AW | 73 | 10/03/2015 | 7.3 | P | 1 | 5 | 1a | 16 | F | P | 3+4 | 4, 6 | P | 3+3 |
| | | | | | | 2 | 5 | 3p | 25 | | | | | | NO |
| 16 | T0016RD | 69 | 02/06/2015 | 11.7 | P | 1 | 5 | (14,15)as,(10,12)a | 25 | F | N | | | P | 3+4 |
| 17 | T0017NM | 58 | 02/06/2015 | 11.2 | P | 1 | 5 | ,5P,6P,7,8,9,10,1 | 40 | F | P | 4+3 | EXP 2 | P | 4+3 |
| 19 | T0019NM | 69 | 16/06/2015 | 9.7 | P | 1 | 5 | (7-10)p | 15 | F | P | 4+3 | 6 | P | 3+4 |
| | | | | | | 2 | 5 | 1p, 2p, 4p, 9p | 15 | | | | | | 4+3 |
| 23 | T0023DN | 63 | 30/06/2015 | 10.8 | P | 1 | 5 | 1p, 2p, 7p | 28 | F | P | 4+3 | 2-6, 10, 12 | P | 3+4 |
| | | | | | | 2 | 5 | 5p, 11p | 15 | | | | | | 4+3 |
| | | | | | | 3 | 5 | 13as | 21 | | | | | | |
| 24 | T0024JN | 65 | 30/06/2015 | 7.7 | P | 1 | 5 | 9p, 10p, 129 | 16 | F | P | 4+4 | 7 | P | 5+4 |
| | | | | | | 2 | 4 | 6a, 15as | 12 | | | | | | NO |
| | | | | | | 3 | 4 | 1p, 7p | 32 | | | | | | |
| 27 | T0027SF | 60 | 15/07/2015 | 6.2 | P | 1 | 5 | 6a, 6p, 5p | 16 | F | N | | | N | NO |
| | | | | | | 2 | 3 | 1a | 25 | | | | | | NO |
| 28 | T0028JS | 73 | 15/07/2015 | 5 | P | 1 | 4 | 11p, 12p | 11 | F | N | | | P | 3+4 |
| | | | | | | 2 | 3 | 7a | 19 | | | | | | 3+4 |
| 34 | T0034ED | 68 | 13/08/2015 | 13.8 | P | 1 | 3 | 1a | 20 | F | N | | | N | NO |
| 35 | T0035RM | 70 | 18/08/2015 | 12.4 | P | 1 | 5 | all | 44 | F | P | 4+4 | 10 | P | 4+3 |
| 38 | T0038IM | 70 | 01/11/2015 | 12.6 | P | 1 | 3 | 14as | 22 | F | P | 3+3 | 1 | N | NO |
| 39 | T0039TM | 72 | 18/11/2015 | 9.9 | P | 1 | 5 | 10p, 10a | 17 | F | N | | | P | 3+4 |
| | | | | | | 2 | 5 | 13as | 16 | | | | | | NO |
| 40 | T0040PH | 66 | 18/11/2015 | 5.9 | P | 1 | 4 | 1a | 10 | F | P | 3+3 | 7 | P | 3+3 |
| | | | | | | 2 | 3 | 12p | 9 | | | | | | 3+3 |
| 42 | T0042DM | 70 | 02/12/2015 | 8.7 | P | 1 | 4 | 6p, 5p | 12 | F | P | 3+4 | 2,3,6,7,8,9,10 | P | 3+4 |
| | | | | | | 2 | 4 | 12p | 10 | | | | | | NO |
| | | | | | | 3 | 3 | 9a | 19 | | | | | | |
| 46 | T0046JS | 62 | 22/12/2015 | 7.3 | P | 1 | 4 | 3a, 5a | 13 | F | N | | | P | 3+3 |
| | | | | | | 2 | 4 | 12p | 7 | | | | | | 3+4 |
| | | | | | | 3 | 4 | 12a, 12p | 6 | | | | | | |
| 49 | T0049RM | 75 | 13/01/2016 | 5.7 | P | 1 | 5 | , 2a, (4-6)a, 9p | 36 | F | P | 5+4 | 4, 6 | P | 4+5 |
| 51 | T0051LE | 74 | 20/01/2016 | 6.8 | P | 1 | 5 | (1-4)a, 2p, 4p | 15 | F | P | 3+4 | 5,6 | P | 3+4 |
| | | | | | | 2 | 4 | 10p | 10 | | | | | | 3+3 |
| 55 | T0055AR | 51 | 10/02/2016 | 14.5 | P | 1 | 4 | 12p | 11 | F | N | | | N | NO |
| 58 | T0058JT | 59 | 02/03/2016 | 9.1 | p | 1 | 5 | 7-12)pa, 3p, 5 | 36 | F | P | 4+3 | 7,8,11,12 | P | 4+5 |
| | | | | | | 2 | 4 | 4a, 6a | 11 | | | | | | 3+3 |
| 59 | T0059JM | 62 | 09/03/2016 | 6.6 | P | 1 | 5 | 8a 8p 10a 10p | 18 | F | P | 3+3 | 5,9,12 | P | 3+4 |
| | | | | | | 2 | 5 | 1p 3p 4p | 15 | | | | | | NO |
| 63 | T0063GR | 69 | 23/03/2016 | 14.4 | P | 1 | 5 | 3,7,9)a, (13-15 | 33 | F | N | | | N | NO |
| | | | | | | 2 | 5 | 9a,12a,12p | 15 | | | | | | NO |
| 64 | T0064TD | 57 | 30/03/2016 | 4.6 | P | 1 | 5 | (7-10)p | 18 | F | P | 4+3 | 1,3,4,6 | P | NO |
| | | | | | | 2 | 4 | 10a | 9 | | | | | | 4+3 |
| 68 | T0068IM | 57 | 19/04/2016 | 4.5 | P | 1 | 4 | 2p, 1p | 10 | F | P | 3+3 | 7, 9 | N | NO |
| | | | | | | 2 | 3 | 10a | 9 | | | | | | NO |
| 70 | T0070SS | 74 | 04/05/2016 | 11.3 | P | 1 | 5 | 6a, 5a, 6p, 15as | 20 | F | N | | | P | 3+3 |
| | | | | | | 2 | 5 | 9a | 15 | | | | | | 3+5 |
| | | | | | | 3 | 4 | 10a, 10p | 10 | | | | | | |
| | | | | | | 4 | 4 | 12a | 10 | | | | | | |
| 71 | T0071IC | 52 | 04/05/2016 | 10.2 | P | 1 | 4 | 2A,2p, 4a,4p | 11 | F | N | | | N | NO |

| # | Code | Age | Date | | | | | | | | | | | | |
|---|---|---|---|---|---|---|---|---|---|---|---|---|---|---|---|
| 73 | T0073AD | 70 | 18/05/2016 | 7.1 | P | 1 | 5 | a,p | 33 | F | N | | | P | 3+4 |
| | | | | | | 2 | 5 | p | 15 | | | | | | NO |
| 75 | T0075JS | 74 | 25/05/2016 | 8.2 | P | 1 | 5 | 10p,12p | 15 | F | P | 3+3 | 7, 8 | N | NO |
| 78 | T0078DO | 57 | 08/06/2016 | 4.8 | P | 1 | 4 | 4p | 10 | F | N | | | N | NO |
| | | | | | | 2 | 4 | 10p | 9 | | | | | | NO |
| 80 | T0080SS | 65 | 15/06/2016 | 14 | P | 1 | 5 | (3-6)p | 16 | F | P | 3+4 | 6 | P | 3+4 |
| | | | | | | 2 | 4 | 12a | 8 | | | | | | NO |
| 83 | T0083DF | 63 | 05/10/2016 | 5.5 | P | 1 | 5 | 3p,9p | 15 | F | N | | | P | 3+3 |
| | | | | | | 2 | 4 | 6p,5p | 8 | | | | | | 3+3 |
| 84 | T0084AH | 62 | 29/06/2016 | 3 | P | 1 | 3 | 3a | 10 | F | N | | | N | NO |
| 90 | T0090WL | 74 | 20/07/2016 | 14.4 | P | 1 | 4 | 5p,6p | 12 | F | N | | | N | NO |
| | | | | | | 2 | 4 | 6a | 10 | | | | | | NO |
| 93 | T0093AD | 66 | 09/08/2016 | 7 | P | 1 | 4 | 15as | 12 | F | N | | | N | NO |
| 94 | T0094mm | 51 | 10/08/2016 | 9.1 | P | 1 | 3 | 1a,13as | 15 | F | P | 4+3 | 9,11 | P | NO |
| | | | | | | 2 | 3 | 15as | 9 | | | | | | 3+3 |
| 99 | T0099PT | 63 | 07/09/2016 | 10.2 | P | 1 | 5 | 10p,12a,12p | 15 | F | N | | | P | 4+3 |
| | | | | | | 2 | 4 | 1p,2p,3p,4p | 9 | | | | | | 4+3 |
| | | | | | | 3 | 3 | 1a,7a | 18 | | | | | | |
| 101 | T0101DM | 59 | 14/09/2016 | 1.7 | P | 1 | 5 | 10p,8a,8p,11, | 31 | F | N | | | N | NO |
| | | | | | | 2 | 5 | 3p,4a,4p,6p | 19 | | | | | | NO |
| 107 | T0107GP | 63 | 12/10/2016 | 11 | P | 1 | 5 | 13as,7a | 30 | F | N | | | P | 3+3 |
| | | | | | | 2 | 4 | 9p,10p | 19 | | | | | | NO |
| 112 | T0112JR | 57 | 09//11/2016 | 4.4 | P | 1 | 4 | 1A | 10 | F | N | | | N | NO |
| | | | | | | 2 | 4 | 11A | 7 | | | | | | NO |
| | | | | | | 3 | 3 | 9A | 12 | | | | | | |
| 114 | T0114DK | 68 | 16/11/2016 | 2.2 | P | 1 | 5 | 12P | 16 | F | N | | | N | NO |
| 116 | T0116SB | 61 | 23/11/2016 | 8.6 | P | 1 | 5 | 3P,4P | 20 | F | P | 4+4 | ALL | P | 4+4 |
| | | | | | | 2 | 4 | 10P,9P | 18 | | | | | | NO |
| | | | | | | 3 | 4 | 3P | 8 | | | | | | |
| | | | | | | 4 | 4 | 3P,9P | 6 | | | | | | |
| 118 | T0118JW | 70 | 02/12/2016 | 9.9 | P | 1 | 5 | 3P | 13 | F | P | 4+4 | 3 7 8 11 | P | 4+4 |
| 120 | T0120ER | 71 | 07/12/2016 | 10.1 | P | 1 | 3 | 11p, 12p | 17 | F | N | | | N | NO |
| 123 | T0123BA | 55 | 15/12/2016 | 6.1 | P | 1 | 5 | 13as, 14as | 24 | F | P | 3+3 | 1, 9, 10 | N | NO |
| | | | | | | 2 | 4 | 12p | 8 | | | | | | NO |
| 124 | T0124RW | 68 | 21/12/2016 | 7.6 | P | 1 | 3 | 7a | 20 | F | N | | | N | NO |
| 129 | T0129JC | 69 | 11/01/2017 | 5.4 | P | 1 | 4 | 10a, 10p | 10 | F | N | | | N | NO |
| 131 | T0131FR | 64 | 18/01/2017 | 12.1 | P | 1 | 5 | 2a,3a,4a,13as,1 | 22 | F | P | 3+3 | 9 10 | P | 4+3 |
| | | | | | | 2 | 4 | 10p | 10 | | | | | | NO |
| 133 | T0133PM | 69 | 25/01/2017 | 11.7 | P | 1 | 5 | 10p,9p,12p | 16 | F | P | 4+5 | 10 11 12 | P | NO |
| | | | | | | 2 | 4 | 4a | 13 | | | | | | 4+4 |
| | | | | | | 3 | 4 | 10a | 7 | | | | | | |
| 135 | T0135ID | 71 | 01/02/2017 | 4.7 | P | 1 | 3 | m4 | 7 | F | N | | | N | NO |
| 138 | T0138BF | 66 | 15/02/2017 | 12.2 | P | 1 | 4 | m4 | 27 | F | N | | | N | NO |
| | | | | | | 2 | 4 | a3 | 5 | | | | | | NO |
| | | | | | | 3 | 4 | a4 | 4 | | | | | | |
| 140 | T0140RM | 70 | 22/02/2017 | 9.7 | P | 1 | 5 | m2 | 17 | F | P | 3+4 | 9 | P | NO |
| | | | | | | 2 | 4 | a3 | 9 | | | | | | 3+4 |
| 142 | T0142IW | 60 | 01/03/2017 | 7.7 | P | 1 | 3 | m2 | 14 | F | N | | | N | NO |
| 145 | T0145GC | 61 | 08/03/2017 | 14.4 | P | 1 | 4 | m3 | 11 | F | P | 4+3 | 3 | P | NO |
| | | | | | | 2 | 3 | a4 | 10 | | | | | | 3+4 |
| 149 | T0149RC | 67 | 29/03/2017 | 8.5 | P | 1 | 5 | b1,b2,m1 | 25 | F | N | | | N | NO |
| 150 | T0150AM | 63 | 29/03/2017 | 16.4 | P | 1 | 5 | ,b4,m2,m4,a2, | 30 | F | P | 4+3 | 8 9 10 11 12 | P | 4+4 |
| 154 | T0154NJ | 64 | 12/04/2017 | 9.3 | P | 1 | 5 | b1,m1,b3,m3 | 32 | F | P | 3+4 | 10 | P | 4+5 |
| | | | | | | 2 | 5 | m2 | 22 | | | | | | 3+3 |
| 159 | T0159NM | 67 | 26/04/2017 | 9.1 | P | 1 | 4 | m1,m3 | 21 | F | N | | | N | NO |

| No | ID | Age | Date | Value | P | Core | Grade | Location | Len | F | Res1 | Gl1 | Sites | Res2 | Gl2 |
|---|---|---|---|---|---|---|---|---|---|---|---|---|---|---|---|
| 162 | T0162RH | 73 | 10/05/2017 | 9.3 | P | 1 | 4 | m3 | 16 | F | P | 4+3 | 1 2 5 | N | NO |
| 165 | T0165HH | 68 | 17/05/2017 | 8.3 | P | 1 | 5 | m3,m4 | 20 | F | N | | | N | NO |
| 167 | T0167JS | 73 | 24/05/2017 | 8.2 | P | 1 | 4 | a3 | 11 | F | P | 3+4 | 2 3 4 6 | P | NO |
| | | | | | | 2 | 4 | a4 | 10 | | | | | | 3+3 |
| 169 | T169ND | 58 | 01/06/2017 | 6.5 | P | 1 | 5 | b2,m1,m2,a1, | 35 | F | P | 3+4 | 3 | P | NO |
| | | | | | | 2 | 5 | a3 | 22 | | | | | | 3+4 |
| | | | | | | 3 | 4 | a4 | 13 | | | | | | |
| 170 | T0170LB | 62 | 01/06/2017 | 16.4 | P | 1 | 5 | b4,m1,m2,m3 | 39 | F | P | 5+4 | 12 | P | 4+4 |
| | | | | | | 2 | 5 | m2 | 15 | | | | | | 4+5 |
| 173 | T0173CS | 64 | 14/06/2017 | 6.3 | P | 1 | 3 | m2 | 11 | F | N | | | P | 3+3 |
| 174 | T0174FC | 67 | 14/06/2017 | 19.6 | P | 1 | 5 | m4,a4 | 21 | F | P | 4+3 | 8,9,10,11 | P | 3+4 |
| | | | | | | 2 | 5 | b3,m3 | 16 | | | | | | 3+4 |
| 179 | T0179DB | 69 | 29/06/2017 | 6.1 | P | 1 | 3 | m3,m4,a3,a4 | 37 | F | N | | | N | NO |
| 181 | T0181SM | 50 | 05/07/2017 | 10.8 | P | 1 | 5 | b3,b4,m2,m3, | 30 | F | P | 5+4 | 5, 7…11 | P | 4+5 |
| | | | | | | 2 | 4 | a4 | 5 | | | | | | 5+4 |
| 184 | T0184AG | 66 | 02/08/2017 | 6.3 | P | 1 | 3 | m1,m3 | 16 | F | N | | | N | NO |
| 187 | T0187GE | 69 | 16/08/2017 | 5.4 | P | 1 | 5 | 1,b2,m1,m3,a | 22 | F | P | 4+5 | 7 | P | 4+5 |
| | | | | | | 2 | 4 | a4 | 9 | | | | | | 4+5 |
| 188 | T0188JM | 74 | 16/08/2017 | 9.3 | P | 1 | 5 | b2,b4,m2,m4 | 22 | F | N | | | N | NO |
| 191 | T0191AT | 71 | 23/08/2017 | 18.3 | P | 1 | 5 | ,b4,m3,m4,a3 | 36 | F | P | 4+5 | 3 5 11 | P | 4+5 |
| 193 | T0193RH | 73 | 30/08/2017 | 6.7 | P | 1 | 4 | a4 | 14 | F | P | 4+5 | 7 9 10 | N | NO |
| | | | | | | 2 | 4 | a4 | 4 | | | | | | NO |
| 196 | T0196DH | 67 | 13/09/2017 | 6.9 | P | 1 | 4 | m4 | 13 | F | P | 4+3 | 11 | P | 3+4 |
| | | | | | | 2 | 4 | a3,a4 | 12 | | | | | | 3+4 |
| 204 | T0204BA | 55 | 04/10/2017 | 6.5 | P | 1 | 3 | m4 | 15 | F | N | | | N | NO |
| 207 | T0207SP | 60 | 20/10/2017 | 7.2 | P | 1 | 4 | m4 | 12 | F | P | 3+3 | 12 | P | 3+3 |
| 210 | T0210AR | 70 | 01/11/2017 | 8.5 | P | 1 | 5 | b1,b2 | 18 | F | N | | | P | 4+4 |
| | | | | | | 2 | 3 | m4 | 13 | | | | | | N0 |
| 213 | T0213JS | 61 | 08/11/2017 | 12.5 | P | 1 | 3 | m2 | 15 | F | N | | | N | NO |
| 215 | T0215PN | 64 | 15/11/2017 | 7 | P | 1 | 4 | m3 | 13 | F | N | | | P | 4+4 |
| | | | | | | 2 | 3 | m1 | 10 | | | | | | NO |
| 219 | T0219IM | 75 | 29/11/2017 | 3.3 | P | 1 | 5 | ,b4,m2,m4,a2 | 28 | F | P | 4+5 | 11 | P | 3+4 |
| 223 | T0223RR | 71 | 13/12/2017 | 6.5 | P | 1 | 5 | b4 | 15 | F | P | 3+4 | 2 | P | 3+3 |
| 226 | T0226HA | 57 | 03/01/2018 | 6 | P | 1 | 3 | a4 | 11 | F | P | 4+3 | 8,12 | P | 3+4 |
| 228 | T0228TM | 67 | 10/01/2018 | 10.2 | P | 1 | 5 | m2,m4 | 19 | F | P | 3+3 | 7,8 | N | NO |
| | | | | | | 2 | 4 | m4 | 13 | | | | | | |
| | | | | | | 3 | 4 | b3 | 11 | | | | | | |
| 231 | T0231SD | 65 | 24/01/2018 | 6.9 | P | 1 | 5 | b1,b3 | 30 | F | P | 3+4 | 3,5,6 | N | NO |
| 234 | T0234RP | 67 | 31/01/2018 | 6.7 | P | 1 | 5 | b4 | 30 | F | P | 4+5 | 7-9,11 | P | 4+5 |
| 237 | T0237NS | 71 | 14/02/2018 | 10.6 | P | 1 | 5 | m3,a3 | 15 | F | P | 3+4 | 12 | P | 3+4 |
| | | | | | | 2 | 4 | a4 | 12 | | | | | | NO |
| | | | | | | 3 | 4 | m1 | 8 | | | | | | |
| | | | | | | 4 | 4 | b4 | 6 | | | | | | |
| | | | | | | 5 | 4 | m2 | 5 | | | | | | |
| 240 | T0240JP | 74 | 21/02/2018 | 10.5 | P | 1 | 5 | b4,m4 | 16 | F | P | 3+4 | 3 | P | 3+3 |
| | | | | | | 2 | 4 | m2 | 6 | | | | | | 3+4 |
| 241 | T0241TJ | 71 | 28/02/2018 | 14.7 | P | 1 | 5 | b2,b4,m2,m4 | 16 | F | P | 4+3 | 7,8,9,19 | P | 3+4 |
| 243 | T0243WM | 56 | 07/03/2018 | 11.4 | P | 1 | 4 | b4,m4 | 12 | F | P | 3+3 | ALL | N | NO |
| 248 | T0248GK | 68 | 21/03/2018 | 9.3 | P | 1 | 3 | b3 | 10 | F | P | 3+4 | 11 | P | 3+3 |
| 249 | T0249RR | 69 | 28/03/2018 | 6.7 | P | 1 | 5 | b1,b3,m1,m3, | 18 | F | P | 4+5 | 3,6 | P | 4+3 |
| | | | | | | 2 | 4 | m2 | 8 | | | | | | 3+4 |
| 253 | T0253JK | 73 | 09/04/2018 | 13.4 | P | 1 | 4 | m2 | 14 | F | N | | | P | 3+4 |
| 255 | T0255TC | 61 | 11/04/2018 | 18.9 | P | 1 | 5 | 4,m1,m2,m3, | 45 | F | P | 4+4 | | P | 4+5 |
| 257 | T0257SP | 52 | 18/04/2018 | 6.7 | P | 1 | 4 | m1,m2 | 11 | F | P | 3+3 | 1,3 | N | NO |
| 260 | T0260PH | 72 | 30/04/2018 | 10.3 | P | 1 | 5 | m1,a1 | 18 | F | N | | | N | NO |

Check for updates

**OPEN**

# Prediction of prostate cancer Gleason score upgrading from biopsy to radical prostatectomy using pre-biopsy multiparametric MRI PIRADS scoring system

Saeed Alqahtani[1,2,5], Cheng Wei[1,6], Yilong Zhang[2], Magdalena Szewczyk-Bieda[3], Jennifer Wilson[4], Zhihong Huang[2] & Ghulam Nabi[1] ✉

An increase or 'upgrade' in Gleason Score (GS) in prostate cancer following Transrectal Ultrasound (TRUS) guided biopsies remains a significant challenge to overcome. to evaluate whether MRI has the potential to narrow the discrepancy of histopathological grades between biopsy and radical prostatectomy, three hundred and thirty men treated consecutively by laparoscopic radical prostatectomy (LRP) between July 2014 and January 2019 with localized prostate cancer were included in this study. Independent radiologists and pathologists assessed the MRI and histopathology of the biopsies and prostatectomy specimens respectively. A multivariate model was constructed using logistic regression analysis to assess the ability of MRI to predict upgrading in biopsy GS in a nomogram. A decision-analysis curve was constructed assessing impact of nomogram using different thresholds for probabilities of upgrading. PIRADS scores were obtained from MRI scans in all the included cases. In a multivariate analysis, the PIRADS v2.0 score significantly improved prediction ability of MRI scans for upgrading of biopsy GS (p = 0.001, 95% CI [0.06–0.034]), which improved the C-index of predictive nomogram significantly (0.90 vs. 0.64, p < 0.05). PIRADS v2.0 score was an independent predictor of postoperative GS upgrading and this should be taken into consideration while offering treatment options to men with localized prostate cancer.

Histology from biopsies categorised into Gleason score is the only confirmatory test for cancer diagnosis and is most commonly used for risk stratification of men with a recent diagnosis of prostate cancer. Based on this men are counselled for various treatment options. MR imaging data is not considered in risk stratification at present. With increasing therapeutic options available to men with a diagnosis of prostate cancer, scrutiny of information from biopsy grade becomes increasingly important. There is around 35.5% (range: 14–51%) upgrading of biopsy GS on LRP[1]. Many factors contribute to the discrepancy between needle biopsy and corresponding radical surgery GS. Under calling of Gleason cribriform Gleason pattern 4 as pattern 3 or the presence of borderline grades due to barely appreciable glandular differentiation under microscope and lack of sampling of tertiary grade disease on biopsies are known contributors. Factors such as age, size of prostate, extent of cancer on biopsy needle and number of biopsy samples (extended/ or mapping) have also been known to impact on the incidence of upgrading[2].

In light of a number of studies reporting upgrading or under-grading of prostate cancer on needle biopsies, there is the potential for under treatment or overtreatment (i.e. radiotherapy and hormone duration). Several publications[3,4] and consensus updates on the Gleason grading system have partially addressed this issue including recommendation of deriving GS by adding the most common and highest Gleason pattern on biopsy rather than

[1]Division of Imaging Sciences and Technology, School of Medicine, Ninewells Hospital, University of Dundee, Dundee, UK. [2]School of Science and Engineering, University of Dundee, Dundee, UK. [3]Department of Clinical Radiology, Ninewells Hospital, Dundee, UK. [4]Department of Pathology, Ninewells Hospital, Dundee, UK. [5]Department of Radiological sciences, college of applied medical science, Najran University, Najran, Saudi Arabia. [6]These authors contributed equally: Saeed Alqahtani and Cheng Wei. ✉e-mail: g.nabi@dundee.ac.uk
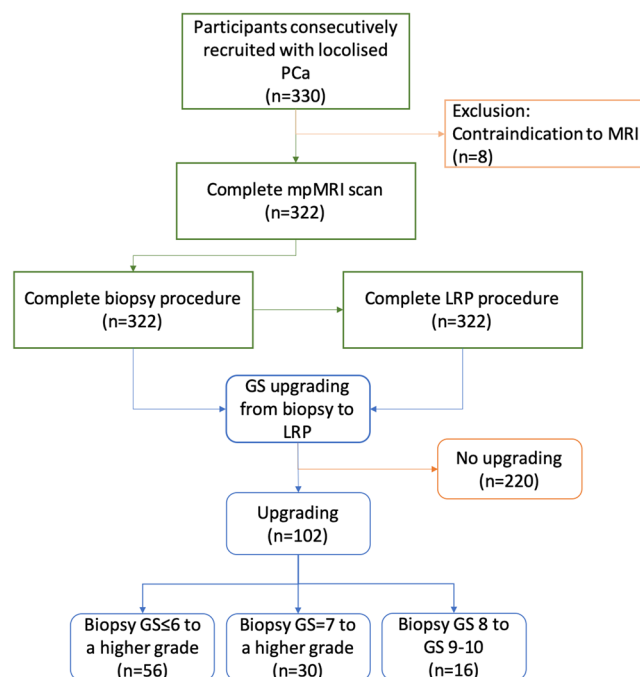
**Figure 1.** Flowchart of the study.

original method of adding the primary and second most common patterns[5]. Moreover, upgrading if suspected, has long-term outcome implications. Corcoran *et al.*[6] have shown that even after adjusting for known preoperative variables (including clinical stage, prostate-specific antigen (PSA), number of positive cores and percentage of positive cores) upgrade to a higher Gleason Score (GS) remained a strong and independent predictor of biochemical recurrence after attempted local curative therapy, this underscores the importance of gaining more information to predict upgrading of biopsy GS in men diagnosed with prostate cancer as this may serve as a marker of biologically aggressive disease.

Pre-biopsy MRI has recently been shown to hold great promise in the detection and characterisation of prostate cancer[7]. A negative scan (no lesion seen on the MRI scan) showed a high negative predictive value for the presence of significant prostate cancer[8]. Song *et al.*[9] reported a high predictive value of PIRADS v2 in predicting upgrading of GS from biopsy, however this study was retrospective and MR Imaging was obtained at least 3 weeks following biopsies - an approach known to impact interpretation of images. Post-biopsy haemorrhage is the most common false-positive finding for prostate cancer[10]. In this study, there was no attempt to align histopathological sectioning to MRI using recently reported 3D-mould technology. Therefore, this is the first report describing predictive accuracy of pre-biopsy MRI in upgrading biopsy GS following LRP using patient-specific 3D moulds to ensure permitted alignment of excised prostates with MRI scans.

## Patients and methods

**Study population.** This is a study with prior Caldicott institutional approval (Caldicott/IGTCAL5626). All experiments including the study protocol study followed approved institutional guidelines. The study had ethical approval (14/ES/1070) with each participant informed consenting to the use of their imaging data. Between July 2014 and January 2019, 330 men consecutively treated by LRP who were diagnosed with localised prostate cancer with raised PSA or/and abnormal digital rectal examination were included in this study. They were offered mpMRI and those with positive MRI results (PIRADS score 3 and above) were performed transrectal ultrasound (TRUS)-guided prostate biopsy (12 cores) followed. Of these patients, eight were excluded because of contraindication to MRI such as a heart pacemaker and metallic foreign body including three claustrophobic patients. Further analysis included remaining 322 patients (Fig. 1). The clinical, pathological and imaging factors information of the patients, including age, weight, preoperative PSA, PSA density, number of positive cores, maximum percentage of cancer per core and PIRADS v2 score on multiparametric MRI (mpMRI) were recorded. GS upgrading defined as a biopsy GS increasing from lower to higher grade on reported before[2]. Table 1 summarises the baseline characteristics between upgraded and non-upgraded groups of the cohort.

**Hypotheses of the study.** We hypothesised that pre-biopsy MRI with PIRADS classification of suspicious area in prostatic cancer improve prediction of GS upgrading from biopsy to radical prostatectomy. Upgrading of GS on histology was defined as change of GS from lower to higher grade between biopsy and histology from radical prostatectomy.

**MRI protocol and PIRADS score.** All patients' mpMRI scans were performed on 3 T scanner (TIM Trio, Siemens, Erlangen, Germany) 2 weeks before TRUS-guided biopsies. The mpMRI protocol was derived from the European Society of Uro-radiology Guidelines 2012 for the detection of prostate cancer and the subsequent

| | Total | Upgrading | No upgrading |
|---|---|---|---|
| **Number of patients** | **322** | **102** | **220** |
| Age (y), mean ± SD (range) | 66.83 ± 5.9(44–77) | 66.82 ± 6.12(49–77) | 66.85 ± 5.9(44–77) |
| Prostate Weight mean ± SD (range) | 63.7 ± 30.13(12–207) | 65.3 ± 26.2(20–155) | 63.1 ± 31.78(12–207) |
| PSA level (ng/ml), mean ± SD (range) | 11.1 ± 7.39(0.1–47.7) | 12.6 ± 9.98(2–47.7) | 10.39 ± 5.7(0.1–41) |
| PSA Density (ng/ml²), mean ± SD (range) | 0.261 ± 0.234 (0.001–3.48) | 0.212 ± 0.183(0.035–1.11) | 0.203 ± 0.254(0.00198–3.48) |
| Number of positive cores | 4.8 ± 3.4(1–12) | 4.1 ± 3.07(1–12) | 5.08 ± 3.42(1–12) |
| Maximum percentage of cancer per core | 50.2 ± 30.4(5–100) | 42.5 ± 30.6(5–100) | 53.3 ± 29.52(5–100) |
| PIRADS from mpMRI Benign (1,2) | 17 (5%) | 4 (4%) | 13 (6%) |
| PIRADS 3 | 21 (7%) | 6 (6%) | 15(7%) |
| PIRADS 4 | 78 (24%) | 26 (26%) | 52 (23%) |
| PIRADS 5 | 206 (64%) | 66 (65%) | 140 (64%) |

**Table 1.** Patient characteristics.

| | T1WI | | High resolution T2WI | | | DWI | | DCE |
|---|---|---|---|---|---|---|---|---|
| | Axial | Sagittal | Axial | Coronal | DWI | DWI high b-value | | Dyn Gd-MRI |
| TR (ms) | 650 | 6000 | 4000 | 5000 | 3300 | 3300 | | 4.76 |
| Sequence | 2DTSE | 2DTSE | 2DTSE | 2DTSE | 2DEPI | 2DEPI | | 3D VIBE |
| TE (ms) | 11 | 102 | 100 | 100 | 95 | 95 | | 2.45 |
| Flip angle (°) | 150 | 140 | 150 | 150 | — | — | | 10 |
| Slice thickness (mm) | 3 | 3 | 3 | 3 | 3 | 3 | | 3 |
| Slice gap (mm) | 0.6 | 0.6 | 0.6 | 0.6 | 0 | 0 | | 0.6 |
| Resolution (pixels) | 320 | 320 | 320 | 320 | 192 | 192 | | 192 |
| FOV (mm) | 200 | 200 | 200 | 200 | 280 | 280 | | 280 |
| b-values (s/mm²) | — | — | — | — | 50,100,500,1000 | 2000 | | — |
| Temporal resolution (s) | — | — | — | — | — | — | | 4 |

**Table 2.** MRI acquisition parameters.

publication of version 2[11]. Table 2 briefly summarizes the MRI acquisition parameters. Localiser images were acquired in all three imaging planes, whereby the plane of the prostate was defined in relation to the rectal wall.

The mpMRI images were analysed and scored by experienced uro-radiologists using PIRADS v2.0; and the radiologists were blinded to all patients' pathology results. PIRADS v2.0 assessment categories were described as follows: score 1, clinically significant cancer is highly unlikely to be present; score 2, clinically significant cancer is unlikely to be present; score 3, the presence of clinically significant cancer is equivocal; score 4, clinically significant cancer is likely to be present; and score 5, clinically significant cancer is highly likely to be present (Fig. 2).

**Histopathology data and analysis.** The biopsy results were analysed by experienced pathologists; who were blinded to MRI findings. The GS for each patient was obtained. The radical prostate specimens for histology were sliced in patient-specific moulds to aid orientations between imaging and histology, which were fabricated using a 3D printer as described by our group and others previously[12,13]. Specifically, patient specific 3D printed moulds were made prior to surgery based on the T2-weighted MRI prostate capsule the moulds were customised for each patient using MIMICS and Solidworks. Moulds were printed at 200 micro resolution using a consumer grade 3D printer (MakerBot Replicator 5th generation). The average mould required 120 minutes to design, 4 to 7 hours to print and an expense for materials of less than $7[12].

**Statistical analysis.** Baseline characteristics of patients and pathological outcomes were compared using a chi-square test for categorical data (PIRADS score) and a Student t-test or ANOVA for continuous data (age, weight, PSA level, PSAD, number of positive cores and maximum percentage of cancer per core). Univariate logistic regression was applied to investigate the association of clinical variables with the upgrading of biopsy GS. Variables with $P < 0.05$ in the univariate analysis were further assessed using a multivariate logistic regression analysis to identify factors predictive of GS upgrading. In order to estimate the area under the curve (AUC) for predicting GS upgrading to determine the diagnostic performance of clinical variables with or without PIRADS score, a receiver operating characteristic (ROC) curve analysis was conducted.

In addition, logistic regression model coefficients were used to perform a nomogram predicating the probability of GS upgrading. Non-informative or non-significant variables in univariate logistic regression for GS upgrading were removed. The value of concordance indexes (c-index) were calculated and compared. The bias-corrected calibrated values were generated from internal validation based on 200 bootstrap resamples.

A decision-analysis curve was constructed assessing impact of nomogram using different thresholds probabilities of upgrading (none of the GS upgrade to all GS upgrade).
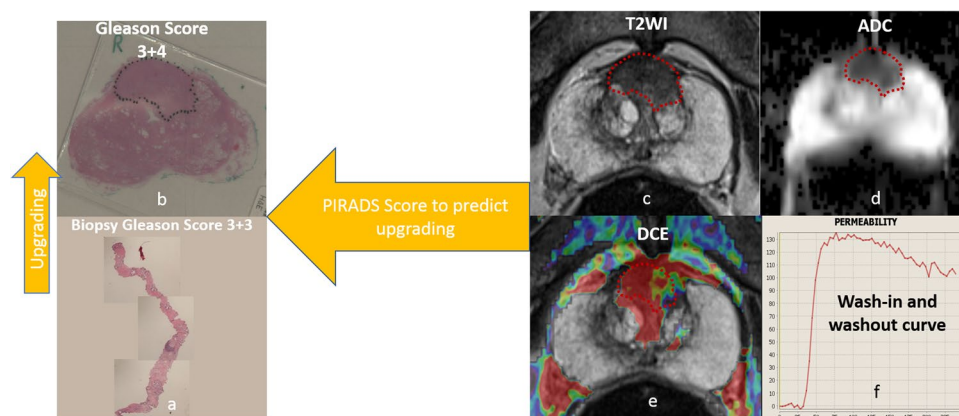
**Figure 2.** (**a**) A 73 year-old man with Gleason score 6 disease on prostate cancer on TRUS-Guided biopsies. (**b**) The grade was upgrading to GS 7 on whole mount radical prostatectomy specimen (**c**) Axial T2-wighted image shows ill-defined homogeneous low-signal-intensity on the central zone (**d**), Apparent diffusion coefficient (ADC) shows restricted diffusion in low-signal mass and (**e**) dynamic contrast enhanced (DCE) shows fast and strong enhancement and early contrast agent washout (type 3 curve), (**e,f**) The lesion was scored as PIRADSv2 5 (>1.5 cm) and based on parameters described here.

| Biopsy Gleason sum | Radical prostatectomy Gleason sum | | | | |
|---|---|---|---|---|---|
| | 6 | 7 | 8 | 9–10 | Total |
| 1–5 | 0 | 3 | 0 | 1 | 4 |
| 6 | 6 | 46 | 2 | 4 | 58 |
| 7 | 0 | 145 | 14 | 16 | 175 |
| 8 | 0 | 19 | 9 | 16 | 44 |
| 9–10 | 0 | 2 | 3 | 36 | 41 |
| Total | 6 | 215 | 28 | 73 | 322 |

**Table 3.** Comparison between biopsy and radical prostatectomy Gleason score sum.

Analyses were performed using SPSS 22 (IBM Corporation, New York, US) and R software. The alpha level was set at 0.05 to determine two-tailed significance.

## Results

**Upgrading cohort characteristics.** In total, 322 men were included in our study. Table 3 shows the concordance between the biopsy and prostatectomy Gleason score sums. Of these, (102/322; 31.6%) had GS upgrading from biopsy to LRP. Almost half of this upgrading was from biopsy GS $\leq$ 6 disease (56/102; 55%). More than half of whole cohort (175/322; 54%) had a GS 7 on prostate biopsy and (30/175; 17%) men had GS upgrading. Finally, eighty five of the cohort (85/322; 26%) had a GS $\geq$ 8 on prostate biopsy and (16/85; 18.8%) men had GS upgrading from GS 8 on prostate biopsy to GS > 8 at LRP.

The correlation between PIRADS score and pathologic GS at LRP is demonstrated in Fig. 3. Of the 322 patients, the distribution of PIRADS score was as follows: score 1 and 2 in 17 (17/322; 5%) patients, score 3 in 21 (21/322; 7%) patients, score 4 in 78 (78/322; 24%) patients, and score 5 in 206 (206/322; 64%) patients.

**Predictions of GS upgrading.** Table 4 shows the outcomes of the logistic regression analysis and predictive variables of GS upgrading. On univariate analyses, increased preoperative PSA levels, number of positive cores, maximum percentage of cancer per core and PIRADS $\geq$ 4 were all significantly associated with GS upgrading (p < 0.05). Age, weight of prostate and PSAD did not show any significance (p > 0.05) which were excluded from further analyses. In the multivariate analyses, PIRADS $\geq$ 4 and higher PSA level were both statistically significant and independently predictive of GS upgrading (p = 0.001 and 0.003, respectively).

In Fig. 4, PIRADS v2 score with PSA value show a higher accuracy than PSA alone for predicting GS upgrading (AUC = 0.90 and 0.64, respectively, p < 0.001).

**Impact of PIRADS score on prediction of GS upgrading in relation to other factors.** Figure 5a$_1$,a$_2$ show the nomograms constructed for upgradation of biopsy GS with and without PIRADS v2 score data. Longer scales indicated higher percentage of impact and larger points were suggesting probability of upgrading. PIRADS score had the greatest impact followed by PSA level. C-index of the established nomogram which had PIRADS v2 score variable to predict the GS upgrading in the cohort was significantly higher than that of the nomogram
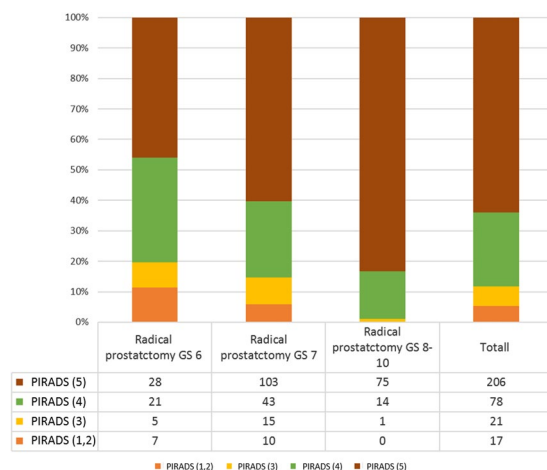
**Figure 3.** Radical prostatectomy Gleason score stratified according to PIRADS score.

| | Univariate | | Multivariate | |
|---|---|---|---|---|
| | OR (95% CI) | *P*-value | OR (95% CI) | *P*-value |
| Age | 1.005 (0.962–1.041) | 0.799 | | |
| Pathology weight | 1.002(0.931–1.009) | 0.540 | | |
| Number of positive cores | 0.86(0.87–0.96) | 0.005 | 0.970(0.98–1.01) | 0.69 |
| PSA level (ng/ml) | 1.040 (1.009–1.073) | 0.001 | 1.09(1.030–1.160) | 0.003 |
| PSA Density (ng/ml²) | 1.15 (0.44–3.04) | 0.76 | | |
| Maximum percentage of cancer per core | 0.988 (0.980–0.96) | 0.002 | 0.970 (0.84–1.12) | 0.62 |
| PIRADS | | | | |
| ≤3 | 1 (reference) | — | 1 (reference) | — |
| >3 | 0.017(0.08–0.04) | 0.001 | 0.014 (0.06–0.034) | 0.001 |

**Table 4.** Univariate and multivariate logistic regression analysis.

without PIRADS score (0.90 [95% CI 0.87–0.89] vs. 0.64 [95% CI, 0.57–0.70], p = 0.001). The nomograms were then validated using 200 bootstrap samples, internal calibration curves are shown in Fig. 5b$_1$,b$_2$.

**Decision curve analysis.** The decision analysis curve is shown in Fig. 6. The net benefit for the model using PIRADS score was significantly higher at all thresholds compared with the model without PIRADS score. As seen in Fig. 6, the decision curve line (depicted by a red line) of the model without the PIRADS scores remained close to the line with threshold probabilities ranging from 0 to 0.25. In contrast, a higher positive net benefit was obtained in the range of threshold probabilities ranging from 0.05 to 1.0 in the model with PIRADS scores.

## Discussion

**Principal findings of the study.** This is the first study to bring together information of PIRADS scores in pre-biopsy MRI and an improved image oriented histopathological grossing of RP specimen by making the use of the mould, bridging the gap in the existing literature. Our results indicate a significant advantage (C-index 0.90 vs 0.64) of using the prediction model including PIRADS scores added to conventional clinic-pathological characteristics (PSA level, percentage of cancer on core-biopsies, gland size etc.) of men with prostate cancer confirmed by systematic transrectal random biopsies relative to a model without PIRADS scores. Prostate biopsy GS upgrading remains a challenge for physicians managing localised prostate cancer, as better knowledge of contributing factors and how to narrow the gap is lacking[2]. To inform any consensus, we need an improved understanding of the role imaging can play, in particular pre-biopsy MRI, in predicting GS change and adverse downstream oncological outcomes. Although, recent improvements have been made in refining biopsy strategies and in reducing sampling errors, a significant and continued effort is still needed to identify men at risk of GS upgrading.

**Study findings in context of the reported literature.** Wang JY *et al.*[14] reported a nomogram with C-index of 0.795 using preoperative factors without imaging data in a non-screened population from China. This is similar to our study as the healthcare system for the cohort reported here did not have men screened for prostate cancer. Table 5 shows the predictive ability of various reported nomograms in upgrading of biopsy GS of prostate cancer in screened populations[1,14–17]. The upgrading rate of biopsy GS seen in our cohort is similar to a larger cohort of 2982 patients reported previously[15]. A higher percentage of men with a GS of 6 were upgraded in the present study. It is interesting that despite the higher number of cores obtained in the present study (12 in
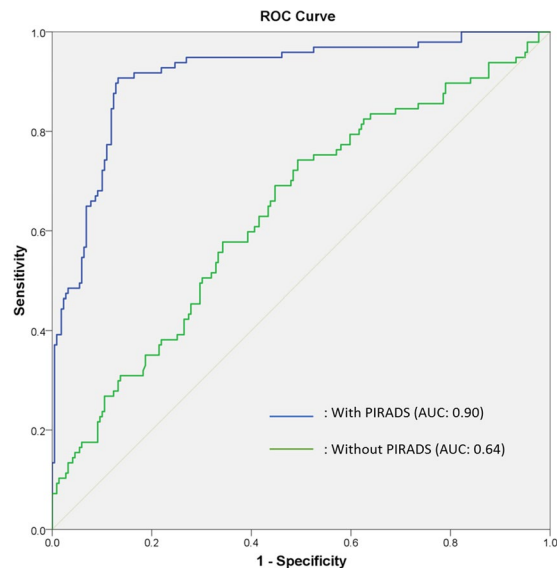
**Figure 4.** Receiver operating characteristic (ROC) curve of the clinical variables with and without PIRADS score.
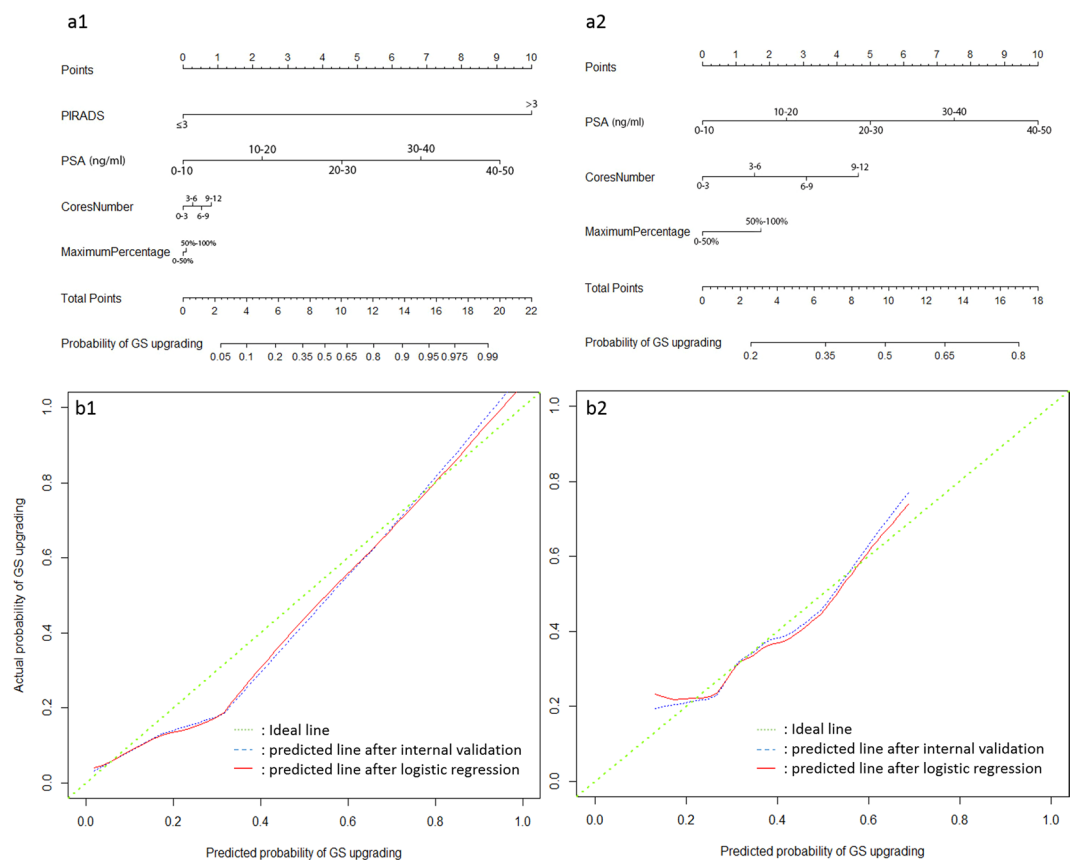


**Figure 5.** The nomograms of Gleason score upgrading prediction with (a1) and without PIRADS score (a2). Calibration plots of observed and predicted probability of GS upgrading with (b1) and without PIRADS score (b2).

number) in comparison with 6–10 biopsy cores obtained in study by Chun FK *et al.*[15]; upgrading rates remain comparable.

A number of previous studies have carried out multivariate analyses of factors responsible for upgrading of biopsy GS including construction of nomograms (Table 5). In predictive oncology, nomograms have huge
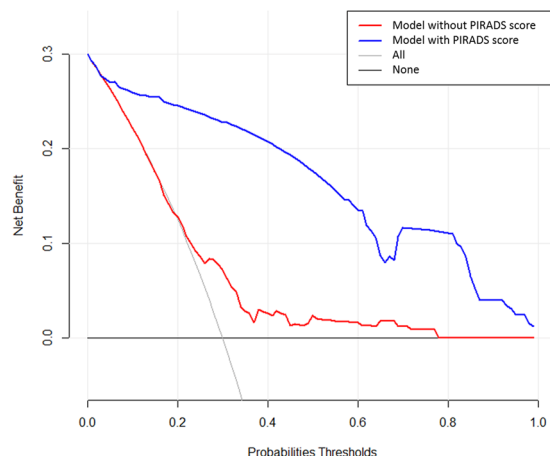
**Figure 6.** Decision analysis demonstrated a high net benefit of PIRADS score model across a wide range of threshold probabilities. Prediction model without PIRADS score (red line); prediction model with PIRADS score (blue line).

| Author | year | Number of patients | Performance (C-index) | Significant parameters on multivariate analysis |
|---|---|---|---|---|
| Chun, FK | 2006 | 2982 | 0.804 | PSA level, clinical stage and primary and secondary GS |
| Kulkarni, GS | 2007 | 175 | 0.71 | PSA level and the level of pathologist expertise |
| Budäus, L | 2010 | 414 | 0.708 | PSA level, clinical stage, prostate volume and percent of positive cores |
| Wang, JY | 2014 | 220 | 0.789 | PSA level, clinical stage, and primary and secondary GS |
| Biming, He | 2016 | 411 | 0.753 | Primary and secondary GS and obesity |
| This study | 2019 | 322 | 0.90 | PSA level and PIRADS score on mp-MRI |

**Table 5.** literature review and comparison between previous and current studies.

potential to help clinicians determine the risk of disease progression and identify those who would experience a greater benefit from multimodality therapy. This approach may result in avoiding unnecessary treatment and improve quality of life by reducing side effects of therapy through better and more precise approach. However, a careful approach is needed to construct nomogram based on specific question, the study population, the method of construction, and its ability to apply to a particular clinical situation. We have followed guidelines described in previous publications[18–20] in constructing nomogram in this study including selection of variables and statistical methods. The nomogram in the present study has been internally validated (Cross-validation and bootstrapping). External validation of nomogram was not carried out in the present study as this would require further prospective multi-centre recruitment of a cohort. Since D'Amico pioneered this approach[21], none of the reported predictive nomograms have included imaging features of the disease. Furthermore, the advantage of our nomogram is a higher overall accuracy (discriminant properties) and closer agreement between predicted and observed values (superior calibration). Estimating clinical utility of nomograms in prognosticating an outcome of intervention remains core value of translational research in precision medicine. Vickers and Elkin[22] have introduced decision analysis curves estimating probabilities of benefits and harms that a diagnostic test or intervention can trigger at various thresholds. Addition of PIRADS score to nomogram achieved a higher net benefit of decisions making in comparison to leaving out PIRADS score as shown in the decision analysis curve constructed in the present study. The thresholds ranged from no upgrading of disease to all men having upgrading of disease following LRP.

**Clinical implications of the study findings.** Predicting final histopathological Gleason score of prostate cancer remains a highly desirable information for physicians counselling men with localised prostate cancer for various modalities of treatment and long-term disease recurrence. At present, various nomograms are used mainly taking into consideration clinical factors such as age, pre-operative PSA level and number of biopsy cores involved with the cancer. Notwithstanding this, there is still a large histopathological discrepancy between biopsy and final radical prostatectomy Gleason score. The present study reports a nomogram based on pre-biopsy multiparameteric MRI grade (PIRADS score) of cancer alongwith other known clinical parameters. The nomogram clearly showed an improved prediction of final Gleason score and the findings have a large implications for clinicians and researchers in this area. We envisage that this and further research should take us close to precise prediction of final Gleason score of histopathology in prostate cancer and thereby an improved and informed decision making by stakeholders including patients in the management of localised prostate cancer. This will have huge benefits for improved GS prediction for men opting for active surveillance and focal therapy besides those opting for radical prostatectomy.

**Limitation of the study.**   There are limitations to our study. This is a single centre study with dedicated uro-radiologist and pathologist, and the rate of upgrading may be different in small centres. Moreover, overall accuracy of our model, although higher than previous was not perfect (90%). Additionally, performance of our model needs further validation in an external data set. Finally, the accuracy of our model could still be improved by integrating additional predictor variables, such as the novel genomic and other biomarkers[23,24]. The growing field of artificial intelligence and machine learning using radiomics approach may improve our ability to define tumour characteristics and classification. This, undoubtly may impact results of the study in the future. Finally, with emerging evidence supporting MRI facilitated biopsy targeting of suspicious areas using ultrasound, the rate of upgrading and the future implications for the practice may change[25]. There is an emerging evidence that targeted biopsy may improve our ability to narrow the upgrading gap between the biopsies and radical prostatectomy histology[26,27]; however no predictive nomogram information was available from both the studies. Our ongoing work through randomised intervention in MR/US fusion should be able to provide more information[28]

In Conclusions, PIRADS version 2 score of 4 or 5 are associated with an increased risk of biopsy Gleason Score upgrading. Pre-biopsy MRI and PIRADS score significantly and independently predict GS upgrading. If proven by external validation, this information should help in decision making by offering treatment options to men with localised prostate cancer.

## References

1. Budäus, L. *et al*. The novel nomogram of Gleason sum upgrade: Possible application for the eligible criteria of low dose rate brachytherapy. *Int. J. Urol.* **17**, 862–868 (2010).
2. Epstein, J. I., Feng, Z., Trock, B. J. & Pierorazio, P. M. Upgrading and Downgrading of Prostate Cancer from Biopsy to Radical Prostatectomy: Incidence and Predictive Factors Using the Modified Gleason Grading System and Factoring in Tertiary Grades. *Eur. Urol.* **61**, 1019–1024 (2012).
3. Amin, M. *et al*. Prognostic and predictive factors and reporting of prostate carcinoma in prostate needle biopsy specimens. *Scand. J. Urol. Nephrol. Suppl.* **39**, 20–33 (2005).
4. Epstein, J. I. *et al*. The 2005 International Society of Urological Pathology (ISUP) consensus conference on Gleason grading of prostatic carcinoma. *Am. J. Surg. Pathol.* **29**, 1228–1242 (2005).
5. Garnett, J. E., Oyasu, R. & Grayhack, J. T. The accuracy of diagnostic biopsy specimens in predicting tumor grades by Gleason's classification of radical prostatectomy specimens. *J. Urol.* **131**, 690–693 (1984).
6. Corcoran, N. M. *et al*. Upgrade in Gleason score between prostate biopsies and pathology following radical prostatectomy significantly impacts upon the risk of biochemical recurrence. *BJU Int.* **108**, 202–210 (2011).
7. Ahmed, H. U. *et al*. Diagnostic accuracy of multi-parametric MRI and TRUS biopsy in prostate cancer (PROMIS): a paired validating confirmatory study. *Lancet (London, England)* **389**, 815–822 (2017).
8. Itatani, R. *et al*. Negative predictive value of multiparametric MRI for prostate cancer detection: Outcome of 5-year follow-up in men with negative findings on initial MRI studies. *Eur. J. Radiol.* **83**, 1740–1745 (2014).
9. Song, W. *et al*. Role of PI-RADS Version 2 for Prediction of Upgrading in Biopsy-Proven Prostate Cancer With Gleason Score 6. *Clin. Genitourin. Cancer* **16**, 281–287 (2018).
10. White, S. *et al*. Prostate Cancer: Effect of Postbiopsy Hemorrhage on Interpretation ofMR Images' From the Departments of Radiology. *Radiology* **195**, 385–390 (1995).
11. Padhani, A. R. *et al*. Prostate Imaging-Reporting and Data System Steering Committee: PI-RADS v2 Status Update and Future Directions. *Eur. Urol.*, https://doi.org/10.1016/J.EURURO.2018.05.035 (2018).
12. Sheikh, N. *et al*. Combined T2 and diffusion-weighted MR imaging with template prostate biopsies in men suspected with prostate cancer but negative transrectal ultrasound-guided biopsies. *World J. Urol.* **35**, 213–220 (2017).
13. Wei, C. *et al*. Quantitative parameters in dynamic contrast-enhanced magnetic resonance imaging for the detection and characterisation of prostate cancer. *Oncotarget* **9**, 15997–16007 (2018).
14. Wang, J. Y. *et al*. A nomogram to predict gleason sum upgrading of clinically diagnosed localized prostate cancer among Chinese patients. *Chin. J. Cancer* **33**, 241–248 (2014).
15. Chun, F. K.-H. *et al*. Development and Internal Validation of a Nomogram Predicting the Probability of Prostate Cancer Gleason Sum Upgrading Between Biopsy and Radical Prostatectomy Pathology. *Eur. Urol.* **49**, 820–826 (2006).
16. Kulkarni, G. S. *et al*. Clinical predictors of gleason score upgrading. *Cancer* **109**, 2432–2438 (2007).
17. He, B. *et al*. Nomograms for predicting Gleason upgrading in a contemporary Chinese cohort receiving radical prostatectomy after extended prostate biopsy: development and internal validation. Oncotarget 7 (2016).
18. Iasonos, A., Schrag, D., Raj, G. V. & Panageas, K. S. How to build and interpret a nomogram for cancer prognosis. *J. Clin. Oncol.* **26**, 1364–1370 (2008).
19. Harrell, F. E. Regression Modeling Strategies [electronic resource]: With Applications to Linear Models, Logistic and Ordinal Regression, and Survival Analysis in Springer Series in Statistics. Springer (2015).
20. Balachandran, V. P., Gonen, M., Smith, J. J. & DeMatteo, R. P. Nomograms in oncology: More than meets the eye. *Lancet Oncol.* **16**, e173–e180 (2015).
21. D'AMICO, A. V. *et al*. The Combination Of Preoperative Prostate Specific Antigen And Postoperative Pathological Findings To Predict Prostate Specific Antigen Outcome In Clinically Localized Prostate Cancer. *J. Urol.* **160**, 2096–2101 (1998).
22. Vickers, A. J. & Elkin, E. B. Decision curve analysis: A novel method for evaluating prediction models. *Med. Decis. Mak.* **26**, 565–574 (2006).
23. Kornberg, Z., Cooperberg, M. R., Spratt, D. E. & Feng, F. Y. Genomic biomarkers in prostate cancer. *Transl. Androl. Urol.* **7**, 459–471 (2018).
24. Sanhueza, C. & Kohli, M. Clinical and Novel Biomarkers in the Management of Prostate Cancer. Curr. Treat. Options Oncol. 19 (2018).
25. Kasivisvanathan, V. *et al*. MRI-targeted or standard biopsy for prostate-cancer diagnosis. *N. Engl. J. Med.* **378**, 1767–1777 (2018).
26. Nassiri, N. *et al*. Targeted Biopsy to Detect Gleason Score Upgrading during Active Surveillance for Men with Low versus Intermediate Risk Prostate Cancer. *J. Urol.* **197**, 632–639 (2017).
27. Le, J. D. *et al*. Magnetic resonance imaging-ultrasound fusion biopsy for prediction of final prostate pathology. *J. Urol.* **192**, 1367–1373 (2014).
28. Szewczyk-Bieda, M. *et al*. A multicentre parallel-group randomised trial assessing multiparametric MRI characterisation and image-guided biopsy of prostate in men suspected of having prostate cancer: MULTIPROS study protocol. *Trials* **20**, 638 (2019).

### Competing interests

The authors declare no competing interests.

### Additional information

**Correspondence** and requests for materials should be addressed to G.N.

**Reprints and permissions information** is available at www.nature.com/reprints.

**Publisher's note** Springer Nature remains neutral with regard to jurisdictional claims in published maps and institutional affiliations.

*cancers*

*Article*

# Predicting the Performance of Concurrent Systematic Random Biopsies during Image Fusion Targeted Sampling of Multi-Parametric MRI Detected Prostate Cancer. A Prospective Study (PRESET Study)

**Saeed Alqahtani [1,2,3], Xinyu Zhang [4], Cheng Wei [1], Yilong Zhang [2], Magdalena Szewczyk-Bieda [5], Jennifer Wilson [6], Zhihong Huang [2] and Ghulam Nabi [1,\*]**

1   Division of Imaging Sciences and Technology, School of Medicine, Ninewells Hospital, University of Dundee, Dundee DD1 9SY, UK; szalqahtani@dundee.ac.uk (S.A.); c.wei@dundee.ac.uk (C.W.)
2   School of Science and Engineering, University of Dundee, Dundee DD1 9SY, UK; y.y.zhang@dundee.ac.uk (Y.Z.); z.y.huang@dundee.ac.uk (Z.H.)
3   Department of Radiological sciences, College of Applied Medical Science, Najran University, Najran 11001, Saudi Arabia
4   Division of Population Health and Genomics, School of Medicine, University of Dundee, Dundee DD1 9SY, UK; xzhang001@dundee.ac.uk
5   Department of Clinical Radiology, Ninewells Hospital, University of Dundee, Dundee DD1 9SY, UK; m.szewczykbieda@dundee.ac.uk
6   Department of Pathology, Ninewells Hospital, University of Dundee, Dundee DD1 9SY, UK; jennifer.wilson7@nhs.scot
\*   Correspondence: g.nabi@dundee.ac.uk

check for **updates**

**Simple Summary:** The study provides a predictive model by using clinical factors in selecting men who may benefit from the addition of systematic biopsies with an image fusion targeted approach. The approach is likely to improve the detection of csPCa and avoid unnecessary detection of indolent prostate cancers.

**Abstract:** The study was aimed to develop a predictive model to identify patients who may benefit from performing systematic random biopsies (SB) in addition to targeted biopsies (TB) in men suspected of having prostate cancer. A total of 198 patients with positive pre-biopsy MRI findings and who had undergone both TB and SB were prospectively recruited into this study. The primary outcome was detection rates of clinically significant prostate cancer (csPCa) in SB and TB approaches. The secondary outcome was net clinical benefits of SB in addition to TB. A logistic regression model and nomogram construction were used to perform a multivariate analysis. The detection rate of csPCa using SB was 51.0% (101/198) compared to a rate of 56.1% (111/198) for TB, using a patient-based biopsy approach. The detection rate of csPCa was higher using a combined biopsy (64.6%; 128/198) in comparison to TB (56.1%; 111/198) alone. This was statistically significant ($p < 0.001$). Age, PSA density and PIRADS score significantly predicted the detection of csPCa by SB in addition to TB. A nomogram based on the model showed good discriminative ability (C-index; 78%). The decision analysis curve confirmed a higher net clinical benefit at an acceptable threshold.

**Keywords:** prostate cancer; magnetic resonance imaging; prostatectomy; systematic random biopsy; targeted biopsy

## 1. Introduction

Recent trends and evidence support pre-biopsy MRI with selective targeting of suspected malignant lesions using MRI/ultrasound (US) and TB methods [1]. The burgeoning interest in fusion imaging has arisen to address the main limitations of SB: overdetection of clinically insignificant cancers and possibly underdetection of csPCa. A number of recent

reports support the utility of pre-biopsy multi-parametric magnetic resonance imaging (mpMRI) to address the limitations of SB, and the advantage of increased csPCa detection [2–4]. Pre-biopsy MRI in MRI directed pathways have been reported to detect a higher number of csPCa. However, benefits of image-guided targeting performed in combination with systematic sampling or alone remains poorly defined. Drost et al., in a recent systematic review, used a mixed population (with or without image fusion targeting of suspicious areas) to answer this question; however, image fusion methods were not used in all the cases of included studies, and hence, the benefits of targeting suspicious areas with the image fusion approach, with or without addition of systematic biopsy sampling, remains unclear [5].

Image fusion approach makes use of information from MRI to direct biopsy needles under real-time US guidance [2,6,7]. Studies have shown that mpMRI combined with TB technology is a promising tool in the diagnosis of PCa [2,8,9]. In light of a number of previous trials showing the significant benefits of image TB, research is now focused on whether random biopsies are required at all in the detection of prostate cancer [10–12]. This question is pertinent to settle an ongoing debate as studies have also highlighted that TB with the addition of systematic random biopsy is superior to systematic random biopsy alone either in terms of capturing csPCa or even in terms of post-procedural morbidity [1]. In a large retrospective study, from centres in Europe and the USA, Dell'Oglio et al. aimed at findings a group of men where systematic biopsies could be avoided altogether in men with MRI-facilitated targeted biopsy approach. The authors failed to achieve their objectives and concluded that systematic sampling should be combined with the image-guided fusion biopsies [13]. In a large multicentre prospective study, researchers concluded a higher detection rate for clinically significant prostate cancer for a combined approach (TB and SB) biopsy method; however, different image fusion systems including cognitive guidance were used in the targeted biopsy approach [11]. Furthermore, the study did not use PIRADS v2 categorisation and no standardised protocol was used for MRI imaging. This allowed biases and heterogeneity into the reported data. Our study is a protocol-driven prospective investigation with a standardised US/MRI fusion protocol. We assessed clinical variables that could help in identifying patients who may benefit from systematic random biopsies in addition to fusion targeted approach. The comprehensive analysis and outcomes using methodology of this study has not been reported in the literature [14,15], in particularly the net clinical benefit of the approach.

The aim of this study was to:

(1) Compare the diagnostic accuracy of MRI/US fusion targeted biopsies, systematic biopsies and combined approaches in the detection of csPCa and define predictive factors where a combined approach could be used.
(2) Quantify additional benefits of adding systematic biopsies to the targeted biopsies approach by constructing a nomogram and assessing its net clinical benefits.

## 2. Materials and Methods

### 2.1. Study Population

The study had ethical approval (14/ES/1070) and all participants provided informed consent for their imaging data to be used. The study also had Caldicott institutional approval through the East of Scotland Ethical committee and Caldicott permission (Caldicott/ IGTCAL6358) to link data with electronic system wherever follow-up outcomes were needed. The study period was between April 2015 and March 2020.

The inclusion criteria were age between 40 to 76, abnormal digital rectal examination (DRE), PSA $\leq 20$ ng/mL and MRI < T3 disease. Exclusion criteria were repeat biopsies, prior radiotherapy to prostate and diagnosis of acute prostatitis with the last 12 months or a history of PCa. All participants had pre-biopsy mpMRI and only MRI positive (PIRADS $\geq 3$) were recruited into the study ($n = 198$). Patients then underwent prostate biopsy by the MRI/US fusion technique (Hitachi HI-RVS; Europe Holding, Steinhausen, Switzerland) by

operator 1. This was followed by a standard 12-core TRUS biopsy by a second operator (blinded to the MRI results). In total, 78/198 (39%) underwent radical prostatectomy (RP).

### 2.2. Outcomes

The primary outcome was to compare detection rates of csPCa using both SB and TB approaches alone and in combination. This was assessed both at biopsy and RP stages. csPCa was defined as the presence of prostate cancer with Gleason Score $\geq 3 + 4$ (International Society for Urological Pathology [ISUP] grade 2 or more).

The secondary outcome was to assess the net clinical benefit of the approaches using nomogram and decision-analysis methods.

### 2.3. Sample Size Estimation

In considering performing a McNemar matched test, a minimum sample size of 110 men undergoing both SB and TB prostate biopsy approaches would be required to yield 90% power with a significance level of 0.05 ($\alpha = 0.05$), which would also allow 20% of the dropout rate. The csPCa detection rate via Sb and TB were found in a previous study [16]. Therefore, we recruited more patients than the minimum required number from the sample estimation to ensure achievement of study power and significance level.

### 2.4. Multi-Parametric MRI

All mpMRI scans were performed using 3T scanner (TIM Trio, Siemens, Erlangen, Germany) approximately 2 weeks before TRUS and MRI/US fusion biopsies. The mpMRI protocol was derived from the European Society of Uro-radiology Guidelines 2012 for the detection of prostate cancer and the subsequent publication of version 2 (Table S1—Supplementary file). Briefly, Table S1 summarises the MRI acquisition parameters. Prostate images were acquired in all three imaging planes, whereby the plane of the prostate was defined in relation to the rectal wall.

The mpMRI images were analysed and scored by experienced uro-radiologists (with more than 5 years post-certification experience using PIRADS v2.0). PIRADS v2.0 assessment categories were described as follows: score 1, clinically significant cancer is highly unlikely to be present; score 2, clinically significant cancer is unlikely to be present; score 3, the presence of clinically significant cancer is equivocal; score 4, clinically significant cancer is likely to be present; and score 5, clinically significant cancer is highly likely to be present.

### 2.5. Biopsy Procedures

All mpMRI scans were prepared by an experienced uro-radiologist (MSB) and fusion-targeted biopsies were performed by an experienced radiologist or in their presence using the Hitachi HI-RVS platform (Europe Holding, Steinhausen, Switzerland) using a pre-recorded lesion location. Three cores of tissue were obtained in TB approach from previously identified mpMRI lesions using a superimposed T2-weighted sequence on the real-time TRUS image. The systematic random 12-core biopsies were performed by an experienced urologist or specialist nurse following targeting.

The systematic random biopsy was typically a 12-core approach, collected in an extended sextant template of biopsies from the lateral and medial aspects of the base, mid, and apical prostate from the left and right sides. The biopsy results were analysed by experienced uro-pathologists who were blinded to the MRI findings. The Gleason Score for each patient was obtained.

A subset of the cohort ($n = 78$) underwent RP and their pathological stages were as follows: T2a = 2, T2c = 47, T3a = 24 and T3b = 5. Figure 1 summarises the study protocol in brief. The radical prostate specimens for histology were sliced in patient-specific moulds to aid orientation between imaging and histology per lesion, which were then fabricated using a 3D printer, as described previously by our group and others [17]. Specifically, patient-specific 3D printed moulds were made prior to surgery based on the T2-weighted MRI prostate capsule. The moulds were then customised for each patient using MIMICS

and Solidworks. This was used as a reference standard to assess the diagnostic accuracy of both SB and TB in detecting csPCa.
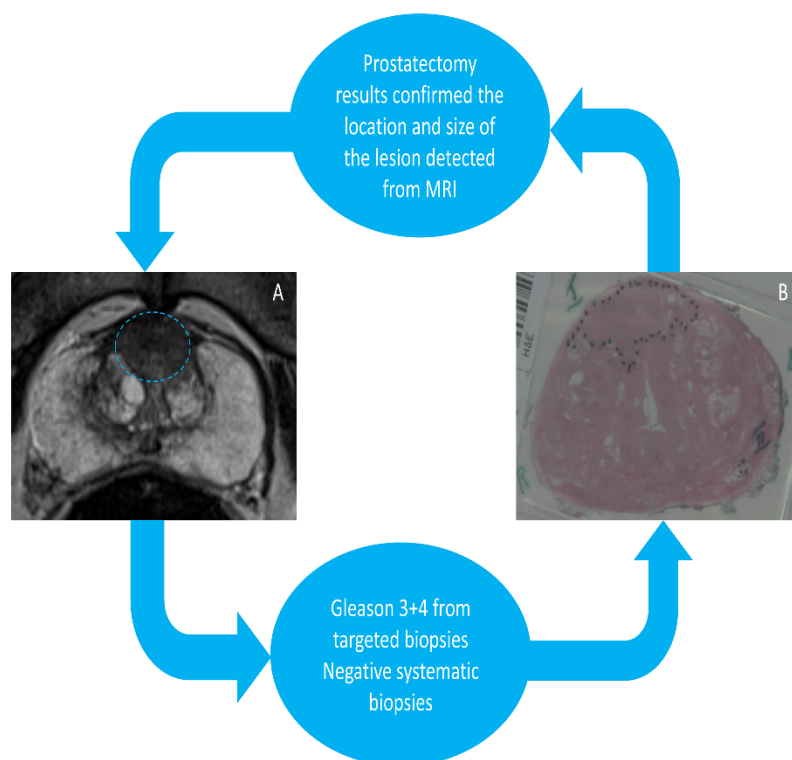


**Figure 1.** (**A**) A 76-year-old patient with a PIRADS 5 lesion detected from 3T MRI in anterior zone with a high PSA and abnormal DRE. (**B**) Patient-specific 3D mould-based grossing of a radical prostatectomy slice shows a 3 + 4 GS cancer located in the anterior zone.

### 2.6. Statistical Analysis

Patients' age, PSA, prostate volume (mL) and PSAD were collected. PSAD was calculated using PSA divided by the MRI-derived prostate volume (ellipsoid method). The number of MRI lesions, index lesion size (mm), PIRADS category and lesion location were measured by mpMRI. Each lesion was counted only once. The index lesion size was the size of the lesion with the highest PIRADS score. Continuous data were first tested to see if they were normally distributed by the Kolmogorov–Smirnov Test of Normality. The mean (m) and standard deviation (SD) were described if the variable followed a normal distribution. The median (M) and interquartile range (IQR) were presented if the variable was not normally distributed. Categorical variables are reported as frequencies and proportions. Cross tabulation was carried out in order to compare the proportions of csPCa patients by SB, TB, and combined SB + TB. The McNemar chi-square test was conducted in patients who were given both diagnostic tests. McNemar chi-square, degree of freedom (df) and $p$-value were calculated and presented. A two-step logistic regression was performed to identify explanatory variables of csPCa. First, patients' age, PSAD, lesion size, PIRADS and number of lesions were individually put into a univariate logistic regression model, where the outcome was defined as having csPCa or not. Statistically significant variables were then put into the multivariate logistic regression model. Odds ratio (OR), 95% confidence interval (95% CI) of odds ratio and $p$ values were recorded. A nomogram was created based on the statistically significant variables in the final model. The discriminative ability of the predictive model was tested by receiver operating characteristics (ROC) curve and the concordance statistic (c-statistic) was presented. The predicted probabilities of csPCa were plotted against observed probabilities to test the calibration of the model. Decision curve analysis was applied to determine the benefit of the nomogram. In the subgroup analysis,

prostatectomies were performed in a group of 78 patients (112 lesions). The detection rate of true significant prostate cancer lesions via SB, TB and combined SB+TB was compared using McNemar chi-square test. Statistical analyses were conducted by SPSS V23.0 and R V4.0.3. The Bonferroni adjustment, which adjusted *p* value by times of tests, was used accounting for multiple testing. The alpha level (adjusted *p*-value) was set at 0.05/times of tests to determine two-tailed significance for McNemar chi-square test.

## 3. Results

### 3.1. Patient Characteristics

The participating patients' demographic data are shown in in Table 1. A total of 198 patients who underwent both systematic random and TB in the same setting were recruited into the study. Several clinical variables included baseline information (age, PSA level (ng/mL), PSA density (ng/mL$^2$) and prostate volume (mL)), multi-parametric magnetic resonance imaging features (number of lesions seen on MRI, index lesion size (mm)) and PIRADS score.

**Table 1.** Characteristics of participating patients.

| | **Variables** | **Overall (*n* = 198)** |
|---|---|---|
| Basic information | Age, median (IQR), in years | 67 (71–61) |
| | Prostate specific antigen (PSA), median (IQR), ng/mL | 8.2 (10.6–6.4) |
| | Prostate volume, median (IQR), mL | 47 (63–33) |
| | PSA Density, median (IQR), ng/mL$^2$ | 0.18 (0.27–0.11) |
| mp-MRI | Number of lesions, *n* (%) | |
| | 1 | 102 (51.5%) |
| | 2 | 75 (38%) |
| | 3 | 14 (7%) |
| | 4 | 6 (3%) |
| | 5 | 1 (0.5%) |
| | Index lesion size, median (IQR), mm | 16 (25–13) |
| | Prostate Imaging Reporting and Data System (PIRADS score), *n* (%) | |
| | PIRADS 3 | 22 (11%) |
| | PIRADS 4 | 55 (28%) |
| | PIRADS 5 | 121 (61%) |
| | Lesion location, *n* (%) | |
| | Peripheral zone (PZ) | 79 (40%) |
| | Transition zone (TZ) | 44 (22%) |
| | Both zones (TZ-PZ) | 75 (38%) |
| Targeted (TB)/Systematic random (SB) biopsy | Detection of prostate cancer in TB, *n* (%) | 129 (65%) |
| | Detection of prostate cancer in SB, *n* (%) | 127 (64%) |

### 3.2. Comparison of the Detection Rate of csPCa between SB, TB and Combined Approaches

The detection rate of csPCa using random biopsy was 51.0% (101/198) and using targeted biopsy was 56.1% (111/198). This was not statistically significant (McNemar chi-square test was $\chi^2$ = 2.273, df = 1, *p* = 0.132, Odds ratio (OR) = 0.63 (95% CI, 0.34 to 1.16). The results are shown in Figure 2. There were 17 patients (17/198; 8.5%) where the TB approach alone missed csPCa (eight from the same site and nine from normal-looking prostate on MRI). There were 84 patients (84/198; 42.4%) where the positive cores on systematic sampling and TB detected csPCa (72 from the same sector of index lesion and 12 from different sectors away from index lesion). When the TB is negative (69/198; 34.8%), the SB detected clinically insignificant cancer in 12 patients (12/69; 17.3%) and detected csPCa in eight patients (8/69; 11.6%). Twenty-seven (27/198; 13.6%) men were upgraded to csPCa based on TB, while 17 patients (17/198; 8.5%) were upgraded based on SB ($\chi^2$ = 2.27, *p* = 0.13).
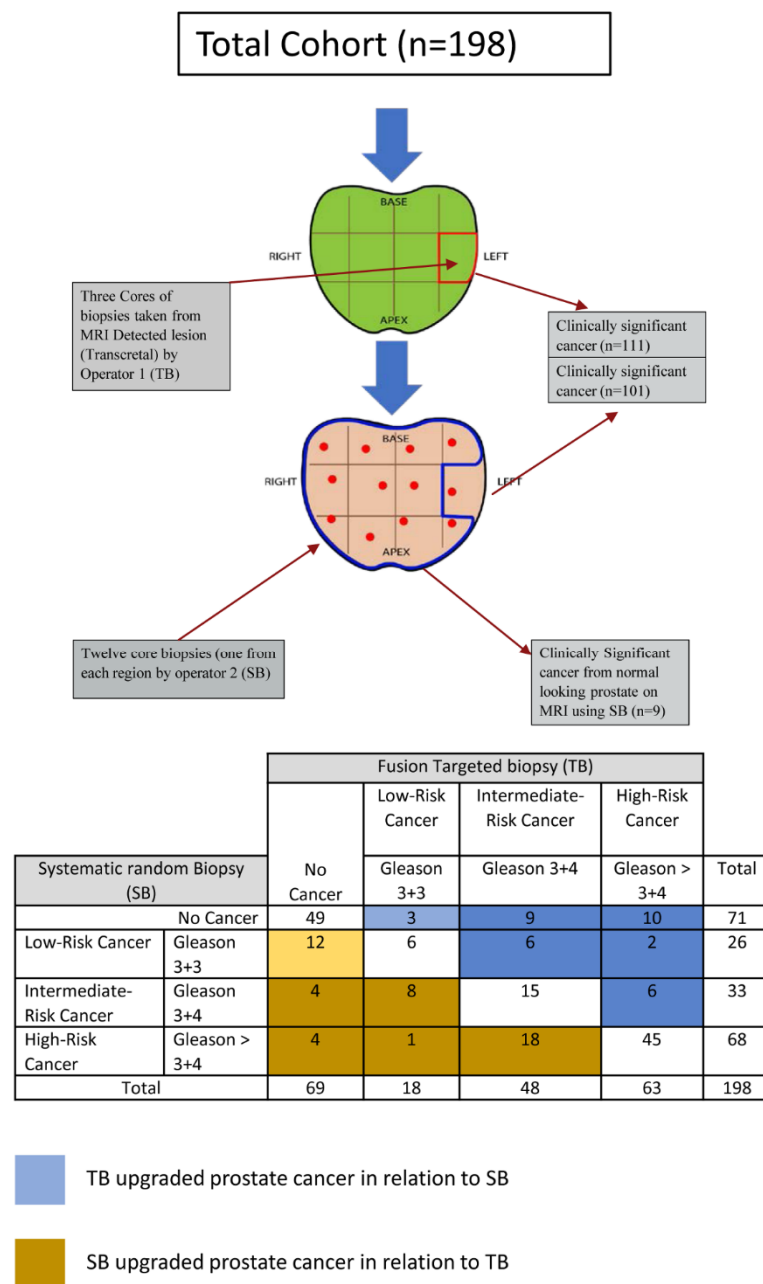
| | | | Fusion Targeted biopsy (TB) | | | |
| --- | --- | --- | --- | --- | --- | --- |
| | | | Low-Risk Cancer | Intermediate-Risk Cancer | High-Risk Cancer | |
| Systematic random Biopsy (SB) | | No Cancer | Gleason 3+3 | Gleason 3+4 | Gleason > 3+4 | Total |
| | No Cancer | 49 | 3 | 9 | 10 | 71 |
| Low-Risk Cancer | Gleason 3+3 | 12 | 6 | 6 | 2 | 26 |
| Intermediate-Risk Cancer | Gleason 3+4 | 4 | 8 | 15 | 6 | 33 |
| High-Risk Cancer | Gleason > 3+4 | 4 | 1 | 18 | 45 | 68 |
| Total | | 69 | 18 | 48 | 63 | 198 |

TB upgraded prostate cancer in relation to SB

SB upgraded prostate cancer in relation to TB

**Figure 2.** The detection rate of significant prostate cancer between SB and TB based on patients' level.

The detection rate of csPCa was higher using combined biopsy (64.6%; 128/198) in comparison to TB (56.1%; 111/198). The McNemar chi-square test result with the Yates correction was statistically significant ($\chi^2$ = 15.06, df = 1, $p < 0.001$). There was an 8.5% increase in significant prostate cancer detection rate at the patient level using combined biopsy methods compared to using TB alone.

We further validated findings using a subset of the cohort, where the histopathology of RP was used as a reference standard (Figure 3). There were 170 csPCa (170/190; 89.4%) seen on RP histopathology using mould-based approach and counting each focus of cancer. In total, 112 were targeted using MRI/US image fusion method. The TB approach detected 70 of these (70/112; 62.5%), whereas the SB approach detected 54 (54/112; 48.2%). The difference was statistically significant (the McNemar chi-square test result with the Yates correction was $\chi^2$ = 6.618, df = 1, $p = 0.010$, OR = 0.36 (95% CI, 0.17 to 0.77)). The combined approach to 112 lesions detected more cancers than SB or TB alone (79/112; 70.5%). Compared to SB, the combined approach detected 22.3% more cancers (70.5% vs. 48.2%).

The McNemar chi-square test result with the Yates correction was statistically significant ($\chi^2$ = 23.04, df = 1, $p$ < 0.001). Similarly, the combined approach detected 8% more cancers in comparison to TB (70.5% vs. 62.5%). The McNemar chi-square test result with the Yates correction was statistically significant ($\chi^2$ = 7.111, df = 1, $p$ = 0.008.)
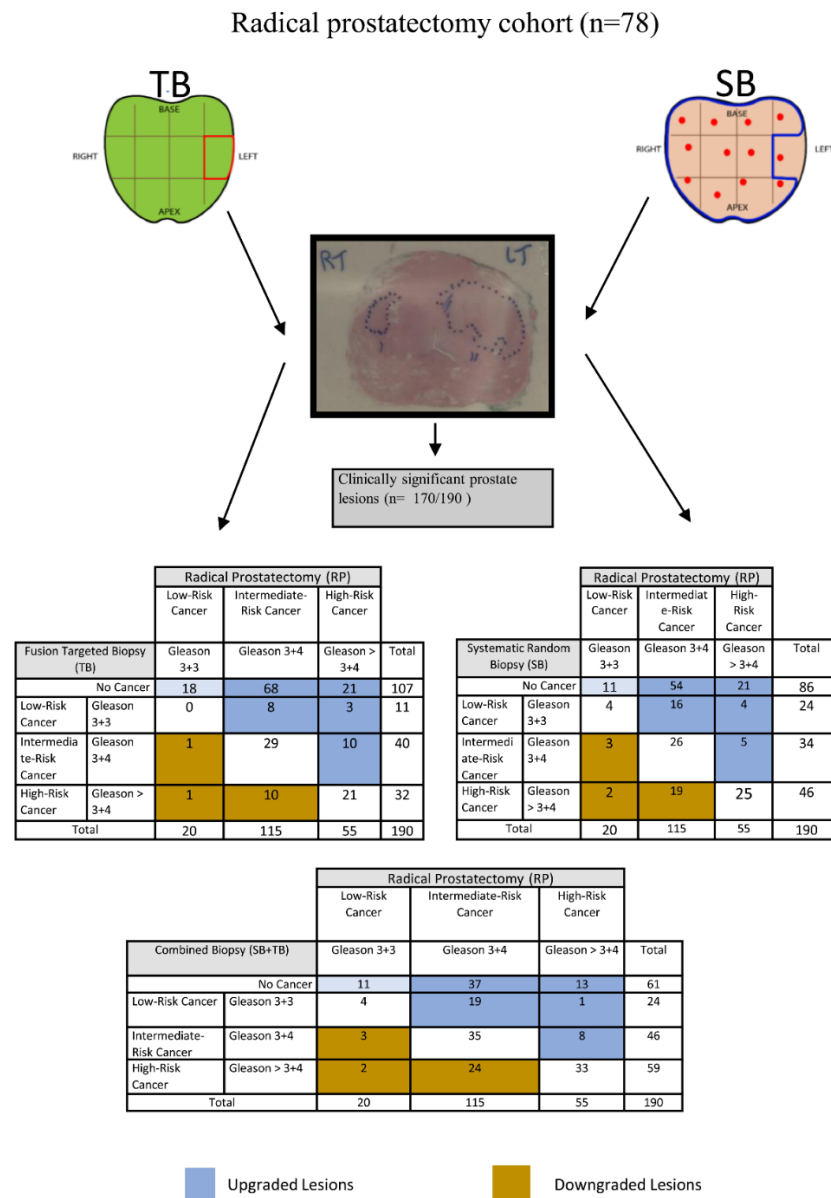


**Figure 3.** The detection rate of significant prostate cancer via SB, TB and combined SB+TB on RP lesions.

Interestingly, there were 11 cancers (11/190; 5.8%) which were labelled as clinically insignificant and all were upgraded to clinically significant using the TB approach. In comparison, there were 24 (24/190; 12.6%) cancers labelled as clinically insignificant and 20 (20/190; 10.5%) were upgraded using the SB approach. The McNemar chi-square test result with the Yates correction was $\chi^2$ = 0.450, df = 1, $p$ = 0.502, OR = 1.50 (95% CI, 0.61 to 3.67). This was not statistically significant.

### 3.3. Univariate and Multivariate Logistic Regression Analysis and Developed Nomogram

In univariate logistic regression, patient's age, PSAD, Index lesion size and PIRADS were all significant predictors of csPCa detected by random biopsy (Table 2) and were,

therefore, inputted into the multivariate analysis. A 6% increase in odds of csPCa by random biopsy was associated with each one-year increase in age (OR = 1.06, 95% CI 1.01–1.12). A PSAD increase of 1 ng/mL was associated with an almost 26-fold increase in odds of csPCa (OR = 25.63, 95% CI 1.93–341.27). Having PIRADS-5 was another significant predictor of csPCa using random biopsy, which was associated with a six-fold increase in odds compared to those with PIRADS-3 (OR = 5.94, 95% CI 1.77–19.93).

**Table 2.** Univariate and multivariate logistic regression analysis.

| Covariate | N | Univariate Logistic Regression | | | | Multivariate Logistic Regression | | | |
|---|---|---|---|---|---|---|---|---|---|
| | | OR | 95% CI Lower | Upper | *p* Value | OR | 95% CI Lower | Upper | *p* Value |
| Age (year) | 198 | 1.07 | 1.02 | 1.12 | 0.009 | 1.06 | 1.01 | 1.12 | 0.036 |
| PSAD | 198 | 92.79 | 7.61 | 1130.69 | <0.001 | 25.63 | 1.93 | 341.27 | 0.014 |
| Index lesion size | 198 | 1.06 | 1.03 | 1.10 | <0.001 | 1.02 | 0.98 | 1.06 | 0.399 |
| PIRADS | 198 | | | | <0.001 | | | | 0.001 |
| 3 | 22 | Ref | - | | - | Ref | - | | - |
| 4 | 55 | 1.69 | 0.49 | 5.80 | 0.406 | 1.51 | 0.42 | 5.43 | 0.525 |
| 5 | 121 | 9.46 | 3.00 | 29.84 | <0.001 | 5.94 | 1.77 | 19.93 | 0.004 |
| Number of Lesions | | | | | 0.309 | | | | |
| 1 | 102 | Ref | - | | - | | | | |
| 2 | 75 | 1.11 | 0.61 | 2.02 | 0.730 | | | | |
| 3 and above | 21 | 2.16 | 0.81 | 5.80 | 0.125 | | | | |

The statistically significant independent variables from the multivariate logistic regression model (age, PSAD and PIRADS) were used to develop a nomogram to predict the probability of csPCa using SB (Figure 4). The model demonstrated good discriminative ability (C-statistic = 0.779, 95% CI 0.714–0.843 (Figure S1—Supplementary Material)).
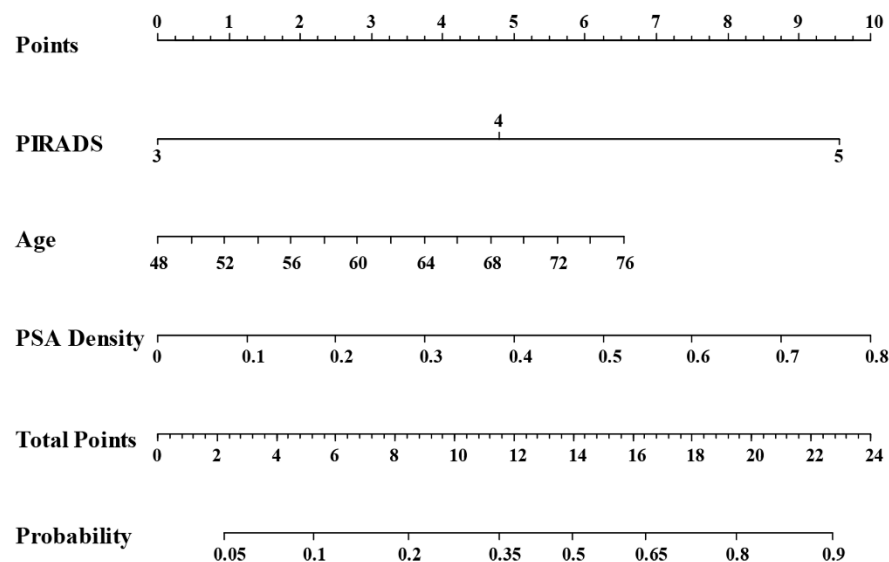


**Figure 4.** Nomogram with significant clinical variables to predict patients who will benefit from performing systematic random biopsy in addition to TB.

The calibration plot demonstrated a good agreement between the model predictions and actual observations for detecting csPCa via SB (Figure 5).
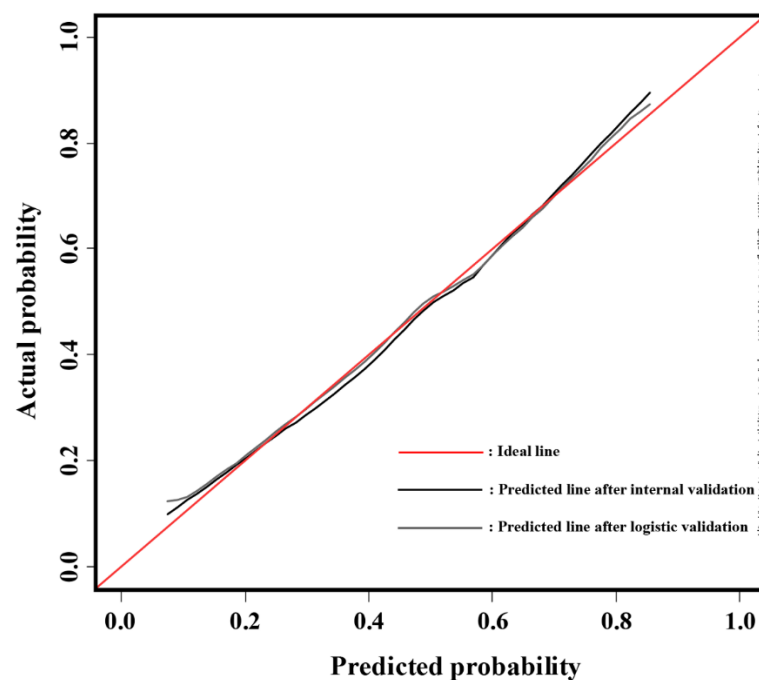
**Figure 5.** Model calibration plot for observed and predicted probability.

### 3.4. Decision Curve Analysis

The outcomes of the decision analysis curve are shown in Figure 6. The net benefit of performing SB in addition to TB on all cases is depicted by the grey line, whereas the black line represents the net benefit of not performing SB (only TB performed). To avoid the harm of unnecessarily intervening on the patients who are disease free and over intervening in the patients with disease, the net benefit of performing SB in addition to TB based on our prediction model with a reasonable range of threshold probabilities is shown as a red line in Figure 6. The net benefit of using our prediction model is to identify patients at risk of having csPCa who will benefit from SB in addition to TB. Our nomogram increased the overall net clinical benefit when the threshold probability was <60% and improved the diagnosis of csPCa compared to avoiding SB biopsy in all.
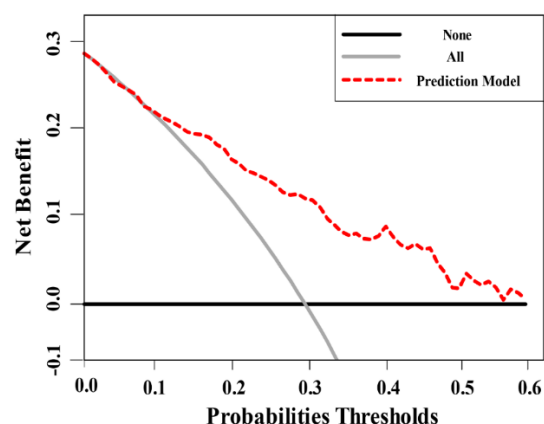


**Figure 6.** Decision analysis demonstrated a high net benefit of the model across a wide range of threshold probabilities.

## 4. Discussion

### 4.1. Principal Findings of the Study

This study assessed detection rate of csPCa using image fusion targeting, random systematic sampling and combination approaches. Patient-based analyses were further

validated using lesion-based data from RP histology. There were statistically significant higher detection rates for the combined biopsy approach in comparison to SB or TB alone. The TB approach alone would have missed 17 csPCas. Therefore, the combined approach detected more csPCa than either SB or TB alone. These results are similar to those reported by Filson et al. [18]; however, they were different to those reported in the PRECISION trial [1]. Therefore, in our observations, omitting concurrent SB during image-fusion may run the risk of missing csPCas in around 8.5% of patients. Similar to Cash et al. [19], we observed TB missing a small number csPCa in targeted areas. It is essential that we balance the advantages of concurrent sampling of the prostate during targeting against the risk of side effects and increased detection of clinically insignificant prostate cancers. Avoiding or adding systematic random biopsy at the time of TB remains a challenge for physicians, as knowledge and evidence of decision-making contributing factors still remains known [20]. Our outcomes from the nomogram indicated the excellent advantage (C-index 78% vs. 70%) of using a multivariable prediction model adjusting for clinical and radiological features (age, PSAD and PIRADS). The nomogram could be used to assist in selecting a group of men where a combined biopsy approach would be more useful.

We have also observed no significant advantage of improved characterisation of csPCa using the TB approach as all cancers labelled as clinically insignificant were upgraded on the final histopathology of RP. The challenge of upgrading or under grading would continue with both biopsy approaches as seen in our previous study [21]. There could be various reasons, such as inadequate sampling due to cancer heterogeneity and poor visibility of cribriform architecture on MRI and in biopsies [22].

### 4.2. Study Findings in Context of the Reported Literature

Several retrospective studies have assessed the outcomes of SB in addition to TB for the detection of csPCa. Sathianathen [23] et al. reported a nomogram with C-index = 70%. This nomogram was based on the clinical variables (biopsy naïve, previous biopsy and active surveillance patients) and imaging variables (number of MRI lesions and PIRADS score). The model provided a higher net clinical benefit at a threshold probability of <30%. The model was meant to predict csPCa in systematic random cores only (when TB was negative); however, our findings focused on predicting those patients who will benefit from performing systematic random biopsy in addition to TB (irrespective of target biopsy being positive or negative). Additionally, unlike their study, our nomogram, along with age, PSAD and PIRADS, found that adding these clinical variables to a model yielded a higher C-index (78% vs. 70%). In contrast to the present study, Sathianathen et al. [23] did not report on a validation cohort using RP as a reference standard. Furthermore, and similar to our study, others have reported the possibility of missing significant cancers if the image fusion targeted approach was offered alone [3,24–26]. Dell'Oglio et al. [13] failed to identify patients who might benefit from TB alone; therefore, they supported a combination of TB and SB as the preferred approach. In their study, there was no attempt to predict and assess the clinical variables that could help in identifying patients who might derive a greater benefit from systematic random biopsies. Lastly, Falagario et al. [27], highlighted that smaller lesions in big prostates are more likely to be missed in TB biopsies; therefore, they developed a nomogram based on MRI volumetric parameters and clinical information for deciding when SB should be performed in addition to TB. In their study, all patients underwent biparamtric MRI; however, in our analysis, we followed the standard mpMRI using PIRADS [28]. Moreover, the study was a multi-institutional retrospective data analysis of two previously published prospective trials with predominant fusion biopsies being cognitive rather than image-fusion using software. All men in the MULTI-IMPROD study [29,30] had transrectal systematic biopsies; therefore, these trials were not appropriate in answering the research question of the present study. In contrast to this study, however, Falagario et al. [27] provided a range of probabilities of men missing clinically significant cancers, if SB was to be avoided altogether. We reported a set of measurable imaging criteria which could predict the likely benefit of adding SB to TB.

To our knowledge, this study is the first where lesion-based analyses were carried out using mould-based approach for a comprehensive pathological analysis. This confirmed that most csPCas were detected using a combined biopsy approach. csPCas were still missed by biopsies, which may be due to smaller lesions or the cribriform pattern seen on histopathology [31].

*4.3. Clinical Implications of the Study Findings and Limitation of the Study*

Decision-making using critical analysis, especially in situations of uncertainty, cost pressures and likely patient morbidity, is inevitably based on evidence or on a set of observations. In this study, we presented a decision-curve analysis estimating the net clinical benefits of offering a diagnostic test (combined approach to biopsy) in comparison to TB or SB approaches alone. The clinical and radiological observations were used to construct a nomogram, which is then the basis of a decision-making curve. The curve includes intervention for all and intervention for none and provides a background to facilitate discussions with patients. A balance has to be achieved between maximising detection of csPCas and avoiding detection of clinically insignificant cancers.

At present, various nomograms are used mainly for taking into consideration clinical factors, such as age, pre-operative PSA level and PIRADS score of the suspicious cancers. The present study reports a nomogram based on clinical parameters (age, PSAD and PIRADS). The nomogram clearly showed an improved prediction rate, which can be used to perform additional biopsies and the findings have substantial implications for clinicians and researchers in this area. We envisage that this and further research should bring us closer to precise decision-making. There will remain a group of men where systematic the random biopsy approach would bring value in addition to the TB approach, and thereby, improve informed decision-making in the management of men suspected of having prostate cancer.

However, there are some limitations to this study. This is a single-centre study with dedicated uro-radiologist and pathologists. We wanted to explore the association between lesion location in prostate and csPCa via SB but due to low numbers of lesions in TZ, which was not possible. It was not possible to use PIRADS v2.1, since the enrolment to study started before its publication, and this is a similar challenge to any other study published recently on this topic [11]. The nomogram in the present study has been internally validated (cross-validation and bootstrapping). External validation of the nomogram was not carried out in this study, as this would require further prospective multi-centre recruitment of a cohort to test external validity.

## 5. Conclusions

The study reports a nomogram using clinical variables which can assist decision-making during counselling. Patients could be directed towards having systematic sampling of the prostate in addition to an image fusion biopsy approach. The decision analysis curve confirmed a higher net clinical benefit of a combined biopsy approach compared to targeted or random sampling at an acceptable threshold.

**Institutional Review Board Statement:** This was a prospective, protocol-driven study with ethical approval obtained through the East of Scotland Ethical committee and Caldicott permission (IGTCAL6358)) to access healthcare follow-up data.

**Informed Consent Statement:** Informed consent was obtained from all subjects involved in the study.

**Data Availability Statement:** The data are available for scrutiny from external requests.

**Conflicts of Interest:** The authors declare no conflict of interest.

## References

1. Kasivisvanathan, V.; Rannikko, A.S.; Borghi, M.; Panebianco, V.; Mynderse, L.A.; Vaarala, M.H.; Briganti, A.; Budäus, L.; Hellawell, G.; Hindley, R.G.; et al. MRI-Targeted or Standard Biopsy for Prostate-Cancer Diagnosis. *N. Engl. J. Med.* **2018**, *378*, 1767–1777. [CrossRef]

2. Ahmed, H.U.; El-Shater Bosaily, A.; Brown, L.C.; Gabe, R.; Kaplan, R.; Parmar, M.K.; Collaco-Moraes, Y.; Ward, K.; Hindley, R.G.; Freeman, A.; et al. Diagnostic accuracy of multi-parametric MRI and TRUS biopsy in prostate cancer (PROMIS): A paired validating confirmatory study. *Lancet* **2017**, *389*, 815–822. [CrossRef]

3. Pokorny, M.R.; de Rooij, M.; Duncan, E.; Schröder, F.H.; Parkinson, R.; Barentsz, J.O.; Thompson, L.C. Prospective study of diagnostic accuracy comparing prostate cancer detection by transrectal ultrasound-guided biopsy versus magnetic resonance (MR) imaging with subsequent mr-guided biopsy in men without previous prostate biopsies. *Eur. Urol.* **2014**, *66*, 22–29. [CrossRef] [PubMed]

4. Mottet, N.; van den Bergh, R.C.N.; Briers, E.; Van den Broeck, T.; Cumberbatch, M.G.; De Santis, M.; Fanti, S.; Fossati, N.; Gandaglia, G.; Gillessen, S.; et al. EAU-EANM-ESTRO-ESUR-SIOG Guidelines on Prostate Cancer—2020 Update. Part 1: Screening, Diagnosis, and Local Treatment with Curative Intent. *Eur. Urol.* **2021**, *79*, 243–262. [CrossRef] [PubMed]

5. Drost, F.J.H.; Osses, D.; Nieboer, D.; Bangma, C.H.; Steyerberg, E.W.; Roobol, M.J.; Schoots, I.G. Prostate Magnetic Resonance Imaging, with or Without Magnetic Resonance Imaging-targeted Biopsy, and Systematic Biopsy for Detecting Prostate Cancer: A Cochrane Systematic Review and Meta-analysis. *Eur. Urol.* **2020**, *77*, 78–94. [CrossRef] [PubMed]

6. Padhani, A.R.; Weinreb, J.; Rosenkrantz, A.B.; Villeirs, G.; Turkbey, B.; Barentsz, J. Prostate Imaging-Reporting and Data System Steering Committee: PI-RADS v2 Status Update and Future Directions. *Eur. Urol.* **2019**, *75*, 385–396. [CrossRef]

7. Kasivisvanathan, V.; Stabile, A.; Neves, J.B.; Giganti, F.; Valerio, M.; Shanmugabavan, Y.; Clement, K.D.; Sarkar, D.; Philippou, Y.; Thurtle, D.; et al. Magnetic Resonance Imaging-targeted Biopsy Versus Systematic Biopsy in the Detection of Prostate Cancer: A Systematic Review and Meta-analysis. *Eur. Urol.* **2019**, *76*, 284–303. [CrossRef]

8. Sonn, G.A.; Natarajan, S.; Margolis, D.J.A.; MacAiran, M.; Lieu, P.; Huang, J.; Dorey, F.J.; Marks, L.S. Targeted biopsy in the detection of prostate cancer using an office based magnetic resonance ultrasound fusion device. *J. Urol.* **2013**, *189*, 86–92. [CrossRef]

9. Wysock, J.S.; Rosenkrantz, A.B.; Huang, W.C.; Stifelman, M.D.; Lepor, H.; Deng, F.-M.; Melamed, J.; Taneja, S.S. A Prospective, Blinded Comparison of Magnetic Resonance (MR) Imaging–Ultrasound Fusion and Visual Estimation in the Performance of MR-targeted Prostate Biopsy: The PROFUS Trial. *Eur. Urol.* **2014**, *66*, 343–351. [CrossRef]

10. Ahdoot, M.; Wilbur, A.R.; Reese, S.E.; Lebastchi, A.H.; Mehralivand, S.; Gomella, P.T.; Bloom, J.; Gurram, S.; Siddiqui, M.; Pinsky, P.; et al. MRI-Targeted, Systematic, and Combined Biopsy for Prostate Cancer Diagnosis. *N. Engl. J. Med.* **2020**, *382*, 917–928. [CrossRef]

11. Rouvière, O.; Puech, P.; Renard-Penna, R.; Claudon, M.; Roy, C.; Mège-Lechevallier, F.; Decaussin-Petrucci, M.; Dubreuil-Chambardel, M.; Magaud, L.; Remontet, L.; et al. Use of prostate systematic and targeted biopsy on the basis of multiparametric MRI in biopsy-naive patients (MRI-FIRST): A prospective, multicentre, paired diagnostic study. *Lancet Oncol.* **2019**, *20*, 100–109. [CrossRef]

12. Elkhoury, F.F.; Felker, E.R.; Kwan, L.; Sisk, A.E.; Delfin, M.; Natarajan, S.; Marks, L.S. Comparison of Targeted vs Systematic Prostate Biopsy in Men Who Are Biopsy Naive: The Prospective Assessment of Image Registration in the Diagnosis of Prostate Cancer (PAIREDCAP) Study. *JAMA Surg.* **2019**, *154*, 811–818. [CrossRef] [PubMed]

13. Dell'Oglio, P.; Stabile, A.; Soligo, M.; Brembilla, G.; Esposito, A.; Gandaglia, G.; Fossati, N.; Bravi, C.A.; Dehò, F.; De Cobelli, F.; et al. There Is No Way to Avoid Systematic Prostate Biopsies in Addition to Multiparametric Magnetic Resonance Imaging Targeted Biopsies. *Eur. Urol. Oncol.* **2020**, *3*, 112–118. [CrossRef]

14. Siddiqui, M.M.; Rais-Bahrami, S.; Turkbey, B.; George, A.K.; Rothwax, J.; Shakir, N.; Okoro, C.; Raskolnikov, D.; Parnes, H.L.; Linehan, W.M.; et al. Comparison of MR/ultrasound fusion-guided biopsy with ultrasound-guided biopsy for the diagnosis of prostate cancer. *JAMA* **2015**, *313*, 390–397. [CrossRef]

15. Sonn, G.A.; Chang, E.; Natarajan, S.; Margolis, D.J.; MacAiran, M.; Lieu, P.; Huang, J.; Dorey, F.J.; Reiter, R.E.; Marks, L.S. Value of targeted prostate biopsy using magnetic resonance-ultrasound fusion in men with prior negative biopsy and elevated prostate-specific antigen. *Eur. Urol.* **2014**, *65*, 809–815. [CrossRef]

16. Puech, P.; Rouvière, O.; Renard-Penna, R.; Villers, A.; Devos, P.; Colombel, M.; Bitker, M.-O.; Leroy, X.; Mège-Lechevallier, F.; Comperat, E.; et al. Prostate cancer Diagnosis: Multiparametric MR-targeted Biopsy with Cognitive and Transrectal US–MR Fusion Guidance versus Systematic Biopsy—Prospective Multicenter Study. *Radiology* **2013**, *268*, 461–469. [CrossRef]

17. Wei, C.; Jin, B.; Szewczyk-Bieda, M.; Gandy, S.; Lang, S.; Zhang, Y.; Huang, Z.; Nabi, G. Quantitative parameters in dynamic contrast-enhanced magnetic resonance imaging for the detection and characterisation of prostate cancer. *Oncotarget* **2018**, *9*, 15997–16007. [CrossRef]

18. Filson, C.P.; Natarajan, S.; Margolis, D.J.A.; Huang, J.; Lieu, P.; Dorey, F.J.; Reiter, R.E.; Marks, L.S. Prostate cancer detection with magnetic resonance-ultrasound fusion biopsy: The role of systematic and targeted biopsies. *Cancer* **2016**, *122*, 884–892. [CrossRef] [PubMed]

19. Cash, H.; Günzel, K.; Maxeiner, A.; Stephan, C.; Fischer, T.; Durmus, T.; Miller, K.; Asbach, P.; Haas, M.; Kempkensteffen, C. Prostate cancer detection on transrectal ultrasonography-guided random biopsy despite negative real-time magnetic resonance imaging/ultrasonography fusion-guided targeted biopsy: Reasons for targeted biopsy failure. *BJU Int.* **2016**, *118*, 35–43. [CrossRef] [PubMed]

20. Connor, M.J.; Miah, S.; Jayadevan, R.; Khoo, C.C.; Eldred-Evans, D.; Shah, T.; Ahmed, H.U.; Marks, L. Value of systematic sampling in an mp-MRI targeted prostate biopsy strategy. *Transl. Androl. Urol.* **2020**, *9*, 1501–1509. [CrossRef]

21. Alqahtani, S.; Wei, C.; Zhang, Y.; Szewczyk-Bieda, M.; Wilson, J.; Huang, Z.; Nabi, G. Prediction of prostate cancer Gleason score upgrading from biopsy to radical prostatectomy using pre-biopsy multiparametric MRI PIRADS scoring system. *Sci. Rep.* **2020**, *10*, 1–9. [CrossRef]

22. Epstein, J.I.; Feng, Z.; Trock, B.J.; Pierorazio, P.M. Upgrading and Downgrading of Prostate Cancer from Biopsy to Radical Prostatectomy: Incidence and Predictive Factors Using the Modified Gleason Grading System and Factoring in Tertiary Grades. *Eur. Urol.* **2012**, *61*, 1019–1024. [CrossRef] [PubMed]

23. Sathianathen, N.J.; Warlick, C.A.; Weight, C.J.; Ordonez, M.A.; Spilseth, B.; Metzger, G.J.; Murugan, P.; Konety, B.R. A clinical prediction tool to determine the need for concurrent systematic sampling at the time of magnetic resonance imaging-guided biopsy. *BJU Int.* **2019**, *123*, 612–617. [CrossRef]

24. Sathianathen, N.J.; Butaney, M.; Bongiorno, C.; Konety, B.R.; Bolton, D.M.; Lawrentschuk, N. Accuracy of the magnetic resonance imaging pathway in the detection of prostate cancer: A systematic review and meta-analysis. *Prostate Cancer Prostatic Dis.* **2019**, *22*, 39–48. [CrossRef]

25. Muthigi, A.; George, A.K.; Sidana, A.; Kongnyuy, M.; Simon, R.; Moreno, V.; Merino, M.J.; Choyke, P.L.; Turkbey, B.; Wood, B.J.; et al. Missing the Mark: Prostate Cancer Upgrading by Systematic Biopsy over Magnetic Resonance Imaging/Transrectal Ultrasound Fusion Biopsy. *J. Urol.* **2017**, *197*, 327–334. [CrossRef]

26. Siddiqui, M.M.; Rais-Bahrami, S.; Truong, H.; Stamatakis, L.; Vourganti, S.; Nix, J.; Hoang, A.N.; Walton-Diaz, A.; Shuch, B.; Weintraub, M.; et al. Magnetic Resonance Imaging/Ultrasound–Fusion Biopsy Significantly Upgrades Prostate Cancer Versus Systematic 12-core Transrectal Ultrasound Biopsy. *Eur. Urol.* **2013**, *64*, 713–719. [CrossRef] [PubMed]

27. Falagario, U.; Jambor, I.; Taimen, P.; Syvänen, K.T.; Kähkönen, E.; Merisaari, H.; Montoya Perez, I.; Knaapila, J.; Steiner, A.; Verho, J.; et al. Added value of systematic biopsy in men with a clinical suspicion of prostate cancer undergoing biparametric MRI-targeted biopsy: Multi-institutional external validation study. *World J. Urol.* **2020**, *39*, 1879–1887. [CrossRef] [PubMed]

28. Schieda, N.; Quon, J.S.; Lim, C.; El-Khodary, M.; Shabana, W.; Singh, V.; Morash, C.; Breau, R.H.; McInnes, M.D.F.; Flood, T.A. Evaluation of the European Society of Urogenital Radiology (ESUR) PI-RADS scoring system for assessment of extra-prostatic extension in prostatic carcinoma. *Eur. J. Radiol.* **2015**, *84*, 1843–1848. [CrossRef] [PubMed]

29. Perez, I.M.; Jambor, I.; Kauko, T.; Verho, J.; Ettala, O.; Falagario, U.; Merisaari, H.; Kiviniemi, A.; Taimen, P.; Syvänen, K.T.; et al. Qualitative and Quantitative Reporting of a Unique Biparametric MRI: Towards Biparametric MRI-Based Nomograms for Prediction of Prostate Biopsy Outcome in Men With a Clinical Suspicion of Prostate Cancer (IMPROD and MULTI-IMPROD Trials). *J. Magn. Reson. Imaging* **2020**, *51*, 1556–1567. [CrossRef]

30. Jambor, I.; Boström, P.J.; Taimen, P.; Syvänen, K.; Kähkönen, E.; Kallajoki, M.; Perez, I.M.; Kauko, T.; Matomäki, J.; Ettala, O.; et al. Novel biparametric MRI and targeted biopsy improves risk stratification in men with a clinical suspicion of prostate cancer (IMPROD Trial). *J. Magn. Reson. Imaging* **2017**, *46*, 1089–1095. [CrossRef] [PubMed]

31. Truong, M.; Hollenberg, G.; Weinberg, E.; Messing, E.M.; Miyamoto, H.; Frye, T.P. Impact of Gleason Subtype on Prostate Cancer Detection Using Multiparametric Magnetic Resonance Imaging: Correlation with Final Histopathology. *J. Urol.* **2017**, *198*, 316–321. [CrossRef] [PubMed]